

University of Southampton Research Repository ePrints Soton

Copyright © and Moral Rights for this thesis are retained by the author and/or other copyright owners. A copy can be downloaded for personal non-commercial research or study, without prior permission or charge. This thesis cannot be reproduced or quoted extensively from without first obtaining permission in writing from the copyright holder/s. The content must not be changed in any way or sold commercially in any format or medium without the formal permission of the copyright holders.

When referring to this work, full bibliographic details including the author, title, awarding institution and date of the thesis must be given e.g.

AUTHOR (year of submission) "Full thesis title", University of Southampton, name of the University School or Department, PhD Thesis, pagination

DEPARTMENT OF AERONAUTICS AND ASTRONAUTICS

A UNIFIED UNSTEADY FLOW THEORY OF DELTA WINGS
WITH ATTACHED SHOCK WAVES

by

D.D. Liu

A thesis submitted for the degree of
Doctor of Philosophy

University of Southampton,
Southampton, England

July 1974

ABSTRACT

FACULTY OF ENGINEERING & APPLIED SCIENCES

DEPARTMENT OF AERONAUTICS & ASTRONAUTICS

Doctor of Philosophy

A UNIFIED UNSTEADY FLOW THEORY OF DELTA WINGS WITH ATTACHED
SHOCK WAVES

by Danny Ding-Yu Liu

A unified unsteady flow theory has been developed for flat delta wings performing slow pitching oscillations. The provision is that the shock waves must be attached to the wing leading edges. The present study is considered as a first attempt in the unsteady wing theory in which the shock wave effect, hence the rotationality, is properly accounted for and Mach number ranges unified.

Emphasis is placed on methods of obtaining the unsteady flow solutions over the compression side of the wing which lead to the calculation of its stability derivatives.

The lifts and moments of steady mean flow and the in-phase flow are first obtained. A similarity rule for the delta-wing family with added volume of non-affine shapes is shown to exist. The out-of-phase flow is proved to be 'quasi-conical', thus a formulation in terms of pressure can be realized. In the outer region where the cross flow is supersonic the solution is exact representing parallel surfaces of isobars (and iso-velocities). In the inner region where the cross flow is subsonic the application of the method of spanwise integration yields directly a global formulation of the problem. In all cases, analytical closed-form solutions are obtained. Consequently the stability derivatives can be simply expressed in algebraic form.

Numerical examples are presented to exhibit the dependence of the stability derivatives on the given parameters, namely, the free-stream Mach number, the mean incidence, the sweepback angle, the pitching-axis location and the ratio of specific heats. Some stability boundaries are also given.

Finally, critical assessments of the present theory are presented. In particular, the valid flow regions due to the present perturbation scheme are defined. Improvement schemes toward the refinement of the present theory are outlined. Recommendations are made for a number of cases in which further extensions of the present theory are possible.

ACKNOWLEDGEMENT

The author wishes to express his gratitude to Dr. W.H. Hui for his initiation of the problem and continuing encouragement throughout the course of this work. In many stimulating discussions, his inspiring viewpoint and most valuable consultation on the problem were deeply appreciated.

He would also like to acknowledge Dr. R.A. East for his helpful comments in reviewing the manuscript, and Professor G.M. Lilley for his prolonged interest in the problem.

Among his colleagues, the author wishes to thank Dr. S.S. Desai for numerous helpful discussions, and Mr. H.P. Chou for his efforts in checking the algebra and his consultation in programming.

In particular, he is obliged to Professor and Mrs. P.E. Doak, whose constant concern for the author's non-technical life during his stay in Southampton made the technical one endurable.

The author is greatly indebted to his parents for their unfailing support and patience.

Finally, he wishes to thank Mrs. E. Bell for typing this manuscript.

This work has been carried out with the support of Procurement Executive, Ministry of Defence, for which the author is grateful.

CONTENTS

Chapter		Page
	ABSTRACT	ii
	ACKNOWLEDGEMENT	iv
	LIST OF FIGURES	viii
	NOMENCLATURE	x
1	INTRODUCTION	1
	1.1 Previous Unsteady Wing Theories	1
	1.2 Wedge Perturbation Methods	3
	1.3 Three-dimensional Flow Problems	4
	1.4 An outline of the Present Theory	5
2	STATEMENTS OF THE PROBLEM	8
	2.1 Flow Regions and Geometry Relations	8
	2.2 Perturbation Scheme	11
	2.3 Definition of the Problems	14
3	PROBLEM FORMULATION	16
	3.1 Governing Equations and Boundary Conditions	16
	3.2 Perturbed Equations	19
	3.3 Perturbed Boundary Conditions	21
	3.4 Full Formulation of the Mean-flow Problem and Problems A, B, C AND D	30
4	FORCES AND MOMENTS OF STEADY MEAN FLOW AND IN-PHASE FLOW	37
	4.1 The Mean-flow : Hui's Solutions	38
	4.2 Lift and Moment Coefficients : Mean-flow	44
	4.3 In-phase Flow : Differentiation Method	48
	4.4 A Similarity Rule for Flat Delta Wings	52

CONTENTS (continued)

Chapter		Page
5	FORCES AND MOMENTS OF DELTA WING-BODY COMBINATIONS: A LINEAR FORMULATION	55
	5.1 The Linearized Formulation	56
	5.2 The Method of Solution of the Inner Region	63
	5.3 The Forces and Moments	68
	5.4 The Generalized Similarity Rule	72
6	THE UNSTEADY FLOW SOLUTIONS : PROBLEMS A, B, C & D	75
	6.1 Problem A : The In-phase Flow of the Outer Region	75
	6.2 Problem C : The Out-of-phase Flow of the Outer Region	76
	6.3 Problem B : The In-phase Flow of the Inner Region	81
	6.4 Problem D : The Out-of-phase Flow of the Inner Region	84
7	THE STABILITY DERIVATIVES	100
	7.1 The Definition of the Derivatives	100
	7.2 The Evaluation of the Stability Derivatives	106
	7.3 The Stability Criteria	109
	7.4 The Limits of $C_{M\alpha}$ AND $C_{M\alpha}$ AS $X \rightarrow 0$	111
	7.5 Stability Derivatives for Two-sided Delta Wings	112
8	RESULTS AND DISCUSSION	115
	8.1 Description of the Figures	115
	8.2 The Flow Field Solutions : New Contributions	121
	8.3 The Method of Spanwise Integration	126
	8.4 The Limitations of the Present Theory	128
9	RECOMMENDATIONS	134
	9.1 On Experimental Research	134
	9.2 On Theoretical Research	134

CONTENTS (continued)

Chapter		Page
10	CONCLUSIONS	136
APPENDICES :		
A	THE GEOMETRICAL RELATION OF THE DELTA-WING FAMILY: ITS DETACHMENT CRITERIA AND EXACT FLOW SOLUTIONS	138
B	THE WAVE-ANGLE FORMULAE FOR THE OBLIQUE-SHOCK RELATION	145
C	THE PERTURBED SHOCK CONDITION (S.C.) FOR A SKEWED WEDGE PERFORMING UNSTEADY MOTIONS	148
D	THE DERIVATIVES OF SOME FLOW PARAMETERS : DIFFERENTIATION METHOD	150
E	ON OPERATORS REPRESENTING SPANWISE INTEGRATION	166
F	APPLICATION OF SPANWISE INTEGRAL IN THE TSCHAPLYGIN PLANE	168
G	THE PRESSURE FORMULATION FOR THE WEDGE FLOW : A SPECIAL CASE	171
H	AN IMPROVED PERTURBATION SCHEME TO THE INNER PROBLEMS	179
I	CONVERSION TABLES FOR VARIABLES AND COEFFICIENTS : FOR VARIOUS PROBLEMS IN THE PRESENT FORMULISM	184
	REFERENCES	187-191

FIGURES

LIST OF FIGURES

Figure

- 1-A Flat-Bottom Delta Wing placed in the Cartesian Co-ordinate
- 1-B Problems A, B, C & D and the Defined Regions
- 1-C Delta Wing showing Notations
- 1-D Caret Wing showing Notations
- 1-E Diamond Wing showing Notations
- 1-F Applicable Configurations
- 1-G Caret Wings with added Volumes of non-Affine Shapes
- 1-H Two-sided Wing Geometry
- 1-I Projection Plane of a Caret Wing
- 1-J The Tschaplygin Transform Plane

- 2 Shock-attachment Criterion for Cone, Wedge and Flat Delta Wings
($M_\infty - \alpha_0$ Diagram) ($\gamma = 1.4$)
- 3 Shock-attachment Criterion for Flat Delta Wings ($\chi - \alpha_0$ Diagram)
($\Gamma = 90^\circ$) ($\gamma = 1.4$)
- 4 Shock-attachment Criterion for Caret Wings ($\chi - \alpha_0$ Diagram)
($\Gamma = 80^\circ$) ($\gamma = 1.4$)
- 5 Shock-attachment Criterion for Caret Wings ($\chi - \alpha_0$ Diagram)
($\Gamma = 60^\circ$) ($\gamma = 1.4$)
- 6 Typical Pressure Distribution according to Hui's Theory (Ref. 7)
($\gamma = 1.4$)
- 7 $C_{L\alpha}$ vs α_0 according to Different Methods ($\gamma = 1.4$)
- 8 $C_{L\alpha}$ vs χ according to Different Methods ($\gamma = 1.4$)
- 9 $C_{L\alpha}$ vs α_0 for various Wing-Body Combinations ($\gamma = 1.4$)
- 10 $C_{M\alpha}$ vs M_∞ : Comparison with Experimental Data ($\gamma = 1.4$)
- 11 $-C_{M\alpha}$ vs x_0 at Different Incidences ($\gamma = 1.4$)
- 12 $-C_{M\alpha}$ vs x_0 at High Mach Numbers ($\gamma = 1.4$)
- 13 Comparison of Stiffness Derivative and Damping Derivatives for
Delta Wing of $\chi = 50^\circ$ ($\gamma = 1.4$)
- 14 $-C_{M\dot{\alpha}}$ vs x_0 for Delta Wing & Wedge ($\gamma = 1.4$)

LIST OF FIGURES (continued)

Figure

- 15 $-C_{M\dot{\alpha}}$ vs x_0 : Contribution due to Inner and Outer Regions
($\gamma = 1.4$)
- 16 $-C_{M\dot{\alpha}}$ vs x_0 Comparison of Damping Derivatives for a Cone, a
Wedge and a Delta Wing of $\chi = 30^\circ$ all with
semi-Apex Angle $\alpha_0 = 9^\circ$ ($\gamma = 1.4$)
- 17 $C_{N\dot{\alpha}}$ vs M_∞ : Comparison of out-of-phase Lifts for a Cone, Wedges
and Delta Wing of $\chi = 30^\circ$ all with semi-Apex
Angle $\alpha_0 = 10^\circ$ ($\gamma = 1.4$)
- 18 $-C_{M\dot{\alpha}}$ in Lower Mach Number Range ($\gamma = 1.4$)
- 19 $-C_{M\dot{\alpha}}$ Variation from Low to High Mach Numbers ($\gamma = 1.4$)
- 20 $-C_{M\dot{\alpha}}$ vs α_0 at Various x_0 s. ($\gamma = 1.4$)
- 21 $-C_{M\dot{\alpha}}$ vs α_0 : Comparison of a Wedge and a Delta Wing of $\chi = 45^\circ$
at various x_0 s. ($\gamma = 1.4$)
- 22 $-C_{M\dot{\alpha}}$ vs χ at Various x_0 s. ($M_\infty = 10$) ($\gamma = 1.4$)
- 23 $-C_{M\dot{\alpha}}$ vs χ at Various x_0 s. ($M_\infty = 1.5$) ($\gamma = 1.4$)
- 24 Stability Boundaries of a Wedge and a Delta Wing ($\gamma = 1.4$)
- 25 Stability Boundaries of Damping for Wedges and a Delta Wing
($\gamma = 1.4$)
- 26 Stability Boundaries for Delta Wings of various χ . ($\gamma = 1.4$)
- 27 Stability Boundaries showing in $\chi - x_0$ Diagram ($\gamma = 1.4$)
- 28 $-C_{M\dot{\alpha}}$ vs x_0 for Different Ratios of Specific Heats
- 29 Effects of the Ratios of Specific Heats on Damping-in-Pitch $C_{M\dot{\alpha}}$

NOMENCLATURE

<u>small letters</u>		<u>Equation</u>
a a_1 $\tilde{a}_V, \tilde{b}_V, \tilde{c}_V, \tilde{d}_V$ $a_{10}, c_{10}, b_{20}, a_{40}$ \tilde{d}_{50}	$= w_*/u_*$ 	 (4.2)b or (4.9) (6.9) (6.10)
a_{30}, c_{30}		(6.6)
b_k, \hat{c}_k $(k = 1, 2, 3, \dots)$		(4.2)a
$b^{(o)}$		(6.18)
$c_1, c_2, c_3, c_5, d_4, d_5$ $e_4, e_5, e_6, g_6, t_1, t_2$ t_3, s_1, s_2, s_3	See Appendix C	(3.21)a
$\hat{d}_1, \hat{d}_2, \hat{d}_3, \hat{d}_5, \hat{e}_5$	Coefficients of $\phi(\eta, \zeta)$	(6.35)
$\tilde{d}_5, \tilde{e}_5, \tilde{f}_5$	Coefficients of Q^0	(6.2)
d_{10}	Coefficient of p^1	(6.4)f
$f_\delta(\zeta)$	Perturbed mean-flow shock shape	(3.4)a
$g(\zeta)$	Perturbed shock shape of axis solution	(6.20)d
h_o	Pitch axis location for two-side wing (Fig. 1-H)	
i	$= \sqrt{-1}$	
$\vec{i}, \vec{j}, \vec{k}$	Unit vectors in Cartesian coordinate	
k_o, k_*	Reduced frequencies defined for inner and outer regions respectively	(2.11)
k	$= \frac{\bar{\omega}L}{U_\infty}$, conventional definition of reduced frequency	(2.11)

NOMENCLATURE (continued)

<u>small letters</u>		<u>Equation</u>
$(\bar{p}, \bar{u}, \bar{v}, \bar{w})$	Physical pressure and velocities	(2.12)
(p_o, u_o, v_o)	Pressure and velocities of 2-D wedge flow	
(p_*, u_*, v_*, w_*)	Pressure and velocities of skewed wedge flow	(2.5)
(p_s, u_s, v_s, w_s)		(2.6)
$(p_\delta, u_\delta, v_\delta, w_\delta)$	Perturbed solutions of the mean flow	(2.12), (3.7) and (4.1)
p_Δ	$= p_o \left[1 + \frac{\gamma M_o^2}{\lambda} p_\delta \right]$; (Ref. 7)	
p_c	Centre line pressure	(4.6)
\tilde{p}_δ	Stretched p_δ (Ref. 7)	
(p^I, v^I, w^I)	$O(\delta)$, linearized formulation	(5.1)
(p^{II}, v^{II}, w^{II})	$O(\delta \hat{\tau})$, linearized formulation	(5.1)
(p_s', v_s', w_s')		(3.24)a, (4.5) and (5.15)a
(p_s'', v_s'', w_s'')		(5.15)b
q_∞	$= \frac{1}{2} U_\infty^2$, dynamic pressure	
\bar{s}	$= \bar{s}(\bar{x}, \bar{y}, \bar{z}, t)$, general surface	(3.2)
t_c	$= \tan \varphi_1 \cos \chi$	
t_s	$= \tan \varphi_1 \sin \chi$	
$(\bar{x}, \bar{y}, \bar{z}, \bar{t})$	Physical Cartesian coordinate and time	
(x, y, z, t)	Non-dimensional coordinates (outer region)	(2.10)
\bar{x}_o	Pitch axis location (physical)	
x_o	$= \frac{\bar{x}_o}{L}$, pitch axis location (non-dimensional)	

NOMENCLATURE (continued)

<u>Capital letters</u>		<u>Equation</u>
A, B, C, D, E, F, G, J, K	2-D perturbed coefficients of (S.C.)	(3.17)
$\tilde{A}_1, \tilde{A}_2, \tilde{B}, \tilde{C}_1, \tilde{C}_2, \tilde{D}$ $\tilde{E}_1, \tilde{E}_2, \tilde{F}, \tilde{G}_1, \tilde{G}_2, \tilde{J}$ $\tilde{K}_1, \tilde{K}_2, \tilde{L}$	3D perturbed coefficients of (S.C.) see also Appendix I	(3.20)
A_0	$= \frac{A}{C}$	
B_0	$= -\frac{K}{C}$	
A_1, B_1, C_1, D_1	Coefficients of P^1	(6.4)
A_2, B_2, C_2, D_2	Coefficients of V^1	(6.5)
A_3, B_3, C_3, D_3	Coefficients of W^1	(6.6)
A_4, B_4, C_4, D_4	Coefficients of U^1	(6.7)
$A_5, B_5, C_5, D_5, E_5, F_5$	Coefficients of Q^1	(6.8)
C_I, C_{II}		(6.32)
C_f	$= \frac{2}{M_\infty^2} \frac{P_0}{P_\infty} \kappa^2$	
C_L	Lift coefficient	(4.12), (7.10)
C_{L_0}	2-D component of C_L	(4.14)a
C_{L_1}	3-D correction of C_L	(4.14)b
\bar{C}_L	C_L due to sweepback angle χ	
$\cup C_L$	C_L due to added volume σ_v	(5.26)
\hat{C}_L	C_L due to small bend	
$C_{L\alpha}$	in-phase lift (or lift slope)	(4.17)
$C_{L_0\alpha}$	2-D component of C_L	(4.17)a
$C_{L_1\alpha}$	3-D correction C_L	(4.17)b
$C_L \alpha$	Out-of-phase lift	(7.25)
C_M	Moment coefficient	(4.13), (7.11)

NOMENCLATURE (continued)

Capital letters

Equation

$-C_{M\alpha}$	Stiffness derivative (or in-phase moment)	(4.18)
$-C_{M\dot{\alpha}}$	Damping-in-pitch (or out-of-phase moment)	(7.26)
C_p	Pressure coefficient	(4.10)
C_{pHDP}	Pressure coefficient of HDP	(7.6)b
C_{p0}	Pressure coefficient (2-D)	(4.11)
C_{p1}	Pressure coefficient (3-D correction)	(4.11)
E_o	$= \frac{E}{C}$	
$F(\zeta)$	$= \frac{f_s(\zeta)}{X}$, perturbed shock shape of HDP	(4.1)
$F^I(\zeta), F^{II}(\zeta)$	Perturbed shock shapes	(5.9)a
$\hat{G}(\zeta)$	Body shape of the added volume	(5.2)a
\bar{G}	General shock shape	(3.4)
\bar{G}_o	2-D planar shock shape	(3.4)a
\bar{G}_*	3-D planar shock shape	(3.4)b
H	$= \lambda \tan \varphi_o$	
H'	$= \sqrt{1 - H^2}$	
I		(4.14)c
I_G	$= P_G(0)$	
I_{GS}	$= P_{GS}(0)$	
I_{LS}	$= P_{LS}(0)$	
I_u		(5.24)b
L	Physical length of the root chord	
\bar{L}	Total lift	
\bar{M}	Total Moment	
M_∞	Free stream Mach number	
M_s	Mach number defined in	(2.8)
M_n	Mach number defined in	(2.4)
M_o	2-D, aft-shock Mach number	
M_x	3-D, aft-shock Mach number (skewed wedge)	(2.8)

NOMENCLATURE (continued)

<u>Capital letters</u>		<u>Equation</u>
$(\hat{P}, \hat{U}, \hat{V}, \hat{W}, \hat{R})$	Flow variables of oscillatory flow $\sim O(\epsilon)$	(2.12)
$(P^0, U^0, V^0, W^0, R^0)$	Flow variables of Problem A	(2.15)
$(P^{(0)}, U^{(0)}, V^{(0)},$ $W^{(0)}, R^{(0)})$	Flow variables of Problem B	(2.14)
$(P^1, U^1, V^1, W^1, R^1)$	Flow variables of Problem C	(2.15)
$(P^{(1)}, U^{(1)}, V^{(1)},$ $W^{(1)}, R^{(1)})$	Flow variables of Problem D	(2.14)
$(P_*^{(0)}, V_*^{(0)}, W_*^{(0)})$	Exact flow solutions of Problem A appeared in M.C. of Problem B	(3.28)
$(P_*^{(1)}, V_*^{(1)}, W_*^{(1)})$	Exact flow solution of Problem C appeared in M.C. of Problem D	(3.30)
$(P_t^{(0)}, W_t^{(0)}, V_t^{(0)})$		(6.16)
$\hat{Q}(X, Y, Z, T)$	Oscillatory shock shape	
$Q_0(X, T)$	Perturbed oscillatory shock shape (inner region)	(3.26)a
$Q_*(x, z, t)$	Perturbed oscillatory shock shape (outer region)	(3.26)b
$Q^0, Q^{(0)}, Q^1, Q^{(1)}$	Perturbed shock shapes of Problems A, B, C and D respectively	(3.26)a, (3.26)b
S	= $L \cot \chi$, planform area	
U_∞	Free stream uniform flow	
\vec{V}	Total velocity vector	
\tilde{W}	= $M_0^2 \sin^2 \varphi_0$	
(X, Y, Z, T)	Non-dimensional Cartesian coordinates (inner region)	(2.9)

NOMENCLATURE (continued)

<u>Italic symbols</u>		<u>Equation</u>
$\mathcal{A}_1, \mathcal{B}_1, \mathcal{C}_1, \mathcal{D}_1$	Coefficients of $p_*^{(1)}$	(6.19)
$\mathcal{A}_2, \mathcal{B}_2, \mathcal{C}_2, \mathcal{D}_2$	Coefficients of $v_*^{(1)}$	(6.19)
$\mathcal{A}_3, \mathcal{B}_3, \mathcal{C}_3, \mathcal{D}_3$	Coefficients of $w_*^{(1)}$	(6.19)
L_ϕ		(6.23)b
$P_G(\eta)$	Half-range spanwise integral	(4.3)
$P_G(0)$		(4.4)
$\tilde{P}_{GS}(0)$	'Global-stretched' pressure	(4.7)
$\tilde{P}_{LS}(0)$	'Local-stretched' pressure	(4.8)
$P(\eta)$	Full-range spanwise integral of pressure $\mathcal{P}(\eta, \zeta)$	(6.24)a
$P^I(\eta)$	Full-range spanwise integral of pressure p	(5.16)a
$P^{II}(\eta)$	Full-range spanwise integral of pressure p	(5.16)b
$P^e(0)$		(5.23)a
$P^i(0)$		(5.23)b
$(\mathcal{P}, \mathcal{V}, \mathcal{W})$	Apex solutions (Problem D)	(6.20)
\mathcal{P}_0		(6.23)
\mathcal{P}_ϕ		(6.23)b
$(\mathcal{P}^*, \mathcal{V}^*, \mathcal{W}^*)$		(6.28)
$(\mathcal{P}_+, \mathcal{V}_+, \mathcal{W}_+)$		(6.25)
$(\tilde{p}, \tilde{v}, \tilde{w})$	Axis solution (Problem D)	(6.34)
$\tilde{P}(\eta)$	Spanwise integral of $\tilde{p}(\eta, \zeta)$	(6.40)
$\mathcal{S}_0, \mathcal{T}_0, \mathcal{V}_0$	Similarity functions due to χ , \hat{c} and σ_v respectively	(5.27)
$V(\eta)$	Full-range spanwise integral of $\mathcal{V}(\eta, \zeta)$	(6.24)b

NOMENCLATURE (continued)

<u>Greek symbols</u>		<u>Equation</u>
α_0	Mean flow incidence (Fig. 1-A)	
α_1	Incidence measured in oblique plane	(2.1)
$\bar{\alpha}$	$= \frac{\lambda}{\gamma M_0^2} P^*/P_0$	
α_I, α_{II}		(6.31)
β_0	Oblique shock wave angle (see Appendix B)	
β_1	Shock wave angle measured in oblique plane	(2.3)
$\bar{\beta}$	$= u^*/u_0$	
γ	Ratios of specific heats	
Γ	Half-wing angle of caret wings (Fig. 1-I)	
δ	Small parameter indicating 2-D departure	
$\bar{\Delta}$	$= (\bar{x}, \bar{z}, \bar{t})$ perturbed surface due to amplitude	(3.2)
Δ	Oscillatory surface (outer region)	(3.26)a
$\hat{\Delta}$	Oscillatory surface (inner region)	(3.26)b
ϵ	Small amplitude of oscillation	
(η, ζ)	$= \left(\frac{Y}{X}, \frac{Z}{X} \right)$	
(η^*, ζ^*)	Intersection of 3-D Mach cone and the wing surface	(4.6)
(η^*, ζ^*)	Intersection of 3-D Mach cone and the 3-D planar shock	(6.29)
θ	3-D Mach cone angle	(2.8)b
κ	$= \frac{M_0}{\lambda}$	
λ	$= \sqrt{M_0^2 - 1}$	
λ^*	$= \sqrt{M_*^2 - 1}$	
ζ_d	$= \cot \chi$	

NOMENCLATURE (continued)

Greek symbols

Equation

Λ	= $\cot \Gamma$	
μ	= $\sin^{-1} \frac{\zeta}{\sqrt{1-\eta^2}}$, Tschplygin coordinate
ν	= $\frac{1}{\gamma M_*^2}$	
ξ	= X or x	
$\bar{\rho}$	Physical flow density	
ρ_0	2-D flow density (wedge)	
ρ_*	3-D flow density (skewed wedge)	(2.5)
ρ_δ	Perturbed density of the mean flow	(2.12)
$\hat{\sigma}$	= $\tan \chi$	
σ_0	= $\tanh^{-1} H$	
(σ, μ)	= $(\tanh^{-1} \eta, \sin^{-1} \frac{\zeta}{\sqrt{1-\eta^2}})$	Tschplygin Transform
σ_v	Added volume parameter	
τ	An angle in the side plane (see Fig. 1-C)	
$\hat{\tau}$	Small-bend parameter	
$\tilde{\tau}$	Wing thickness (Fig. 1-F)	
φ_0	= $\beta_0 - \alpha_0$	
φ_1	= $\beta_1 - \alpha_1$	
Φ_{AB}, Φ_C		(6.31)
χ	Sweepback angle	
$\bar{\chi}$	Sweepback angle of a caret wing (Fig. 1-J)	
χ_*	3-D Mach cone as measured by χ	
Ψ	= $\frac{\partial \mathcal{P}_\phi}{\partial \zeta}$	
ψ_0	Design angle of a caret wing	
$\bar{\omega}$	Circular frequency	

Subscripts and Superscripts

- ($\bar{\quad}$) : Physical quantities, real time and velocities
- ()_∞ : Free stream flow properties and velocities
- ()_o : Aft-shock, uniform flow properties and velocities
(wedge flow)
- ()_{*} : Aft-shock, uniform flow properties and velocities
(skewed wedge flow)
- ()_Δ : Hui's delta wing solution (Ref. 7)
- ()_ξ : Steady mean flow solution (Ref. 7) inner region
- ()_ξ : Steady mean flow solution (Ref. 7) outer region
- ()⁰ : Dependent variables of Problem A
- ()⁽⁰⁾ : Dependent variables of Problem B
- ()¹ : Dependent variables of Problem C
- ()⁽¹⁾ : Dependent variables of Problem D
- ()['] : Linear representation of the exact flow quantities
in the outer region

Operational symbols

Differentiation :

$$(\)' = \frac{d}{d\eta}$$

Total differentiation, e.g.

$$P'(\eta) = \frac{dP}{d\eta}$$

$(\)_{\eta}$, $(\)_{\zeta}$, $(\)_{\eta\zeta}$, $(\)_{\eta\eta}$... etc. Partial differentiation, e.g.

$$P_{\eta} = \frac{\partial P}{\partial \eta} \quad \& \quad P_{\eta\zeta} = \frac{\partial^2 P}{\partial \eta \partial \zeta}$$

Integration :

$$\int [P(\eta, \zeta)]$$

Full-range spanwise integral
(see Appendix E)

ABBREVIATIONS

D.E.	Differential equation
S.C.	Shock condition
M.C.	Mach cone condition
SYM.C.	Symmetric condition
T.C.	Tangency condition
E.C.	Extra condition
HDP	Hui's delta wing Problem (Ref. 7)
HWP	Hui's wedge Problem (Ref. 34)
GS	Global stretched
LS	Local stretched
LL	Local Linear
RHS	Right hand side
LHS	Left hand side
WRT	With respect to
2-D	Two-dimensional
3-D	Three-dimensional
O.D.E.	Ordinary Differential Equation
P.D.E.	Partial Differential Equation

1. INTRODUCTION

With the advance of the present space technology, the detailed knowledge of space vehicle design, such as space shuttle, is of increasing demand. One fundamental aspect of the design of a re-entry hypersonic/supersonic lifting vehicle is its aerodynamic stability during its complete course of atmospheric flight. When the vehicle descends to earth, for example, its entry path generally introduces a fairly large flow incidence. Consequently, the shock waves encountered are generally strong and may be either detached or attached to the wing edges. To achieve a higher aerodynamic efficiency (i.e lift to drag ratio) for a delta shape wing, it has been suggested that the shock attachment case is more favourable for this purpose, owing to the fact that no 'flow spillage' could come from the lower surface, as it is enclosed by the shock waves (Refs. 1 & 2). Since there is no communication between the upper and lower surfaces in this situation, the aerodynamic problem can be tackled independently by first examining the flow field of the lower surface (e.g. Refs. 3-8). Besides, in the moderately high supersonic and hypersonic speed range, nearly all the aerodynamic forces and moments are contributed mainly from the compression side. The present attempt, therefore, is to develop a unified unsteady flow theory for delta wings at certain mean incidence performing pitching oscillations in hypersonic/supersonic flow. The provision is that the shock waves must be attached to the wing leading edges. Emphasis will be placed on analysing the unsteady flow disturbances over the lower surface and the calculations of its stability derivatives.

1.1 Previous unsteady wing theories

Research work in the past dealing with the unsteady supersonic flow problems was mostly restricted to the linearized potential flow model.

The unsteady linearized potential flow equation for thin wings has been studied by many (e.g. Refs. 9-14). The methods used can be classified broadly as the moving source method proposed by Garrick & Rubinow (Ref. 9), and the model of integral transform suggested by Gunn (Ref. 16) and Stewartson (Refs. 10 and 11). Following the first approach, a series of NACA technical reports (Refs. 17-19) have extensively applied the method for sweepback wings of different configurations. Malvestuto et al (Ref. 17) and Martin et al (Ref. 18) studied how the tapered and tip effects could influence the damping moment for delta wings. Nelson (Ref. 19) and Froelich (Ref. 20) have studied the pitching problem of 'wide' delta wings and both presented the stability boundaries. The integral transform methods on the other hand were adopted by many investigators to study wings of different aspect ratios and bodies of revolution, notably Miles (Ref. 14) and Adam-Sears (Ref. 15) in supersonic flow and Landahl (Ref. 21) in transonic flow. The quasi steady approach of Miles (Ref. 13) has also provided simple damping formula for wide delta wings, but with a crude approximation to the flow field.

The advantage of the unsteady linearized potential flow approach is that the solutions obtained generally allow higher order frequency variations, thus opening ways for flutter analysis, and for analysing other aeroelasticity problems. These theories, however, break down as the supersonic Mach number increases and/or the wing thickness and the mean incidence are no longer small. The deficiency of the potential model is that the shock wave is replaced by a series of Mach waves, thus no effect of rotationality can be taken into consideration. Various attempts were made to further incorporate the non-linear effects into the potential model by rendering a second order expansion in M_∞^{-2} (Landahl 1957, Ref. 22), or in the thickness parameter (Van Dyke, Ref. 23).

Nevertheless, the validity of their methods still suffer from the basic deficiencies of the potential model.

In order to handle problems in higher Mach ranges, many investigators adopted more physical models, such as the well-known piston theory and Newtonian theory. Based on the unsteady analogies of the shock expansion theory, the tangent wedge theory (see Ref. 24), or in extending Hayes-Lighthill piston theory (Ref. 25), Morgan et al (Ref.26), Zartarian et al (Ref. 27) and Ashley et al (Ref. 28) have vastly explored various aeroelastic aspects of airfoils and bodies. Unsteady Newtonian flow approaches were studied by Miles (Ref. 29) and by Aroesty et al (Ref. 30). These methods usually avoided the small perturbation scheme, and yet the Mach ranges applicable were still limited. In contrast to the potential model, the shock wave effect in some cases was overestimated (e.g. Newtonian theory). Apparently, in these cases, the Rankine-Hugoniot conditions were not properly satisfied in the formulation.

1.2 Wedge perturbation methods

To achieve a unified approach, the shock wave conditions must be formulated properly. Rigorous treatment in dealing with the shock wave-reflected wave interaction was first given by Lighthill (Ref. 31) and further extended by Chu (Ref. 32), and reviewed by Chernyi (Ref.33). Lighthill's formulation is a perturbation method based on the exact and uniform flow over the wedge behind the shock wave (called 'wedge perturbation' from hereon). The merits of this method are many, i.e. the wedge-like body can be of arbitrary thickness, the flow rotationality can be accounted for, and hence the Mach ranges are unified provided that the shock attaches to the apex. Furthermore, unlike the usual free-stream perturbation scheme (e.g. linearized potential flow), the

wedge perturbation scheme results in a linear formulation but with a basic flow in which the flow nonlinearity and deflection are fully imbedded. Following the same line, Hui (Ref. 34) has further developed an unsteady theory in which he found a new set of unsteady reflected waves associated with higher order thickness effect. His unsteady wedge solution appeared to include all the previous unsteady wedge solutions (Refs. 33, 35 and 36) as special cases. For low frequency oscillation Hui's solution is proved to be an exact one. (This solution will be reformulated and solved in Appendix G by a new method). His method of solution also indicated the possibility of studying the three-dimensional problem, such as a caret wing.

1.3 Three-dimensional flow problems

Including the shock-wave treatment, the three-dimensional methods have been developed by many researchers in the past decade. Prolonged interest in the blunt-body flow problem has yielded numerous methods of approach, direct or indirect. One analytical direct method called the method of series truncation (Ref. 38) was devised by Swigart (Ref. 39) to deal with the steady problem. Chang (Ref. 40) further generalized the method to the unsteady case which serves the analytical counterpart of an earlier numerical work by Telenin & Lipinskii (Ref. 41).

For low aspect ratio delta wings with shock detachment, there exists the thin shock layer theory proposed by Messiter (Ref. 42). Extensive applications to different wing configurations were performed by Hida (Ref. 43) and Squire (Ref. 44). For delta wings with shock attachment, its steady problem has drawn the attention of many researchers. Numerical solutions were first obtained by Fowell (Ref. 3) and Babaev (Ref. 4). The recent numerical developments were given by Voskrenskii (Ref. 5), South and Klunker (Ref. 6), among others (see Ref. 6).

Analytical approaches were given by Malmuth & Hui (Refs. 58 and 7). Based on the hypersonic small disturbance theory, Malmuth's theory is restricted to the hypersonic flow range and to slightly swept angles and small incidences. Hui further generalized Malmuth's approach in constituting a unified supersonic/hypersonic theory, in the shock attachment domain, for delta wings inclined at any incidence. Hui's solution consists of an exact flow solution in the outer region (the region between the oblique shock waves and Mach cone, regions I and II Fig. 1.B), and a wedge perturbation solution in the inner region (within the Mach cone, region III, Fig. 1.B). Rendering Lighthill's technique of strained coordinate, he then matched the solutions of two regions along the spanwise direction. The theory gives almost identical results when compared with those of the numerical methods (Fig. 6) except in the neighbourhood of the cross flow sonic line. Perhaps an improved matching scheme may refine the solution in this region.

Although the steady flow development of the delta wing has reached a mature stage, no unsteady work has been done for either the detached shock case or the attached shock case. It is therefore the purpose of the present study to generalize Hui's theories (Ref. 7 and 34) to a three-dimensional unsteady theory. This work is to be considered a first attempt in the unsteady wing theory in which the shock-wave effect is properly accounted for and Mach ranges unified.

1.4 An outline of the present theory

The premises of the unsteady flow assumptions are that the wing performs pitching oscillations with a small amplitude ϵ and at reduced frequency, k (both being much less than one).

Let p_{Δ} be the steady solution due to the mean flow past the delta wing at its mean position (Hui, Ref. 7), $p^{(0)}$ and $p^{(1)}$ be the pressures due to in-phase and out-of-phase flow respectively, all being

functions of space coordinates $(\bar{x}, \bar{y}, \bar{z})$ then the total pressure \bar{p} is sought in the following form

$$\bar{p}(\bar{x}, \bar{y}, \bar{z}, t) = p_{\Delta} + \epsilon \cdot \left[p^{(0)} + ikp^{(1)} \right] \cdot e^{ikt}$$

Clearly, both the mean flow and the in-phase flow are conical, as no characteristic length appears in the problem. As the mean flow solution p_{Δ} is given as a function of α_0 , the mean incidence, the in-phase flow $p^{(0)}$ is obtained by exact differentiation of p_{Δ} with respect to α_0 . The lifts and moments are then obtained in closed forms by integration (Chapter 4). Furthermore, a similarity rule is shown to exist. The rule states for given free-stream M_{∞} and α_0 , the steady lifts, moments and the stiffness derivatives can be expressed as a combination of terms, which separately account for the sweepback angle effect, the added volume effect and the small anhedral effect (e.g. caret wing), or the dihedral effect (Chapter 5).

Out-of-phase flow is again divided into the outer and the inner regions (see Section 1.3). An exact solution of $p^{(1)}$ in closed form is obtained in the outer region. Interestingly enough, $p^{(1)}$ and out-of-phase velocities and densities are found as linear functions of the space coordinates $(\bar{x}, \bar{y}, \bar{z})$ (see Fig. 1-A), and the outer shock shape is quadratic. This then suggests the 'quasi-conical' nature of the out-of-phase flow*. The inner flow solution thus can be expressed in the form of

$$p^{(1)}(\bar{x}, \bar{y}, \bar{z}) = \bar{x}^n \bar{O}(\bar{\eta}, \bar{\zeta}) + \bar{x}_0 \bar{P}(\bar{\eta}, \bar{\zeta})$$

where $\bar{\eta} = \bar{y}/\bar{x}$ and $\bar{\zeta} = \bar{z}/\bar{x}$, and \bar{x}_0 is the position of the

* This point was suggested in Ref. 17 for unsteady supersonic potential flow but without proof.

pitch axis location with $n = 1$ for the case of flat-bottom delta wing. The boundary value problem is then formulated solely in terms of a single dependent variable $\bar{\phi}$ (and \bar{p}) with two independent variables $\bar{\eta}$ and $\bar{\zeta}$ (the conical coordinates). The boundary conditions are specified at the wing surface, the shock surface and the Mach cone surfaces. Upon application of the method of spanwise integration (Refs. 45 and 46), the problem is further reduced to an ordinary differential equation with two-point boundary conditions, one being at the shock, the other at the wing surface. Again, an exact solution is found in a close form for the inner flow (Chapter 6). After matching the inner and outer solutions, damping derivatives are obtained in simple algebraic expressions. Finally, the formula for stability criterion is given and stability boundaries are presented for various cases (Figs. 24-27)(Chapter 7).

It is noted that the outer flow solution is based on an exact formulation, whereas the inner formulation for out-of-phase flow is an approximate one. The approximation in essence ignores the interaction between the mean flow and the out-of-phase contribution of the reference wedge flow (see Appendix H). However, the terms ignored can be recovered, if one wishes, in a straightforward manner following the present method of approach. In fact, the terms ignored will eventually turn out to be the inhomogeneous terms in the ordinary differential equation obtained. Thus, the present theory should expect to give accurate results for cases in which :

- (a) the mean flow incidence and/or the sweepback angle is not too large where the interaction effect is small ;
- (b) the Mach number is high enough so that the outer flow region dominates the inner one over the planform.

2. STATEMENTS OF THE PROBLEM

Consider a flat-bottom delta wing of sweepback angle χ in a supersonic/hypersonic flow with the shock waves attached to its leading edges. The right-handed Cartesian coordinate system $(\bar{x}, \bar{y}, \bar{z})$ fixed with the lower wing surface (flat-bottom side), is employed as shown in Figure 1-A. The origin is set at the apex of the wing. The \bar{x} -axis is placed along the root chord of the wing; \bar{y} -axis is normal to the wing surface and \bar{z} -axis normal to the $\bar{x}\bar{y}$ plane. (see Fig. 1-A).

Restricting the present interest to the lower surface of the wing, (i.e. the windward side), figure 1-A is drawn bottom up with the uniform supersonic/hypersonic flow $\hat{V}_\infty = (U_\infty, 0, 0)$ approaching the wing surface at an inclined angle α_0 (i.e. the mean flow incidence). Denote by \bar{u} , \bar{v} and \bar{w} respectively, the velocity components of the flow field in the \bar{x} , \bar{y} and \bar{z} directions, and by \bar{p} and $\bar{\rho}$ the pressure and the density of the flow field. These flow velocities and properties are considered generally to be functions of \bar{x} , \bar{y} , \bar{z} and \bar{t} , the real time. The barred notation hence indicates the physical lengths or quantities. Also, denote by u_0 , v_0 , w_0 , p_0 and ρ_0 the corresponding flow velocities and properties in the flow field over the flat plate whose condition is given by reducing the sweepback angle to zero. Clearly, $v_0 = w_0 = 0$ under the present coordinate system.

2.1 Flow regions and geometry relations

The flow field of interest is enclosed by the attached shock waves and the wing surface. According to the flow nature, it is sub-divided into two regions by the Mach core (see Fig. 1-B), namely the outer region (Region I and II) and the inner region (Region III), defined in Sec. 1.3. The cross flow in the outer region is of hyperbolic type and the cross flow in the inner region is of elliptic type. For steady

mean flow, the flow in the outer region is a uniform one, and in the inner region a non-uniform one. For unsteady flow in general, they are both non-uniform. Further specification of the related problems in these regions encountered in oscillatory case will be given later in Sec. 2.3 .

In the outer region, the geometry of the wing and the flow incidence constitute different planes as shown in Figure 1-C . The oblique plane is defined as one which is normal to the leading edges and the side plane as one which contains free stream vector \vec{V}_∞ and one side of the leading edges.

Let τ be the angle in the side plane measured from the leading edge to \vec{V}_∞ , α_1 the angle between the wing surface and side plane, and β_1 be the shock angle measured from the side plane to the plane of the oblique shock surface, the following relations hold,

$$\tan \alpha_1 = \frac{\tan \alpha_0}{\cos \chi} \quad (2.1)$$

$$\cos \tau = \cos \alpha_0 \sin \chi \quad (2.2)$$

$$\left[1 + \frac{\gamma-1}{2} M_n^2 \right] \tan^3 \beta_1 - \left[(M_n^2 - 1) \cot \alpha_1 \right] \tan^2 \beta_1 + \left[1 + \frac{\gamma+1}{2} M_n^2 \right] \tan \beta_1 + \cot \alpha_1 = 0 \quad (2.3)$$

$$M_n = M_\infty \sin \tau \quad (2.4)$$

where M_∞ is defined as the freestream Mach number.

Thus, for a given set of M_∞ , α_0 and χ one obtains α_1 , τ and β_1 from the above relations. The generalisation of equations (2.1) and (2.2) for a delta-wing family is given in the Appendix A . Equation (2.3) is the well-known oblique shock relation, the explicit form of $\beta_1 = \beta_1(\alpha)$ is derived through the cubic formulae in

Appendix B .

Let the notation subscript ()₀ indicate the flow properties and geometry quantities corresponding to the wedge flow. Thus, for given M_∞ and α_0 , the aft-shock Mach number M_0 , and the shock wave angle β_0 can be found from the oblique shock relation (Appendix B). Hence, the uniform flow in regions I and II can be represented as :

$$\left\{ \begin{array}{l} u_* = u_0 (1 + u_s) \quad \text{a} \\ v_* = u_0 v_s \quad \text{b} \\ w_* = u_0 w_s \quad \text{c} \\ p_* = p_0 \left(1 + \frac{\gamma M_0^2}{\lambda} p_s \right) \quad \text{d} \\ \rho_* = \rho_0 \left(1 + \frac{M_0^2}{\lambda} \rho_s \right) \quad \text{e} \end{array} \right. \quad (2.5)$$

where

$$\left\{ \begin{array}{l} u_s = \frac{\cos \varphi_0}{\cos \beta_0} \cdot \left[\cos \tau \sin \chi + \frac{\sin \tau \cos \beta_1}{\cos \varphi_1} \cos \chi \right] - 1 \quad \text{(a)} \\ v_s = 0 \quad \text{(b)} \\ w_s = \frac{\cos \varphi_0}{\cos \beta_0} \left[\cos \tau \cos \chi - \frac{\sin \tau \cos \beta_1}{\cos \varphi_1} \sin \chi \right] \quad \text{(c)} \\ p_s = \frac{2 \lambda M_\infty^2}{M_0^2} \left[\frac{\sin^2 \beta_1 \sin^2 \tau - \sin^2 \beta_0}{2 \gamma M_\infty^2 \sin^2 \beta_0 - (\gamma - 1)} \right] \quad \text{(2.6) (d)} \\ \rho_s = \frac{2 \lambda}{M_0^2 \sin^2 \beta_0} \left[\frac{\sin^2 \beta_1 \sin^2 \tau - \sin^2 \beta_0}{2 + (\gamma - 1) M_\infty^2 \sin^2 \tau \sin^2 \beta_1} \right] \quad \text{(e)} \end{array} \right.$$

In the equations (2.6), $\varphi_1 = \beta_1 - \alpha_1$, $\lambda = \sqrt{M_0^2 - 1}$ and γ is the specific heat ratio of the gas.

Note that when $\chi \rightarrow 0$, $u_s = v_s = w_s = p_s = \rho_s = 0$, implying $u_* = u_0$, $v_* = 0$, $w_* = w_0$, $p_* = p_0$ and $\rho_* = \rho_0$, a reduction to two-dimensional wedge flow.

Furthermore, the oblique plane shock surface is defined as

$$\bar{y} = \tan \varphi_1 (\bar{x} \cos \chi - \bar{z} \sin \chi) \quad (2.7)$$

and the three dimensional Mach cone, which divides the flow regions, is described by the following formula

$$(M_*^2 - 1) \frac{\bar{y}^2}{\bar{y}} + (\bar{x} \sin \theta - \bar{z} \cos \theta)^2 = (\bar{x} \cos \theta + \bar{z} \sin \theta)^2 \quad (2.8)$$

where M_* is the uniform flow Mach number in regions I and II, i.e.

$$M_* = \left[\frac{\rho_* (u_*^2 + w_*^2)}{\gamma p_*} \right]^{\frac{1}{2}} \quad (2.8a)$$

and θ is the angle between the x-axis and the flow velocity in the regions, i.e.

$$\theta = \tan^{-1} \frac{w_*}{u_*} \quad (2.8b)$$

2.2 Perturbation scheme

Let L be the characteristic length (the root chord) of the delta wing, two sets of non-dimensional coordinate systems are defined :

In the inner region,

$$\begin{cases} X = \bar{x}/L \\ Y = \lambda \bar{y}/L \\ Z = \lambda \bar{z}/L \\ T = \bar{t} u_0/L \end{cases} \quad (2.9)$$

* The brief notation for Mach cone surface is written as

$$M_s(\bar{x}, \bar{y}, \bar{z}) = 0$$

and in the outer region,

$$\left\{ \begin{array}{l} x = \bar{x}/L \\ y = \bar{y}/L \\ z = \bar{z}/L \\ t = \bar{t} u_*/L \end{array} \right. \quad (2.10)$$

When the delta wing performs a small amplitude oscillation with respect to its mean incidence α_0 , there exist two physical parameters namely the small amplitude parameter ϵ , $\epsilon \ll 1$ and the oscillation circular frequency $\bar{\omega}$. Two reduced frequencies are introduced for inner and outer regions, i.e.

$$\left\{ \begin{array}{l} k_0 = \frac{\bar{\omega} L}{u_0} \\ k_* = \frac{\bar{\omega} L}{u_*} \end{array} \right. \quad (2.11) \quad \begin{array}{l} a \\ b \end{array}$$

Also the commonly-used reduced frequency k based on the freestream velocity U_∞ is defined as

$$k = \frac{\bar{\omega} L}{U_\infty} \quad (2.11)^* \quad c$$

* The relations then read $k_0 = \frac{U_\infty}{u_0} \cdot k$ and $k_* = \frac{U_\infty}{u_*} \cdot k$.

From here to Chapter 6, the perturbation schemes are based on small parameters k_0 and k_* . But in the final evaluation of the oscillatory force and Moment coefficients in Chapter 7, they are based on reduced frequency k . (see equation (7.7)).

In the present study, it is considered the wing performs slow oscillation at a low circular frequency $\bar{\omega}$ much smaller than the chord length travelled per unit time as measured by U_∞ . Consequently

$$k \ll 1$$

$$\text{hence } k_0, k_* \ll 1 \quad \text{as } u_0, u_* \sim O(U_\infty)$$

Thus, the five dependent variables can be written in the following perturbation forms :

In the inner region

$$\left\{ \begin{array}{l} \bar{p} = p_0 + \frac{\gamma M_0^2 p_0}{\lambda} \left[p_\delta + \epsilon \cdot \hat{p}(X, Y, Z, T) \right] \\ \bar{u} = u_0 + u_0 \left[u_\delta + \epsilon \cdot \hat{U}(X, Y, Z, T) \right] \\ \bar{v} = u_0 \left[v_\delta + \epsilon \cdot \hat{V}(X, Y, Z, T) \right] \\ \bar{w} = u_0 \left[w_\delta + \epsilon \cdot \hat{W}(X, Y, Z, T) \right] \\ \bar{\rho} = \rho_0 + \frac{\rho_0 M_0^2}{\lambda} \left[\rho_\delta + \epsilon \cdot \hat{R}(X, Y, Z, T) \right] \end{array} \right. \quad (2.12)$$

where subscript $()_\delta$ indicates perturbed flow properties and velocities of $O(\delta)$; and δ is a small parameter representing the three dimensional departure from the wedge flow. The subscript $()_\Delta$ denotes the mean flow solution previously obtained by Hui (Ref. 7).

In the outer region

$$\left\{ \begin{array}{l} \bar{p} = p_* + \epsilon \cdot p_* P(x, y, z, t) \\ \bar{u} = u_* + \epsilon \cdot u_* U(x, y, z, t) \\ \bar{v} = \epsilon \cdot u_* V(x, y, z, t) \\ \bar{w} = w_* + \epsilon \cdot u_* W(x, y, z, t) \\ \bar{\rho} = \rho_* + \epsilon \cdot \rho_* R(x, y, z, t) \end{array} \right. \quad (2.13)$$

It is assumed that the oscillation is simple harmonic with small

frequency and the following expansions in k_0 (and k_*) are introduced.

In the inner region,

$$\left\{ \begin{array}{l} \hat{P}(X,Y,Z,T) = \left[p^{(0)}(X,Y,Z) + ik_0 p^{(1)}(X,Y,Z) \right] \cdot e^{ik_0 T} \\ \hat{U}(X,Y,Z,T) = \left[u^{(0)}(X,Y,Z) + ik_0 u^{(1)}(X,Y,Z) \right] \cdot e^{ik_0 T} \\ \hat{V}(X,Y,Z,T) = \left[v^{(0)}(X,Y,Z) + ik_0 v^{(1)}(X,Y,Z) \right] \cdot e^{ik_0 T} \\ \hat{W}(X,Y,Z,T) = \left[w^{(0)}(X,Y,Z) + ik_0 w^{(1)}(X,Y,Z) \right] \cdot e^{ik_0 T} \\ \hat{R}(X,Y,Z,T) = \left[r^{(0)}(X,Y,Z) + ik_0 r^{(1)}(X,Y,Z) \right] \cdot e^{ik_0 T} \end{array} \right. \quad (2.14)$$

In the outer region,

$$\left\{ \begin{array}{l} P(x,y,z,t) = \left[p^0(x,y,z) + ik_* p^1(x,y,z) \right] \cdot e^{ik_* t} \\ U(x,y,z,t) = \left[u^0(x,y,z) + ik_* u^1(x,y,z) \right] \cdot e^{ik_* t} \\ V(x,y,z,t) = \left[v^0(x,y,z) + ik_* v^1(x,y,z) \right] \cdot e^{ik_* t} \\ W(x,y,z,t) = \left[w^0(x,y,z) + ik_* w^1(x,y,z) \right] \cdot e^{ik_* t} \\ R(x,y,z,t) = \left[r^0(x,y,z) + ik_* r^1(x,y,z) \right] \cdot e^{ik_* t} \end{array} \right. \quad (2.15)$$

where the superscripts $()^{(0)}$ and $()^0$ indicate the in-phase components of the oscillatory flow and the superscripts $()^{(1)}$ and $()^1$ indicate the out-of-phase components of the flow.

2.3 Definition of the problems

According to the above perturbation scheme, four problems are categorised here (see Fig. 1-B)

i) Problem A : p^0 , the in-phase flow problem of the outer region.

The flow field is conical and is uniform. The mathematical formulation is an initial valued problem (Hyperbolic-type P.D.E.)

ii) Problem B : $p^{(0)}$, the in-phase flow problem of the inner region.
The flow field is conical but non-uniform. The mathematical formulation is a boundary valued problem (Elliptic-type P.D.E.)

iii) Problem C : p^1 , the out-of-phase flow problem of the outer region.
The flow field is proved later to be quasi-conical and is an initial valued problem (Hyperbolic-type P.D.E.)

iv) Problem D : $p^{(1)}$, the in-phase flow problem of the inner region.
The flow field is quasi conical and is non-uniform. The mathematical formulation is a boundary valued problem. (Elliptic-type P.D.E.).

3. PROBLEM FORMULATION

3.1 Governing equations and boundary conditions

For an inviscid adiabatic flow of a gas, the continuity, momentum and energy equations can be written as

$$\frac{\partial \bar{\rho}}{\partial \bar{t}} + \bar{\nabla} \cdot (\bar{\rho} \bar{\mathbf{V}}) = 0 \quad \text{a}$$

$$\frac{\partial \bar{\mathbf{V}}}{\partial \bar{t}} + (\bar{\mathbf{V}} \cdot \bar{\nabla}) \bar{\mathbf{V}} = -\frac{1}{\bar{\rho}} \bar{\nabla} \bar{p} \quad \text{(3.1) b}$$

$$\frac{\partial}{\partial \bar{t}} \left(\frac{\bar{p}}{\bar{\rho}^\gamma} \right) + (\bar{\mathbf{V}} \cdot \bar{\nabla}) \left(\frac{\bar{p}}{\bar{\rho}^\gamma} \right) = 0 \quad \text{c}$$

where $\bar{\mathbf{V}} = \bar{u} \hat{i} + \bar{v} \hat{j} + \bar{w} \hat{k}$

$$\bar{\nabla} = \frac{\partial}{\partial \bar{x}} \hat{i} + \frac{\partial}{\partial \bar{y}} \hat{j} + \frac{\partial}{\partial \bar{z}} \hat{k}$$

The general tangency condition (T.C.) requires no normal velocity at the wing surface for all time, i.e.

$$\frac{D\bar{s}}{D\bar{t}} = 0 \quad \text{at } \bar{s}(\bar{x}, \bar{y}, \bar{z}, \bar{t}) = 0 \quad \text{(3.2)}$$

where \bar{s} represents the general wing surface, i.e.

$$\bar{s} = \bar{y} - \epsilon \bar{\Delta}(\bar{x}, \bar{y}, \bar{z}, \bar{t}) = 0 \quad \text{(3.2a)}$$

$\bar{\Delta}$ being the amplitude perturbed surface and

$$\frac{D}{D\bar{t}} = \frac{\partial}{\partial \bar{t}} + \bar{\mathbf{V}} \cdot \bar{\nabla}, \quad \text{the substantial derivative.}$$

The shock condition (S.C.) requires the conservation of mass, momentum and energy across the shock wave, i.e. the Rankine-Hugoniot condition. Denoting $()_\infty$ as the flow quantities upstream of the

shock and $()_s$ as the flow quantities immediately downstream behind the shock, the conditions are

(continuity)

$$\left[\bar{\rho} \left(\frac{\partial \bar{G}}{\partial \bar{t}} + \vec{v} \cdot \bar{\nabla} \bar{G} \right) \right]_s = 0 \quad a$$

(normal momentum)

$$\left[\bar{\rho} \left(\frac{\partial \bar{G}}{\partial \bar{t}} + \vec{v} \cdot \bar{\nabla} \bar{G} \right)^2 + (\bar{\nabla} \bar{G})^2 \bar{p} \right]_s = 0 \quad b$$

(tangential momentums)

(3.3)

$$\left[\vec{v} \cdot \vec{\tau} \right]_s = 0 \quad c$$

$$\left[\vec{v} \cdot \vec{\delta} \right]_s = 0 \quad d$$

(energy)

$$\left[\frac{1}{2} \left(\frac{\partial \bar{G}}{\partial \bar{t}} + \vec{v} \cdot \bar{\nabla} \bar{G} \right)^2 + (\bar{\nabla} \bar{G})^2 \cdot \bar{h} \right]_s = 0 \quad e$$

where \bar{G} is the shock surface, given by

$$\bar{G} = \bar{G}_0(x, y) + \bar{f}_\delta(\bar{x}, \bar{z}) + \epsilon \cdot \bar{Q}(\bar{x}, \bar{z}, \bar{t}) = 0 \quad (3.4) \quad a$$

for the inner region

$$\bar{G} = \bar{G}_*(\bar{x}, \bar{y}, \bar{z}) + \epsilon \cdot \bar{Q}_*(\bar{x}, \bar{z}, \bar{t}) = 0 \quad (3.4) \quad b$$

for the outer region g

and $\bar{G}_0 = \bar{x} \tan \varphi_0 - \bar{y} = 0$

$$\bar{G}_* = (\bar{x} \cos \chi - \bar{z} \sin \chi) \tan \varphi_1 - \bar{y} = 0$$

\bar{f}_δ is the perturbed shock shape of the mean flow,

\bar{Q} and \bar{Q}_* are the amplitude perturbed shock shapes. Also, $\vec{\tau}$ and $\vec{\delta}$ represent the tangential vectors along the shock surface.

The slowly oscillatory motion of the wing ensures the shock attachment condition (S.A.C.) along the leading edges at all time, i.e.

$$\bar{Q}_* (\bar{x}, \bar{y}, \bar{z}, t) = \bar{\Delta} (\bar{x}, \bar{t}) \quad (3.5)^*$$

$$\text{at } \bar{z} = \bar{x} \cot \chi$$

Furthermore, the Mach cone condition (M.C.) is introduced so that the solution of the inner region can be matched toward that of the outer region. The condition simply ensures that all the flow velocities and properties remain the same on the interface of the Mach cone (eqn.(2.8)) i.e.

For the mean flow,

$$\left\{ \begin{array}{l} p_\delta = p_s \\ u_\delta = u_s \\ v_\delta = v_s \\ w_\delta = w_s \end{array} \right. \quad \text{at } M_s(\bar{x}, \bar{y}, \bar{z}) = 0 \quad (3.6)a$$

For the oscillatory flow,

$$\left\{ \begin{array}{l} \hat{p} = \left(\frac{\lambda p_*}{\gamma M_o^2 p_o} \right) \cdot p \\ \hat{u} = \left(\frac{u_*}{u_o} \right) \cdot u \\ \hat{v} = \left(\frac{u_*}{u_o} \right) \cdot v \\ \hat{w} = \left(\frac{u_*}{u_o} \right) \cdot w \\ \hat{r} = \left(\frac{\rho_* \lambda}{\rho_o M_o^2} \right) \cdot r \end{array} \right. \quad \text{at } M_s(\bar{x}, \bar{y}, \bar{z}) = 0 \quad (3.6)b$$

* For a flat surface delta wing here the relation is simply $\bar{Q}_* = \bar{\Delta} (\bar{x}, \bar{t})$

3.2 Perturbed equations

According to the perturbation schemes proposed in Sec. 2.2, the equations for the mean flow (of order δ) and for the oscillatory flow (of order ϵ), in the inner and the outer regions are linearized. For the oscillatory flow, the inner flow equations are approximate, accurate to $O(\delta\epsilon, \delta^2, \epsilon^2)^*$, the outer flow equations are accurate to $O(\epsilon^2)$ but otherwise exact, i.e. the effect due to sweepback angle χ is fully accounted for.

i) Mean-flow equations :

Making use of the inner non-dimensional coordinates in equation (2.9) and substituting the inner perturbation expression equation (2.12) into the governing equations (3.1), and collecting terms of like order of $O(\delta)$, yield the inner equations

$$\left. \begin{aligned}
 p_{\delta X} + v_{\delta Y} + w_{\delta Z} &= 0 & a \\
 \lambda u_{\delta X} + p_{\delta X} &= 0 & b \\
 v_{\delta X} + p_{\delta Y} &= 0 & c \\
 w_{\delta X} + p_{\delta Z} &= 0 & d \\
 p_{\delta X} - p_{\delta X} &= 0 & e
 \end{aligned} \right\} \quad (3.7)$$

Eliminating v_{δ} and w_{δ} from equations (3.7) a, c and d, a second order equation with one single variable p_{δ} results, i.e.

$$p_{\delta XX} - (p_{\delta YY} + p_{\delta ZZ}) = 0 \quad (3.8)$$

* By means of differentiation with respect to the mean-flow solution (Hui, Ref. 7) the in-phase flow solution is improved to include at least the terms of $O(\delta\epsilon)$ (See Chapter 4).

The uniform outer flow solutions (exact) are given previously in equations (2.5). The derivation and solution of the mean flow problem were given in Ref. 7 (Hui). Further application of the solution and extension of the formulation will be given later in the next chapter in achieving the more accurate in-phase solutions.

ii) Oscillatory flows.

Inner region :

Making use of the inner non-dimensional coordinates in equation (2.9) and substituting the inner perturbation expression equation (2.12) into the governing equations (3.1), dropping terms of order $O(\delta\epsilon)$, $O(\delta^2)$ and $O(\epsilon^2)$, and collecting terms of like order of $O(\epsilon)$, yield the following equations

$$\left. \begin{aligned} \kappa^2 (\hat{p}_T + \hat{p}_X) + \frac{1}{\lambda} \hat{u}_X + \hat{v}_Y + \hat{w}_Z &= 0 & a \\ \lambda (\hat{u}_T + \hat{u}_X) + \hat{p}_X &= 0 & b \\ \hat{v}_X + \hat{p}_Y &= 0 & c \\ \hat{w}_X + \hat{p}_Z &= 0 & d \\ \hat{r}_X - \hat{p}_X &= 0 & e \end{aligned} \right\} \quad (3.9)$$

where $\kappa = \frac{M_0}{\lambda}$

Eliminating \hat{u} , \hat{v} and \hat{w} from equations (3.9) a,b,c and d, a second order equation with one single variable \hat{p} results, i.e.

$$\hat{p}_{XX} - (\hat{p}_{YY} + \hat{p}_{ZZ}) + \kappa^2 (2 \hat{p}_{XT} + \hat{p}_{TT}) = 0 \quad (3.10)$$

Notice that equations (3.9) and (3.10) reduce to mean-flow equations (3.5) and (3.6) as $T \rightarrow \infty$

Outer region :

Making use of the outer non-dimensional coordinate equations (2.10)

and substituting the outer perturbation expressions equations (2.13) into the governing equations (3.1) and collecting terms of like order of $O(\epsilon)$ yield the following perturbed equations

$$\left. \begin{aligned}
 P_t + P_x + a P_z &= -\gamma (U_x + V_y + W_z) & a \\
 U_t + U_x + a U_z &= -\nu P_x & b \\
 V_t + V_x + a V_z &= -\nu P_y & c \\
 W_t + W_x + a W_z &= -\nu P_z & d \\
 \gamma (R_t + R_x + a R_z) &= P_t + P_x + a P_z & e
 \end{aligned} \right\} \quad (3.11)$$

where $a = w_*/u_*$

$$\nu = \frac{1}{\gamma M_*^2}$$

Eliminating U, V and W from equation (3.9) a, b, c and d results in a second order equation with one single variable P , i.e.

$$\begin{aligned}
 (M_*^2 - 1) P_{xx} - P_{yy} - P_{zz} + 2M_*^2 P_{xt} + M_*^2 P_{tt} \\
 + a \cdot \left[2M_*^2 (P_{xz} + P_{zt}) + a M_*^2 P_{zz} \right] = 0
 \end{aligned} \quad (3.12)$$

Notice that letting $w_* = 0$ and $M_* \rightarrow M_0$, (with changes in non-dimensional coordinates systems) reduces outer equations (3.11) and (3.12) to inner equations (3.7) and (3.8).

3.3 Perturbed boundary conditions

i) Perturbed tangency condition (T.C.)

For the mean flow,

$$v = 0 \quad \text{at } Y = 0 \quad (3.13)$$

For oscillatory flow let $\bar{\Delta}(\bar{x}, \bar{t})$ represent the flat delta wing surface in oscillatory motion, associated with ϵ , and let

$$\frac{\lambda \bar{\Delta}}{L} = \hat{\Delta}(X, T) \quad \text{and} \quad \frac{\Delta}{L} = \Delta(x, t), \quad \text{thus the tangency condition (3.2)}$$

can be written, to the order of $O(\epsilon)$, for the inner flow as

$$\hat{v} = \frac{\partial \hat{\Delta}}{\partial T} + \frac{\partial \hat{\Delta}}{\partial X} \quad \text{at} \quad Y = \epsilon \cdot \hat{\Delta}(X, T) \quad (3.14a)$$

and for the outer flow as

$$v = \frac{\partial \Delta}{\partial t} + \frac{\partial \Delta}{\partial x} \quad \text{at} \quad y = \epsilon \cdot \Delta(x, t) \quad (3.14b)$$

ii) Perturbed shock conditions (S.C.)

Inner region :

Substituting the perturbed shock surface equation (3.4a) into the shock condition equations (3.3) yield the following sets of perturbed conditions

To the order of $O(\delta)$, the shock conditions (S.C.) of the mean-flow read (see Hui, Ref. 7)

$$\left\{ \begin{array}{ll} p_{\delta} = C f_{\delta X}(X, Z) & \text{a} \\ u_{\delta} = E f_{\delta X}(X, Z) & \text{b} \\ v_{\delta} = A f_{\delta X}(X, Z) \quad \text{at} \quad Y = HX & \text{c} \\ w_{\delta} = K f_{\delta Z}(X, Z) & \text{d} \\ \rho_{\delta} = G f_{\delta X}(X, Z) & \text{e} \end{array} \right. \quad (3.15)$$

where

$$f_{\delta} = \frac{\lambda \bar{f}_{\delta}}{L}$$

$$H = \lambda \tan \varphi_0$$

and the coefficients A, C, E, K and G are functions of given M_{∞} and α_0

defined in equation (3.17) .

To the order of $O(\epsilon)$, the shock conditions (S.C.) of the oscillatory flow reads

$$\left\{ \begin{array}{l} \hat{P} = C\hat{Q}_X (X,Z,T) + D\hat{Q}_T (X,Z,T) \quad a \\ \hat{U} = E\hat{Q}_X (X,Z,T) + F\hat{Q}_T (X,Z,T) \quad b \\ \hat{V} = A\hat{Q}_X (X,Z,T) + B\hat{Q}_T (X,Z,T) \quad \text{at } Y = HX \quad (3.16) \quad c \\ \hat{W} = K\hat{Q}_Z (X,Z,T) \quad d \\ \hat{R} = G\hat{Q}_X (X,Z,T) + J\hat{Q}_T (X,Z,T) \quad e \end{array} \right.$$

where

$$\hat{Q} = \hat{Q}(X,Z,T) = \frac{\lambda \bar{Q}(\bar{X}, \bar{Z}, \bar{Y})}{L}$$

and the coefficients are defined as

$$\left\{ \begin{array}{l} A = \left(1 - \frac{\rho_\infty}{\rho_0}\right) \cos^4 \varphi_0 \left[1 + \frac{\rho_0}{\rho_\infty} H^2 - \gamma \tilde{w} \left(\frac{\rho_0}{\rho_\infty} - 1\right) \right] / (1 - \tilde{w}) \lambda \\ B = \left(1 - \frac{\rho_\infty}{\rho_0}\right) \cos^2 \varphi_0 \left[1 + \left(\frac{\rho_0}{\rho_\infty}\right) \tilde{w} - \gamma \tilde{w} \left(\frac{\rho_0}{\rho_\infty} - 1\right) \right] / (1 - \tilde{w}) \lambda \\ C = 2\kappa H \left(1 - \frac{\rho_\infty}{\rho_0}\right) \cos^4 \varphi_0 \left[1 - \frac{\gamma-1}{2} \tilde{w} \left(\frac{\rho_0}{\rho_\infty} - 1\right) \right] / M_0 (1 - \tilde{w}) \\ D = C / \cos^2 \varphi_0 \\ E = (A - B) \cot \varphi_0 \quad (3.17) \\ F = -B \tan \varphi_0 \\ G = \kappa H \left(1 - \frac{\rho_\infty}{\rho_0}\right) \cos^4 \varphi_0 \left[(\gamma + 1) - (\gamma - 1) \frac{\rho_0}{\rho_\infty} \right] / M_0 (1 - \tilde{w}) \\ J = G / \cos^2 \varphi_0 \\ K = -\sin \varphi_0 \cos \varphi_0 \left(\frac{\rho_0}{\rho_\infty} - 1\right) \end{array} \right.$$

and

$$\tilde{w} = M_0^2 \sin^2 \varphi_0$$

Outer region :

Substituting equations (2.13) and (3.4b) into S.C. (3.3) and collecting the lowest order terms (i.e. $O(1)$) results in the exact outer flow solutions of the mean-flow problem, i.e.

$$\frac{\rho_{\infty} U_{\infty}}{\rho_* u_*} = \frac{\cos \chi - a \sin \chi}{\cos \alpha_0 \cos \chi + \sin \alpha_0 \cot \varphi_1} \quad a$$

$$\frac{p_{\infty} - p_*}{\rho_* u_*^2} = \sin^2 \varphi_1 (\cos \chi - a \sin \chi)^2 \cdot \left\{ 1 - \left(\frac{U_{\infty}}{u_*} \right) \left[\frac{\cos \alpha_0 \cos \chi + \sin \alpha_0 \cot \varphi_1}{\cos \chi - a \sin \chi} \right] \right\} \quad b$$

$$\frac{h_{\infty} - h_*}{(u_*^2/2)} = \sin^2 \varphi_1 \left\{ (\cos \chi - a \sin \chi) - \left(\frac{U_{\infty}}{u_*} \right)^2 (\cos \alpha_0 \cos \chi + \sin \alpha_0 \cot \varphi_1)^2 \right\} \quad e$$

$$\frac{u_*}{U_{\infty}} = \cos \alpha_0 - \sin \alpha_0 \tan \varphi_1 \cos \chi \quad c$$

$$\begin{aligned} \frac{u_*}{U_{\infty}} &= \tan^2 \varphi_1 \cos \chi \sin \chi + (1 + \tan^2 \varphi_1 \cos^2 \chi) \left(\frac{w_*}{U_{\infty}} \right) \quad d \\ &= \tan \varphi_1 \sin \chi (\tan \varphi_1 \cos \alpha_0 \cos \chi + \sin \alpha_0) \end{aligned}$$

(3.18)

Note that solving these relations gives exactly the same solutions for u_* , v_* , w_* , θ_* and p_* as previously obtained in equations (2.5). Moreover, as $\chi \rightarrow 0$, the above relations reduce identically to those of the two-dimensional oblique shock relations. Hence, it is stated here that equations (3.18) derived are generalizations of the wedge oblique shock relations (due to the steady mean flow) - called the skewed wedge oblique shock relations.

Next, substituting equation (3.4b) into equation (3.3) and collecting terms of like order of $O(\epsilon)$ yield the perturbed S.C. of the oscillatory flow (see Appendix C), which in turn provide the S.C. in the following form :

$$\left\{ \begin{array}{l} P = \tilde{C}_1 Q_x + \tilde{C}_2 Q_z + \tilde{D} Q_t \\ U = \tilde{E}_1 Q_x + \tilde{E}_2 Q_z + \tilde{F} Q_t \\ V = \tilde{A}_1 Q_x + \tilde{A}_2 Q_z + \tilde{B} Q_t \\ W = \tilde{K}_1 Q_x + \tilde{K}_2 Q_z + \tilde{L} Q_t \\ R = \tilde{G}_1 Q_x + \tilde{G}_2 Q_z + \tilde{J} Q_t \end{array} \right. \quad \text{at } y = (t_c)x - (t_s)z \quad (3.19)$$

where

$$\left\{ \begin{array}{l} t_c = \tan \varphi_1 \cos \chi \\ t_s = \tan \varphi_1 \sin \chi \\ Q = Q(x, z, t) = \frac{\bar{Q}(\bar{x}, \bar{z}, \bar{t})}{L} \end{array} \right.$$

and the coefficients $\tilde{A}_1, \tilde{A}_2, \tilde{B} \dots$ etc. are functions of given M_∞, α_0 and χ , defined as :-

$$\begin{aligned}
\tilde{A}_1 &= \frac{t_x - t_1 \cdot \tilde{E}_1}{t_2} \\
\tilde{A}_2 &= -\frac{t_1}{t_2} \tilde{E}_2 \\
\tilde{B} &= -\frac{t_1}{t_2} \tilde{F} \\
\tilde{C}_1 &= \frac{e_x - e_5 \tilde{G}_1 - m_x}{e_4} \\
\tilde{C}_2 &= \frac{e_z - e_5 \tilde{G}_2 - m_z}{e_4} \\
\tilde{D} &= \frac{e_t - e_5 \tilde{J} - m_t}{e_4} \\
\tilde{E}_1 &= \frac{s_3 (t_2 m_x - c_2 t_x) + c_3 (s_2 t_x - t_2 s_x)}{e_6} \\
\tilde{E}_2 &= \frac{s_3 t_2 m_z - t_2 s_z c_3}{e_6} \\
\tilde{F} &= \frac{m_t t_2 s_3}{e_6} \\
\tilde{G}_1 &= \frac{e_4 (c_x - d_x) - d_4 (c_x - e_x)}{g_6} \\
\tilde{G}_2 &= \frac{e_4 (c_z - d_z) - d_4 (c_z - e_z)}{g_6} \\
\tilde{J} &= \frac{e_4 c_t - d_4 (c_t - e_t)}{g_6} \\
\tilde{K}_1 &= \frac{s_x - s_1 \tilde{E}_1 - s_2 \tilde{A}_1}{s_3} \\
\tilde{K}_2 &= \frac{s_z - s_1 \tilde{E}_2 - s_2 \tilde{A}_2}{s_3} \\
\tilde{L} &= -\frac{s_1 \tilde{F} + s_2 \tilde{B}}{s_3}
\end{aligned} \tag{3.20}$$

where

$$\left\{ \begin{aligned}
 c_1 &= \tan \varphi_1 \cos \chi \\
 c_2 &= -1 \\
 c_3 &= -\tan \varphi_1 \sin \chi \\
 c_5 &= \tan \varphi_1 (\cos \chi - a \sin \chi) \\
 d_4 &= \frac{\nu}{2} \cdot \frac{1}{\sin \varphi_1 \cos \varphi_1 (\cos \chi - a \sin \chi)} \\
 d_5 &= \frac{1}{2} c_5 \\
 e_4 &= \frac{1}{(\gamma - 1) M_*^2 \sin \varphi_1 \cos \varphi_1} \cdot \frac{1}{(\cos \chi - a \sin \chi)} \\
 e_5 &= -e_4 \\
 e_6 &= s_3 (t_2 c_1 - t_1 c_2) + c_3 (s_2 t_1 - s_1 t_2) \\
 g_6 &= (c_5 - d_5) e_4 - (c_5 - e_5) d_4 \\
 t_1 &= 1 \\
 t_2 &= c_1 \\
 s_1 &= -c_1 c_3 \\
 s_2 &= c_3 \\
 s_3 &= 1 + \tan^2 \varphi_1 \cos^2 \chi
 \end{aligned} \right. \quad (3.21) \text{ a}$$

and

$$\left\{ \begin{aligned}
 c_t &= \frac{\rho_\infty}{\rho_*} - 1 \\
 c_x &= \frac{\rho_\infty U_\infty}{\rho_* u_*} \cos \alpha_0 - 1 \\
 c_z &= -a
 \end{aligned} \right. \quad (3.21) \text{ b}$$

continued ...

$$d_x = \left\{ (\cos \chi - a \sin \chi) \left[\left(\frac{U_\infty}{u_*} \right) \cos \alpha_0 - 1 \right] + \left(\frac{p_\infty - p_*}{\rho_* u_*^2} \right) \cos \chi \right\} / (\cos \chi - a \sin \chi)$$

$$d_z = - \left\{ \left(\frac{p_\infty - p_*}{\rho_* u_*^2} \right) \sin \chi + a (\cos \chi - a \sin \chi) \right\} / (\cos \chi - a \sin \chi)$$

$$e_x = \frac{1}{\cos \chi - a \sin \chi} \cdot \left[\left(\frac{U_\infty}{u_*} \right)^2 (\cos \alpha_0 \cos \chi + \sin \alpha_0 \cot \varphi_1) \cos \alpha_0 + 2 \left(\frac{h_\infty - h_*}{u_*^2} \right) \cdot \cos \chi \right] - 1$$

$$e_z = - \left\{ \frac{1}{\cos \chi - a \sin \chi} \cdot 2 \left(\frac{h_\infty - h_*}{u_*^2} \right) \sin \chi + a \right\}$$

$$e_t = \frac{1}{\cos \chi - a \sin \chi} \cdot \left[\left(\frac{U_\infty}{u_*} \right) (\cos \alpha_0 \cos \chi + \sin \alpha_0 \cot \varphi_1) - 1 \right]$$

$$t_x = - \left(\frac{U_\infty}{u_*} \right) \sin \alpha_0 \quad \begin{aligned} m_t &= c_t - c_5 \tilde{J} \\ m_x &= c_x - c_5 \tilde{G}_1 \\ m_z &= c_z - c_5 \tilde{G}_2 \end{aligned} \quad (3.21)b$$

$$s_x = - \left\{ \left[1 - \left(\frac{U_\infty}{u_*} \right) \cos \alpha_0 \right] \tan \varphi_1 \sin \chi + 2a \tan \varphi_1 \cos \chi \right\}$$

$$s_z = \left[1 - \frac{U_\infty}{u_*} \cos \alpha_0 \right] \tan \varphi_1 \cos \chi - \left(\frac{U_\infty}{u_*} \right) \sin \alpha_0$$

Equations (3.19) are the generalized perturbed skewed wing shock conditions which contain previous 2D perturbed wedge shock conditions (3.16) and (3.17) as its special case. That is to say, letting $\chi \rightarrow 0$ gives

$$\tilde{C}_2 = \tilde{E}_2 = \tilde{A}_2 = \tilde{K}_2 = \tilde{G}_2 = \tilde{L} = 0$$

and reduces

$$\begin{aligned} \tilde{A}_1 &= \lambda A; & \tilde{B} &= \lambda B; & \tilde{C}_1 &= \gamma M_0^2 C; \\ \tilde{D} &= \gamma M_0^2 D; & \tilde{E}_1 &= \lambda E; & \tilde{F} &= \lambda F; \end{aligned} \quad (3.22)$$

$$\tilde{G}_1 = M_0^2 F; \quad \tilde{J} = M_0^2 J \quad \text{and} \quad \tilde{K}_1 = K$$

(see Appendix I)

iii) Perturbed Mach cone conditions (M.C.)

The inner region is based on the wedge perturbation scheme (equation 2.12). Hence, the exact Mach cone surface (equation 2.8) is now replaced by a two-dimensional Mach cone in order to be consistent with the perturbation scheme. This Mach cone is obtained simply by taking the limit $\chi \rightarrow 0$, and $M_* = M_0$, thus equation (2.8) becomes (see Fig. 1-B),

$$y^2 + z^2 = x^2 \quad (3.23)$$

Thus, at constant x , the exact Mach cone (equation 2.8) is of elliptical cross section and it is now a circular cross-section for the 2-D Mach cone.

For steady mean flow, the M.C. of equation (3.6)a reduces to

$$\left\{ \begin{array}{l} p_\delta = p_s' = 0 \\ v_\delta = v_s' = 0 \\ w_\delta = w_s' = \chi \frac{\sin \varphi_0}{\cos \beta_0} \sin \alpha_0 \end{array} \right. \quad \text{at } y^2 + z^2 = x^2 \quad (3.24)a$$

For detailed derivations, one is referred to Hui (equations (6) and (8) of Ref. 7).

For oscillatory flow let P' , U' , V' , W' and R' be the perturbed solutions obtained from the outer region (Problems A and C), the perturbed Mach cone conditions can be expressed as

$$\begin{aligned}\hat{P} &= \left(\frac{\lambda P_*}{\gamma M_o^2 P_o} \right) P' \\ \hat{U} &= \left(\frac{U_*}{U_o} \right) U' \\ \hat{V} &= \left(\frac{U_*}{U_o} \right) V' \quad \text{at } Y^2 + Z^2 = X^2 \quad (3.24) \text{ b} \\ \hat{W} &= \left(\frac{U_*}{U_o} \right) W' \\ \hat{R} &= \left(\frac{\rho_* \lambda}{\rho_o M_o^2} \right) R'\end{aligned}$$

These ()' solutions need not be determined as they will be replaced by their exact expressions P, U, V, W , and R at a later stage (see chapter 6).

iv) Perturbed shock-attachment condition :

The non-dimensional perturbed S.A.C. is simply

$$Q_* = \Delta(x, t) \quad \text{at } z = x \cot \chi \quad (3.25)$$

3.4 Full formulation of the mean-flow problem and problems A, B, C and D

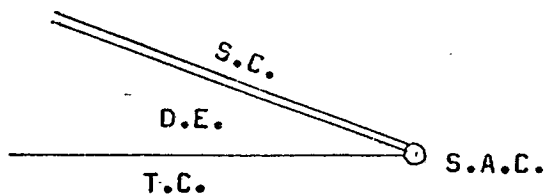
Now, if it is further assumed that the oscillatory motion is of simple harmonic type, the following time dependent function can be written as :-

$$\left\{ \begin{array}{l} \hat{\Delta}(X,T) = (X - X_0) e^{ik_0 T} \\ Q_0(X,T) = Q^{(0)}(X) + ik_0 Q^{(1)}(X) e^{ik_0 T} \end{array} \right. \quad (3.26) \text{ a}$$

$$\left\{ \begin{array}{l} \Delta(x,t) = (x - x_0) e^{ik_* t} \\ Q_*(x,z,t) = Q^0(x,z) + ik_* Q^1(x,z) e^{ik_* t} \end{array} \right. \quad (3.26) \text{ b}$$

Thus, substituting equations (2.14) and (3.26)a into equations (3.9), (3.10) (3.14)a, (3.16) and (3.24), and collecting terms of the like order of $O(\epsilon)$ and $O(\epsilon k_0)$ yield the problems of the inner region, namely Problem B and Problem D. Similarly, substituting equations (2.15) and (3.26)b into equations (3.11), (3.12), (3.14)b, (3.19) and (3.25), and collecting terms of the like order of $O(\epsilon)$ and $O(\epsilon k_*)$ yield the problems of the outer region, namely Problem A and Problem C. For the convenience of later analyses, the full formulation of Problems A, B, C and D are presented separately in the following pages.

PROBLEM A



D.E.

$$(M_*^2 - 1) p_{xx}^0 - p_{yy}^0 - p_{zz}^0 + a \cdot (2M_*^2 p_{xz}^0 + aM_*^2 p_{zz}^0) = 0$$

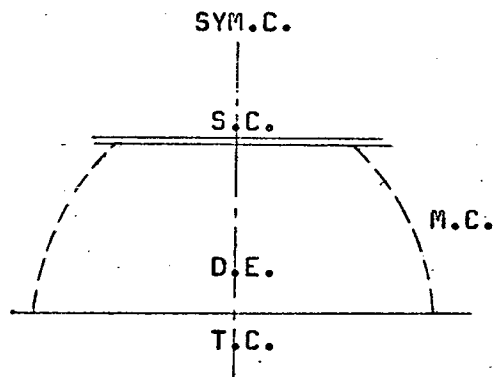
$$\left\{ \begin{array}{l} p_x^0 + a p_z^0 = -\gamma (U_x^0 + V_y^0 + W_z^0) \\ U_x^0 + a U_z^0 = -\nu p_x^0 \\ V_x^0 + a V_z^0 = -\nu p_y^0 \\ W_x^0 + a W_z^0 = -\nu p_z^0 \end{array} \right.$$

T.C. $V^0 = 1$ at $y = 0$ (3.27)

S.C.
$$\left\{ \begin{array}{l} p^0 = \tilde{C}_1 Q_x^0 + \tilde{C}_2 Q_z^0 \\ U^0 = \tilde{E}_1 Q_x^0 + \tilde{E}_2 Q_z^0 \\ V^0 = \tilde{A}_1 Q_x^0 + \tilde{A}_2 Q_z^0 \\ W^0 = \tilde{K}_1 Q_x^0 + \tilde{K}_2 Q_z^0 \end{array} \right.$$
 at $y = (\tan \varphi_1 \cos \chi) \cdot x - (\tan \varphi_1 \sin \chi) \cdot z$

S.A.C. $Q^0 = x - x_0$ at $z = x \cot \chi$

PROBLEM B



D.E.
$$p_{XX}^{(o)} - p_{YY}^{(o)} - p_{ZZ}^{(o)} = 0$$

$$\left\{ \begin{aligned} p_X^{(o)} + v_Y^{(o)} + w_Z^{(o)} &= 0 \\ v_X^{(o)} + p_Y^{(o)} &= 0 \\ w_X^{(o)} + p_Z^{(o)} &= 0 \end{aligned} \right.$$

T.C.
$$v^{(o)} = 1 \quad \text{at } Y = 0$$

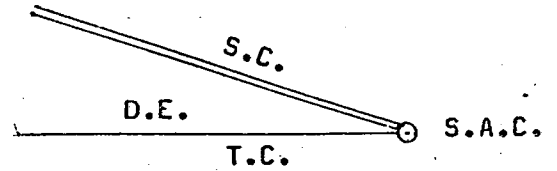
S.C.
$$\left\{ \begin{aligned} p^{(o)} &= cQ_X^{(o)}(X,Z) \\ v^{(o)} &= aQ_X^{(o)}(X,Z) \\ w^{(o)} &= kQ_Z^{(o)}(X,Z) \end{aligned} \right. \quad \text{at } Y = HX \quad (3.28)$$

M.C.
$$\left\{ \begin{aligned} p^{(o)} &= p_*^{(o)} \\ v^{(o)} &= v_*^{(o)} \\ w^{(o)} &= w_*^{(o)} \end{aligned} \right. \quad \text{at } Y^2 + Z^2 = X^2$$

SYM.C.
$$p_Z^{(o)} = 0 \quad \text{at } Z = 0$$

Note that here $p_*^{(o)}$, $v_*^{(o)}$ and $w_*^{(o)}$ are given by the exact values of the exact solution of Problem A, through the matching procedure discussed later in chapter 6.

PROBLEM C



D.E.

$$(M_*^2 - 1)p_{xx}^1 - p_{yy}^1 - p_{zz}^1 + a M_*^2 (2 p_{xz}^1 + a p_{zz}^1) = -2 M_*^2 (p_x^0 + a p_z^0)$$

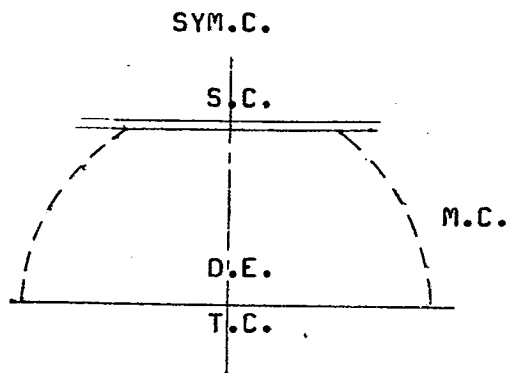
$$\left\{ \begin{array}{l} p_x^1 + a p_z^1 + \gamma (U_x^1 + V_y^1 + W_z^1) = -p^0 \\ U_x^1 + a U_z^1 + \gamma p_x^1 = -U^0 \\ V_x^1 + a V_z^1 + \gamma p_y^1 = -V^0 \\ W_x^1 + a W_z^1 + \gamma p_z^1 = -W^0 \end{array} \right.$$

T.C. $V^1 = x - x_0$ at $y = 0$ (3.29)

S.C. $\left\{ \begin{array}{l} p^1 = \tilde{C}_1 Q_x^1 + \tilde{C}_2 Q_z^1 + \tilde{D} Q^0 \\ U^1 = \tilde{E}_1 Q_x^1 + \tilde{E}_2 Q_z^1 + \tilde{F} Q^0 \\ V^1 = \tilde{A}_1 Q_x^1 + \tilde{A}_2 Q_z^1 + \tilde{B} Q^0 \\ W^1 = \tilde{K}_1 Q_x^1 + \tilde{K}_2 Q_z^1 + \tilde{L} Q^0 \end{array} \right.$ at $y = (\tan \varphi_1 \cos \chi) x - (\tan \varphi_1 \sin \chi) z$

S.A.C. $Q^1 = 0$ at $z = x \cot \chi$

PROBLEM D



D.E.
$$P_{XX}^{(1)} - P_{YY}^{(1)} - P_{ZZ}^{(1)} = -2\kappa^2 P_X^{(0)}$$

$$\left\{ \begin{aligned} P_X^{(1)} + V_Y^{(1)} + W_Z^{(1)} &= -\kappa^2 P^{(0)} + \frac{1}{\lambda} U^{(0)} \\ V_X^{(1)} + P_Z^{(1)} &= -V^{(0)} \\ W_X^{(1)} + P_Z^{(1)} &= -W^{(0)} \end{aligned} \right.$$

T.C.
$$V^{(1)} = X - X_0 \quad \text{at } Y = 0$$

(3.30)

S.C.
$$\left\{ \begin{aligned} P^{(1)} &= CQ_X^{(1)}(X,Z) + DQ^{(0)}(X,Z) \\ V^{(1)} &= AQ_X^{(1)}(X,Z) + BQ^{(0)}(X,Z) \quad \text{at } Y = HX \\ W^{(1)} &= KQ_Z^{(1)}(X,Z) \end{aligned} \right.$$

M.C.
$$\left\{ \begin{aligned} P^{(1)} &= P_*^{(1)} \\ V^{(1)} &= V_*^{(1)} \\ W^{(1)} &= W_*^{(1)} \end{aligned} \right. \quad \text{at } Y^2 + Z^2 = X^2$$

SMY.C.
$$P_Z^{(1)} = 0 \quad \text{at } Z = 0$$

Again, $P_*^{(1)}$, $V_*^{(1)}$, $W_*^{(1)}$ are given by the exact solutions of given Problem C. These values will be/in the later matching scheme.

Form the foregoing formulation of these problems, it is clear that the solving procedure must be carried out in a particular sequence. Problem A will be first solved. Then Problem B can be solved as its boundary condition is given at M.C. from Problem A. Next, Problem C is solved by knowing all the inhomogeneous terms provided by Problem A. Finally, Problem D, whose solution depends on knowing all the solutions given by Problems A, B and C, can then be completely solved.

Furthermore, it is understood now that Problems A and C are exact (WRT δ) but Problems B and D are approximate in which the effect of δ only enters through M.C. from the exact solutions of A and C (i.e. through the Z-dependence). Thus, for cases close to the shock detachment region (see Figs. 2 and 3) where the inner region dominates the planform area, the approximate scheme of Problems B and D may introduce inaccurate results. In order to improve the approximate scheme for Problem B, it is found possible to make use of Hui's mean flow solution by differentiating it with respect to α_0 . Hence the improved problem B can fully include terms of order $O(\delta\epsilon)$. However, unless a pulsating mean flow solution is found or before other improved schemes can be achieved, the solution of Problem D will remain as an approximate one.*

In the next Chapter, the exact differentiation method for the improved Problems A and B will be presented. Expressions for force, moments and stability derivatives for steady mean flow and in-phase flow will be given. In Chapter 5 a generalized similarity rule will be derived. The solutions of Problems A, B, C and D formulated based on the so-called 'perturbation method' will be given in Chapter 6, so that the damping derivatives can be presented last (Chapter 7).

* See Appendix H for an improved scheme.

4. FORCES AND MOMENTS OF STEADY MEAN FLOW AND IN-PHASE FLOW

The conventional way to obtain in-phase lift and moment has been to perturb the steady mean flow solution, as presented in Sec. 3.3,

e.g.

$$\bar{p} = p_o \left[1 + \frac{\gamma M_o^2}{\lambda} (p_\delta + \epsilon p^{(o)}) \right]$$

Once $p^{(o)}$ is obtained from the formulation, Problem B say, one then can integrate $p^{(o)}$ over the platform to get the lift and moment coefficients, C_L and C_M say. As $p^{(o)}$ is a perturbed solution, this method is termed the 'perturbation method' from now on. To determine stability derivatives at zero mean incidence, the perturbation method appears to be the only practical way and has been widely used for wings and bodies. As in the linearized potential flow problems, for example, the steady mean flow is represented by source distribution and in-phase (or oscillatory) flow by doublet distributions. However, the determination of the source strength is quite different from that of the doublet strength (e.g. see Adam Sears, Ref. 15). Hence, to relate the mean-flow solution to the in-phase solution is by no means obvious in the source methods of the potential flow theories.

Unlike the 'source doublet' method, the present approach to the delta wing problem provides a simple means of obtaining the in-phase-flow when the mean flow solution is known. Since the mean-flow solution p_Δ , say, given by Hui (Ref. 7), generally contains α_o as a parameter the associated in-phase flow solution is simply its derivative $\partial p_\Delta / \partial \alpha_o$. This procedure is then termed exact differentiation method. Thus, integrating p_Δ results in C_L and differentiating C_L with respect to α results in C_{L_α} , the in-phase lift coefficient (or the lift slope).

To begin with, it is required to revisit Hui's theories (Refs. 7 and 46) for the steady mean flow solutions.

4.1 The mean-flow : Hui's solutions

Introducing the conical coordinate

$$\begin{cases} \eta = \frac{Y}{X} \\ \zeta = \frac{Z}{X} \end{cases}$$

and writing the shock shape (equation 3.4a) in the form

$$\eta = H + F(\zeta)$$

where $F(\zeta) = \frac{f_\zeta}{X}$, the mean-flow is formulated as below :

i) Linear solutions : $O(\delta)$

Inner region

$$\text{D.E.} \quad (\eta^2 - 1) P_{\delta \eta \eta} + 2\eta P_{\delta \eta \zeta} + (\zeta^2 - 1) P_{\delta \zeta \zeta} + 2\eta P_{\delta \eta} + 2\zeta P_{\delta \zeta} = 0$$

$$\text{T.C.} \quad P_{\delta \eta} = 0 \quad \text{at} \quad \eta = 0$$

$$\text{S.C.} \quad H'^2 \zeta P_{\delta \eta} + [HB_0 - (A_0 + H)\zeta^2] P_{\delta \zeta} = 0 \quad \text{at} \quad \eta = H$$

$$\text{M.C.} \quad P_{\delta} = 0 \quad \text{at} \quad \eta^2 + \zeta^2 = 1$$

$$\text{SYM.C.} \quad P_{\delta \zeta} = 0 \quad \text{at} \quad \zeta = 0$$

$$\text{E.C.} \quad \int_0^{H'} \frac{dP_{\delta}}{\zeta} = \frac{w'_s}{B_0} \quad \text{at} \quad \eta = H$$

(4.1)

where

$$A_0 = \frac{A}{C}$$

$$B_0 = -\frac{K}{C}$$

$$H' = \sqrt{1 - H^2}$$

and

$$w_s' = \chi \cdot \frac{\sin \varphi_0}{\cos \beta_0} \cdot \sin \alpha_0^*$$

The details of the formulation and method of solution are given by Hui (Ref. 7). Hui's solution on the wing surface thus reads

$$P_\zeta(0, \zeta) = \sum_{n=1}^{\infty} a_n' \cos \left[(2n-1) \sin^{-1} \zeta \right] \quad (4.2)$$

($|\zeta| \leq 1$)

where

$$a_n' = \frac{a_1' b_n}{(2n-1) \cosh(2n-1) \sigma_0}$$

$$b_1 = \frac{1}{H'}$$

$$b_2 (A_0 + \hat{c}_2) - b_1 (A_0 + \hat{c}_1 - 2D_0) = 0 \quad (4.2) \text{ a}$$

$$b_K (A_0 + \hat{c}_K) + 2D_0 b_{K-1} + b_{K-2} (A_0 - \hat{c}_{K-2}) = 0$$

$$(K = 3, 4, 5 \dots)$$

$$\hat{c}_K = \tanh(2K-1) \sigma_0$$

$$\sigma_0 = \tanh^{-1} H$$

$$a_1' = -\frac{2w_s' H'}{\pi B_0 \sum_{n=1}^{\infty} b_n} \quad (4.2) \text{ b}$$

* From the linear χ expansion of w_s , also $w_s' = -K \tan \varphi_0 \cdot \chi$

On the other hand, if one defines the half-range spanwise pressure integral, following Hui (Ref. 46)*

$$P_G(\eta) = \int_0^{\sqrt{1-\eta^2}} P_\delta(\eta, \zeta) d\zeta \quad (4.3)$$

An ordinary differential equation (O.D.E.) based on the integral formulation can be derived resulting in a global formulation of the problem. The 'spanwise-integral' solution was found in a simple form, on the wing surface (For details, see Ref. 45 and 46, or see Chapter 5 and Appendix E)

$$P_G(0) = - \frac{H w_s'}{A_0 + H} \quad (4.4)$$

Clearly, integration of $P_\delta(0, \zeta)$ (equation 4.2) along the span results in $P_G(0)$ (equation 4.4). Thus, for convenience, the former solution is called the 'local' solution, the latter is called the 'global' solution.

In the outer region, the exact pressure and velocities are consistently expanded to the order of $O(\delta)$, or χ .

Thus,

$$\begin{aligned} p_s' &= 0 \\ v_s' &= 0 \\ w_s' &= \chi \cdot \frac{\sin \varphi_0}{\cos \beta_0} \sin \alpha_0 \end{aligned} \quad (4.5)$$

The full expression of the pressure solutions with regard to the present formulation of $O(\delta)$ is precisely equation (4.2) and equation (4.4), called the 'local-linear' solution (LL) and the 'global-linear' solution

* For detailed derivation and discussion on the method of spanwise integration see Sec. 5.2, Appendix E and Sec. 8.3

(GL), respectively.

ii) Improved solutions :

Knowing the exact uniform flow in the outer region (equation (2.6)), one can then match the inner linear solution (equation 4.2) towards the exact pressure (equation (2.6.d) by the method of strained coordinates, i.e. following Hui's procedure,

$$\tilde{p}_\delta(0, \zeta) = p_s + \frac{p_c - p_s}{p_c} \sum_{n=1}^{\infty} a_n' \cos \left[(2n-1) \sin \frac{\zeta}{\zeta_*} \right] \quad (0 \leq \zeta \leq \zeta_d) \quad (4.6)$$

where $p_c = \sum_{n=1}^{\infty} a_n'$, representing the perturbed pressure along the root chord

$\zeta_d = \lambda \cot \chi$, 'conical' distance from root chord to the leading edge

and $\zeta_* = \lambda \left(\frac{\lambda_* \sin \theta + \cos \theta}{\lambda_* \cos \theta - \sin \theta} \right)$, the intersecting point of

3-D Mach cone surface and the wing surface, resulting from equation (2.8)

$$\lambda_* = \sqrt{M_*^2 - 1}$$

Solution (4.6), \tilde{p}_δ is called the 'local-stretched' solution (LS). An example of $M_\infty = 4.0$, $\alpha_0 = 15^\circ$ and $\chi = 50^\circ$ is plotted in Fig. 6 which exhibits excellent comparison with other numerical solutions (Refs. 4, 5 and 6).

The 'global-linear' solution (equation 4.4) can also be sketched in a slightly different manner. To stretch the inner flow,

$$\tilde{P}_G(o) = P_G(o) \cdot \zeta_*$$

whereas the outer flow is exact again

$$\tilde{P}_S(o) = \int_{\zeta_*}^{\zeta_d} P_S d\zeta = P_S (\zeta_d - \zeta_*)$$

Hence, the 'global-stretched' solution is defined as the addition of these two parts

$$\begin{aligned} \tilde{P}_{GS}(o) &= \tilde{P}_G(o) + \tilde{P}_S(o) - \\ &= -\left(\frac{w'_s H}{A_o + H}\right) + P_S (\zeta_d - \zeta_*) \end{aligned} \quad (4.7)$$

Integrating the 'local-stretched' solution throughout the span gives the 'local-stretched' spanwise pressure integral (see equation 4.3) in the form

$$\begin{aligned} \tilde{P}_{LS}(o) &= \int_0^{\zeta_d} \tilde{P}_\delta(o, \zeta) d\zeta \\ &= P_S \lambda \cot \chi + \left(1 - \frac{P_S}{P_C}\right) \cdot \frac{\pi \zeta_*}{4} \cdot a_1' \end{aligned} \quad (4.8)$$

The following observations are made :-

(a) The 'global-linear' solution $\tilde{P}_G(o)$ is exactly the same as the 'local-linear' spanwise pressure $\tilde{P}_L(o) = \int_0^1 P_\delta(o, \zeta) d\zeta$.

Hence, a convenient form is provided for a_1' , i.e.

$$a_1' = -\frac{4}{\pi} \cdot \left(\frac{Hw'_s}{A_o + H}\right) \quad (4.9)$$

and

$$\tilde{P}_L(o) = \frac{\pi}{4} \cdot a_1'$$

Note that the expression (4.2)b for a_1' is not closed, equation (4.9)

for a_1' here is an exact expression.

(b) The 'global-stretched' solution $\tilde{P}_{GS}(o)$, based on a novel idea, is different from the 'local-stretched' solution $\tilde{P}_{LS}(o)$. The latter solution is a more reliable one as it is based on a good 'local' solution (equation 4.6) (see Ref. 7).

As indicated by numerical studies on $P_c = \sum_{n=1}^N a_n'$, Hui (Ref. 7) found that a_1' converges very rapidly. With the approximation $P_c \approx a_1'$ the difference between \tilde{P}_{GS} and \tilde{P}_{LS} can be roughly estimated as

$$\tilde{P}_{GS} - \tilde{P}_{LS} = \zeta_* P_s \left(1 - \frac{\pi}{4}\right)$$

For example, in the case of $M_\infty = 4.0$, $\alpha_0 = 15^\circ$, $\chi = 50^\circ$

$$a_1' = - .02435$$

$$a_2' = - .0007435$$

$$a_3' = - .00015 \dots$$

and $\sum_{n=1}^{20} a_n' = - .0249$

$$P_s = .01312$$

Thus

$$\tilde{P}_{GS} - \tilde{P}_{LS} = .0036$$

and if it is normalized by P_s ,

$$\frac{\tilde{P}_{GS} - \tilde{P}_{LS}}{P_s} \approx .27$$

This is an acceptable differential error, since they only produce .5% difference resulting in the normalized lift coefficients (C_L/C_{L0}),

(See Table 1, page 47).

(c) Numerically, all P_G , \tilde{P}_{GS} and \tilde{P}_{LS} are of very small order. For example, for given condition of $M_\infty = 4.0$, $\alpha_0 = 15^\circ$, $\chi = 50^\circ$

$$P_G(0) = - .018$$

$$\tilde{P}_{GS}(0) = - .0102$$

$$\tilde{P}_{LS}(0) = - .007 \quad (- .0066, \text{ for } p_c \approx a_1')$$

It will be shown later (Sec. 4.2) this substantiates the fact that 3-D effects are indeed small in lift contribution, as pointed out earlier by Babaev (Ref. 4). Moreover, it is seen that $\tilde{P}_{GS}(0)$ is closer to $\tilde{P}_{LS}(0)$, indeed an improvement on $P_G(0)$

(d) It is seen that the global formulation due to the method of spanwise integration (equation (4.3)) is indeed a much simpler one than the 'local' formulation (equation (4.1)). In fact, in Chapter 6, both the in-phase and the out-of-phase flow in the inner region are obtained by means of this method. Since the stretching scheme in global formulation is different from the 'local' one, care must be exercised in detecting their difference. Thus, equation (4.8) is presented to compare with equation (4.7). From the numerical example given in items (b) and (c) it partly justifies that the difference due to the 'global-stretched' solution and the 'local-stretched' solution may not be large for the cases of in-phase and the out-of-phase flow (Chapter 6).

4.2 Life and Moment coefficients : mean flow

The pressure coefficient is defined in the usual way

$$\bar{c}_p = \frac{2}{\gamma M_\infty^2} \left(\frac{\bar{p}}{p_\infty} - 1 \right) \quad (4.10)$$

where

$$\frac{\bar{p}}{P_\infty} = \frac{P_0}{P_\infty} \left[1 + \left(\frac{\gamma M_0^2}{\lambda} \right) P_\delta (0, \zeta) \right] - 1$$

Thus \bar{C}_p can be written in two terms

$$\bar{C}_p = C_{P_0} + C_{P_1}$$

$$\begin{cases} C_{P_0} = \frac{2}{\gamma M_\infty^2} \left(\frac{P_0}{P_\infty} - 1 \right) \\ C_{P_1} = \frac{2}{\gamma M_\infty^2} \cdot \left(\frac{P_0}{P_\infty} \right) \left(\frac{\gamma M_0^2}{\lambda} \right) P_\delta (0, \zeta) \end{cases} \quad (4.11)$$

where C_{P_0} is the 2-D pressure coefficient and C_{P_1} is the 3-D 'correction' pressure coefficient due to P_δ .

The Lift coefficient for the full wing is simply defined as

$$C_L = \frac{2 \cos \alpha_0}{S} \int_{\bar{x}=0}^{\bar{x}=L} \int_{\bar{z}=0}^{\bar{z}=\bar{x} \cot \chi} \bar{C}_p \, d\bar{x} \, d\bar{z} \quad (4.12)$$

where S is the wing platform area, $S = L^2 \cot \chi$

The moment coefficient is then defined as

$$C_M = \frac{2}{S \cdot L} \int_{\bar{x}=0}^{\bar{x}=L} \int_{\bar{z}=0}^{\bar{z}=\bar{x} \cot \chi} \bar{C}_p \cdot (\bar{x} - \bar{x}_0) \cdot d\bar{x} \, d\bar{z} \quad (4.13)$$

Equation (4.12) can be written in two terms in the same manner as the pressure coefficient, i.e.

$$C_L = C_{L_0} + C_{L_1} \quad (4.14)$$

$$\left\{ \begin{array}{l} C_{L_0} = C_{p_0} \cdot \cos \alpha_0 \end{array} \right. \quad (4.14) \text{ a}$$

$$\left\{ \begin{array}{l} C_{L_1} = \frac{\cos \alpha_0}{\lambda \cot \chi} \left(\frac{2}{\gamma_M^2} \right) \left(\frac{p_0}{p_\infty} \right) \left(\frac{\gamma M_0^2}{\lambda} \right) \end{array} \right. \quad (4.14) \text{ b}$$

where
$$I = \int_0^{S_d} p_\delta(0, \zeta) d\zeta \quad (4.14) \text{ c}$$

The integral (4.14)c is indeed the spanwise pressure integral defined in the last section. Thus, I is assigned to the value of $\tilde{P}_G(0)$ (equation 4.4), \tilde{P}_{GS} (equation 4.7) or \tilde{P}_{LS} (equation 4.8), according to different approximate schemes chosen, respectively, the 'global-linear' (or local-linear), the 'global-stretched' or the 'local-stretched' methods.

Once C_L is known, the moment coefficient (equation 4.13) can be obtained in a simple form

$$C_M = \frac{C_L}{\cos \alpha_0} \cdot \left(\frac{2}{3} - x_0 \right) \quad (4.15)$$

The aerodynamic center is located at 2/3 chord as expected, independent of $M_\infty (>1)$, α_0 and χ . Now, if the lift coefficient C_L is normalized by its corresponding two-dimensional lift coefficient C_{L_0} , equation (4.14) becomes

$$\frac{C_L}{C_{L_0}} = 1 + \frac{C_{L_1}}{C_{L_0}}$$

where

$$\frac{C_{L1}}{C_{L0}} = \gamma \kappa^2 \tan \chi \left(\frac{P_0/P_\infty}{1 - P_0/P_\infty} \right) \quad I$$

To further demonstrate the smallness of the three-dimensional effect on the lift, a table is shown below :

M_∞	α_0	χ	C_L / C_{L0}			C_{L0}
			Lin.	L.S.	G.S.	
4	5°	50°	.9667	.999	.998	.055
4	10°	50°	.964	.992	.993	.1324
4	15°	50°	.959	.981	.986	.2326
17	10°	75°	.970	.975	.984	.0767

TABLE 1

The steady pressure distribution due to mean flow of these cases is given by Hui (Ref. 7) (Roy.Soc. 1971). Some immediate conclusion may be drawn from these examples. First, the difference between the 'local-stretched' method and the 'global-stretched' method are within 3% , and the linear method at most gives 9% error, if the 'local-stretched' method is taken as the standard one.

Secondly, the ratio (C_{L1}/C_{L0}) ranges from roughly 1% to 4% substantiating Bahaev's conclusion (Ref. 4), from his numerical solutions that the lift is insensitive to the sweepback angle χ .

4.3 In-phase flow: Differentiation method

As mentioned earlier, the static stability derivatives $C_{L\alpha}$ and $C_{M\alpha}$ can be directly derived from the mean flow C_L and C_M through direct differentiation with respect to α_0 . With the explicit expressions available in the last section, (equation 4.14, 4.15), it is possible to apply the exact differentiation.

Although the principle of exact differentiation is sound and direct, the procedure is laborious. In order to apply the procedure systematically, the previous expressions for spanwise pressure integrals

P_G , \tilde{P}_{GS} and \tilde{P}_{LS} are rewritten in more unified form.

Let $I_G = P_G$, $I_{GS} = \tilde{P}_{GS}$ and $I_{LS} = \tilde{P}_{LS}$, then

$$I_G = - \frac{w_s' H}{A_0 + H} \quad a$$

$$I_{GS} = - \zeta_* \cdot I_G + P_s \cdot (\zeta_d - \zeta_*) \quad (4.15) \quad b^*$$

$$I_{LS} = - \zeta_* \cdot \left[I_G \cdot \left(\frac{P_s}{P_c} - 1 \right) - P_s \right] + P_s \cdot (\zeta_d - \zeta_*) \quad c$$

All expressions are now presented in the form with the first term representing the inner flow contribution and the second term the outer-flow contribution. Thus, by the elementary differentiation formula, the following derivatives are obtained

$$\frac{\partial I_G}{\partial \alpha_0} = \frac{-1}{(A_0 + H)^2} \left\{ \left[w_s' \frac{\partial H}{\partial \alpha_0} + H \frac{\partial w_s'}{\partial \alpha_0} \right] (A_0 + H) - w_s' H \cdot \left(\frac{\partial A_0}{\partial \alpha_0} + \frac{\partial H}{\partial \alpha_0} \right) \right\} \quad (4.16) \quad a$$

* Note that $P_{GS} \rightarrow P_G$ as $\zeta_* \rightarrow 1$ and $P_s \rightarrow 0$

$$\frac{\partial I_{GS}}{\partial \alpha_0} = - \left(\zeta_* \frac{\partial I_G}{\partial \alpha_0} + I_G \cdot \frac{\partial \zeta_*}{\partial \alpha_0} \right) + \left\{ \frac{\partial P_s}{\partial \alpha_0} (\zeta_d - \zeta_*) + P_s \left(\frac{\partial \zeta_d}{\partial \alpha_0} - \frac{\partial \zeta_*}{\partial \alpha_0} \right) \right\} \quad (4.16) \text{ b}$$

$$\frac{\partial I_{LS}}{\partial \alpha_0} = - \left\{ \zeta_* \cdot \left[\left(\frac{P_s}{P_c} - 1 \right) \frac{\partial I_G}{\partial \alpha_0} + \frac{I_G}{P_c^2} \left(P_c \frac{\partial P_s}{\partial \alpha_0} - P_s \frac{\partial P_c}{\partial \alpha_0} \right) \right] - \frac{\partial P_s}{\partial \alpha_0} + \frac{\partial \zeta_*}{\partial \alpha_0} \left[I_G \left(\frac{P_s}{P_c} - 1 \right) - P_s \right] + (\zeta_d - \zeta_*) \frac{\partial P_s}{\partial \alpha_0} + P_s \left(\frac{\partial \zeta_d}{\partial \alpha_0} - \frac{\partial \zeta_*}{\partial \alpha_0} \right) \right\} \quad (4.16) \text{ c}$$

It is seen now, for the inner-flow part, three derivatives

$\frac{\partial H}{\partial \alpha_0}$, $\frac{\partial w_s}{\partial \alpha_0}$ and $\frac{\partial A_0}{\partial \alpha_0}$ are yet to be derived. For the outer-flow

part, $\frac{\partial \zeta_d}{\partial \alpha_0}$, $\frac{\partial \zeta_*}{\partial \alpha_0}$, $\frac{\partial P_s}{\partial \alpha_0}$ and $\frac{\partial P_c}{\partial \alpha_0}$ are required. These are very

complicated and lengthy functions of M_∞ , α_0 and χ , the derivation of these expressions is given in Appendix D.

Hence, differentiating equation (4.14) WRT α_0 the in-phase life coefficient is written as

$$C_{L\alpha} = \frac{\partial C_L}{\partial \alpha_0} = C_{L_0\alpha} + C_{L1\alpha} \quad (4.17)$$

where

$$C_{L_0\alpha} = \frac{\partial C_{L_0}}{\partial \alpha_0} = \cos \alpha_0 \frac{\partial C_{p_0}}{\partial \alpha_0} - \sin \alpha_0 \cdot C_{p_0} \quad (4.17) \text{ a}$$

with
$$\frac{\partial C_{p_0}}{\partial \alpha_0} = \frac{2}{\gamma M_\infty^2} \cdot \frac{\partial (P_0/P_\infty)}{\partial \alpha_0}$$

For convenience C_{L_1} is written in the following form

$$C_{L_1} = C_{P_I} \cdot \cos \alpha_0$$

where

$$C_{P_I} = \tan \chi \cdot C_f \cdot I$$

and

$$C_f = \frac{2}{M_\infty^2} \frac{P_0}{P_\infty} \kappa^2 \quad \kappa = \frac{M_0}{\sqrt{M_0^2 - 1}}$$

$$I = I_G \quad (\text{Linear})$$

$$= I_{GS} \quad (\text{Global-stretched})$$

$$= I_{LS} \quad (\text{Linear-stretched})$$

The derivative C_{L_1} in equation (4.17) thus reads

$$C_{L_1 \alpha} = \cos \alpha_0 \frac{\partial C_{P_I}}{\partial \alpha_0} - \sin \alpha_0 \cdot C_{P_I} \quad (4.17) \text{ b}$$

$$\frac{\partial C_{P_I}}{\partial \alpha_0} = \tan \chi \cdot \left(\frac{\partial C_f}{\partial \alpha_0} I + \frac{\partial I}{\partial \alpha_0} \cdot C_f \right)$$

$$\frac{\partial C_f}{\partial \alpha_0} = \frac{2}{M_\infty^2} \cdot \frac{\partial}{\partial \alpha_0} \left(\frac{P_0}{P_\infty} \right) \kappa^2 + \left(\frac{P_0}{P_\infty} \right) \cdot 2\kappa \frac{\partial \kappa}{\partial \alpha_0}$$

$$\frac{\partial I}{\partial \alpha_0} = \frac{\partial I_G}{\partial \alpha_0} \quad (\text{Linear})$$

$$= \frac{\partial I_{GS}}{\partial \alpha_0} \quad (\text{Global-stretched})$$

$$= \frac{\partial I_{LS}}{\partial \alpha_0} \quad (\text{Linear-stretched})$$

Here, the derivatives of equations (4.17) a and (4.17) b,

$$\frac{\partial}{\partial \alpha_0} \left(\frac{P_0}{P_\infty} \right) \quad \text{and} \quad \frac{\partial \kappa}{\partial \alpha_0}$$

are also presented in the Appendix D.

From equation (4.15) the in-phase moment can be expressed as

$$C_{M\alpha} = \frac{\partial C_M}{\partial \alpha_0} = \frac{1}{\cos \alpha_0} \cdot \left[C_{L\alpha} - \tan \alpha_0 C_L \right] \cdot \left(\frac{2}{3} - x_0 \right) \quad (4.18)$$

It is seen that the static stability boundary is given at $x_0 = \frac{2}{3}$, a unique pitch location for all delta wings under the present assumptions.

Finally, comparison of the numerical results on $C_{L\alpha}$ of previous example cases (in Table 1) is presented in the following table.

M_∞	α_0	χ	$C_{L\alpha} / C_{L_0\alpha}$			$C_{L_0\alpha}$
			Lin.	L.S.	G.S.	
4	5°	50°	.962	.992	.993	.754
4	10°	50°	.948	.978	.983	1.018
4	15°	50°	.931	.955	.969	1.273
17	10°	75°	.975	.996	.997	1.273

TABLE 2

Some immediate conclusions may be drawn from these examples :

First, it is observed from Table 2 that the largest deviation between these three methods is no more than 8%, produced by the 'linear' method. In order to check out the 'exact differentiation' method, a numerical differentiation scheme was devised - (unpublished here). It was found that for wide ranges of cases, almost identical numerical results were obtained between the 'exact differentiation' method and the numerical one.

Second, Babœv's statement on the insensitivity of C_L can be further extended to the in-phase lift $C_{L\alpha}$, based on the observation

from TABLE 2 and Figures 7 and 8. However, it should be pointed out that this fact may not be so when the flow region approaches the zone of shock detachment (e.g. see Figures 7 and 8).

For further discussion on this point, see Sections 8.1 and 8.3.

4.4 A similarity rule for flat delta wings

It has been shown that the lifts and moments for mean flow and the in-phase flow can be split into two terms (e.g. equations 4.14 and 4.17)*.

Based on the 'linear' formulation (i.e. $O(\delta)$), see equations (4.1), (4.4) and (4.15)a), it is then possible to devise a similarity rule for flat delta wings at different sweepback angles, χ_1 say, and χ_2 but placed at the same flow conditions M_∞ , α_0 and γ .

i) The mean flow :

Equation (4.14) gives

$$C_L = C_{L_0} + C_{L_1}$$

Now, if the flow conditions are the same for both wings, this implies

$$C_{L_0}(\chi_1) = C_{L_0}(\chi_2)$$

as C_{L_0} is independent of χ .

The second term can be expressed as for the wing of χ_1 ,

$$C_{L_1}(\chi_1) = \cos \alpha_0 \cdot C_f \cdot I_G(\chi_1) \cdot \tan \chi_1$$

for the wing of χ_2

$$C_{L_1}(\chi_2) = \cos \alpha_0 \cdot C_f \cdot I_G(\chi_2) \cdot \tan \chi_2$$

* With the first term attributed to the corresponding 2-D flow and the second term to the 3-D correction.

Also, C_f is independent of χ . This allows the relation

$$\frac{C_{L_1}(\chi_1)}{C_{L_1}(\chi_2)} = \frac{I_G(\chi_1)}{I_G(\chi_2)} \cdot \left(\frac{\tan \chi_1}{\tan \chi_2} \right) = \frac{w_s'(\chi_1)}{w_s'(\chi_2)} \cdot \left(\frac{\tan \chi_1}{\tan \chi_2} \right)$$

as the parameters A_0 and H are independent of χ . From equation

$$(4.1) \quad w_s' = \chi \cdot \frac{\sin \varphi_0}{\cos \beta_0} \sin \alpha_0$$

thus,

$$C_{L_1}(\chi_2) = C_{L_1}(\chi_1) \cdot \left(\frac{\chi_2 \tan \chi_2}{\chi_1 \tan \chi_1} \right) \quad (4.19)$$

According to equations (4.14) and (4.15) the moment coefficient can also be written in two terms, i.e.

$$C_M = C_{M_0} + C_{M_1} \quad (4.20)$$

where

$$C_{M_0} = \frac{C_{L_0}}{\cos \alpha_0} \left(\frac{2}{3} - x_0 \right)$$

$$C_{M_1} = \frac{C_{L_1}}{\cos \alpha_0} \left(\frac{2}{3} - x_0 \right)$$

Thus, for two wings having the same pitching-axis location x_0 , the rule gives

$$C_{M_0}(\chi_2) = C_{M_0}(\chi_1) \quad (4.21)$$

$$C_{M_1}(\chi_2) = C_{M_1}(\chi_1) \frac{\chi_2 \tan \chi_2}{\chi_1 \tan \chi_1}$$

ii) The in-phase flow :

Equations (4.17), (4.19), (4.20) and (4.21) thus provide the similarity rule for the stability derivative as follows

$$\begin{aligned}c_{L_{0\alpha}}(\chi_2) &= c_{L_{0\alpha}}(\chi_1) \\c_{L_{1\alpha}}(\chi_2) &= c_{L_{1\alpha}}(\chi_1) \cdot \left(\frac{\chi_2 \tan \chi_2}{\chi_1 \tan \chi_1} \right)\end{aligned}\tag{4.22}$$

and

$$\begin{aligned}c_{M_{0\alpha}}(\chi_2) &= c_{M_{0\alpha}}(\chi_1) \\c_{M_{1\alpha}}(\chi_2) &= c_{M_{1\alpha}}(\chi_1) \cdot \left(\frac{\chi_2 \tan \chi_2}{\chi_1 \tan \chi_1} \right)\end{aligned}\tag{4.23}$$

for two wings having the same pitching-axis location x_0 .

Note that a more general expression includes different x_0 and can be easily obtained, if one wishes.

In the next chapter, a generalization of the present similarity rule will be derived, in which the effects of added-volume for wing-body combinations and the effect of small-bend for caret wings and V-shape (diamond) wings will also be included.

5. FORCES AND MOMENTS OF DELTA WING-BODY COMBINATIONS: A LINEAR FORMULATION

In the previous Chapter, it was shown that based on the linear formulation, the lifts and moments of a flat delta wing can be split into terms of purely two-dimensional contribution and three-dimensional sweep-back effects. Thus, a similarity rule was shown to exist for wings of different swept-back angles.

In the present Chapter, a formal generalization will be made in order to treat a wing of delta platform but with small bend along its root chord (i.e. V-shape wing of small detached caret wing of small anhedral) and with an added volume. From Appendix A, the geometry equation and outer flow solutions clearly show that the caret wing is indeed a generalization of the delta wing. Hence, for ^asmall-bend caret wing, one may apply the Taylor's expansion taking the flat delta wing solution as a first order approximation to include the small bend effect in the next higher order approximation. On the other hand, the added volume refers here to a symmetrical conical body enclosed in the linearized Mach cone (i.e. $\eta^2 + \zeta^2 \leq 1$) (see Figure 1-B). Outside of the Mach cone, the wing surfaces are required to be that of a caret wing of small bend.

The problem for a flat delta wing with added volume, or the wing-body combination, has been treated by Malmuth (Ref. 45) and generalized by Hui (Ref. 46) in their so-called 'hypersonic/supersonic area rule'. The basic technique used for such a study is termed 'the spanwise integral method' (see Chapter 4, or Sec. 5.2) or 'the method of spanwise integration' by which one can arrive directly at the global information, such as lifting forces, without explicitly seeking the detailed knowledge of the local flow field. This method is particularly

advantageous for the present force and moment derivation. Making use of the method, the present study further investigates how the effects of sweep-back angle, of added volume, and of small bend contribute to the steady and in-phase lifts and moments. Consequently, a generalized similarity rule (of Sec. 4.4) accounts for these effects and will be presented.

5.1 The linearized formulation

Let Γ be the half angle between two inner surfaces of the caret wing measured in the plane normal to the lower ridge (see Figs. 1-I, 1-G) the small-bend parameter \hat{c} is thus defined as

$$\hat{c} = \frac{\pi}{2} - \Gamma$$

as a first term of the expansion series of $\cot \Gamma$ for large enough Γ . Hence, the following perturbation scheme is introduced for P_δ , v_δ and w_δ

$$P_\delta(\eta, \zeta) = P^I(\eta, \zeta) + \hat{c} P^{II}(\eta, \zeta) + \hat{c}^2 P^{III}(\eta, \zeta) + \dots \quad a$$

$$v_\delta(\eta, \zeta) = v^I(\eta, \zeta) + \hat{c} v^{II}(\eta, \zeta) + \hat{c}^2 v^{III}(\eta, \zeta) + \dots \quad b$$

$$w_\delta(\eta, \zeta) = w^I(\eta, \zeta) + \hat{c} w^{II}(\eta, \zeta) + \hat{c}^2 w^{III}(\eta, \zeta) + \dots \quad c$$

(5.1)

When equations (5.1) are substituted into the linear formulation (4.1), all the equations and the boundary condition remain the same for P^I and P^{II} except the tangency condition. This condition is complicated by the added volume and the small bend effects.

i) The tangency conditions : the inner region

Formally, the surface for a caret wing of angle Γ with added volume surface $\eta = \hat{G}(\zeta)$ can be written generally as

$$\eta = \Lambda \cdot \zeta + \hat{G}(\zeta) \quad (5.2) \text{ a}$$

where $\Lambda = \cot \Gamma$

and $\hat{G}(\zeta) \simeq O(\delta)$

The tangency condition to the order of $O(\delta)$ reads

$$v_\delta - \Lambda w_\delta = \frac{1}{\lambda} \left[\hat{G}(\zeta) - \zeta \hat{G}'(\zeta) \right] \quad \text{at} \quad \eta = \Lambda \zeta \quad (5.2) \text{ b}$$

Writing equation (3.7) in conical coordinates

$$\begin{aligned} \eta v_{\delta \eta} + \zeta v_{\delta \zeta} &= P_\delta \eta \\ \eta w_{\delta \eta} + \zeta w_{\delta \zeta} &= P_\delta \zeta \\ \eta P_{\delta \eta} + \zeta P_{\delta \zeta} &= v_{\delta \eta} + w_{\delta \zeta} \end{aligned} \quad (5.3)$$

Combining equations (5.2)b and (5.3) provides the tangency condition purely in P_δ alone, i.e.

$$P_{\delta \eta}(\eta, \zeta) - \Lambda P_{\delta \zeta}(\eta, \zeta) = -\frac{\zeta^2}{\lambda} \hat{G}''(\zeta) \quad (5.4) \text{ a}$$

at $\eta = \Lambda \zeta$

For the caret wing with small bend, i.e. $\Lambda \simeq \hat{\tau}$, equation (5.4) reads

$$P_{\delta \eta}(\hat{\tau} \zeta, \zeta) - \hat{\tau} P_{\delta \zeta}(\hat{\tau} \zeta, \zeta) = -\frac{\zeta^2}{\lambda} \hat{G}''(\zeta) \quad (5.4) \text{ b}$$

Now, it is essential to apply the Taylor's expansion about $\eta = 0$ so that the tangency condition can be expressed explicitly in terms of $\hat{\tau}$.

Thus, the expansion of P_δ and its derivatives are given as follows

$$P_\delta(\hat{\tau}\zeta, \zeta) = P_\delta(0, \zeta) + \hat{\tau}\zeta P_{\delta\eta}(0, \zeta) + \hat{\tau}^2 \zeta^2 P_{\delta\eta\eta}(0, \zeta) \quad a$$

$$P_{\delta\eta}(\hat{\tau}\zeta, \zeta) = P_{\delta\eta}(0, \zeta) + \hat{\tau}\zeta P_{\delta\eta\eta}(0, \zeta) + \hat{\tau}^2 \zeta^2 P_{\delta\eta\eta\eta}(0, \zeta) \quad b$$

$$P_{\delta\zeta}(\hat{\tau}\zeta, \zeta) = P_{\delta\zeta}(0, \zeta) + \hat{\tau}\zeta P_{\delta\zeta\eta}(0, \zeta) + \hat{\tau}^2 \zeta^2 P_{\delta\zeta\eta\eta}(0, \zeta) \quad c$$

(5.5)

Substituting equations (5.1)a into equation (5.4)b and making use of the above expression (5.5), the tangency conditions are obtained, in accord with the like order of $O(1)$, $O(\hat{\tau})$ and $O(\hat{\tau}^2)$, i.e.

$$O(1): \quad P_{\eta}^I(0, \zeta) = -\frac{\zeta^2}{\lambda} \hat{G}''(\zeta) \quad a$$

$$O(\hat{\tau}): \quad P_{\eta}^{II}(0, \zeta) = P_{\zeta}^I(0, \zeta) - \zeta P_{\eta\eta}^I(0, \zeta) \quad (5.6) \quad b$$

$$O(\hat{\tau}^2): \quad P_{\eta}^{III}(0, \zeta) = P_{\zeta}^{II}(0, \zeta) - \zeta P_{\eta\eta}^{II}(0, \zeta) \\ + \zeta P_{\zeta\eta}^I(0, \zeta) - \zeta^2 P_{\eta\eta\eta}^I(0, \zeta) \quad c$$

ii) The formulations

The inner region :

Substituting the perturbed expression (5.1)a into the formulation equations (4.1) and adding the tangency conditions obtained previously the formulation of $O(\delta)$ reads :-

$$\text{D.E.} \quad (\eta^2 - 1)P_{\eta\eta}^I + 2\eta\zeta P_{\eta\zeta}^I + (\zeta^2 - 1)P_{\zeta\zeta}^I + 2\eta P_{\eta}^I + 2\zeta P_{\zeta}^I = 0$$

$$\text{T.C.} \quad P_{\eta}^I(0, \zeta) = -\frac{\zeta^2}{\lambda} \hat{G}''(\zeta)$$

$$\text{SYM.C.} \quad P_{\zeta}^I(\eta, 0) = 0 \quad (5.7)$$

$$\text{S.C.} \quad H'^2 \zeta P_{\eta}^I(H, \zeta) + [H B_0 - (A_0 + H)\zeta^2] P_{\zeta}^I(H, \zeta) = 0$$

$$\text{M.C.} \quad P^I = P'_s \quad \text{at } \eta^2 + \zeta^2 = 1$$

$$\text{E.C.} \quad \int_{-H'}^{H'} \frac{1}{\zeta} \frac{dP^I}{d\zeta} d\zeta = \frac{2w'_s}{B_0} \quad \text{at } \eta = H$$

with $P'_s = 0$ and $w'_s = -K \tan \varphi_0 \cdot X$ given from the outer flow from the flat delta wing solution. It is seen that the above formulation is the same as that for a flat delta wing (equations (4.1)), except the tangency condition.

The $O(\hat{\tau}\delta)$ formulation thus reads

$$\text{D.E.} \quad (\eta^2 - 1)P_{\eta\eta}^{II} + 2\eta\zeta P_{\eta\zeta}^{II} + (\zeta^2 - 1)P_{\zeta\zeta}^{II} + 2\eta P_{\eta}^{II} + 2\zeta P_{\zeta}^{II} = 0$$

$$\text{T.C.} \quad P_{\eta}^{II}(0, \zeta) = P_{\zeta}^I(0, \zeta) - \zeta P_{\eta\eta}^I(0, \zeta)$$

$$\text{SYM.C.} \quad P_{\zeta}^{II}(\eta, 0) = 0 \quad (5.8)$$

$$\text{S.C.} \quad H'^2 \zeta P_{\eta}^{II}(H, \zeta) + [H B_0 - (A_0 + H)\zeta^2] P_{\zeta}^{II}(H, \zeta) = 0$$

$$\text{M.C.} \quad P^{II} = P''_s \quad \text{at } \eta^2 + \zeta^2 = 1$$

continued ...

$$\text{E.C.} \quad \int_{-H'}^{H'} \frac{1}{S} \frac{dP^{\text{II}}}{d\zeta} d\zeta = \frac{2w_s''}{B_0} \quad \text{at } \eta = H \quad (5.8)$$

with P_s'' and w_s'' given from the outer region flow, which will be derived in the next step.

Note that again the formulation here is the same as the previous one except the tangency condition.

The outer region :

The conical shock shape can be expressed as (equation (3.4)a)

$$\eta_s = H + f_s(\zeta) = H + F^{\text{I}}(\zeta) + \hat{\tau} F^{\text{II}}(\zeta) \quad (5.9) \text{ a}$$

and the outer wing surface is described by

$$\eta_w = \lambda \zeta \approx \hat{\tau} \zeta \quad (5.9) \text{ b}$$

The shock attachment condition demands η_s equal to η_w at the leading edge $\eta = \lambda \cot \chi$, and results in

$$\begin{aligned} F^{\text{I}}(\lambda \cot \chi) &= -H \\ F^{\text{II}}(\lambda \cot \chi) &= \lambda \cot \chi \end{aligned} \quad (5.10)$$

From equations (3.15) the following shock condition in conical coordinates can be derived, i.e. :-

$$\begin{cases} p^I(H, \zeta) = C \cdot [F^I(\zeta) - \zeta F^{I'}(\zeta)] \\ v^I(H, \zeta) = A \cdot [F^I(\zeta) - \zeta F^{I'}(\zeta)] \\ w^I(H, \zeta) = K \cdot [F^{I'}(\zeta)] \end{cases} \quad (5.11) \text{ a}$$

and

$$\begin{cases} p^{II}(H, \zeta) = C \cdot [F^{II}(\zeta) - \zeta F^{II'}(\zeta)] \\ v^{II}(H, \zeta) = A \cdot [F^{II}(\zeta) - \zeta F^{II'}(\zeta)] \\ w^{II}(H, \zeta) = K \cdot [F^{II'}(\zeta)] \end{cases} \quad (5.11) \text{ b}$$

Next, the tangency condition for v_δ and w_δ are expanded in Taylor's series as was previously done for p_δ

$$O(1) \quad v^I(0, \zeta) = 0 \quad (5.12) \text{ a}$$

$$O(\hat{\tau}) \quad v^{II}(0, \zeta) = w^I(0, \zeta) - \zeta v_{\eta}^I(0, \zeta) \quad (5.12) \text{ b}$$

Since the flow in the outer region is a uniform one (for all orders), the downwash v^I is identically zero, hence for $1 < \zeta < \lambda \cot \chi$

$$v^I(\eta, \zeta) = v_{\eta}^I(\eta, \zeta) = 0 \quad (5.13)$$

Equation (5.12)b thus becomes

$$v^{II}(0, \zeta) = w^I(0, \zeta)$$

From equations (5.11)a, (5.12)a and (5.13), the shock shape $F^{II'}(\lambda \cot \chi)$ is obtained and from equation (5.11)b and (5.12)b,

the shock shape $F^{\text{II}'}$ ($\lambda \cot \chi$) is obtained, i.e.

$$\begin{cases} F^{\text{I}'}(\lambda \cot \chi) = -\tan \varphi_0 \tan \chi & \text{a} \\ F^{\text{II}'}(\lambda \cot \chi) = 1 + \frac{K \tan \varphi_0}{A \lambda} \chi \tan \chi & \text{b} \end{cases} \quad (5.14)$$

Notice that in arriving at these expressions, the sidewash velocity w^{I} has been approximated as

$$w^{\text{I}} = -K \cdot \tan \varphi_0 \tan \chi \approx -K \tan \varphi_0 \cdot \chi$$

which is consistent with the value used previously (last equation of (4.1)).

Knowing the perturbed shock locations and their slopes at the leading edges, the solutions for the outer region can be written down as

$$O(\delta) : \begin{cases} p^{\text{I}} = p_s^{\text{I}} = 0 \\ v^{\text{I}} = v_s^{\text{I}} = 0 \\ w^{\text{I}} = w_s^{\text{I}} = -K \cdot \tan \varphi_0 \cdot \chi \end{cases} \quad (5.15) \text{ a}$$

$$O(\delta \hat{\tau}) : \begin{cases} p^{\text{II}} = p_s^{\text{II}} = -\frac{K}{A_0} \cdot \tan \varphi_0 \cdot \chi \\ v^{\text{II}} = v_s^{\text{II}} = -K \cdot \tan \varphi_0 \cdot \chi \\ w^{\text{II}} = w_s^{\text{II}} = K \left[1 + \frac{K \tan \varphi_0}{A \lambda} \chi \tan \chi \right] \\ \approx K + O(\chi^2) \end{cases} \quad (5.15) \text{ b}$$

With the outer-flow perturbed pressures and velocities given, the

formulations for the inner region flow equations (5.7) and (5.8) are thus complete.

5.2 The method of solution of the inner region

i) The 'full-range' spanwise integral :

In their previous analyses, both Malmuth and Hui (Refs. 45 and 46) have used the half-range spanwise integral of pressure, i.e.

$$0 \leq \zeta \leq \sqrt{1 - \eta^2}$$

Instead of the half-range, the present analysis will use the spanwise integral in the full range, i.e.

$$-\sqrt{1 - \eta^2} \leq \zeta \leq \sqrt{1 - \eta^2}$$

The merits of the full range spanwise integral are essentially two : first, no information about pressure, say, along the root chord is required; second, one may fully exploit the symmetry properties and the anti-symmetry properties of the pressure and its higher derivatives. These points will be further demonstrated as follows.

The full-range spanwise integration is defined as

$$P^I(\eta) = \int_{-\sqrt{1 - \eta^2}}^{\sqrt{1 - \eta^2}} p^I(\eta, \zeta) d\zeta = \mathcal{J}[p^I(\eta, \zeta)] \quad (5.16) \text{ a}$$

likewise for P^{II} , i.e.

$$P^{II}(\eta) = \mathcal{J}[p^{II}(\eta, \zeta)] \quad (5.16) \text{ b}$$

Since the wing and the added volume is symmetric with respect to $\zeta = 0$, the pressures P^I and P^{II} , say, are therefore also symmetric, a priori; hence they are even functions.

Clearly P_ζ^I and P_ζ^{II} and their higher derivatives in ζ are antisymmetric with $\zeta = 0$, and hence are odd functions.

The following properties can then be defined for any given function P in $(-\sqrt{1-\eta^2}, \sqrt{1-\eta^2})$, i.e.

$$\int_{-\sqrt{1-\eta^2}}^{+\sqrt{1-\eta^2}} \zeta^{n+1} \frac{\partial^n P}{\partial \zeta^n} d\zeta = \mathcal{D} \left[\zeta^{n+1} \frac{\partial^n P}{\partial \zeta^n} \right] = 0 \quad \text{a}$$

('odd' integrand)

(5.17)

$$\int_{-\sqrt{1-\eta^2}}^{+\sqrt{1-\eta^2}} \zeta^{2n+1} \frac{\partial^n P}{\partial \zeta^n} d\zeta = \mathcal{D} \left[\zeta^{2n+1} \frac{\partial^n P}{\partial \zeta^n} \right] \neq 0 \quad \text{b}$$

('even' integrand)

where $n = 0, 1, 2, 3 \dots$ $(-\sqrt{1-\eta^2} \leq \zeta \leq \sqrt{1-\eta^2})$
 $(0 \leq \eta \leq H)$

This leaves only the integrand with even functions to be evaluated.

To write down a few, i.e.

$$\mathcal{D} [P_\eta(\eta, \zeta)] = P'(\eta) + \frac{2\eta}{\sqrt{1-\eta^2}} P(\eta, \sqrt{1-\eta^2}) \quad \text{c}$$

(5.17)

$$\mathcal{D} [\zeta P_\zeta(\eta, \zeta)] = 2 \cdot \sqrt{1-\eta^2} P(\eta, \sqrt{1-\eta^2}) - P(\eta) \quad \text{d}$$

More evaluations of these integrals for higher derivatives can be found in the Appendix E.

ii) The integral formulation and the solutions :

Applying the spanwise integral, equations (5.16) and (5.17), to the previous local formulations, equations (5.7) and (5.8), the global formulations are obtained as two ordinary differential equations in order of $O(\delta)$ and of $O(\delta\hat{\tau})$, each with two end point conditions :
 $O(\delta)$:

$$\text{D.E.} \quad P^{\text{I}''}(\eta) = - \frac{2 P_s'}{(1 - \eta^2)^{3/2}}$$

$$\text{T.C.} \quad P^{\text{I}'}(0) = - 2 \sigma_v / \lambda \quad (5.18)$$

$$\text{S.C.} \quad P^{\text{I}'(H)} + \left(\frac{A_0 + H}{1 - H^2} \right) P^{\text{I}(H)} = \left(\frac{2 A_0}{H'} \right) P_s' - \left(\frac{2H}{H'^2} \right) w_s'$$

where σ_v is the added volume parameter defined as

$$\sigma_v = \int_{-1}^1 \hat{G}(\zeta) d\zeta$$

with

$$\hat{G}(\zeta) = 0 \quad \text{for} \quad |\zeta| \geq 1$$

since $\hat{G}(\zeta) \sim O(\delta)$ as stated previously, the order of σ_v is also of $O(\delta)$. Notice the above formulation is exactly what Hui has obtained (Ref. 46). The next higher order formulation of order $O(\delta\hat{\tau})$ reads :-

$0(\delta\hat{\tau}) :$

$$\text{D.E.} \quad P^{\text{II}''}(\eta) = - \frac{2 P_s''}{(1-\eta^2)^{3/2}} \quad (5.19)$$

$$\text{T.C.} \quad P^{\text{II}'}(0) = 0$$

$$\text{S.C.} \quad P^{\text{II}'}(\eta) + \left(\frac{A_0 + H}{1 - H^2} \right) P^{\text{II}}(\eta) = \left(\frac{2 A_0}{H'} \right) P_s'' - \left(\frac{2 H}{H'^2} \right) w_s''$$

It is interesting to note that the added volume parameter σ_v does not appear in equations (5.19). This is due to the fact that as observed from equation (5.6)b, all terms on the RHS of the tangency condition are odd functions. However, for the next higher order formulation of $0(\hat{\tau}^2\delta)$, as observed from equation (5.6)c, the added volume parameter σ_v will enter through the tangency condition, since the last two terms on the RHS are even functions.

The solutions of equations (5.18) and (5.19) can be immediately obtained, i.e.

$$P^{\text{I}}(\eta) = - \frac{2 w_s' H}{A_0 + H} + \frac{2 \sigma_v}{\lambda} \cdot \left[\left(\frac{1 + A_0 H}{A_0 + H} \right) - \eta \right] \quad (5.20)$$

$$P^{\text{II}}(\eta) = 2 \cdot \left[P_s'' \sqrt{1-\eta^2} - \frac{w_s'' H}{A_0 + H} \right] \quad (5.21)$$

The total spanwise pressure integral for the inner region then reads

$$P^{\text{I}}(\eta) = P^{\text{I}}(\eta) + \hat{\tau} P^{\text{II}}(\eta) \quad (5.22)$$

Notice that when letting $\sigma_v = \hat{\tau} = 0$ and evaluating equation (5.22) at $\eta = 0$ $P^{\text{I}}(0) = 2P_G(0)$ as expected. (see equation (4.4)).

The pressure integral in the outer region is defined as

$$P^{\circ}(0) = 2 \int_1^{\zeta_d} \left[P^{\text{I}}(0, \zeta) + \hat{\tau} P^{\text{II}}(0, \zeta) \right] d\zeta$$

With the values of P^{I} and P^{II} given in equations (5.15)a and (5.15)b, the above expression becomes

$$P^{\circ}(0) = \hat{\tau} \chi \cdot \left[\frac{2K}{A_0} \tan \varphi_0 \right] (\zeta_d - 1) \quad (5.23) \text{ a}$$

Explicitly the pressure integral in the inner region (equation 5.22) reads

$$P^{\text{i}}(0) = \chi \cdot \left[\frac{2KH \tan \varphi_0}{A_0 + H} \right] + \sigma_v \cdot \left[\frac{2(1 + A_0 H)}{A_0 + H} \right] + \hat{\tau} \cdot \left[\frac{-2K}{A_0} \tan \varphi_0 \cdot \chi - \frac{KH}{A_0 + H} \right] \quad (5.23) \text{ b}$$

Further let the total pressure integral be I_U , then

$$I_U = P^{\text{i}}(0) + P^{\circ}(0) \quad (5.24) \text{ a}$$

and

$$\frac{I_U}{\lambda \cot \chi} = \chi \tan \chi \cdot \left[\frac{2KH^2}{\lambda^2(A_0 + H)} \right] \quad (5.24) \text{ b}$$

$$+ \sigma_v \tan \chi \cdot \left[\frac{2(1 + A_0 H)}{\lambda^2(A_0 + H)} \right]$$

$$+ \hat{\tau} \tan \chi \cdot \left[\frac{-2KH(2A_0 + H)}{\lambda A_0(A_0 + H)} \right]$$

It is seen now in equation (5.24)b the three-dimensional effects and the added volume effect are separated from the corresponding two-dimensional effects. This thus provides ground for the later development of the general similarity rule.

5.3 The forces and moments

i) The mean flow :

Following the expression for lift coefficients given in equations (4.14), its general form can now be expressed as

$$C_L = C_{L_0} + C_{L_1} \quad (5.25) \text{ a}$$

$$\left\{ \begin{array}{l} C_{L_0} = C_{P_0} \cos \alpha_0 \end{array} \right. \quad (5.25) \text{ b}$$

$$\left\{ \begin{array}{l} C_{L_1} = C_f \cdot \cos \alpha_0 \frac{I_U}{\lambda \cot \chi} \end{array} \right. \quad (5.25) \text{ c}$$

Let \bar{C}_L , \check{C}_L and \hat{C}_L be the lift coefficients due to the contribution of sweepback effect, the added-volume effect and the small-bend effect respectively, equation (2.25)c can be expressed as

$$C_{L_1} = \bar{C}_L + \check{C}_L + \hat{C}_L \quad (5.26)$$

where

$$\left\{ \begin{array}{l} \bar{C}_L = \chi \tan \chi \cdot \mathcal{S}_0(M_\infty, \alpha_0) \\ \check{C}_L = \sigma_v \tan \chi \cdot \mathcal{V}_0(M_\infty, \alpha_0) \\ \hat{C}_L = \hat{\tau} \tan \chi \cdot \mathcal{J}_0(M_\infty, \alpha_0) \end{array} \right. \quad (5.26) \begin{array}{l} \text{a} \\ \text{b} \\ \text{c} \end{array}$$

with the corresponding two-dimensional functions \mathcal{S}_0 , \mathcal{V}_0 and \mathcal{J}_0

explicitly written as

$$\left\{ \begin{array}{l} \mathcal{D}_0(M_\infty, \alpha_0) = C_f \cdot \cos \alpha_0 \cdot \left(\frac{KH^2}{\lambda^2(A_0 + H)} \right) \quad \text{a} \\ \mathcal{V}_0(M_\infty, \alpha_0) = C_f \cdot \cos \alpha_0 \left(\frac{1 + A_0 H}{\lambda^2(A_0 + H)} \right) \quad \text{(5.27) b} \\ \mathcal{J}_0(M_\infty, \alpha_0) = C_f \cdot \cos \alpha_0 \left(\frac{-KH(2A_0 + H)}{\lambda A_0(A_0 + H)} \right) \quad \text{c} \end{array} \right.$$

Note that the factor $\tan \chi$ appeared in equations (5.26) and is introduced by the definition of the lift coefficient, i.e. the platform area $S = L^2 \cot \chi$.^{*} Hence, if one is only interested in the total lifting force, by definition

$$\bar{L} = q_\infty \cdot S \cdot C_L \quad \text{(5.28) a}$$

where $q_\infty = \frac{1}{2} \rho_\infty U_\infty^2$ the dynamic pressure, it is found that

$$\frac{\partial \bar{L}}{\partial \sigma_v} = \mathcal{V}_0(M_\infty, \alpha_0) \quad \text{(5.28) b}$$

and

$$\frac{\partial \bar{L}}{\partial \hat{\tau}} = \mathcal{J}_0(M_\infty, \alpha_0) \quad \text{(5.28) c}$$

* In all the lift coefficients defined herein it is only for convenience that the reference area used being that of a flat delta and the circumferencial area of the added volume is not included.

Thus, in the present linearized formulation, the function \mathcal{V}_0 represents the total lift force changing rate due to added volume and the function \mathcal{J}_0 due to small bend. Furthermore, it is seen in equations (5.27), $\mathcal{S}_0(M_\infty, \alpha_0) < 0$, $\mathcal{V}_0(M_\infty, \alpha_0) > 0$ and $\mathcal{J}_0(M_\infty, \alpha_0) > 0$, since all the coefficients on the RHS are positive except for K which is negative. These lead to the following conclusion :

According to equations (5.25) and (5.26), increasingly the sweepback angle χ results in a reduction of lift, whereas increasing either the added volume or the caret-wing small bend results in an increment of lift.

Clearly, the present lift expression equations (5.25), (5.26) include the previous lift expression for a flat delta wing, equations (4.14) and (4.15), as a special case.

Finally, the moment coefficient is defined in the usual way (see equation (4.15))

$$C_M = \frac{C_L}{\cos \alpha_0} \left(\frac{2}{3} - x_0 \right).$$

ii) The in-phase flow :

The in-phase lift and moment can also be easily found by exact differentiation of the mean-flow lift and moment, in the same way described in Chapter 4. Thus, following equation (4.17)

$$C_{L\alpha} = C_{L_0\alpha} + C_{L_1\alpha} \quad (5.29)$$

where $C_{L_0\alpha}$ is given in equation (4.17)a

$$c_{L1\alpha} = \frac{\partial c_{L1}}{\partial \alpha_0} \quad (5.29) \text{ a}$$

$$= \frac{\partial \bar{c}_L}{\partial \alpha_0} + \frac{\partial \check{c}_L}{\partial \alpha_0} + \frac{\partial \hat{c}_L}{\partial \alpha_0}$$

and

$$\left\{ \begin{array}{l} \frac{\partial \bar{c}_L}{\partial \alpha_0} = \chi \tan \chi \frac{\partial \mathcal{S}_0}{\partial \alpha_0} \quad \text{a} \\ \frac{\partial \check{c}_L}{\partial \alpha_0} = \sigma_v \tan \chi \frac{\partial \mathcal{V}_0}{\partial \alpha_0} \quad (5.30) \text{ b} \\ \frac{\partial \hat{c}_L}{\partial \alpha_0} = \hat{\tau} \tan \chi \frac{\partial \mathcal{J}_0}{\partial \alpha_0} \quad \text{c} \end{array} \right.$$

All derivatives $\frac{\partial \mathcal{S}_0}{\partial \alpha_0}$, $\frac{\partial \mathcal{V}_0}{\partial \alpha_0}$ and $\frac{\partial \mathcal{J}_0}{\partial \alpha_0}$ depend on knowing

$\frac{\partial c_f}{\partial \alpha_0}$, $\frac{\partial \kappa}{\partial \alpha_0}$, $\frac{\partial A_0}{\partial \alpha_0}$, $\frac{\partial H}{\partial \alpha_0}$ and $\frac{\partial \lambda}{\partial \alpha_0}$, whose expressions were given

in Appendix D. Since the differentiation procedure used here for obtaining equations (5.30) is quite elementary and is similar to the one used in Chapter 4, no further detail will be given. However, it should be stated that their behaviour is :

$\frac{\partial \mathcal{S}_0}{\partial \alpha_0} < 0$, $\frac{\partial \mathcal{V}_0}{\partial \alpha_0}$, $\frac{\partial \mathcal{J}_0}{\partial \alpha_0} > 0$, similar to the behaviour of \mathcal{S}_0 ,

\mathcal{V}_0 and \mathcal{J}_0 . Again, the in-phase moment coefficient is defined as in equation (4.18)

$$c_{M\alpha} = \frac{\partial c_M}{\partial \alpha_0} = \left[c_{L\alpha} - \tan \alpha_0 c_L \right] \cdot \left(\frac{2}{3} - x_0 \right)$$

In Figure 9, the in-phase lift coefficients are plotted against α_0 , at freestream Mach $M_\infty = 4$ and 20, for the cases of the flat delta wing and two delta wings of small-bend (small anhedral and

dihedral) with the same sweepback angle χ and added volume ($\sigma_v = 1$ for $M_\infty = 4$ and for $M_\infty = 20$). It is seen that the caret wing configuration with added volume achieves the highest $C_{L\alpha}$ as expected.

5.4 The generalized similarity rule

i) The mean flow :

As mentioned previously, the results of equations (5.26) invite the establishment of a more general similarity rule.

The basic features of the present similarity rule are :

- For given M_∞ and α_0 , the steady and in-phase lifts and moments can be expressed in a combination of terms which separately account for the effects of sweepback angle χ , of the added volume σ_v and of the small bend $\hat{\tau}$.

- It is a generalized similarity rule for non-affine bodies of the added volume (see Figure 1-H).

The rule can be derived as follows :

Consider two wing-bodies of different sweepback angles, χ_1 and χ_2 say, of different added volumes, σ_{v_1} and σ_{v_2} say, and of different small bend, $\hat{\tau}_1$ and $\hat{\tau}_2$ say, but both are cruising at the same freestream Mach M_∞ and at the same incidence α_0 (see Figures 1-F and 1-G). Let the superscript 1 indicate the lift and moment coefficients of the wing 1 and superscript 2 of the wing 2.

Equations (5.25) and (5.26) provide the following relations for the lift, i.e.

$$C_{L_0}^2 = C_{L_0}^1 \quad (5.31) \text{ a}$$

$$\left\{ \begin{array}{l} \bar{c}_L^2 = \bar{c}_L^1 \cdot \frac{\chi_2 \tan \chi_2}{\chi_1 \tan \chi_1} \\ \check{c}_L^2 = \check{c}_L^1 \cdot \frac{\sigma_{v_2} \tan \chi_2}{\sigma_{v_1} \tan \chi_1} \\ \hat{c}_L^2 = \hat{c}_L^1 \cdot \frac{\hat{\tau}_2 \tan \chi_2}{\hat{\tau}_1 \tan \chi_1} \end{array} \right. \quad \begin{array}{l} b \\ (5.31) \text{ c} \\ d \end{array}$$

Hence, knowing the lift components of wing 1 and knowing the configuration of both wings, the lift components, and hence the total lift, of wing 2 can be found from equations (5.31).

Employing the same notation and superscripts for the moment coefficient, the same rule also applies to it, at the same pitching-axis location x_o ,

$$\begin{array}{l} c_{M_o}^2 = c_{M_o}^1 \quad (5.32) \text{ a} \\ \left\{ \begin{array}{l} \bar{c}_M^2 = \bar{c}_M^1 \cdot \frac{\chi_2 \tan \chi_2}{\chi_1 \tan \chi_1} \\ \check{c}_M^2 = \check{c}_M^1 \cdot \frac{\sigma_{v_2} \tan \chi_2}{\sigma_{v_1} \tan \chi_1} \\ \hat{c}_M^2 = \hat{c}_M^1 \cdot \frac{\hat{\tau}_2 \tan \chi_2}{\hat{\tau}_1 \tan \chi_1} \end{array} \right. \quad \begin{array}{l} b \\ c \\ d \end{array} \end{array}$$

The total moment coefficient thus reads

$$c_M^n = c_{M_o}^n + (\bar{c}_M^n + \check{c}_M^n + \hat{c}_M^n) \quad \begin{array}{l} n = 1 \text{ (wing 1)} \\ = 2 \text{ (wing 2)} \end{array} \quad (5.32) \text{ e}$$

ii) The in-phase flow :

Similar to the mean-flow lifts and moments, the rule for the in-phase lifts and moments can also be expressed as

$$\begin{aligned}
 c_{L_0 \alpha}^2 &= c_{L_0 \alpha}^1 & \text{a} \\
 \left\{ \begin{aligned}
 \bar{c}_L^2 &= \bar{c}_L^1 \frac{\chi_2 \tan \chi_2}{\chi_1 \tan \chi_1} & \text{b} \\
 \check{c}_L^2 &= \check{c}_L^1 \frac{\sigma_{v_2} \tan \chi_2}{\sigma_{v_1} \tan \chi_1} & \text{c} \\
 \hat{c}_L^2 &= \hat{c}_L^1 \frac{\hat{\tau}_2 \tan \chi_2}{\hat{\tau}_1 \tan \chi_1} & \text{d}
 \end{aligned} \right. & (5.33)
 \end{aligned}$$

and

$$\begin{aligned}
 c_{M_0 \alpha}^2 &= c_{M_0 \alpha}^1 & \text{a} \\
 \left\{ \begin{aligned}
 \bar{c}_M^2 &= \bar{c}_M^1 \frac{\chi_2 \tan \chi_2}{\chi_1 \tan \chi_1} & \text{b} \\
 \check{c}_M^2 &= \check{c}_M^1 \frac{\sigma_{v_2} \tan \chi_2}{\sigma_{v_1} \tan \chi_1} & \text{c} \\
 \hat{c}_M^2 &= \hat{c}_M^1 \frac{\hat{\tau}_2 \tan \chi_2}{\hat{\tau}_1 \tan \chi_1} & \text{d}
 \end{aligned} \right. & (5.34)
 \end{aligned}$$

The total stiffness derivatives thus reads

$$\begin{aligned}
 c_{M \alpha}^n &= c_{M_0 \alpha}^n + (\bar{c}_M^{\alpha n} + \check{c}_M^{\alpha n} + \hat{c}_M^{\alpha n}) & n = 1 \text{ (wing 1)} \\
 & & n = 2 \text{ (wing 2)}
 \end{aligned}$$

6. THE UNSTEADY FLOW SOLUTIONS: PROBLEMS A, B, C & D

The present chapter aims at providing methods of solution for Problems A, B, C and D, previously formulated in chapter 3 (i.e. equations (3.27), (3.28), (3.29) and (3.30) respectively). The method of solution employed here for Problems A and C of the outer region is similar to that of Hui's work for wedges and caret wings. In each case the solutions yield constant properties on parallel planar surfaces for the out-of-phase flow. The method of solution for solving Problems B and D depends on the extensive application of the spanwise integration technique, discussed in chapters 4 and 5, to the out-of-phase flow in the inner region.

6.1 PROBLEM A : The in-phase flow of the outer region

Based on the formulation in equations (3.27), exact solutions are found. They represent uniform in-phase flow solutions in the region as expected, i.e.

$$\left\{ \begin{array}{l} p^0 = \tilde{C}_1 \tilde{d}_5 + \tilde{C}_2 \tilde{e}_5 \\ v^0 = 1 \\ u^0 = \tilde{E}_1 \tilde{d}_5 + \tilde{E}_2 \tilde{e}_5 \\ w^0 = \tilde{K}_1 \tilde{d}_5 + \tilde{K}_2 \tilde{e}_5 \end{array} \right. \quad \begin{array}{l} a \\ b \\ c \\ d \end{array} \quad (6.1)$$

and the outer shock shape is an oblique planar surface described by

$$Q^0(x, z) = \tilde{d}_5 x + \tilde{e}_5 z + \tilde{f}_5 \quad (6.1) \quad e$$

where

$$\left\{ \begin{array}{l} \tilde{d}_5 = \frac{1 - \tilde{A}_2 \hat{\sigma}}{\tilde{A}_1 - \tilde{A}_2 \hat{\sigma}} \\ \tilde{e}_5 = \hat{\sigma} (1 - \tilde{d}_5) \\ \hat{\sigma} = \tan \chi \\ \tilde{f}_5 = -x_0 \end{array} \right. \quad (6.2)$$

Note that as $\chi \rightarrow 0$, implying $\hat{G} = 0$, P^0 , V^0 , U^0 and Q^0 reduce identically to the in-phase wedge solutions previously obtained by Hui (Ref.37, 1969) and $W^0 \equiv 0$ as expected.

6.2 PROBLEM C : The out-of-phase flow of the outer region

Based on the formulation given in equation (3.29), solutions of the following form are sought, namely

$$\left\{ \begin{array}{l} P^1 = A_1 x + B_1 y + C_1 z + D_1 \quad a \\ V^1 = A_2 x + B_2 y + C_2 z + D_2 \quad b \\ W^1 = A_3 x + B_3 y + C_3 z + D_3 \quad c \\ U^1 = A_4 x + B_4 y + C_4 z + D_4 \quad d \end{array} \right. \quad (6.3)$$

together with the out-of-phase shock shape in quadratic form

$$Q^1(x,z) = A_5 x^2 + B_5 xz + C_5 z^2 + D_5 x + E_5 z + F_5 \quad (6.3) \quad e$$

They are indeed the exact solutions of the Problem C. Thus, as a part of the solutions, the coefficients $A_1, B_1, C_1 \dots$ etc. are given as follows :

For P^1 ,

$$\left\{ \begin{array}{l} A_1 = 2\tilde{C}_1 A_5 + \tilde{C}_2 B_5 + (\tilde{D} \tilde{d}_5 - B_1 t_c) \quad a \\ B_1 = - \left(\frac{1 + V^0}{\nu} \right) \quad b \\ C_1 = \tilde{C}_1 B_5 + 2\tilde{C}_2 C_5 + (\tilde{D} \tilde{e}_5 + B_1 t_s) \quad c \\ D_1 = \tilde{C}_1 D_5 + \tilde{C}_2 E_5 = d_{10} \cdot x_0 \quad d \end{array} \right. \quad (6.4)$$

where $\nu = \frac{1}{\gamma M_*^2}$ e

$$d_{10} = - \frac{\tilde{C}_2 \hat{G} - \tilde{C}_1}{\tilde{A}_2 \hat{G} - \tilde{A}_1} \quad f$$

For v^1 ,

$$\left\{ \begin{array}{l} A_2 = 1 \\ B_2 = \frac{1}{t_c} \left[2\tilde{A}_1 \cdot A_5 + \tilde{A}_2 \cdot B_5 + (\tilde{B} \cdot \tilde{d}_5 - 1) \right] \\ C_2 = 0 \\ D_2 = -x_0 \end{array} \right. \quad \begin{array}{l} a \\ b \\ c \\ d \end{array} \quad (6.5)$$

For w^1 ,

$$\left\{ \begin{array}{l} A_3 = \left(\frac{2a \hat{\sigma} \tilde{K}_1}{a \hat{\sigma} - 1} \right) \cdot A_5 + \left(\frac{a(\tilde{K}_2 \hat{\sigma} + \tilde{K}_1) + \nu \tilde{C}_1}{a \hat{\sigma} - 1} \right) \cdot B_5 \\ \quad + \left(\frac{2a \tilde{K}_2 + 2 \nu \tilde{C}_2}{a \hat{\sigma} - 1} \right) \cdot C_5 + a_{30} \\ B_3 = \frac{1}{t_c} \left[2\tilde{K}_1 \cdot A_5 + \tilde{K}_2 \cdot B_5 + (\tilde{L} \tilde{d}_5 - A_3) \right] \\ C_3 = \left(\frac{2\tilde{K}_1 \hat{\sigma}}{1 - a \hat{\sigma}} \right) \cdot A_5 + \left(\frac{\tilde{K}_2 \hat{\sigma} + \tilde{K}_1 + \nu \tilde{C}_1 \hat{\sigma}}{1 - a \hat{\sigma}} \right) \cdot B_5 \\ \quad + \left(\frac{2\tilde{K}_2 + 2 \nu \hat{\sigma} \tilde{C}_2}{1 - a \hat{\sigma}} \right) \cdot C_5 + c_{30} \\ D_3 = \tilde{K}_1 D_5 + \tilde{K}_2 E_5 \end{array} \right. \quad \begin{array}{l} a \\ b \\ c \\ d \end{array} \quad (6.6)$$

where

$$a_{30} = \left[a \tilde{L} (\hat{\sigma} \tilde{d}_5 + \tilde{e}_5) + \nu (\tilde{D} \tilde{e}_5 + B_1 \cdot t_s) + w^0 \right] / (a \hat{\sigma} - 1)$$

$$c_{30} = \left[\nu \hat{\sigma} (\tilde{D} \tilde{e}_5 + B_1 t_s) + w^0 \hat{\sigma} + \tilde{L} (\hat{\sigma} \tilde{d}_6 + \tilde{e}_5) \right] / (1 - a \hat{\sigma})$$

For U^1 ,

$$\left\{ \begin{array}{l}
 A_4 = \left(\frac{2a\tilde{E}_1 \hat{\sigma} + 2\nu\tilde{C}_1}{a\hat{\sigma} - 1} \right) \cdot A_5 + \left(\frac{a(\tilde{E}_2 \hat{\sigma} + \tilde{E}_1) + \nu\tilde{C}_2}{a\hat{\sigma} - 1} \right) \cdot B_5 \\
 \quad + \left(\frac{2a\tilde{E}_2}{a\hat{\sigma} - 1} \right) \cdot C_5 + a_{40} \quad a \\
 B_4 = \frac{1}{t_c} \left[2\tilde{E}_1 \cdot A_5 + \tilde{E}_2 \cdot B_5 + \tilde{F} \cdot \tilde{d}_5 - A_4 \right] \quad b \\
 C_4 = \tilde{E}_1 \cdot B_5 + 2\tilde{E}_2 \cdot C_5 + \tilde{F} \cdot \tilde{e}_5 + B_4 \cdot t_s \quad c \\
 D_4 = \tilde{E}_1 D_5 + \tilde{E}_2 \cdot E_5 \quad d
 \end{array} \right. \quad (6.7)$$

where a_{40} is defined in equation (6.10)

In the previous equations (equations (6.4), (6.5), (6.6) and (6.7), certain coefficients are still dependent on the values of A_5 , B_5 , C_5 , D_5 and E_5 given below. Thus

For Q^1

$$\left\{ \begin{array}{l}
 A_5 = \frac{\tilde{d}_{50} \cdot (\tilde{b}_v - \hat{\sigma} \tilde{c}_v) - \tilde{d}_v}{(\tilde{a}_v - \hat{\sigma}^2 \tilde{c}_v) - 2\hat{\sigma}(\tilde{b}_v - \hat{\sigma} \tilde{c}_v)} \quad a \\
 B_5 = -2\hat{\sigma} A_5 - \tilde{d}_{50} \quad b \\
 C_5 = -\hat{\sigma}^2 A_5 - \hat{\sigma} B_5 \quad c \\
 D_5 = \frac{x_0}{\hat{\sigma} \tilde{A}_2 - \tilde{A}_1} \quad d \\
 E_5 = -\hat{\sigma} D_5 \quad e \\
 F_5 = 0 \quad f
 \end{array} \right. \quad (6.8)$$

where

$$\left\{ \begin{array}{l}
 \tilde{a}_v = 2\tilde{C}_1 + 2\gamma \cdot \left[\frac{\tilde{A}_1}{t_c} + \frac{(\nu\tilde{C}_1 + a\hat{\sigma}\tilde{E}_1) - \hat{\sigma}\tilde{K}_1}{a\hat{\sigma} - 1} \right] \\
 \tilde{b}_v = (\tilde{C}_2 + a\tilde{C}_1) + \gamma \cdot \left[\frac{\tilde{A}_2}{t_c} + \frac{\nu\tilde{C}_2 + a(\tilde{E}_2 \hat{\sigma} + \tilde{E}_1)}{a\hat{\sigma} - 1} - \frac{\tilde{K}_2 \hat{\sigma} + \tilde{K}_1 + \nu\hat{\sigma}\tilde{C}_1}{a\hat{\sigma} - 1} \right]
 \end{array} \right.$$

continued ...

$$\left\{ \begin{array}{l} \tilde{c}_v = 2a\tilde{c}_2 + 2\gamma \cdot \left[\frac{a\tilde{E}_2 - (\tilde{K}_2 + \nu)\hat{\sigma}\tilde{c}_2}{a\hat{\sigma} - 1} \right] \\ \tilde{d}_v = a_{10} + ac_{10} + \gamma \cdot (a_{40} + b_{20} + c_{30}) + p^0 \end{array} \right. \quad (6.9)$$

and with

$$\left\{ \begin{array}{l} a_{10} = \tilde{D} \cdot \tilde{d}_5 - B_1 t_c \\ c_{10} = \tilde{D} \cdot \tilde{e}_5 + B_1 t_s \\ b_{20} = (\tilde{B} \cdot \tilde{d}_5 - 1)/t_c \\ a_{40} = \left[\nu (\tilde{D} \cdot \tilde{d}_5 - B_1 \cdot t_c) + a\tilde{F} \cdot (\tilde{e}_5 + \hat{\sigma} \tilde{d}_5) + U^0 \right] / (a\hat{\sigma} - 1) \\ \tilde{d}_{50} = \frac{\tilde{B} \cdot \tilde{e}_5 + \hat{\sigma} (\tilde{B} \cdot \tilde{d}_5 - 1)}{\tilde{A}_1 - \tilde{A}_2 \hat{\sigma}} \end{array} \right. \quad (6.10)$$

Some remarks are in order to describe the pressure solutions p^0 and p^1 of Problems A and C.

i) According to the perturbation scheme for the outer region equations (2.13) and (2.15), the following identity holds

$$p^0 = \frac{1}{P_*} \frac{\partial P_*}{\partial \alpha_0} \quad (6.11)$$

This is to say that in the outer region the in-phase flow obtained from the present perturbation formulation is exactly the same as that obtained by the previous differentiation method.

ii) The present solutions constitute the exact in-phase and out-of-phase skewed wedge solutions (the skewed angle being the sweepback

angle χ (see Appendix C)). As $\chi \rightarrow 0$, the present solutions reduce to the exact two-dimensional wedge solutions given by Hui.

iii) In Problem C, all the flow pressure and velocities are found to be linear functions of (x, y, z) . Hence, they assume constant values along each parallel planar surface. For example, the gradient of p^1 is a constant vector $\nabla p^1 = A_1 \vec{i} + B_1 \vec{j} + C_1 \vec{k}$, along any planar surface, S^1 say, normal to ∇p^1 , p^1 therefore is constant. S^1 is hence called the iso-baric surface.

iv) In view of the above argument, the flow pressure p^1 can be written as *

$$p^1 = x \cdot \mathcal{O}^1\left(\frac{y}{x}, \frac{z}{x}\right) \quad \text{a} \quad (6.12)$$

$$\text{and} \quad \mathcal{O}^1 = A_1 + B_1 \left(\frac{y}{x}\right) + C_1 \left(\frac{z}{x}\right) \quad \text{b}$$

Now, it is seen that function \mathcal{O}^1 is expressed in the conical variables. The separable form of p^1 indicates that the flow field is the so-called quasi-conical flow. The 'quasi-conical' nature of the out-of-phase flow in the outer region provides information for one to seek the flow solution in the inner region in the same form. This will be discussed further in detail in Sec. 6.4, and in Chapter 8 ((iii)a and (iii)b of Sec. 8.2)

* Here, x_0 is set to be zero for convenience, hence D_1 is zero, and this will not affect the generality of the statement

6.3 PROBLEM B : The in-phase flow of the inner region

i) The formulation :

Adopting the conical coordinates, Problem B (equation 3.28) can be formulated in the same manner as the mean-flow problem.

Thus ,

$$\text{D.E.} \quad (\eta^2 - 1)P_{\eta\eta}^{(0)} + 2\eta\zeta P_{\eta\zeta}^{(0)} + (\zeta^2 - 1)P_{\zeta\zeta}^{(0)} + 2\eta P_{\eta}^{(0)} + 2\zeta P_{\zeta}^{(0)} = 0$$

$$\begin{cases} \eta V_{\eta}^{(0)} + \zeta V_{\zeta}^{(0)} = P_{\eta}^{(0)} \\ \eta W_{\eta}^{(0)} + \zeta W_{\zeta}^{(0)} = P_{\zeta}^{(0)} \\ \eta P_{\eta}^{(0)} + \zeta P_{\zeta}^{(0)} = V_{\eta}^{(0)} + W_{\zeta}^{(0)} \end{cases}$$

$$\text{T.C.} \quad P_{\eta}^{(0)} = 0 \quad \text{at} \quad \eta = 0$$

$$\text{S.C.} \quad H^2 \zeta P_{\eta}^{(0)} + [HB_0 - (A_0 + H)\zeta^2 P_{\zeta}^{(0)}] = 0 \quad \text{at} \quad \eta = H$$

$$\begin{cases} P^{(0)}(H, \zeta) = C [G^{(0)}(\zeta) - \zeta G^{(0)'(\zeta)}] \\ V^{(0)}(H, \zeta) = A [G^{(0)}(\zeta) - \zeta G^{(0)'(\zeta)}] \\ W^{(0)}(H, \zeta) = K G^{(0)'(\zeta)} \end{cases} \quad (6.13)$$

$$\text{M.C.} \quad \begin{cases} P^{(0)} = P_*^{(0)} \\ V^{(0)} = V_*^{(0)} \\ W^{(0)} = W_*^{(0)} \end{cases} \quad \text{at} \quad \eta^2 + \zeta^2 = 1$$

$$\text{SYM.C.} \quad P_{\zeta}^{(0)} = 0 \quad \text{at} \quad \zeta = 0$$

$$\text{E.C.} \quad \int_{-H}^{H'} \frac{d P^{(0)}}{\zeta} = \frac{2 W_*^{(0)}}{B_0} \quad \text{at} \quad \eta = H$$

Note that the D.E. and the S.C. for $U^{(0)}$ reads respectively

$$-\lambda (\eta U_{\eta}^{(0)} + \zeta U_{\zeta}^{(0)}) = \eta P_{\eta}^{(0)} + \zeta P_{\zeta}^{(0)} \quad (\text{D.E.})$$

$$U^{(0)}(H, \zeta) = \epsilon \cdot [G^{(0)}(\zeta) - \zeta G^{(0)'}(\zeta)] \quad (\text{S.C.})$$

The shock shape (3.4)a is written in conical form as

$$\eta_{\zeta} = H + f_{\delta}(\zeta) + \epsilon \cdot [G^{(0)}(\zeta) + ik_0 G^{(1)}(\xi, \zeta)] e^{ik_0 t}$$

where

(6.14)*

$G^{(0)}(\zeta)$ is the in-phase shock shape as in the above S.C.

$G^{(1)}(\xi, \zeta)$ is the out-of-phase shock shape where $\xi = X$

Relating to the Problem A, the values of $p^{(0)}$, $v^{(0)}$ and $w^{(0)}$ at Mach cone are

$$p_*^{(0)} = \bar{\alpha} \cdot p^0$$

$$v_*^{(0)} = \bar{\beta} \cdot v^0$$

$$w_*^{(0)} = \bar{\beta} \cdot w^0$$

(6.15)

where

$$\bar{\alpha} = \frac{\lambda}{\gamma M_0^2} \frac{p_*}{p_0}$$

$$\bar{\beta} = u_*/u_0$$

* Here, it is to assume $Q^{(0)}(X, Z)/X = G^{(0)}(\zeta)$, similar to the mean-flow shock shape.

ii) The method of Spanwise Integration :

Now, the method of full-range spanwise integration introduced in equations (5.16) is applied to the above formulation. Hence defining

$$P^{(0)}(\eta) = \int_{-\sqrt{1-\eta^2}}^{\sqrt{1-\eta^2}} p^{(0)}(\eta, \zeta) d\zeta$$

and making use of the properties at the Mach cone together with the operations derived in Appendix E, the integral form of equation (6.13) can be represented as

$$\text{D.E. } P^{(0)''}(\eta) = - \frac{2 P_*^{(0)}}{(1-\eta^2)^{3/2}} \quad \text{a}$$

$$\text{T.C. } P^{(0)'}(0) = 0 \quad \text{(6.16) b}$$

$$\text{S.C. } P^{(0)'}(H) + \left(\frac{A_0 + H}{1-H^2} \right) P^{(0)}(H) = \left(\frac{2A_0}{H} \right) P_+^{(0)} - \left(\frac{2H}{H^2} \right) W_+^{(0)} \quad \text{c}$$

where $P_+^{(0)} = P^{(0)}(H, H')$

$$W_+^{(0)} = W^{(0)}(H, H') \quad \text{d}$$

and $G^{(0)}(H') = \tilde{d}_5 + \tilde{e}_5 H'$ given from Problem A

The solution of (6.16) can be written down immediately

$$P^{(0)}(\eta) = 2P_*^{(0)} \sqrt{1-\eta^2} + \frac{2}{A_0 + H} \left[A_0 H' (P_+^{(0)} - P_*^{(0)}) - H W_+^{(0)} \right]$$

In order to match the present solution toward the outer solution of Problem A, $p_+^{(0)}$ and $w_+^{(0)}$ are then replaced by $p_*^{(0)}$ and $w_*^{(0)}$. The global solution above is then simplified

$$P^{(0)}(\eta) = 2p_*^{(0)} \sqrt{1-\eta^2} - \frac{2Hw_*^{(0)}}{A_o + H} \quad (6.17) a$$

Evaluating the above equation at the wing surface, $\eta = 0$ results

$$P^{(0)}(0) = 2 \left(p_*^{(0)} - \frac{Hw_*^{(0)}}{A_o + H} \right) \quad (6.17) b$$

6.4 PROBLEM D : The out-of-phase flow of the inner region

The present problem attempted to be solved here is the most complex one of all. The complexity is mainly due to the non-uniform nature of the three-dimensional flow field. Furthermore, as observed from the previous formulation equation (3.30), the solutions of Problems A, B and C enter into the present formulation as a result of the perturbation scheme. To be more precise, the solution of Problem B enters through the inhomogeneous terms of the D.E. and the S.C. of equation (3.30); the solutions of Problems A and C enter through the M.C. of the equation (3.30).

i) Method of solution :

In order to deal with the three-dimensionality of the problem, the following generalized conical coordinate is first introduced

$$\begin{cases} \xi = x \\ \eta = \frac{y}{x} \\ \zeta = \frac{z}{x} \end{cases}$$

The formulation equations (3.30) written in the generalized conical coordinates become

$$\begin{aligned} \text{D.E.} \quad \xi^2 p_{\xi\xi}^{(1)} - 2\xi(\eta p_{\eta\xi}^{(1)} + \zeta p_{\zeta\xi}^{(1)}) + (\eta^2 - 1)p_{\eta\eta}^{(1)} \\ + 2\eta\zeta p_{\eta\zeta}^{(1)} + (\zeta^2 - 1)p_{\zeta\zeta}^{(1)} + 2(\eta p_{\eta\eta}^{(1)} + \zeta p_{\zeta\zeta}^{(1)}) = \\ - 2\kappa^2 \xi(\eta p_{\eta\eta}^{(0)} + \zeta p_{\zeta\zeta}^{(0)}) \end{aligned}$$

$$\begin{cases} \xi p_{\xi\xi}^{(1)} - (\eta p_{\eta\eta}^{(1)} + \zeta p_{\zeta\zeta}^{(1)}) + v_{\eta}^{(1)} + w_{\zeta}^{(1)} = \xi b^{(0)}(\eta, \zeta) \\ \xi v_{\xi\xi}^{(1)} - (\eta v_{\eta\eta}^{(1)} + \zeta v_{\zeta\zeta}^{(1)}) + p_{\eta}^{(1)} = -\xi v^{(0)}(\eta, \zeta) \\ \xi w_{\xi\xi}^{(1)} - (\eta w_{\eta\eta}^{(1)} + \zeta w_{\zeta\zeta}^{(1)}) + p_{\zeta}^{(1)} = -\xi w^{(0)}(\eta, \zeta) \end{cases}$$

where $b^{(0)}(\eta, \zeta) = \frac{1}{\lambda} u^{(0)}(\eta, \zeta) - \kappa^2 p^{(0)}(\eta, \zeta)$ (6.18)

T.C. $p_{\eta}^{(1)} = -2\xi$ at $\eta = 0$

S.C.
$$\begin{cases} p^{(1)} = C \cdot [G^{(1)} + \xi G_{\xi}^{(1)} - \zeta G_{\zeta}^{(1)}] + D \cdot [\xi G^{(0)}(\zeta)] \\ v^{(1)} = A \cdot [G^{(1)} + \xi G_{\xi}^{(1)} - \zeta G_{\zeta}^{(1)}] + B \cdot [\xi G^{(0)}(\zeta)] \\ w^{(1)} = K G_{\zeta}^{(1)} \end{cases}$$
 at $\eta = H$

M.C.
$$\begin{cases} p^{(1)} = p_*^{(1)} \\ v^{(1)} = v_*^{(1)} \\ w^{(1)} = w_*^{(1)} \end{cases}$$
 at $\eta^2 + \zeta^2 = 1$

SYM.C. $p_{\zeta}^{(1)} = 0$ at $\zeta = 0$

where
$$\begin{cases} p_*^{(1)} = \xi[\mathcal{A}_1 + \mathcal{B}_1\eta + \mathcal{C}_1\zeta] + \mathcal{D}_1 \\ v_*^{(1)} = \xi[\mathcal{A}_2 + \mathcal{B}_2\eta + \mathcal{C}_2\zeta] + \mathcal{D}_2 \\ w_*^{(1)} = \xi[\mathcal{A}_3 + \mathcal{B}_3\eta + \mathcal{C}_3\zeta] + \mathcal{D}_3 \end{cases}$$
 (6.19)*

* Note that D_1, D_2 and D_3 , hence $\mathcal{D}_1, \mathcal{D}_2$ and \mathcal{D}_3 , are linearly proportional to x_0 , the pitching axis location.

and

$$\begin{cases} \mathcal{A}_1 = \bar{\alpha} A_1 \\ \mathcal{B}_1 = \bar{\alpha} B_{1/\lambda} \\ \mathcal{C}_1 = \bar{\alpha} C_{1/\lambda} \\ \mathcal{D}_1 = \bar{\alpha} D_1 \end{cases} \quad \begin{cases} \mathcal{A}_2 = \bar{\beta} A_2 \\ \mathcal{B}_2 = \bar{\beta} B_{2/\lambda} \\ \mathcal{C}_2 = \bar{\beta} C_{2/\lambda} \\ \mathcal{D}_2 = \bar{\beta} D_2 \end{cases} \quad \begin{cases} \mathcal{A}_3 = \bar{\beta} A_3 \\ \mathcal{B}_3 = \bar{\beta} B_{3/\lambda} \\ \mathcal{C}_3 = \bar{\beta} C_{3/\lambda} \\ \mathcal{D}_3 = \bar{\beta} D_3 \end{cases}$$

The out-of-phase shock shape $G^{(1)}(\xi, \zeta)$ remains its general form here and is related to $Q^{(1)}(X, Z)$ as

$$\frac{Q^{(1)}(X, Z)}{X} = G^{(1)}(\xi, \zeta)$$

Unlike all the previous problems, the present formulation equation (6.18) is difficult to recast into the single independent variable $\rho^{(1)}$ alone. Apparently the difficulty arises because of the S.C., After eliminating $V^{(1)}$ and $W^{(1)}$ in the S.C., although the resulting S.C. can be expressed solely in $\rho^{(1)}$ it becomes a second-order differential relation, compatible with the order of the D.E. Also, the S.C. is further complicated by the unknown shock shape $G^{(1)}(\xi, \zeta)$. It is essential to further specify the form of the shock shape $G^{(1)}$, since it appears as the lowest-order (in differentiation) of the whole problem.

The latter problem is settled by the confirmation that Problem D is indeed a quasi-conical flow field. This is recognized from two viewpoints. First, it is known that the flow field of Problem C is quasi-conical (equation 6.12), which transmits the characteristic through the Mach cone into Problem D (as in equation 6.19). Second, by inspection, all the boundary conditions and the D.E. of Problem D (equation 6.18) admit solutions which are linearly dependent in ξ .

Based on the above argument, the solutions of the Problem D are sought in the following forms

$$p^{(1)}(\xi, \eta, \zeta) = \xi \mathcal{P}(\eta, \zeta) + x_0 \cdot \phi(\eta, \zeta) \quad a$$

$$v^{(1)}(\xi, \eta, \zeta) = \xi \mathcal{V}(\eta, \zeta) + x_0 \cdot \nu(\eta, \zeta) \quad b$$

$$w^{(1)}(\xi, \eta, \zeta) = \xi \mathcal{W}(\eta, \zeta) + x_0 \cdot \omega(\eta, \zeta) \quad c$$

$$G^{(1)}(\xi, \zeta) = \xi G(\zeta) + x_0 g(\zeta) \quad d$$

(6.20)

The solutions are then split in two terms, the first term being the 'quasi-conical' term. Evidently, with the absence of the second term, the flow field represents one which results from the wing oscillating about the apex. Hence $\mathcal{P}(\eta, \zeta) \dots$ etc. are called the apex solutions, whereas $\phi(\eta, \zeta), \nu(\eta, \zeta) \dots$ etc. are called the axis solutions, indicating the latter solutions add the effect of pitching-axis location to the total solution.

ii) The apex solution :

Substituting equations (6.20) into the total formulation and collecting like terms linear in ξ , the formulation for the apex solution now reads

$$\text{D.E. } (\eta^2 - 1)\mathcal{P}_{\eta\eta} + 2\eta\zeta\mathcal{P}_{\eta\zeta} + (\zeta^2 - 1)\mathcal{P}_{\zeta\zeta} = -2\kappa^2(\eta \mathcal{P}_{\eta}^{(0)} + \zeta \mathcal{P}_{\zeta}^{(0)})$$

$$\begin{cases} \mathcal{P} - (\eta \mathcal{P}_{\eta} + \zeta \mathcal{P}_{\zeta}) + \mathcal{V}_{\eta} + \mathcal{W}_{\zeta} = b^{(0)} \\ \mathcal{V} - (\eta \mathcal{V}_{\eta} + \zeta \mathcal{V}_{\zeta}) + \mathcal{P}_{\eta} = -v^{(0)} \\ \mathcal{W} - (\eta \mathcal{W}_{\eta} + \zeta \mathcal{W}_{\zeta}) + \mathcal{P}_{\zeta} = -w^{(0)} \end{cases} \quad (6.21)$$

$$\text{T.C. } \mathcal{P}_{\eta} = -2 \quad \text{at } \eta = 0$$

$$\text{S.C.} \quad \begin{cases} \mathcal{P} = C \cdot [2G(\zeta) - \zeta G'(\zeta)] + D \cdot G^{(0)}(\zeta) \\ \mathcal{V} = A \cdot [2G(\zeta) - \zeta G'(\zeta)] + B \cdot G^{(0)}(\zeta) \\ \mathcal{W} = K G'(\zeta) \end{cases} \quad \text{at } \eta = H$$

$$\text{M.C.} \quad \begin{cases} \mathcal{P} = \alpha_1 + \beta_1 \eta + \mathcal{C}_1 \zeta \\ \mathcal{V} = \alpha_2 + \beta_2 \eta + \mathcal{C}_2 \zeta \\ \mathcal{W} = \alpha_3 + \beta_3 \eta + \mathcal{C}_3 \zeta \end{cases} \quad \text{at } \eta^2 + \zeta^2 = 1 \quad (6.21)$$

$$\text{SYM.C.} \quad \mathcal{P}_\zeta = 0 \quad \text{at } \zeta = 0$$

where

$$b^{(0)} = \left(\frac{E_0}{\lambda} - \kappa^2 A_0 \right) p^{(0)}(\eta, \zeta), \quad E_0 = \frac{E}{C}$$

$$v^{(0)} = A_0 p^{(0)}(\eta, \zeta), \quad A_0 = \frac{A}{C}$$

Now, making use of the first order equations of the D.E., the S.C. can be written in a second-order form solely in terms of \mathcal{P} as, at $\eta = H$

$$H^2 \zeta \mathcal{P}_{\eta\zeta} + [H B_0 - (A_0 + H) \zeta^2] \mathcal{P}_{\zeta\zeta} = \left[\left(\frac{E_0}{\lambda} - \kappa^2 A_0 \right) H - A_0 \right] \cdot \zeta p_\zeta^{(0)} + \left[\left(\frac{B - A_0 D}{K} \right) \zeta^2 - \frac{DH}{C} \right] \cdot w_\zeta^{(0)} \quad (6.22)$$

Hence, with the S.C. expressed in the form of equation (6.22), the problem of the apex solution, equations (6.21) can be formulated solely in terms of \mathcal{P} . A method of solution is proposed here to solve for $\mathcal{P}(\eta, \zeta)$ formulated in equations (6.21).

The proposed solution is sought in the following steps :

First, let

$$\mathcal{P}(\eta, \zeta) = \mathcal{P}_0(\eta, \zeta) + 2\kappa^2 p^{(0)}(\eta, \zeta)$$

in which the first term represents the complementary solution and the

second term the particular solution given in equations (6.13).

Next, splitting again P_0 in two terms, i.e.

$$P_0(\eta, \zeta) = P_\phi(\eta, \zeta) + L_\phi(\eta, \zeta)$$

where $L_\phi(\eta, \zeta) = \mathcal{A}_1' + \mathcal{B}_1 \eta + \mathcal{C}_1 \zeta$

$$\mathcal{A}_1' = \mathcal{A}_1 - 2\kappa^2 P_*^{(0)}$$

results in the formulation of $P_\phi(\eta, \zeta)$:

D.E. $(\eta^2 - 1)P_{\phi\eta\eta} + 2\eta\zeta P_{\phi\eta\zeta} + (\zeta^2 - 1)P_{\phi\zeta\zeta} = 0$

T.C. $P_{\phi\eta} = -2 - \mathcal{B}_1$ at $\eta = 0$

S.C. $H^2\zeta P_{\phi\eta\zeta} + [HB_0 - (A_0 + H)\zeta^2]P_{\phi\zeta\zeta} = (\nu_a \zeta + \frac{\nu_b}{\zeta}) P_\zeta^{(0)}$

at $\eta = H$

M.C. $P_\phi = 0$ at $\zeta = \sqrt{1 - \eta^2}$

SYM.C. $P_{\phi\zeta} = 0$ at $\zeta = 0$

(6.23) a

where

$$\begin{cases} \nu_a = \nu_0 + \nu_2 B_0 \\ \nu_b = -\nu_1 - \nu_3 B_0 \end{cases}$$

$$\begin{cases} \nu_0 = \left(\frac{E_0}{\lambda} - \kappa^2 A_0 \right) H - A_0 - 2\kappa^2 (A_0 + H) \\ \nu_1 = 2\kappa^2 H B_0 \\ \nu_2 = (B - A_0 D) / K \\ \nu_3 = D \cdot H / C \end{cases}$$

Moreover, introducing the pressure differential function Ψ such that

$$\Psi(\eta, \zeta) = \frac{\partial}{\partial \zeta} \mathcal{P}_\phi(\eta, \zeta)$$

the formulation for \mathcal{P}_ϕ (equation (6.23)a) becomes

$$\text{D.E.} \quad (\eta^2 - 1)\Psi_{\eta\eta} + 2\eta\zeta\Psi_{\eta\zeta} + (\zeta^2 - 1)\Psi_{\zeta\zeta} + 2(\eta\Psi_\eta + \zeta\Psi_\zeta) = 0$$

$$\text{T.C.} \quad \Psi_\eta = 0 \quad \text{at } \eta = 0$$

$$\text{S.C.} \quad H^2 \zeta \Psi_\eta + [HB_0 - (A_0 + H)\zeta^2] \Psi_\zeta = \left(\nu_a \zeta + \frac{\nu_b}{\zeta}\right) P_\zeta^{(0)}$$

at $\eta = H$

$$\text{M.C.} \quad \int^\zeta \Psi d\zeta + \Psi_*(\eta) = 0 \quad \text{at } \zeta = \sqrt{1 - \eta^2}$$

$$\text{Anti-Sym.C.} \quad \Psi(\eta, -\zeta) = -\Psi(\eta, \zeta)$$

(6.23) b

where $\Psi_*(\eta)$ needs to be determined as it is a part of the solution.

Now, it is seen that both D.E. and T.C. are the same as the mean-flow formulation (equation (4.1)). However, in order to cope with the other boundary conditions, care must be exercised upon the S.C. and the M.C. No effort is given here in further derivation of the final 'local' solution.

The Global solution :

For a more direct approach, the global formulation by the method of spanwise integration is once again applied to the equations (6.21). The spanwise integral of pressure and velocity is defined as (for the spanwise integral defined in the Tschaplygin plane (σ, μ) , see Appendix F).

$$\mathcal{J} [\mathcal{P}(\eta, \zeta)] = \int_{-\sqrt{1-\eta^2}}^{\sqrt{1-\eta^2}} \mathcal{P}(\eta, \zeta) d\zeta = P(\eta) \quad \text{a}$$

(6.24)

$$\mathcal{J} [\mathcal{V}(\eta, \zeta)] = \int_{-\sqrt{1-\eta^2}}^{\sqrt{1-\eta^2}} \mathcal{V}(\eta, \zeta) d\zeta = V(\eta) \quad \text{b}$$

First, the spanwise integral is applied to the S.C. According to the operations derived in Appendix E, the first two first-order D.Es. of equation (6.21) evaluated at $\eta = H$ can be written as

$$2P(H) - H P'(H) + V'(H) = \frac{2}{H} \mathcal{P}_+ - \frac{2H}{H} \mathcal{V}_+ - 2\mathcal{W}_+ + \left(\frac{E_0}{\lambda} - \kappa^2\right) P^{(0)}(H) \quad \text{a}$$

(6.25)

$$2V(H) - H V'(H) + P'(H) = \frac{2}{H} \mathcal{V}_+ - \frac{2H}{H} \mathcal{P}_+ - A_0 P^{(0)}(H) \quad \text{b}$$

where $\mathcal{V}_+ = A_0 \mathcal{P}_+ + (B - A_0 D) G^{(0)}(H')$

$$\mathcal{P}_+ = C [2G(H') - H' G'(H')] + DG^{(0)}(H')$$

$$\mathcal{W}_+ = K G'(H)$$

$$P^{(0)}(H) = 2 \left(P_*^{(0)} H' - \frac{H W_*^{(0)}}{A_0 + H} \right)$$

$$G^{(0)}(H') = \lambda \tilde{a}_5 + H' \tilde{e}_5$$

$$G(H') = \mathcal{A}_5 + \mathcal{B}_5 H' + \mathcal{C}_5 H'^2$$

$$G'(H') = \mathcal{B}_5 + 2 \mathcal{C}_5 H'$$

While the first two S.C. of equation (6.21) can be related as

$$\bar{V}(H) = A_0 P(H) + (B - A_0 D) \tilde{G}^{(0)} \quad (6.26)$$

where

$$\tilde{G}^{(0)} = \int_H [G^{(0)}(\zeta)] = \frac{1}{c} P^{(0)}(H) + 2H' G^{(0)}(H')$$

Eliminating $\bar{V}(H)$ and $\bar{V}'(H)$ from equations (6.25)a, (6.25)b and (6.26) results in the S.C. in terms of the spanwise pressure integral alone, i.e.

$$\begin{aligned} P'(H) + 2 \left(\frac{A_0 + H}{H'^2} \right) P(H) &= \left(\frac{2}{H'} \right) \mathcal{V}_+ - \frac{2H}{H'^2} \mathcal{W}_+ \\ &+ \frac{1}{H'^2} \left\{ \left[H \left(\frac{E_0}{\lambda} - \kappa^2 \right) - A_0 \right] P^{(0)}(H) - 2(B - A_0 D) \tilde{G}^{(0)} \right\} \end{aligned} \quad (6.27)$$

In order to match with the exact solutions obtained in the outer region (Problems A and C), the terms \mathcal{V}_+ , \mathcal{P}_+ and \mathcal{W}_+ are replaced by \mathcal{V}^* , \mathcal{P}^* and \mathcal{W}^* as below

$$\begin{cases} \mathcal{V}^* = \alpha_2 + \beta_2 \eta^* + \epsilon_2 \zeta^* & \text{a} \\ \mathcal{P}^* = \alpha_1 + \beta_1 \eta^* + \epsilon_1 \zeta^* & \text{(6.28) b} \\ \mathcal{W}^* = \alpha_3 + \beta_3 \eta^* + \epsilon_3 \zeta^* & \text{c} \end{cases}$$

where η^* and ζ^* indicate the intersection of the three-dimensional Mach cone and the outer oblique plane shock. They are determined by solving equations (2.7) and (2.8) in the conical coordinate, thus :-

$$\left\{ \begin{aligned} \eta^* &= t_c \cdot \lambda - t_s \cdot \zeta^* \\ \zeta^* &= \frac{-\zeta_b + \sqrt{\zeta_b^2 - 4\zeta_a\zeta_c}}{2\zeta_a} \end{aligned} \right. \quad (6.29)$$

where

$$\left\{ \begin{aligned} \zeta_a &= \lambda_*^2 (\cos^2 \theta + t_s^2) - \sin^2 \theta \\ \zeta_b &= -2(\lambda_*^2 + 1) \cdot \lambda \cos \theta \sin \theta - 2t_c \cdot t_s \lambda \lambda_1^2 \\ \zeta_c &= \lambda^2 \cdot [\lambda_*^2 (t_c^2 + \sin^2 \theta) - \cos^2 \theta] \end{aligned} \right.$$

(Similarly, the value of H' appeared in the shock shapes $G^{(0)}(H')$, $G(H')$ and $G'(H')$ is replaced by ζ^* and they become $G^{(0)}(\zeta^*)$, $G(\zeta^*)$ and $G'(\zeta^*)$ respectively. It is seen now that the S.C. (equation (6.27)) becomes an improved 'hybrid' condition in which the coefficients such as A_0 , B_0 and $H \dots$ etc. are from two-dimensional perturbation but the flow velocities are the true three-dimensional ones).

Next, the spanwise integral is applied to the D.E. of equation (6.21). Following the derivation in Appendix F, the spanwise integral form of it reads

$$\begin{aligned} (1 - \eta^2) P''(\eta) + 2\eta P'(\eta) - 2P(\eta) = -2\kappa^2 [\eta P^{(0)'}(\eta) - P^{(0)}(\eta)] \\ - [4\kappa^2 p_*^{(0)}(\sigma) + 6\beta_*(\sigma)] / \sqrt{1 - \eta^2} \end{aligned} \quad (6.30)$$

where

$$\left\{ \begin{aligned} P^{(0)}(\eta) &= 2 p_*^{(0)} \cdot \sqrt{1 - \eta^2} - \frac{2H w_*^{(0)}}{A_0 + H} \\ p_*^{(0)}(\sigma) &= p_*^{(0)} \\ \beta_*(\sigma) &= \alpha_1 + \beta_1 \eta + \epsilon_1 \sqrt{1 - \eta^2} \end{aligned} \right.$$

After some rearrangement, the foregoing equation, together with the T.C. of equation (6.21) and the shock condition equation (6.27) can be written as

$$\text{D.E.} \quad (1 - \eta^2) P''(\eta) + 2\eta P'(\eta) - 2P(\eta) = \alpha_I \cdot \frac{\eta}{\sqrt{1 - \eta^2}} + \alpha_{II} \cdot \frac{1}{\sqrt{1 - \eta^2}} + \alpha_\phi \quad \text{a}$$

$$\text{T.C.} \quad P'(0) = -4 \quad \text{(6.31) b}$$

$$\text{S.C.} \quad P'(H) + 2 \left(\frac{A_0 + H}{1 - H^2} \right) P(H) = \Phi_c + \Phi_{AB} \quad \text{c}$$

where

$$\left\{ \begin{array}{l} \alpha_I = -6\beta_1 \\ \alpha_{II} = -6\alpha_1 \\ \alpha_\phi = -6\mathcal{C}_1 - 4\kappa^2 \left(\frac{H w_*^{(0)}}{A_0 + H} \right) \\ \Phi_c = \left(\frac{2}{H^1} \right) \mathcal{V}^* - \left(\frac{2H}{H^1 2} \right) \mathcal{W}^* \\ \Phi_{AB} = \frac{1}{H^1 2} \left\{ \left[H \left(\frac{E_0}{\lambda} - \kappa^2 \right) - A_0 \right] P^{(0)}(H) - 2(B - A_0 D) \tilde{G}^{(0)} \right\} \end{array} \right.$$

The solution of equations (6.31) can be found as

$$P(\eta) = c_I \eta + c_{II} \cdot (1 + \eta^2) - \alpha_I \left(\frac{1}{3} \sqrt{1 - \eta^2} \right) - \alpha_{II} \left(\frac{1}{3} \eta \sqrt{1 - \eta^2} \right) - \frac{\alpha_\phi}{2} \quad \text{(6.32)}$$

where

$$\begin{cases}
 c_{\text{I}} = \frac{\alpha_{\text{II}}}{3} - 4 \\
 c_{\text{II}} = \frac{H'^2}{2 [HH'^2 + (A_0 + H)(1 + H^2)]} \cdot \left\{ \begin{aligned}
 & \Phi_{\text{C}} + \Phi_{\text{AB}} - c_{\text{I}} \cdot \left[1 + 2H \left(\frac{A_0 + H}{1 - H^2} \right) \right] \\
 & + \alpha_{\phi} \cdot \left(\frac{A_0 + H}{1 - H^2} \right) \\
 & + \alpha_{\text{I}} \cdot \left(\frac{2A_0 + H}{3H} \right) \\
 & + \alpha_{\text{II}} \cdot \left(\frac{2A_0 H + 1}{3H} \right) \end{aligned} \right\}
 \end{cases}$$

Evaluating at the wing surface, the spanwise Pressure Integral becomes

$$P(0) = c_{\text{II}} - \left(\frac{\alpha_{\text{I}}}{3} + \frac{\alpha_{\phi}}{2} \right) \quad (6.33)$$

iii) The Axis Solution :

Substituting equation (6.20) into the total formulation of equation (6.18) and collecting like terms associated with x_0 , the formulation for the axis solution, with the transformation,

$$\begin{cases}
 \tilde{p}(\eta, \zeta) = p(\eta, \zeta) + \lambda D \\
 \tilde{v}(\eta, \zeta) = v(\eta, \zeta) + \lambda B \\
 \tilde{w}(\eta, \zeta) = w(\eta, \zeta)
 \end{cases} \quad (6.34)$$

reads,

$$\text{D.E.} \quad (\eta^2 - 1) \tilde{p}_{\eta\eta} + 2\eta\zeta \tilde{p}_{\eta\zeta} + (\zeta^2 - 1) \tilde{p}_{\zeta\zeta} + 2(\eta \tilde{p}_\eta + \zeta \tilde{p}_\zeta) = 0$$

$$\begin{cases} \eta \tilde{v}_\eta + \zeta \tilde{v}_\zeta = \tilde{p}_\eta \\ \eta \tilde{w}_\eta + \zeta \tilde{w}_\zeta = \tilde{p}_\zeta \\ \eta \tilde{p}_\eta + \zeta \tilde{p}_\zeta = \tilde{v}_\zeta + \tilde{w}_\zeta \end{cases}$$

$$\text{T.C.} \quad \tilde{p}_\eta = 0 \quad \text{at } \eta = 0$$

$$\text{S.C.} \quad H^2 \zeta \tilde{p}_\eta + [HB_0 - (A_0 + H)\zeta^2] \tilde{p}_\zeta = 0 \quad \text{at } \eta = H$$

$$\begin{cases} \tilde{p} = C [g(\zeta) - \zeta g'(\zeta)] \\ \tilde{v} = A [g(\zeta) - \zeta g'(\zeta)] \\ \tilde{w} = K g'(\zeta) \end{cases} \quad (6.35)$$

$$\text{M.C.} \quad \begin{cases} \tilde{p} = \hat{d}_1 + \lambda D = \tilde{p}_* \\ \tilde{v} = \hat{d}_2 + \lambda B = \tilde{v}_* \\ \tilde{w} = \hat{d}_3 = \tilde{w}_* \end{cases} \quad \text{at } \eta^2 + \zeta^2 = 1$$

$$\text{SYM.C.} \quad \tilde{p}_\zeta = 0 \quad \text{at } \zeta = 0$$

$$\text{E.C.} \quad \int_{-H}^H \frac{d\tilde{p}}{\zeta} = \frac{2\tilde{w}_*}{B_0} \quad \text{at } \eta = H$$

where

$$\begin{cases} \hat{d}_1 = \frac{\mathcal{D}_1}{x_0} = \bar{\alpha} \cdot (\tilde{C}_1 \cdot \hat{d}_5 + \tilde{C}_2 \cdot \hat{e}_5 - \tilde{D}) \\ \hat{d}_2 = \frac{\mathcal{D}_2}{x_0} = \bar{\beta} \cdot (\tilde{A}_1 \cdot \hat{d}_5 + \tilde{A}_2 \cdot \hat{e}_5 - \tilde{B}) \\ \hat{d}_3 = \frac{\mathcal{D}_3}{x_0} = \bar{\beta} \cdot (\tilde{K}_1 \cdot \hat{d}_5 + \tilde{K}_2 \cdot \hat{e}_5 - \tilde{L}) \end{cases}$$

and

$$\begin{cases} \hat{d}_5 = \frac{D_5}{x_0} = \frac{\hat{B} - 1}{\hat{A}_1 - \hat{\sigma} \hat{A}_2} \\ \hat{e}_5 = \frac{E_5}{x_0} = -\hat{\sigma} \hat{d}_5 \end{cases}$$

It is seen that the axis-solution formulation is the same as the formulation of the mean flow (equations 4.1) and that of the in-phase flow (equations 6.13). The local solution, if one wishes, can be easily obtained following the same method of solution (equations 4.2) given by Hui.

For a more direct approach, a global formulation of equations (6.35) is more desirable. Hence, the spanwise integral of pressure \tilde{p} is defined as

$$\mathcal{J} [\tilde{p}(\eta, \zeta)] = \int_{-\sqrt{1-\eta^2}}^{\sqrt{1-\eta^2}} \tilde{p}(\eta, \zeta) d\zeta = \underline{\tilde{p}}(\eta) \quad (6.36)$$

The spanwise integral formulation of equations (6.35) is thus obtained in the same manner as equations (6.16), i.e.

D.E. $\underline{\tilde{p}}''(\eta) = - \frac{2\tilde{p}_*}{(1-\eta^2)^{3/2}}$

T.C. $\underline{\tilde{p}}'(0) = 0$ at $\eta = 0$ (6.37)

S.C. $\underline{\tilde{p}}'(H) + \left(\frac{A_0 + H}{1 - H^2}\right) \underline{\tilde{p}}(H) = \left(\frac{2A_0}{H}\right) \tilde{p}_+ - \frac{2H}{H^2} \tilde{w}_+$

where

$$\begin{cases} \tilde{p}_+ = C \frac{\lambda D_5}{x_0} \\ \tilde{w}_+ = K \frac{\lambda E_5}{x_0} \end{cases}$$

Again the values of \tilde{p}_+ and \tilde{w}_+ are replaced by their outer region values \tilde{p}_* and \tilde{w}_* . Hence the solution of equations (6.37) is

$$\tilde{P}(\eta) = 2 \left[\tilde{p}_* \sqrt{1-\eta^2} - \frac{H \tilde{w}_*}{A_0 + H} \right] \quad (6.38)$$

From equation (6.34), the relationship is realized as

$$P(\eta) = \int_{-\sqrt{1-\eta^2}}^{\sqrt{1-\eta^2}} p(\eta, \zeta) d\zeta = \tilde{P}(\eta) - 2\lambda D \sqrt{1-\eta^2} \quad (6.39)$$

Hence, the apex solution becomes

$$P(\eta) = 2 \left[(\tilde{p}_* - \lambda D) \sqrt{1-\eta^2} - \frac{H \tilde{w}_*}{A_0 + H} \right] \quad (6.40)$$

Evaluating at the wing surface, it becomes

$$P(0) = 2 \left[(\tilde{p}_* - \lambda D) - \frac{H \tilde{w}_*}{A_0 + H} \right] \quad (6.41)$$

iv) The total solution : Global formulation

Based on equation (6.20) the total solution of equations (6.21) in the spanwise integral form is derived, i.e.

$$\mathcal{D} [P^{(1)}(\xi, \eta, \zeta)] = P^{(1)}(\xi, \eta) = \xi \mathcal{D} [P(\eta, \zeta)] + x_0 \mathcal{D} [p(\eta, \zeta)]$$

$$\text{Thus } P^{(1)}(\xi, \eta) = \xi \cdot P(\eta) + x_0 p(\eta) \quad (6.42)$$

where $P(\eta)$ and $p(\eta)$ are given previously by equations (6.32) and (6.40).

Evaluating at the wing surface $\eta = 0$, equation (6.42)

becomes

$$P^{(1)}(\xi, 0) = \xi P(0) + x_0 \underline{p}(0) \quad (6.43)$$

where $P(0)$ and $\underline{p}(0)$ are given previously by equations (6.33) and (6.41).

7. THE STABILITY DERIVATIVES

Previously in Sec. 4.2, the lift and moment coefficients were defined for the steady mean flow. In what follows, general expressions of forces and moments for in-phase flow and out-of-phase flow will be defined. Exact integrations of the pressure solutions (from Problems A, B, C and D) obtained in Chapter 6, the stiffness derivative and damping derivative can be expressed simply in algebraic form.

7.1 The Definition of the derivatives

i) The force and moment coefficients :

By definition, the normal force acting on the flat delta wing (windward side) reads

$$\bar{F}_N = \iint_S \bar{p}(\bar{x}, 0, \bar{z}) d\bar{x} d\bar{z}$$

where S represents the area of the wing. Thus, the normal force coefficient is defined as

$$C_N = \frac{\bar{F}_N}{\frac{1}{2} \rho_\infty U_\infty^2 S}$$

hence with the \bar{C}_p defined in equation (4.11)

$$C_N = \frac{2}{S} \int_{\bar{x}=0}^{\bar{x}=L} \int_{\bar{z}=0}^{\bar{z}=\bar{x} \cot \chi} \bar{C}_p d\bar{x} d\bar{z} \quad (7.1)$$

Clearly the lift coefficient is defined as

$$C_L = C_N \cdot \cos \alpha_0 \quad (7.2)$$

The total moment acting on the wing with pitching axis location at \bar{x}_0 therefore follows

$$\bar{M} = \iint_S p(\bar{x}, 0, \bar{z}) \cdot (\bar{x} - \bar{x}_0) d\bar{x} d\bar{z}$$

The moment coefficient is defined as

$$C_M = \frac{\bar{M}}{\frac{1}{2} \rho_\infty U_\infty^2 \cdot S \cdot L}$$

thus

$$C_M = \frac{2}{S \cdot L} \int_{\bar{x}=0}^{\bar{x}=L} \int_{\bar{z}=0}^{\bar{z}=\bar{x} \cot \chi} \bar{c}_p (\bar{x} - \bar{x}_0) d\bar{x} d\bar{z} \quad (7.3)$$

ii) The pressure coefficients :

Defined by equation (4.10), the pressure coefficient

$$\bar{c}_p = \frac{2}{\gamma M_\infty^2} \left(\frac{\bar{p}}{p_\infty} - 1 \right)$$

where from equations (2.12) and (2.14)

$$\bar{p} = p_0 + \frac{\gamma M_0^2 p_0}{\lambda} \left[p_\delta + \epsilon p^{(0)} + ik_0 \epsilon p^{(1)} \right] e^{ik_0 t} \quad (7.4)$$

for the inner region;

from equations (2.12) and (2.15)

$$\bar{p} = p_* + p_* \left[\epsilon p^0 + ik_* \epsilon p^1 \right] e^{ik_* t} \quad (7.5)$$

for the outer region.

Note that $k_0 T = k_* t = \bar{\omega} \bar{t}$

Now, the \bar{C}_p in the inner region can be written as

$$\bar{C}_p = C_{p\Delta} + \left[\epsilon C_{p\alpha}^{(0)} + ik_0 \epsilon \cdot C_{p\alpha}^{(1)} \right]_{\alpha \rightarrow \alpha_0} e^{ik_0 T} \quad a$$

$$C_{p\Delta} = \left(\frac{P_\Delta - P_\infty}{P_\infty} \right) \frac{2}{\gamma M_\infty^2} \quad b$$

$$P_\Delta = P_0 \left[1 + \frac{\gamma M_0^2}{\lambda} p_\delta \right] \quad (7.6)$$

$$\left(C_{p\alpha}^{(0)} \right)_{\alpha \rightarrow \alpha_0} = \frac{2}{\gamma M_\infty^2} \left(\frac{P_0}{P_\infty} \right) \left(\frac{\gamma M_0^2}{\lambda} \right) \cdot p^{(0)} \quad c$$

$$\left(C_{p\alpha}^{(1)} \right)_{\alpha \rightarrow \alpha_0} = \frac{2}{\gamma M_\infty^2} \cdot \left(\frac{\gamma M_0^2}{\lambda} \right) \left(\frac{P_0}{P_\infty} \right) \left(\frac{u_0}{U_\infty} \right) \cdot p^{(1)} \quad d$$

Note that to write $(C_{p\alpha})_{\alpha \rightarrow \alpha_0}$ and $(C_{p\dot{\alpha}})_{\alpha \rightarrow \alpha_0}$ is equivalent to

writing $\left(\frac{\partial C_p}{\partial \epsilon} \right)_{\epsilon \rightarrow 0}$ and $\left(\frac{\partial C_p}{\partial i\epsilon k} \right)_{\epsilon \rightarrow 0}$ with $\alpha = \alpha_0 + \epsilon$.

Furthermore, note that $k = \frac{\bar{\omega} L}{U}$ and is related to k_0 and k_* as

$$\begin{cases} k_0 = \frac{U_\infty}{U_0} k & a \\ k_* = \frac{U_\infty}{U_*} k & b \end{cases} \quad (7.7)$$

Thus the \bar{C}_p in the outer region can be expressed as

$$\bar{C}_p = C_{p*} + \left[\epsilon C_{p\alpha}^0 + ik_* \epsilon \cdot C_{p\alpha}^1 \right]_{\alpha \rightarrow \alpha_0} e^{ik_* t} \quad (7.8) a$$

continued ...

$$\left\{ \begin{array}{l} c_{P_*} = \frac{2}{\gamma M_\infty} \left(\frac{P_* - P_\infty}{P_\infty} \right) \quad b \\ c_{P_\alpha}^{(0)} = \frac{2}{\gamma M_\infty^2} \left(\frac{P_*}{P_\infty} \right) \cdot P^{(0)} \quad (7.8) \quad c \\ c_{P_\alpha}^{(1)} = \frac{2}{\gamma M_\infty^2} \left(\frac{P_*}{P_\infty} \right) \left(\frac{u_*}{U_\infty} \right) \cdot P^{(1)} \quad d \end{array} \right.$$

iii) The stability derivatives :

Next, define the force and moment coefficients in the same form as equations (7.7) and (7.8), i.e.

• In the inner region : The normal force coefficient reads

$$c_N = c_{N_\Delta} + \left[\epsilon c_{N_\alpha}^{(0)} + ik_0 \epsilon \cdot c_{N_\alpha}^{(1)} \right]_{\alpha \rightarrow \alpha_0} e^{ik_0 T} \quad a$$

where

$$\left\{ \begin{array}{l} c_{N_\Delta} = \frac{2}{\cot \chi} \int_{x=0}^{x=1} \int_{z=0}^{z=x \cot \chi_*} c_{P_\Delta} dx dz \quad b \\ c_{N_\alpha}^{(0)} = \frac{2}{\cot \chi} \int_{x=0}^{x=1} \int_{z=0}^{z=x \cot \chi_*} c_{P_\alpha}^{(0)} dx dz \quad (7.9)^* \quad c \\ c_{N_\alpha}^{(1)} = \frac{2}{\cot \chi} \int_{x=0}^{x=1} \int_{z=0}^{z=x \cot \chi_*} c_{P_\alpha}^{(1)} dx dz \quad d \end{array} \right.$$

* Note that from now on the limit $\alpha \rightarrow \alpha_0$ is dropped for convenience.

With the lift coefficient

$$C_L = C_{L\Delta} + \left[\epsilon C_{L\alpha}^{(0)} + ik\epsilon \cdot C_{L\dot{\alpha}}^{(1)} \right]_{\alpha \rightarrow \alpha_0} \cdot e^{ik_0 t} \quad a$$

$$\begin{cases} C_{L\Delta} = \cos \alpha_0 \cdot C_{N\Delta} & b \\ C_{L\alpha}^{(0)} = \cos \alpha_0 \cdot C_{N\alpha}^{(0)} & c \\ C_{L\dot{\alpha}}^{(1)} = \cos \alpha_0 \cdot C_{N\dot{\alpha}}^{(1)} & d \end{cases} \quad (7.10)$$

the moment

$$C_M = C_{M\Delta} + \left[\epsilon \left(-C_{M\alpha}^{(0)} \right) + ik\epsilon \left(-C_{M\dot{\alpha}}^{(1)} \right) \right]_{\alpha \rightarrow \alpha_0} \cdot e^{ik_0 t} \quad a$$

$$\begin{cases} C_{M\Delta} = \frac{2}{\cot \chi} \int_{x=0}^{x=1} \int_{z=0}^{z=x \cot \chi_*} C_{p\Delta} \cdot (x - x_0) dx dz & b \\ -C_{M\alpha}^{(0)} = \frac{2}{\cot \chi} \int_{x=0}^{x=1} \int_{z=0}^{z=x \cot \chi_*} C_{p\alpha}^{(0)} (x - x_0) dx dz & c \\ -C_{M\dot{\alpha}}^{(1)} = \frac{2}{\cot \chi} \int_{x=0}^{x=1} \int_{z=0}^{z=x \cot \chi_*} C_{p\dot{\alpha}}^{(1)} (x - x_0) dx dz & d \end{cases} \quad (7.11)$$

• In the outer region :

the normal force

$$C_N = C_{N_*} + \left[\epsilon C_{N\alpha}^{(0)} + ik\epsilon C_{N\dot{\alpha}}^{(1)} \right]_{\alpha \rightarrow \alpha_0} \cdot e^{ik_* t} \quad a$$

$$C_{N_*} = \frac{2}{\cot \chi} \int_{x=0}^{x=1} \int_{z=x \cot \chi_*}^{z=x \cot \chi} C_{p_*} dx dz \quad b$$

continued ...

$$\left. \begin{aligned}
 C_{N\alpha}^0 &= \frac{2}{\cot\chi} \int_{x=0}^{x=1} \int_{z=x \cot\chi_*}^{z=x \cot\chi} C_{p\alpha}^0 dx dz \\
 C_{N\dot{\alpha}}^1 &= \frac{2}{\cot\chi} \int_{x=0}^{x=1} \int_{z=x \cot\chi_*}^{z=x \cot\chi} C_{p\dot{\alpha}}^1 dx dz
 \end{aligned} \right\} \begin{array}{l} c \\ d \end{array} \quad (7.12)$$

the lift

$$\left. \begin{aligned}
 C_L &= C_{L_*} + \left[\epsilon C_{L\alpha}^0 + ik_* \epsilon C_{L\dot{\alpha}}^1 \right]_{\alpha \rightarrow \alpha_0} \cdot e^{ik_* t} \\
 C_{L_*} &= \cos \alpha_0 \cdot C_{N_*} \\
 C_{L\alpha}^0 &= \cos \alpha_0 \cdot C_{N\alpha}^0 \\
 C_{L\dot{\alpha}}^1 &= \cos \alpha_0 \cdot C_{N\dot{\alpha}}^1
 \end{aligned} \right\} \begin{array}{l} a \\ b \\ c \\ d \end{array} \quad (7.13)$$

the moment

$$\left. \begin{aligned}
 C_M &= C_{M_*} + \left[\epsilon \left(-C_{M\alpha}^0 \right) + ik_0 \epsilon \left(-C_{M\dot{\alpha}}^1 \right) \right]_{\alpha \rightarrow \alpha_0} \cdot e^{ik_0 t} \\
 C_{M_*} &= \frac{2}{\cot\chi} \int_{x=0}^{x=1} \int_{z=x \cot\chi_*}^{z=x \cot\chi} C_{p_*} (x - x_0) dx dz \\
 -C_{M\alpha}^0 &= \frac{2}{\cot\chi} \int_{x=0}^{x=1} \int_{z=x \cot\chi_*}^{z=x \cot\chi} C_{p\alpha}^0 (x - x_0) dx dz \\
 -C_{M\dot{\alpha}}^1 &= \frac{2}{\cot\chi} \int_{x=0}^{x=1} \int_{z=x \cot\chi_*}^{z=x \cot\chi} C_{p\dot{\alpha}}^1 (x - x_0) dx dz
 \end{aligned} \right\} \begin{array}{l} a \\ b \\ c \\ d \end{array} \quad (7.14)$$

7.2 The evaluation of the Stability Derivatives

1) The derivatives in the inner region :

Substituting equations (7.6)c,d into equations (7.10)c,d and (7.11)c,d and after the simple integration the contributions to the stability derivatives become

$$c_{L\alpha}^{(0)} = \left[\frac{\cos \alpha_0}{\cot \chi} \frac{2}{\gamma_{M_\infty}^2} \frac{\gamma_{M_0}^2}{\lambda} \cdot \frac{P_0}{P_\infty} \right] \cdot I_*^{(0)} \quad (7.15)$$

where

$$\begin{cases} I_*^{(0)} = \zeta_* I^{(0)} \\ I^{(0)} = \frac{1}{2} P^{(0)}(0) \end{cases}$$

and $P^{(0)}(0) = \int_{-1}^1 P^{(0)} d\zeta$, given in equation (6.17)b

$$-c_{M\alpha}^{(0)} = \left[\frac{1}{\lambda \cot \chi} \cdot \frac{2}{\gamma_{M_\infty}^2} \frac{\gamma_{M_0}^2}{\lambda} \frac{P_0}{P_\infty} \right] \cdot \left(\frac{2}{3} - x_0 \right) \cdot I_*^{(0)} \quad (7.16)$$

$$c_{L\alpha}^{(1)} = \left[\frac{\cos \alpha_0}{\lambda \cot \chi} \cdot \frac{2}{\gamma_{M_\infty}^2} \frac{\gamma_{M_0}^2}{\lambda} \frac{P_0 U_0}{P_\infty U_\infty} \right] \cdot I_*^{(1)} \quad (7.17)$$

$$\begin{cases} I_*^{(1)} = \zeta_* I^{(1)} \\ I^{(1)} = \frac{1}{3} P(0) + \frac{x_0}{2} \underline{p}(0) \end{cases}$$

$$-c_{M\alpha}^{(1)} = \left[\frac{1}{\lambda \cot \chi} \cdot \frac{2}{\gamma_{M_\infty}^2} \cdot \frac{\gamma_{M_0}^2}{\lambda} \cdot \frac{P_0 U_0}{P_\infty U_\infty} \right] \cdot II_*^{(1)} \quad (7.18)$$

$$\begin{cases} II_*^{(1)} = \zeta_* II^{(1)} \\ II^{(1)} = \frac{1}{4} P(0) + x_0 \left(\frac{1}{3} \underline{p}(0) - \frac{1}{3} P(0) - x_0^2 \left(\frac{1}{2} \underline{p}(0) \right) \right) \end{cases}$$

where $P(0)$ and $\underline{p}(0)$ are given in equations (6.33) and (6.41) respectively.

ii) The derivatives in the outer region :

Substituting equations (7.8)c and (7.8)d into equations (7.13)c, (7.13)d, (7.14)a and (7.14)d, after some simple integration procedure the contributions to the stability derivatives become

$$C_{L\alpha}^0 = \cos \alpha_0 \cdot \frac{2}{\gamma M_\infty^2} \frac{P_*}{P_\infty} \cdot p^0 \cdot (1 - \hat{\sigma} \cot \chi_*) \quad (7.19)$$

where $\hat{\sigma} = \tan \chi$

p^0 is given by equation (6.1)a

$$-C_{M\alpha}^0 = C_{N\alpha}^0 \cdot \left(\frac{2}{3} - x_0 \right) \quad (7.20)$$

where $C_{N\alpha}^0 = \sec \alpha_0 \cdot C_{L\alpha}^0$

$$C_{L\alpha}^1 = \cos \alpha_0 \cdot \left[\frac{2}{\gamma M_\infty^2} \cdot \frac{P_* u_*}{P_\infty U_\infty} \cdot \frac{1}{3} (1 - \hat{\sigma} \cot \chi_*) \right] \cdot I^1 \quad (7.21)$$

where $I^1 = 2A_1 + C_1 (\cot \chi + \cot \chi_*) + 3D_1$

A_1, C_1 and D_1 are given in equations (6.4).

$$-C_{M\alpha}^1 = \left[\frac{1}{3} (1 - \hat{\sigma} \cot \chi_*) \frac{2}{\gamma M_\infty^2} \left(\frac{P_* u_*}{P_\infty U_\infty} \right) \right] \cdot II^1 \quad (7.22)$$

$$\left\{ \begin{array}{l} II^1 = II_0 - x_0 II_1 - x_0^2 II_2 \\ II_0 = \frac{1}{2} \left[3A_1 + \frac{3}{2} C_1 (\cot \chi + \cot \chi_*) \right] \\ II_1 = 2 (A_1 - \hat{d}_{10}) + C_1 (\cot \chi + \cot \chi_*) \\ II_2 = 3 \hat{d}_{10}, \text{ where } \hat{d}_{10} = \tilde{c}_1 \hat{d}_5 + \tilde{c}_2 \hat{e}_5 - \tilde{D} \quad (\text{equation} \end{array} \right.$$

(6.35)).

iii) The total expressions :

The total expression for the stiffness derivatives are obtained by adding the ones in the inner region (equations (7.15) and (7.16) to the outer ones (equations (7.19) and (7.20)), i.e.

the lift :

$$C_{L\alpha} = C_{L\alpha}^{(0)} + C_{L\alpha}^0 \quad (7.23)$$

the moment :

$$-C_{M\alpha} = \left(-C_{M\alpha}^{(0)} \right) + \left(-C_{M\alpha}^0 \right) \quad (7.24)$$

Similarly, the damping derivatives are obtained by adding equations (7.17) and (7.18) to equations (7.21) and (7.22), i.e.

the lift :

$$C_{L\dot{\alpha}} = C_{L\dot{\alpha}}^{(1)} + C_{L\dot{\alpha}}^1 \quad (7.25)$$

the moment :

$$-C_{M\dot{\alpha}} = \left(-C_{M\dot{\alpha}}^{(1)} \right) + \left(-C_{M\dot{\alpha}}^1 \right) \quad (7.26)$$

7.3 The Stability Criteria

It is desirable to find the dynamic stability boundaries for design purposes. When the damping moment $C_M \dot{\alpha}$ is negative, it indicates the wing oscillation is stabilizing. While the damping moment $C_M \dot{\alpha}$ is positive, the wing oscillation becomes destabilizing. Hence the dynamic stability boundary is defined when the oscillation becomes neutral, this is represented by demanding

$$C_M \dot{\alpha} = 0 \quad (7.27)$$

Explicitly, equation (7.27) should read, by combining the expressions obtained in equations (7.18) and (7.22),

$$\left[\frac{\nu_D}{2} \dot{P}(0) + \nu_C \cdot II_2 \right] \cdot x_o^2 + \left[\nu_C \cdot II_1 - \frac{\nu_D (\dot{P}(0) - P(0))}{3} \right] \cdot x_o - \left[\nu_C \cdot II_0 + \frac{\nu_D}{4} P(0) \right] = 0 \quad a$$

(7.28)

where

$$\nu_D = \frac{2}{\gamma M_\infty^2} \cdot \frac{P_o u_o}{P_\infty U_\infty} \cdot \frac{\gamma M_o^2}{\lambda} \cdot \frac{\zeta_*}{\lambda \cot \chi} \quad b$$

$$\nu_C = \frac{2}{\gamma M_\infty^2} \cdot \frac{P_* u_*}{P_\infty U_\infty} \cdot \frac{\cot \chi - \cot \chi_*}{3 \cot \chi} \quad c$$

For given α_o , χ and γ , stability boundaries are presented in the $M_\infty - x_o$ diagrams as shown in Figures 24, 25 & 26. For given M_∞ , x_o and γ , the stability boundaries are presented in the $\chi - x_o$ diagram as shown in Figure 27. It can be generally stated that these unstable regions occur only when the given flow conditions are near the shock detachment zone (see Figure 2), for both flat delta and wedge cases. It is also observed that in the $M_\infty - \alpha_o$ diagrams, the peak of the stability boundaries occurs around $x_o = \frac{1}{3}$ for wedges and $x_o = \frac{1}{2}$ for flat delta wings.

The peak indicates the critical Mach number \hat{M}_∞ of the instability, and also the critical pitching axis location \hat{x}_0 .

The critical Mach number \hat{M}_∞ can be obtained from the condition when equation (7.28) provides double roots of x_0 and the critical pitching axis location \hat{x}_0 is simply given by

$$\hat{x}_0 = - \left\{ \frac{\nu_{c II_1} - \frac{\nu_D p(0) - P(0)}{3}}{2 \left[\frac{\nu_D}{2} p(0) + \nu_{c II_2} \right]} \right\}_{M_\infty = \hat{M}_\infty} \quad (7.29)$$

In the case of $\chi \rightarrow 0$, implying $\nu_D = 0$, equation (7.28)a can be written simply as*

$$\hat{d}_{10} \cdot x_0^2 + \frac{2}{3} (A_1 - \hat{d}_{10}) x_0 - \frac{1}{2} A_1 = 0 \quad (7.30) a$$

consequently it yields

$$\hat{x}_0 = \frac{1}{2} \quad (7.30) b$$

This result seems to represent a conjecture based on observations for all the cases of flat delta wings, that the critical pitching axis location is independent of the given flow condition. However, no proof is given here as the general form of x_0 in equation (7.29) is quite involved.

On the other hand, for the case of 'one-side' wedge (essentially a flat plate), with the pitching axis located on the surface, the stability boundary, as the two-dimensional counterpart of equation 7.28,

* Note that $C_1 \cot \chi \rightarrow 0$ as $\chi \rightarrow 0$

becomes (see Hui AIAA, 1969)

$$\hat{d}_{10} \cdot x_0^2 + \frac{1}{2} (A_1 - \hat{d}_{10}) - \frac{A_1}{3} = 0 \quad (7.31) \text{ a}$$

consequently it yields

$$\hat{x}_0 = \frac{1}{3} \quad (7.31) \text{ b}$$

7.4 The limits of $C_{M\dot{\alpha}}$ and $C_{M\ddot{\alpha}}$ as $\chi \rightarrow 0$

One question may arise as to why the limiting case of $C_{M\dot{\alpha}}$ for a delta wing as $\chi \rightarrow 0$ gives different values to that for a one-sided wedge (see Figure 19). For the same reason, one may ask why the critical pitching axis location \hat{x}_0 differs in both cases (see equations (7.30)b and (7.31)b). This may be explained by the fact that $C_{M\dot{\alpha}}$ wedge is defined by a single integral but $C_{M\dot{\alpha}}$ delta is inherently defined by double integrals; hence, even in the limiting case as $\chi \rightarrow 0$ of $C_{M\dot{\alpha}}$ delta, it differs from $C_{M\dot{\alpha}}$ wedge by a factor due to 'moment' of one-order higher. For example, at the same flow condition for a wedge and a delta wing (of χ) with $x_0 = 0$ whose out-of-phase pressures read respectively

$$p^1_{\text{wedge}}(x, 0) = A_1 x \quad (7.32) \text{ a}$$

$$p^1_{\text{delta}}(x, 0, z; \chi) = A_1 x + C_1 z \quad (7.32) \text{ b}$$

Numerically, as $\chi \rightarrow 0$ $A_1 \rightarrow A_1'$ and $C_1 \rightarrow 0$

thus $\lim_{\chi \rightarrow 0} p^1_{\text{delta}} = p^1_{\text{wedge}}$

However, in using them to evaluate for $C_{M\dot{\alpha}}$, for the case of wedges

$$C_{M\dot{\alpha}\text{ wedge}} = \frac{1}{L} \int_0^L P_{\text{wedge}} x \, dx = \frac{A_1}{3} \quad (7.33) \text{ a}$$

for the case of delta wing, by equation (7.26)

$$\lim_{\chi \rightarrow 0} C_{M\dot{\alpha}\text{ delta}} = C_{M\dot{\alpha}}^1 = \frac{1}{2} A_1 \quad (7.33) \text{ b}$$

Thus

$$\left(\frac{C_{M\dot{\alpha}\text{ wedge}}}{C_{M\dot{\alpha}\text{ delta}}} \right)_{\chi \rightarrow 0} = \frac{2}{3} \quad (7.34)$$

This can be observed in Figure 19.

Consequently, the same explanation is responsible for the different value in \hat{x}_0 for both cases. Also, for stiffness moment $C_{M\alpha}$, the well-known fact that the aerodynamic centre (the neutral static stability, i.e. $C_{M\alpha} = 0$) of a wedge and of a delta wing occur at $x_0 = \frac{1}{2}$ and $x_0 = \frac{2}{3}$ is due to the same argument presented above.

7.5 Stability Derivatives for two-sided delta wings

The purpose of introducing a two-sided delta wing (see Figure 1-H) is a heuristic one. It is difficult to justify by only studying the outer surfaces of such a wing without considering the internal flow field within these two surfaces, particularly for cases where M_∞ is low or α_0 is large. Because the internal flow field may be subject to vortex separations and ^{may} produce internal shock waves as a result of leading edge expansion, both are of a complex nature.

In order to compare the results of the present theory with those of a wedge (planar case) and of a cone (axisymmetric case), only the contribution from the outer surfaces of a two-sided delta wing are considered. Besides, as the external flow field is enclosed by the attached shock waves, the effects due to the internal flow field mentioned above may be subject to a separate study.

Hence, with the pitching axis h_0 defined from 0 to 1 (see Figure 1-H, $h_0 = x_0 \cos \alpha_0$) and the reference plan form area $S' = \cot \chi \cdot \sec \alpha_0$, the out-of-phase lift and moment for the two-sided wing can be written as

In the inner region,

$$C_L^{(1)} \dot{\alpha} = \frac{4}{\cot \chi \sec \alpha_0} \int_{x=0}^{x=\sec \alpha_0} \int_{z=0}^{z=x \cot \chi_*} C_p^{(1)} dx dz \quad (7.35)a$$

$$-C_M^{(1)} \dot{\alpha} = \frac{4}{\cot \chi \sec \alpha_0} \int_{x=0}^{x=\sec \alpha_0} \int_{z=0}^{z=x \cot \chi_*} C_p^{(1)} (x - h_0 \cos \alpha_0) dx dz \quad (7.35)b$$

In the outer region,

$$C_L^1 \dot{\alpha} = \frac{4}{\cot \chi \sec \alpha_0} \int_{x=0}^{x=\sec \alpha_0} \int_{z=x \cot \chi_*}^{z=x \cot \chi} C_p^1 dx dz \quad (7.36)a$$

$$-C_M^1 \dot{\alpha} = \frac{4}{\cot \chi \sec \alpha_0} \int_{x=0}^{x=\sec \alpha_0} \int_{z=x \cot \chi_*}^{z=x \cot \chi} C_p^1 (x - h_0 \cos \alpha_0) dx dz \quad (7.36)b$$

where h_0 represents the pitching axis location lying in the center plane, parallel to the plane of the free stream and $0 \leq h_0 \leq 1$.

Making use of equations (7.6)c and d, equations (7.8)c and d, equations (7.35)a and (7.35)b become

$$\bar{C}_L^{(1)} = \frac{2 \nu_D}{\cos^3 \alpha_0} \left\{ \frac{1}{3} P(0) + \frac{h_0 \cos \alpha_0}{2} \underline{p}(0) \right\} \quad (7.37) \text{ a}$$

$$-\bar{C}_M^{(1)} = \frac{2 \nu_D}{\cos^3 \alpha_0} \cdot \left\{ \left(\frac{1}{4} - \frac{h_0 \cos \alpha_0}{3} \right) P(0) + h_0 \cos \alpha_0 \cdot \left(\frac{1}{3} - \frac{h_0 \cos \alpha_0}{2} \right) \underline{p}(0) \right\} \quad (7.37) \text{ b}$$

and equations (7.36)a and (7.36)b become

$$\bar{C}_L^1 = \frac{2 \nu_C}{\cos^3 \alpha_0} \cdot \left\{ 2 A_1 + C_1 (\cot \chi + \cot \chi_*) + 3 \hat{d}_{10} \cdot h_0 \cos \alpha_0 \right\} \quad (7.38) \text{ a}$$

$$-\bar{C}_M^1 = \frac{2 \nu_C}{\cos^3 \alpha_0} \cdot \left\{ \left(\frac{3}{2} - 2 h_0 \cos \alpha_0 \right) \left[A_1 + \frac{C_1}{2} (\cot \chi + \cot \chi_*) \right] + (2 - 3 h_0 \cos \alpha_0) h_0 \cos \alpha_0 \cdot \hat{d}_{10} \right\} \quad (7.38) \text{ b}$$

Finally, the stability derivatives for a two-sided delta wing read

$$\bar{C}_L = \bar{C}_L^{(1)} + \bar{C}_L^1 \quad (7.39)$$

$$-\bar{C}_M = \left(-\bar{C}_M^{(1)} \right) + \left(-\bar{C}_M^1 \right) \quad (7.40)$$

In Figure 13, the damping derivative (equation (7.40)) for a two-sided wing of $\chi = 30^\circ$ is compared with a wedge and a cone of semi-apex angle of $\alpha_0 = 9^\circ$.

8. RESULTS AND DISCUSSION

In this Chapter, a complete description of the figures (from Figures 2 to 29) will be given first. Subsequently, in the rest of the sections, a full-length discussion will be carried on with regard to the new contributions due to the present theory, its applicability and its limitations.

8.1 Description of the figures

Figures 1 (from 1A to 1J) are all sketches, not necessarily drawn to the physical scale, but to illustrate the descriptions in the text. The solid lines shown in Figure 2 are the shock-attachment (to the leading edges) boundaries, based on equation (A.9). While the dotted lines are the sonic lines, based on equation (A.10). It is seen that as $\chi \rightarrow 0$, the attachment boundary of the flat delta wing approaches to that of the wedge. For axisymmetric flow past a cone, the apex shock attachment boundary encloses a wider range of M_∞ and α_0 (the apex angle); this is expected. In Figures 3, 4 and 5, the shock attachment boundaries and sonic lines are presented in the $\chi - \alpha_0$ diagrams for the flat delta wings ($\Gamma = 90^\circ$) and caret wings of small bend ($\Gamma = 80^\circ$, $\Gamma = 60^\circ$), respectively.

The details of calculation are given in Appendix A. It should be pointed out that the narrow regions enclosed by each solid line and dotted line represent a non-uniform, shock-attached flow field, confined by the 3D Mach cones. Since the present theory is based on a uniform flow field, the valid region of applicability should be bounded away from the sonic line, not the solid line. This point will be further elaborated in Section 8.4 .

A typical pressure distribution based on Hui's theory (Ref. 7) is presented in Figure 6. The pressure is calculated according to

equation (6.4). When compared with other numerical solutions (Refs. 5 and 6), the overall deviation is less than 2% except near the sonic line ($\bar{z}/\bar{x} = .47$). These deviations may be corrected by a second order approximation (i.e. $O(\chi^2)$) (see Ref. 7). Further discussion on this point can be found in Section 8.4 (ii).

Figures 7 and 8 show the in-phase lift $C_{L\alpha}$ (or the lift slope) due to changes of mean incidence α_0 and sweptback angle χ respectively.

In checking with Tables 1 and 2, together by observing Figure 7, it can be stated that C_L and $C_{L\alpha}$ are of small deviation from its corresponding $C_{L_0\alpha}$ value of a wedge. For steady lift, as stated in Chapter 4 (Sec. 4.2), the deviation appears to be no more than 4% for $M_\infty = 4$, $\chi = 50^\circ$ and $\alpha_0 \leq 15^\circ$. For the same case, the in-phase lift, as calculated by all three methods by exact differentiation (equation (4.17)b), the largest deviation is no more than 8%, given by the 'linear' method. However, when the flow region approaches the detachment zone, the in-phase lift due to 'local-stretched' and 'global-stretched' deviate from the wedge value rather rapidly. In the normal applicable range, say $0 < \alpha_0 \leq 15^\circ$, these two methods provide almost identical results for C_L (see Table 1) and $C_{L\alpha}$. This then partly justifies the later application of the 'global-stretched' method to the unsteady flow. When $\alpha_0 \rightarrow 0$, $C_{L\alpha}$ due to Miles' quasi-steady theory is the same as $C_{L_0\alpha}$, given by the well-known

$$\text{formula } C_{L\alpha} = \frac{2}{\sqrt{M_\infty^2 - 1}} = .516 \text{ for } M_\infty = 4.0, \text{ independent of } \chi.$$

Figure 8 indicates $C_{L\alpha}$ is generally insensitive to χ variations, particularly for cases where α_0 is small. A similar conclusion was stated by Babaev (Ref. 4) from his observation of the normal force. The plots of $C_{L\alpha}$ are based on the perturbation method

(equation (7.10)c) and on the exact differentiation (equation (4.17)b). The difference between these two curves represents the measure of the interaction due to the in-phase wedge flow and the 3-D mean flow. Note that when $\alpha_0 = 5^\circ$ the difference becomes indistinguishable. This is expected, since the global feature of the 3-D mean flow becomes essentially two-dimensional, the interaction is negligible. The study in Figure 8 thus partly justifies the later application of the 'perturbation-method' formulation in the inner region (namely, dropping the terms of $O(\epsilon \delta)$ for unsteady flow (see equations (3.28) and (3.30), Problems B and D).

Figure 9 illustrates the application of the similarity rule for the non-affine wing-body combinations. For a fixed added volume parameter, $\overline{G}_V = 1$, the added volume need not be of affine geometry. For moderate and high Mach number it is clearly shown that the caret wing with added volume produces the highest $C_{L\alpha}$. Careful study of equations (5.26), (5.27), (5.29) and (5.30) reveals the similarity functions and their derivatives behave as $S_0, S_{0\alpha} < 0, \mathcal{V}_0, \mathcal{V}_{0\alpha} > 0$ and $\mathcal{T}_0, \mathcal{T}_{0\alpha} > 0$. Hence, it can be stated that the sweptback effect reduces both C_L and $C_{L\alpha}$, whereas the volume and small-bend (dihedral) effects increase both C_L and $C_{L\alpha}$. It is also important to note that in the calculation scheme, the reference line of the basic wedge flow of these configurations should be carefully chosen (see Figure 1-F).

Figure 10 presents the comparison of the present theory (linear formulation) and the experimental data in the low supersonic range. Based on a model (wing A) of $\chi = 49.1^\circ$ and thickness $\tilde{\tau} = 0.05$ suggested by Orlik-Ruckemann et al (Ref. 48), $C_{M\alpha}$ is calculated according to equations (5.30) and (5.34). In the calculation scheme, $\alpha_0 = x_0 = \overline{G}_V = 0$ and the small-bend parameter $\hat{\tau}$ assumes a negative

value. Since upper and lower surfaces of the wing A are symmetric, the total $C_{M\alpha}$ is obtained simply by multiplying the $C_{M\alpha}$ of one side by 2. Good agreement is found with Hall & Osborne's data (Ref. 49). Figures 11 and 12 show the effects of pitching axis location x_0 on the in-phase moments at moderate and high Mach numbers. It is observed that the effect of x_0 on $C_{M\alpha}$ is not large for high Mach numbers. Figure 13 further compares the in-phase moment and out-of-phase moment $C_{M\dot{\alpha}}$ (or damping-in-pitch) for a wedge and a flat delta wing ($\chi = 50^\circ$) at $M_\infty = 4.0$ and $\alpha_0 = 15^\circ$. Figure 14 compares $C_{M\dot{\alpha}}$ for a wedge and a wing at a higher Mach number ($M_\infty = 10$). It is seen that a wing has more positive damping than a wedge (i.e. $-C_{M\dot{\alpha}}$ is positive) when x_0 is placed in the neighbourhood of the apex.

Figure 15 compares the contribution of the damping-in-pitch from the inner and the outer regions. In the case considered contributions from both regions are of the same order. However, if α_0 approaches zero, the outer contribution dominates and $C_{M\dot{\alpha}}$ becoming insensitive to χ , approaches to the corresponding value of the wedge; the latter fact can be cross-checked by Figure 21. Figure 16 exhibits $C_{M\dot{\alpha}} \sim x_0$ variations for a wedge, a two-sided wing and a cone. It is seen that for all x_0 ($0 \leq x_0 \leq 1$), the present case indicates the cone gains highest damping. When the out-of-phase normal forces $C_{N\dot{\alpha}}$ for these configurations are compared at $x_0 = 0$, similar trends are found in the low to moderate Mach range ($M_\infty \approx 2. \sim 7.$).

Figures 18 and 19 study the effect of free stream Mach numbers on $C_{M\dot{\alpha}}$. In Figure 18, drastic changes are observed for $C_{M\dot{\alpha}}$ at different x_0 when the flow region approaches the shock detachment zone. In Figure 19, it is seen that when M_∞ becomes higher, the values of $C_{M\dot{\alpha}}$ for different χ are rather insensitive to the free stream M_∞ . Note that when $\chi \rightarrow 0$, $C_{M\dot{\alpha}}$ for a delta wing does not approach to $C_{M\dot{\alpha}}$

for a wedge (lowest line), but differs by a ratio of 2/3 (equation (7.34)). An explanation of this was given in Section 7.4.

Figures 20 and 21 investigate the mean incidence effect on $C_{M\dot{\alpha}}$. In these two cases studied, it seems that the effect of α_0 appears to be more important than the effects of M_∞ or χ . Particularly, a rapid change of $C_{M\dot{\alpha}}$ at $x_0 = 0$ is observed. Also, it is noticed that in Figure 21, when the flow region approaches the shock detachment zone, $C_{M\dot{\alpha}}$ for the delta wing and for the wedge break down along gradients of opposite direction for the same pitching location x_0 (see (i) of Sec. 8.4 for further discussion).

Figures 22 and 23 examine the sweepback angle effects on $C_{M\dot{\alpha}}$. Similar to the earlier finding in Figure 19, less dependence of $C_{M\dot{\alpha}}$ on χ is observed for $M_\infty = 10$ than for $M_\infty = 1.5$. The highest damping is obtained when x_0 is located at the wing apex in the former case; whereas in the latter case, it is obtained when x_0 is placed at the trailing edge.

Figures 24, 25, 26 and 27 are plots of some stability boundaries for delta wings and wedges. The detailed derivation and partial description of these diagrams can be found in Section 7.3. Further discussion and common features of these stability boundaries can be put forth as follows :

- 1) The unstable regions for delta wings generally shift rearwards from the unstable regions for (one-sided) wedges (Figures 24, 25 & 26). This is due to the locations of the critical pitching axis x_0 for both cases being shifted by an amount of $1/6$ (see equations (7.30)b and (7.31)b).

- 2) In all cases, the unstable regions occur and gradually enlarge when the flow region approaches the zone of shock detachment (Figures 25 and 26).

3) Unlike the stability boundaries for wedges (e.g. Refs. 23 & 37) and for wings given by potential theories (e.g. Refs. 19 and 20), in some cases of the present study (Figures 24 and 26), closed boundaries (of bubble shape) are formed. In Figure 24, two separate unstable regions appear, one of them occurs near the trailing edge, and extends downstream. The bubble-shape stability boundary is not new, and occurs in the results of Miles' study (Ref. 14, p. 83) for rectangular wings. However, to the best of the author's knowledge, the appearance of two separated unstable regions has not been claimed in the previous stability analysis for either wings or bodies. Whether or not the lower unstable region exists needs further investigation (see (i) of Section 8.4).

4) The occurrence of unstable region near the trailing edge and further downstream is interesting and yet needs careful re-examination. As these regions (Figures 24 and 27) occur very near to the shock detachment zone, it is felt that its existence may be subject to the question of the valid region of the present theory. This point will be further discussed in Section 8.4 .

From Figure 2 to Figure 27, all cases assume perfect gas of specific heat ratio of $\gamma = 1.4$. On the last two figures, Figures 28 and 29, effects of real gas of different specific heat ratios ($\gamma = \frac{n+2}{n}$, $n = 3, 5, 7$) are investigated.

In Figure 29, the effect of γ on $C_{M\alpha}$ are shown for a wing of $\chi = 50^\circ$. It is seen that a decrease in damping occurs at lower Mach number $M_\infty = 4$, when the value of γ decreases.

It is realized now, unlike the Newtonian-flow model, the present study can let M_∞ approach to infinity and let γ independently vary (without assuming $\gamma = 1$ simultaneously). Or one can fix γ and vary M_∞ independently. Hence, even in the hypersonic flow range, the present theory embraces a larger scope of applicability than that of the

Newtonian theory. This fact has been pointed out earlier in one of Hui's studies (Ref. 53 , Aeronautical Acta) of hypersonic flow.

8.2 The flow field solutions: new contributions

In the following sub-sections, a brief review will be made in order to assess the new contributions due to the present theory.

i) The steady mean flow :

The uniform flow solutions in the outer region for a delta wing, a caret wing and a V-shaped (or diamond) wing have been rederived in a unified manner (Appendix A). Previously, these solutions have been originally obtained by Hui (see Refs. 7, 8 and 54). However, these solutions he obtained are not unified due to the fact that the geometrical relationship is specified individually for each case considered. It is shown in Appendix A and Ref. 51 (Liu) the geometrical relation of the flat delta wing becomes a special case of that of the delta-wing family, which also contains the caret wing and the diamond wing.

ii) The mean flow and the in-phase flow :

(a) Differentiation Method: Exact differentiation of Hui's mean flow solution provides useful analytical formulae for $C_{L\alpha}$ and $C_{M\alpha}$ (see equations (4.17) and (4.18) and Appendix D).

(b) Similarity Rule : Based on the 'linear' formulation (Chapter 5), the application of the spanwise integral technique yields the generalized similarity rule (Section 5.4). The rule states that for given M_∞ and α_0 , the steady lifts, moments and the in-phase lifts and moments can be expressed in a combination of terms. These terms separately account for the sweepback angle effect (χ), the added volume effects (σ_v), and the small bend effects ($\hat{\tau}$). This rule is most convenient for practical uses such as generating a series of data from one single

experimental result. In fact, it is a generalized similarity rule for non-affine bodies of the added volume; it includes affine body shapes as a special case (see Fig. 1-H). This is because the lifts and moments only depend on the global parameter of added volume, namely σ_v , but do not depend on the body shape distribution, namely $\hat{G}(\zeta)$.

(c) Small bend approximation : The classical technique of thin wing expansion (e.g. see Van Dyke, Ref. 56) is formally employed in Chapter 5 (Sections 5.1 and 5.2) to account for the small-bend effect of a caret wing ($\hat{\tau} > 0$) or a V-shape wing ($\hat{\tau} < 0$). For the first order approximation $O(\hat{\tau})$, the result shows good agreement with experiment (Figure 10). Second order approximation (or higher) (see equation (5.6)) can be carried out in a straight-forward manner if one wishes to account for larger bend effects, without difficulty. Hence, in Van Dyke's sense (Ref. 56), the approximation is a 'rational' one.

(d) Applicable configurations : (see Figure 1-F)

In combining the methods of (a), (b) and (c), the lifts and moments (i.e. C_L , C_M , $C_{L\alpha}$ and $C_{M\alpha}$) of a number of vastly different configurations can thus be calculated by the present theory (Chapters 4 and 5). Some examples are shown in Figure 1-F. Two categories are specified; namely, the large α_0 case ($\alpha_0 > 0$) and the small α_0 case ($\tilde{\tau} > \alpha_0$, $\alpha_0 \geq 0$).

In the former case, the theory is applicable only to the windward side of the wing-body (see Figure 9). In the latter case, closed profiles can be treated provided that the thickness $\tilde{\tau}$ is always larger than α_0 so that the shock waves are attached on the upper and the lower surfaces. These surfaces need not be symmetrical (e.g. full caret), and α_0 need not be zero. When the wing is symmetrical

(e.g. $\tilde{\tau}_1 = \tilde{\tau}_2$ in full diamond wing) and it is placed at zero incidence, the present theory should be compared with the results provided by previous non-linear potential theories (e.g. Landahl, Ref. 22).

iii) Out-of-phase flow :

(a) Exact outer flow solutions : Within the frame of small-amplitude and small-frequency oscillation (to the orders of $O(\epsilon)$ and $O(\epsilon k)$), the solutions of Problem A and C obtained in Chapter 6 are exact. Referring to Section 6.7, solutions (6.3) can be described in the following observation. It is clear that for given conditions M_∞ , α_0 and χ , the gradients of the out-of-phase pressure, density and velocities (i.e. P^1 , R^1 , U^1 , V^1 and W^1) are all constants (see (iii) of Section 6.2). This implies that all these flow properties and velocities are constant along the parallel planar surfaces. Hence, the nature of these solutions are similar to the conical flow field in which flow properties and velocities are constant along conical rays. In fact, solutions (6.3) are special cases of a so-called 'quasi-conical' flow, a generalized conical flow. (See equation (1.2), $n = 1$, or see Ref. 57).

(b) Quasi-conical flow : Suggested by the solutions of outer flow, the inner flow (Problem D, Section 6.4) is proved again quasi-conical, but in a more general sense (see equation (6.20)). In other words, the solutions of Problem D can be written in a similarity form namely, $P^{(1)}(\xi, \eta, \zeta) = \xi^n \mathcal{P}(\eta, \zeta)$, ($n = 1$ for flat delta). This finding is confirmed by checking all the boundary conditions considered (from equation (6.18) to equation (6.21)). Hence, Problem D can be solved as a reduced 2-D problem. This enables a formulation of $\mathcal{P}(\eta, \zeta)$ alone (see equation (6.21)).

It is observed that although the quasi conical form has been suggested previously in Ref. 17, it was only based on the unsteady potential flow model and no proof was given.

(c) Superposition solutions : Since the present theory is based on a linearized formulation, solutions of Problem D can be treated by superposition of two solutions (see equations (6.20)); namely, the apex solution and the axis solution. The apex solution ((ii) of Sec. 6.4) corresponds to a case where $x_0 = 0$, and the axis solution ((iii) of Sec. 6.4) corresponds to a case where $0 < x_0 \leq 1$ ($x_0 \neq 0$). While the apex solution is quasi conical, the axis solution is conical. This method of solution in low frequency unsteady flow is new, which may also be possible in application to the unsteady flow analyses of thin axisymmetric bodies or to low aspect ratio wings with shock waves.

(d) Higher approximations in k : The present study is restricted to the slow oscillation of a rigid delta wing planform. In the range of hypersonic flow, however, the oscillatory frequency, $\bar{\omega}$, need not be small, as the uniform freestream velocity U_∞ becomes very large, rendering the reduced frequency k considerably small. Thus, it may be remarked that in the unified range of Mach number considered, the stability derivatives obtained here are accurate enough for slow oscillatory frequencies so that $\bar{\omega} \ll \frac{U_\infty}{L}$.

From an aeroelastician's viewpoint, it is also important to study the bending oscillation of an elastic delta wing of given modes or to perform the flutter analysis. In these cases, higher frequency solutions are most desirable; the present formulation indeed admits higher approximations for k , as it is a perturbation problem expanded in small parameter k (see equations (2.14) and (2.15)). Hui (Chapter III, Ref. 34) previously pointed out that the exact

formulation procedure for a wedge can be carried out to any order in k ($k < 1$). It is believed that similar statement can be made for the present case, as the present formulation is a formal generalization of Hui's work; hence, it should preserve its nature of being a rational approximation in k .

iv) The pressure formulation :

In the formulation of the inner flow problems of (i), (ii) and (iii), the flow dependent variables are eliminated to a single variable, namely the perturbed pressure. The pressure formulation for the steady mean flow was first proposed by Lighthill (Ref. 71), Malmuth and Hui (Refs. 52 and 7). The pressure formulation for the unsteady flow equations was originated by Hui (Refs. 34 and 37), but he did not completely formulate these problems in terms of pressure alone. The basic difficulty in achieving a pressure formulation arises from the unsteady shock boundary condition. This was overcome, however, by realizing the out-of-phase flow is quasi-conical (see Sec. 6.4).

The benefits of pressure formulation are many, namely :

- (a) it reduces the problem to one similar to the unsteady potential flow problem, with the additions of Mach cone and shock boundary conditions (the present problem is a free boundary problem);
- (b) it allows the application of the spanwise integral method;
- (c) its solution can be readily integrated to yield forces and moments - an exact and direct way of obtaining damping-in-pitch;
- (d) it can be readily extended to the problems of a delta wing in rolling and yawing oscillation; the only alternative will be the tangency condition.

In checking out the pressure formulation, the unsteady wedge flow was re-derived as a special case of the present 3-D formulation (see Appendix G).

8.3 The Method of Spanwise Integration

In their previous studies, Malmuth and Hui (Refs. 45 and 46) originated the method of Spanwise Integration to examine the so-called 'area rule' in hypersonic and supersonic flows. In the present study, this method is further generalized to account for the unsteady flow (Chapter 6) and is used to construct the generalized similarity rule (Chapter 5). Since this method is being employed extensively throughout the present theory (Problems B and D), it is essential to re-examine its principle and its practical applications.

i) The principles : The method is essentially an integral method, which integrates $\mathcal{P}(\eta, \zeta)$ say, over the spanwise direction ζ , resulting in O.D.E. formulation in $P(\eta)$ (see equations (6.24) and (6.25)). It resembles the Fourier transform in the sense that the end point values at Mach cone for $\mathcal{P}(\eta, \zeta)$ and its derivatives need to be specified. On the other hand, unlike the Fourier transform, the present integral space is a physical one (in η) and no inverse transform is available. The method yields an exact global information for steady or unsteady flow most efficiently. The 'local' (or the flow field) solution may be recovered from the global one in solving the integral-equation formulation by a method similar to that of Malmuth (Ref. 50).

ii) The present contributions :

(a) Full-range integration :

Only half-range integration, whose integration limits being from $\zeta = 0$ to the Mach cone, are defined in Refs. 45 and 46. In Chapters 5 and 6, full-range integrations are introduced, whose limits are from one side of the Mach cone to the other side (see Appendix E). In this way, the properties in the centre line $\zeta = 0$ need not be

specified. Hence, one difficulty encountered in the present unsteady formulation can then be avoided.

(b) The operators and the operation :

Operators representing the full-range integration are defined in Appendix E. Based on the definition of the full-range integration, integrals involving odd-function integrands are identically zero (e.g. see equation (5.17)). The operational rules thus greatly simplify the scheme of integration. The effectiveness of using the operator was clearly demonstrated in Chapters 5 and 6.

(c) Generalization to the unsteady flow :

In Chapter 6, Problems B and D are successively solved by means of the full-range spanwise integration. The present method, therefore, is considered as a generalized method which includes the global treatment of the low frequency oscillatory flow.

iii) Other merits :

(a) The exact evaluation of a_1' : When equation (4.2)b and equation (4.9) are compared, it is seen that the latter expression of a_1' is an exact one, as an outcome of the spanwise integration. Also, it should be pointed out that the evaluation of a_1' (or $a_1'^{(0)}$ in Problem B) need not be carried out on the mean shock position ($\eta = H$). In fact, if one applies the operator equation (E.2) on the mean flow problem, it can be shown that for η in ($0 \leq \eta \leq H$) a_1' remains invariant at any η . While this fact has not been mentioned either in Refs. 45 or 46.

Accordingly, the above finding may shed some light in obtaining the 'local' solution of Problem D (see equations (6.23)) in the future.

(b) More direct method : The common practice in obtaining $C_{L\dot{\alpha}}$ and $C_{M\dot{\alpha}}$ say, usually resorts to solving the unsteady flow

field solution first and then upon integration of the pressure results in Forces or Moments. It has been shown that for the same purpose, the present method is more direct in arriving at this global information, and in the same time without loss of the exactness of the problem.

(c) Further applications : In Chapter 5, the method is applied to deal with wings of small bend and added volume (also see (ii) of Sec. 8.2). It is possible that the method can also be used to deal with these wing-bodies for unsteady flow problems (e.g. Problem D).

8.4 The limitations of the present theory

In this section, the general valid region of the present theory and other restrictions will be investigated. The non-uniformity of the mean flow solution (the linear formulation) will be discussed and the improvement of the perturbation scheme will be outlined.

i) The scope of the unified theory :

By 'unified theory' it is meant that the flow region is unified in its Mach number and it makes no distinction for supersonic or the hypersonic flow so long as the shock attachment requirement is fulfilled. However, the valid flow region is subject to the following examination.

(a) Applicable flow region : The region of analyticity

Referring to Figure 2 (the $M_\infty - \alpha_0$ diagram), it can be said that the supersonic potential theory (e.g. Ref. 13) occupies a valid, narrow region in the left-hand corner, whereas the thin shock layer theory (i.e. Ref. 42) is valid in the upper left portion (or further upward) of the diagram. Hence, the requirement for the potential flow field to be valid is that M_∞ and α_0 have to be low enough, but it makes no restriction on χ , whereas for thin shock layer theory, both M_∞ and α_0 need to be high enough (and ^{or} χ be large enough) so that

the shock wave considered is situated quite near to the wing surface. The valid region of the present theory, however, covers the region where both theories cease to apply. Instead of putting explicit restrictions on the parameters M_∞ , α_0 and χ , the present theory only requires shock attachment to the wing leading edges.

On the other hand, the first two theories are based on the free-stream perturbation scheme and the present theory is based on the wedge perturbation scheme (see Chapter 1). In the former case, the basic flow, say U_∞ , is independent of other parameters such as α_0 or χ . In the latter case, the basic flow, say u_0 (or u_*) is indeed a function of the given parameters, namely M_∞ , α_0 and γ (and χ). These differences lead to the following requirements.

- Free-stream perturbation :

No explicit boundaries of the applicable region need to be specified. The validity of the methods requires the perturbation parameter to be small (e.g. for thin shock layer theory $\epsilon \ll 1$, $\epsilon = (\gamma - 1)/(\gamma + 1) + 2/(\gamma + 1) M_\infty^2 \sin^2 \alpha_0$)

- Wedge perturbation :

Explicit boundaries of the applicable region must be specified. The perturbation parameter (e.g. χ) needs to be small only for the purpose of linearization of the problem.

Therefore, the foregoing discussion leads to the two fundamental requirements of the basic-flow region in the present theory :

- ▶ u_0 (or u_*) and other flow properties (P_0 , P_* ... etc.) must be analytic WRT the given flow parameters M_∞ , α_0 , χ and γ (the region of analyticity).

- ▶ u_0 (or u_*) and other flow properties must be a uniform flow.

Rigorously the valid region must then be bounded away from the sonic lines (the dotted lines in Figures 2, 3 and 4) pointing left-

ward. In fact the sonic line shock detachment line 'pocket' contains non-uniform flow (elliptic in nature) but with the shock attached (the region of shock-attached non-uniform flow). It constitutes a completely different problem by itself and is excluded from the present theory. A thorough study of the basic-flow regions of a caret wing at design condition has been given by Liu (Ref. 51). He has shown that the 'pocket' is quite considerable for caret wings at design. But for caret wings at off design or flat delta wings, it is comparatively small, and becomes vanishingly small at high Mach numbers, say 10 (see Figures 2, 3 and 4)

(b) Other restrictions :

- The ratio of specific heats :

As mentioned in Sec. 8.1 (Figures 28 and 29), the present theory puts no restriction on γ ($1 \leq \gamma \leq \frac{5}{3}$) except that the present theory is not applicable for a gas with dissociation or ionization effects.

- The low-frequency assumption : k

The present theory only accounts for linear-k solutions.

- A compression-side analysis :

No expansion flow is allowed in the present theory. Therefore, it amounts to two conditions for shock-attached flow

$$(1) \alpha_0 > 0$$

or $(2) \tilde{\tau} > \alpha_0$ and $\alpha_0 \geq 0$

(see Figure 1-F)

ii) The mean-flow solution :

The present theory is based on Hui's steady mean flow model (Ref. 7). Consequently, it inherits all the basic characteristics of Hui's model. Although Hui's theory compares favourably with many

other recent numerical works in pressure distribution the model (the linear solution, equation (35) Ref. 7) yields a square root singularity in the pressure gradient along the span at the Mach cone*. In his stretching scheme (equation (50), Ref. 7), he is able to improve the overall pressure distribution in rendering the solution uniformly valid but keeping the singularity unchanged. Apparently, the lifts and moments according to the stretched pressure formula would produce errors as a result of this inherent singularity. The accumulative error is negligible when α_0 or χ is small, but it becomes noticeable when α_0 or χ approaches the detachment zone.

It is recognized that the singularity of the surface pressure gradient at the Mach cone does not exist. Roe (Ref. 60) has given a finite slope formula for the pressure solution only valid at the Mach cone-wing surface point. Otherwise, not even a local solution is available at present.

In order to improve Hui's mean flow model, it is felt that the formal procedure of Method of strained coordinate should be applied to the whole problem once more. According to Crocco (Ref. 62), there are two ways of applying the method, namely, Lighthill's method (Ref. 63) and Pritulo's Method (Ref. 64). Both methods require the second order (in χ) analysis be carried out to a certain extent. Lighthill's method may be more suitable to the problem as the complete second order solution is difficult to obtain. In fact, when carried out the differential equation (in χ^2), in terms of second order pressure, it was

* Same behaviour is found in the solutions of Malmuth (Ref. 58), and Clark & Wallace (Ref. 61).

found that the inhomogeneous terms due to the first order solution amount to some forty terms. Transformation of these terms into the new (strained) coordinate will further multiply this number many times. The lengthy procedure makes the method become very involved indeed.

An alternative way is by the method of Matched asymptotic expansion. Once the expansion parameters and the gauge function are properly identified, in principle, one-term 'inner' solutions (from the Mach cone going inboard) can be matched to a one-term 'outer' solution (from the centre going outboard). In this case, it is possible that only first-order (in χ) analysis is sufficient.

iii) The oscillatory flow solutions :

(a) The globally-stretching scheme : The 'global-stretched' solution of Problem B (perturbation method) was compared with the 'local-stretched' solution obtained by a differentiation method in Figure 8. However, the comparison cannot be made for the 'global-stretched' solution of Problem D (equation (6.32)), since the 'local' solution (or the flow field solution) is not yet available. In order to assess the accuracy due to the proposed stretching scheme used for Problem D, it is desirable to obtain the 'local' solution from the formulation equation (6.23).

(b) An improved perturbation scheme : The approximate formulation of Problems B and D amounts to neglecting the interaction terms (in coupling) due to the mean flow and the oscillatory wedge flow. Based on the new perturbation scheme proposed in Appendix H, these terms ignored were explicitly derived. The proposed method of solution was also outlined.

Basically, if one follows the global formulation ((ii) of Sec. 6.4), the 'new' approach leads to the same equation as equation (6.31)a, except with many more inhomogeneous terms on the RHS. This should

not present any difficulty in principle as the solution technique for a second-order O.D.E. is a standard one (e.g. the variation of parameters). The procedure of solving the 'new' formulation may be lengthy, it is nevertheless straightforward. It is suggested that the 'new' formulation be solved so that the interaction effect ignored in the present theory can be fully measured.

9. RECOMMENDATIONS

9.1 On experimental research

Among the literature available, to the best of the author's knowledge, little experimental data was published along the lines of the present study. In terms of numerical comparison this makes the assessment of the present theory very difficult. For this reason, it is first recommended that the dampings-in-pitch be measured in the present flow region for a series of flat delta wings. In the first instance, it is suggested that the sweepback angle be kept small so that one can always check with the corresponding damping-in-pitch for a wedge.

9.2 On theoretical research

Following the discussion in Chapter 8, the following problems are recommended for further studies :

i) Steady mean flow :

A refinement of Hui's delta wing solution (Ref. 7) based on an improved matching scheme is desirable ((ii) of Sec. 8.4)

ii) Unsteady flow :

a) The 'new' formulation based on the improved perturbation scheme (Appendix H) should be carried out so that the present approach can be fully evaluated ((iii)b of Sec. 8.4).

b) The present theory can be immediately extended for calculation of the damping-in-yaw and the damping-in-roll for a flat delta wing ((iv) of Sec. 8.2).

c) Since the region of analyticity ((i)a of Sec. 8.4) for a caret wing at design is clarified (Liu, Ref. 55), a theory can be readily presented to calculate its dampings-in-pitch, in-yaw and in-roll.

(d) Based on the method of spanwise integration, the present unsteady theory can be further generalized to include the effects of wing-body combinations ((iii)c of Sec. 8.3).

(e) Higher-frequency solutions should be evaluated so that investigations such as flutter analysis could be performed ((iii)d of Sec. 8.2).

10. CONCLUSIONS

A unified unsteady flow theory has been developed for flat delta wings performing slow pitching oscillations. The only restriction imposed on the flow condition is that the shock waves must be attached to the wing leading edges. Emphasis is placed on methods of obtaining the perturbed unsteady flow solutions over the compression side of the wing surface leading to the calculation of its stability derivatives.

In the present study, the essential contributions are :

1. A similarity rule for the steady flow and in-phase flow cases was shown to exist. The rule provides a convenient means of obtaining lifts and moments for the delta-wing family with added volumes of non-affine shapes.
2. The out-of-phase flow is proved to be a 'quasi-conical' flow field. The solution of the out-of-phase flow in the outer region is proved to be exact.
3. A pressure formulation in the inner region is made possible as a result of the 'quasi conical' nature of the flow field.
4. The method of spanwise integration is generalized in the full range in order to achieve a global formulation for the out-of-phase flow.
5. In all the formulations, analytical closed-form solutions were obtained.

The numerical results are presented for the stiffness derivatives and the damping derivatives plotted against a number of flow and geometrical parameters; namely, the mean incidence, the freestream Mach number, the sweepback angle, the pitching axis location and the

ratio of specific heats. The effects on damping derivatives for a cone, a wedge and a flat delta wing were compared. Also, the stability boundaries were given for a number of cases in different ranges of Mach numbers.

Finally, critical assessments of the present theory are given. The present work is to be considered a first attempt in the unsteady wing theory in which the shock-wave effect, hence the rotationality, is properly accounted for and Mach number ranges unified. Nevertheless, a rigorous examination restricts the validity of the present theory to the following conditions :

- 1) The given flow region must be bounded away from the sonic line (the region of analyticity);
- 2) The flow region is restricted to that in which the interaction between the unsteady wedge flow and the steady mean flow is smaller than the unsteady flow contribution due to the outer region.

The last restriction can be removed following an improved scheme proposed in Appendix H , which is recommended for a future study.

It is also suggested that the present theory may be extended to study the rolling and yawing problems of wings of the delta family.

APPENDIX A

THE GEOMETRICAL RELATIONS OF THE DELTA-WING FAMILY : ITS DETACHMENT CRITERIA AND EXACT FLOW SOLUTIONS

The delta-wing family defined here generally contains three types of wings with delta planform, namely

- i) the flat delta wing $(\Gamma = \frac{\pi}{2})$
- ii) the caret wing $(\hat{\Gamma} < \Gamma \leq \frac{\pi}{2})$
- iii) the diamond wing $(\hat{\Gamma} < \Gamma \leq \frac{\pi}{2})$

Referred to the notation shown in figures 1-C, 1-D and 1-E, Γ is defined as the dihedral angle, while $\hat{\Gamma}$ is the dihedral (or anhedral) angle corresponding to the occurrence of the leading-edge shock detachment.

A.1 The unified expressions of the geometry relations

Four planes are defined first so that the flow-wing geometry can be related, i.e., the side plane, the oblique plane, the (oblique) shock plane and the leading-edge plane (see figures 1-C, 1-D and 1-E). The first three planes are defined in Sec. 2.1, Chap. 2); the leading-edge plane is defined as a plane which contains the leading edges of the wing considered.

The given parameters to the problem are M_∞ , α_0 , $\bar{\chi}$, ψ_0 and γ ; where $\bar{\chi}$ is the swept-back angle of the wing measured in the leading-edge plane ($\bar{\chi} = \chi$ for flat delta wing) and ψ_0 is the design angle for caret wing or the thickness angle for diamond wing ($\psi_0 = 0$ for flat delta wing).

From the geometry shown in figures 1-C, 1-D and 1-E the following relationship can be established, viz :

$$\theta_0 = \psi_0 + \alpha_0 \quad (\text{A.1})$$

$$\theta_1 = \tan^{-1} \left[\tan \theta_0 / \cos \bar{\chi} \right] \quad (\text{A.2})$$

$$\Gamma = \tan^{-1} \left[\cot \bar{\chi} / \sin \psi_0 \right] \quad (\text{A.3})$$

$$\Gamma'_1 = \sin^{-1} \left[\cos \Gamma / \sin \bar{\chi} \right] \quad (\text{A.4})$$

A table is provided for equivalent angles in each case considered :

	Caret off design	Caret at design	Diamond	Flat Delta
θ_0	$\psi_0 + \alpha_0$	β_0	α_0	α_0
$\bar{\chi}$	$\bar{\chi}$	$\bar{\chi}$	$\bar{\chi}$	χ
ψ_0	ψ_0	φ_0	ψ_0	0
Γ	Γ	Γ_0	Γ	$\pi/2$
Γ'_1	Γ'_1	φ_1	Γ'_1	0
θ_1	$\alpha_1 + \Gamma'_1$	β_1	$\alpha_1 - \Gamma'_1$	α_1

where $\beta_0 = \varphi_0 + \alpha_0$, $\beta_1 = \varphi_1 + \alpha_1$ and $\chi = \tan^{-1} \left[\tan \bar{\chi} \cos \psi_0 \right]$

Making use of the last row of the table together with equations (A.2) and (A.4), the flow incidence angle α_1 in the oblique plane can be found as

$$\begin{aligned} \alpha_1 &= \theta_1 && (\text{Flat delta}) \\ &\theta_1 - \Gamma'_1 && (\text{Caret off design}) \\ &\theta_1 + \Gamma'_1 && (\text{Diamond}) \end{aligned} \quad (\text{A.5})$$

The free stream-leading edge angle on the side plane, τ , is given from the projection of U_∞ as

$$\tau = \cos^{-1} [\cos \theta_0 \sin \bar{\chi}] \quad (\text{A.6})$$

Hence the Mach number associated with U_n is

$$M_n = M_\infty \sin \tau \quad (\text{A.7})$$

Knowing M_n and α_1 , the shock angle β_1 in the oblique plane can be found by solving the oblique shock relations (see Appendix B), i.e.

$$\left\{ 1 + \frac{\gamma-1}{2} M_n^2 \right\} \tan^3 \beta_1 - (M_n^2 - 1) \cot \alpha_1 \tan^2 \beta_1 + \left\{ 1 + \frac{1}{2} (\gamma+1) M_n^2 \right\} \tan \beta_1 + \cot \alpha_1 = 0 \quad (\text{A.8})$$

In the subsequent development, equation (A.8) is written as

$$\beta_i = \beta_i (\alpha_i)$$

when $i = 0$, it refers to the given flow (M_∞, α_0)

$i = 1$, it refers to the given flow (M_n, α_1)

A.2 The shock detachment criteria

Viewed from the oblique plane, the detachment of the oblique shock wave occurs when the shock wave angle $\hat{\beta}_1$, is related to the normal Mach number \hat{M}_n by the following formula (NACA 1135 eqn.(168), Ref. 47)

$$\sin^2 \hat{\beta}_1 = \frac{1}{4\gamma \hat{M}_n^2} \left\{ (\gamma+1) \hat{M}_n^2 - 4 + \sqrt{[(\gamma+1) \hat{M}_n^4 + 8(\gamma-1) \hat{M}_n^2 + 16] (\gamma+1)} \right\} \quad (\text{A.9})$$

In order to present the detachment lines in the $M_\infty - \alpha_0$

diagram or the $\chi - \alpha_0$ diagram (e.g. see solid lines of Figures 2, 3 and 4), an implicit calculation scheme is employed. In other words, the given condition $(M_\infty, \alpha_0, \bar{\chi}, \psi_0)$ is altered to the given condition $(M_n, \alpha_1, \bar{\chi}, \psi_0)$. Thus, specifying M_n, β_1 is found from (A.9); hence, $\hat{\alpha}_1$ is obtained from equation (A.8). On the other hand, geometrical angles such as θ_0, θ_1 and Γ_1' can be readily found from equations (A.2) - (A.4) and the table for given $\bar{\chi}$ and ψ_0 and knowing $\hat{\alpha}_1$. Finally, α_0 is obtained from equation (A.1) and \hat{M}_∞ from equations (A.6) and (A.7). In this way, the $M_\infty - \alpha_0$ diagram as shown in figure 2 is generated. The $\chi - \alpha_0$ diagrams (the solid lines of Figures 3, 4 and 5) can be generated in very much the same way.

Viewed from the oblique plane, the following equation provides the criterion for the flow behind the plane shock to be physically sonic (NACA 1135, equation (167), Ref. 47.)

$$\sin^2 \beta_1^* = \frac{1}{4\gamma M_n^{*2}} \left\{ (\gamma + 1)M_n^{*2} - (3 - \gamma) \right. \\ \left. + \sqrt{(\gamma + 1)[(\gamma + 1)M_n^{*4} - 2(3 - \gamma)M_n^{*2} + (\gamma + 9)]} \right\} \quad (\text{A.10})$$

where β_1^* and M_n^* correspond to β_1 and M_n in the oblique plane. For given condition of $(M_n, \alpha_1, \bar{\chi}, \psi_0)$, an implicit scheme, similar to the detachment case, is employed to obtain the final M_∞^* and α_0^* . The resulting sonic lines (the dotted lines) are plotted together with the shock detachment lines in Figures 2, 3, 4 and 5. It is seen that among all figures presented, the enclosed region between these two sorts of lines is small when compared with the case of caret wing at design (see Ref. 55, Fig. 10). However, it is certain that the flow field for both delta wing and caret wing at off design conditions of fixed geometry will only achieve the shock detachment

pattern after the leading edges are engulfed by the 3D Mach cone (i.e. in the conically elliptic zone). The same conclusion is drawn for the case of caret wing at design (see Ref. 55.)

It is remarked that the conically sonic cone calculated with the present scheme checks identically with that given by equation (2.8) for the same given condition of $(M_\infty, \alpha_0, \chi)$ for a delta wing, say.

A.3 The exact solutions of the outer flow

If the flow pressure and velocities in the outer region of all types of wings are defined as

$$p_* = p_o \left(1 + \frac{\gamma M_o^2}{\lambda} p_s \right) \quad (d)$$

$$u_* = u_o (1 + u_s) \quad (a)$$

(2.5)

$$v_* = u_o v_s \quad (b)$$

$$w_* = u_o w_s \quad (c)$$

a unified expression for the pressure p_s can be written once for all. Based on the notation defined in Sec. A.1, it is read

$$p_s = \frac{\lambda M_\infty^2}{M_o^2} \cdot \left[\frac{\sin^2 \beta_1 \sin^2 \tau - \sin^2 \beta_o}{\gamma M_\infty^2 \sin^2 \beta_o - \frac{1}{2}(\gamma - 1)} \right] \quad (A.11)$$

The expressions for the flow velocities are written individually for each case as below :

i) Flat delta wing

$$\begin{cases} u_s = \frac{U_\infty}{u_o} \cdot [\cos \tau \sin \chi + \bar{u}_1 \cdot \cos \chi] - 1 \\ w_s = \frac{U_\infty}{u_o} \cdot [\cos \tau \cos \chi - \bar{u}_1 \cdot \sin \chi] \\ v_s = 0 \end{cases} \quad (A.12)$$

where $\bar{u}_1 = \frac{u_1}{U_\infty} = \frac{\sin \tau \cos \beta_1}{\cos \varphi_1}$

u_1 being the uniform velocity behind the oblique shock, parallel to the wing surface as measured in the oblique plane

$$\frac{U_\infty}{u_0} = \frac{\cos \varphi_0}{\cos \beta_0}$$

ii) Caret wing at off design condition

$$\left\{ \begin{array}{l} u_s = \frac{U_\infty}{u_0} \cdot [\cos \tau \sin \bar{\chi} + \bar{u}_1 \cdot \cos \bar{\chi}] \cdot \sin \Gamma - 1 \\ w_s = \frac{U_\infty}{u_0} \cdot [\cos \tau \cos \bar{\chi} - \bar{u}_1 \cdot \sin \bar{\chi}] \cdot \sin^2 \Gamma \\ v_s = w_s \cdot \cot \Gamma \end{array} \right. \quad (\text{A.13})$$

With the help of the equations and the table of Section A.1, it can be shown that for the case of caret wing at design condition equations (A.11) and (A.13) reduce to

$$P_s = u_s = w_s = v_s = 0 \quad (\text{A.14})$$

This is expected since a caret wing at design only possesses a simple flow field of the wedge flow, i.e.

$$\begin{array}{l} P_* = P_0 \\ u_* = u_0 \\ v_* = w_* = 0 \end{array} \quad (\text{A.15})$$

iii) Diamond wing

$$\left\{ \begin{aligned} u_s &= \frac{U_\infty}{U_0} \cdot [\cos \tau \sin \bar{\chi} + \bar{u}_1 \cdot \cos \bar{\chi} \cdot \cos \Gamma_1'] - 1 \\ w_s &= \frac{U_\infty}{U_0} \cdot [\cos \tau \cos \bar{\chi} - \bar{u}_1 \cdot \sin \bar{\chi} \cdot \cos \Gamma_1'] \\ v_s &= \frac{U_\infty}{U_0} \cdot \bar{u}_1 \sin \Gamma_1' \end{aligned} \right. \quad (\text{A.16})$$

Finally, it is noted that the equations (A.11), (A.12), (A.13), (A.14) and (A.16) completely check with the expressions derived previously by Hui in his separate works (Refs. 7, 54 and 8).

APPENDIX B

THE WAVE-ANGLE FORMULAE FOR THE OBLIQUE-SHOCK RELATION

For a given freestream Mach number M_∞ and a deflection angle α_0 the usual practice to find the shock-wave angle β_0 has been either by applying the approximate formula (e.g. Ref. 65) or by numerically solving the oblique shock relation (e.g. Ref. 66). In this Appendix, the explicit exact formulae for the shock wave angles by employing the solutions of cubic equations (Ref. 67) are derived.

Following the expression for oblique shock relation given in Ref. 47 (equation 150), the roots of the cubic equation (cubic in $\sin^2 \beta_0$) are solved.

$$\sin^6 \beta_0 + a_2 \sin^4 \beta_0 + a_1 \sin^2 \beta_0 + a_0 = 0 \quad (\text{B.1})$$

where

$$a_2 = -\frac{M_\infty^2 + 2}{M_\infty^2} - \gamma \sin^2 \alpha_0$$

$$a_1 = \frac{2M_\infty^2 + 1}{M_\infty^4} + \left[\left(\frac{\gamma + 1}{4} \right)^2 + \frac{(\gamma - 1)}{M_\infty^2} \right] \sin^2 \alpha_0$$

$$a_0 = -\frac{\cos^2 \alpha_0}{M_\infty^4}$$

and γ is the specific heat ratio of the gas. According to the cubic root formulae, the three solutions of equation (B.1) can be expressed exactly as

$$\sin^2 \beta_x = -\frac{a_2}{3} + 2(r^2 + \rho^2)^{1/6} \cos \frac{\psi}{3} \quad (\text{B.2})$$

$$\sin^2 \beta_{\text{I}} = -\frac{a_2}{3} - (r^2 + \rho^2)^{1/6} \left[\cos \frac{\psi}{3} + \sqrt{3} \sin \frac{\psi}{3} \right] \quad (\text{B.3})$$

$$\sin^2 \beta_{\text{II}} = -\frac{a_2}{3} - (r^2 + \rho^2)^{1/6} \left[\cos \frac{\psi}{3} - \sqrt{3} \sin \frac{\psi}{3} \right] \quad (\text{B.4})$$

where

$$r = \frac{1}{6} (a_1 a_2 - 3a_0) - \frac{1}{27} a_2^3$$

$$q = \frac{1}{3} a_1 - \frac{1}{9} a_2^2$$

$$\rho = |q^3 + r^2|^{1/2}$$

$$\psi = \tan^{-1} \left(\frac{\rho}{r} \right), \quad 0 \leq \psi \leq \pi$$

From physical reasoning, only consider the positive values of β_0 from equations (B.2), (B.3) and (B.4). It should be noted that in general $0 \leq \beta_{\text{II}} < \beta_{\text{III}} < \beta_{\text{I}} \leq \frac{\pi}{2}$. While β_{I} is the strong shock wave angle, β_{III} is the weak shock wave angle and β_{II} , being less than the Mach angle, thus corresponding to a decrease in entropy, is hence disregarded. Also, it is interesting to note that as $\psi = 0$, $\beta_{\text{I}} = \frac{\pi}{2}$, whereas β_{II} equals to β_{III} and both reduce to the Mach angle of the freestream. In particular, as $\psi = \pi$, $\rho = 0$, β_{I} equals to β_{III} and both become β_{omax} , the maximum angle for shock attachment. The relation $\rho = 0$ provides the maximum deflection angle α_{omax} , for a given M_∞ ; hence, β_{omax} can be evaluated from the following formula

$$\sin^2 \beta_{\text{omax}} = -\frac{a_2}{3} + |r|^{1/3} \quad (\text{B.5})$$

Furthermore, an alternative form of the oblique-shock relation was given in Ref. 4, (equation 7) as :-

$$\begin{aligned} & \left\{ 1 + \frac{1}{2}(\gamma - 1)M_\infty^2 \right\} \tan^3 \beta_0 - \left\{ (M_\infty^2 - 1) \cot \alpha_0 \right\} \tan^2 \beta_0 \\ & + \left\{ 1 + \frac{1}{2}(\gamma + 1)M_\infty^2 \right\} \tan \beta_0 + \cot \alpha_0 = 0 \end{aligned} \quad (B.6)$$

Solving this equation by the same cubic root formulae, three solutions β_i , β_{ii} and β_{iii} are obtained and it is found that $\beta_i = \beta_I$ and $\beta_{iii} = \beta_{III}$. However, $\beta_{ii} = -\beta_{II}$ which indicates an improper shock wave propagation angle, hence should be again rejected on physical ground.

Note that in the case of viewing the flow from the oblique plane, the given flow condition (M_∞, α_0) is replaced by (M_n, α_1) and the wave-angle β_0 is replaced by β_1 throughout the equations above. Symbolically, equation (B.6) is expressed as

$$\begin{aligned} \beta_0 &= \beta_0(M_\infty, \alpha_0) \\ \text{and } \beta_1 &= \beta_1(M_n, \alpha_1) \end{aligned} \quad (B.7)^*$$

Clearly, throughout the present work, it is the weak-shock-wave angle β_{iii} (or β_{III}) which is employed for the calculation.

* Even simpler, sometimes they are written as

$$\begin{aligned} \beta_0 &= \beta_0(\alpha_0) \\ \text{and } \beta_1 &= \beta_1(\alpha_1) \text{ for convenience.} \end{aligned}$$

APPENDIX C

THE PERTURBED SHOCK CONDITIONS (S.C.) FOR A SKEWED WEDGE
PERFORMING UNSTEADY MOTIONS

Let the leading edge and the outer region of a delta wing (or a caret wing or a diamond wing) be replaced by a skewed wedge. Thus the skewed angle is properly defined by the swept-back angle χ . Now consider the unsteady motion of such a skewed wedge with attached plane shock waves.

Suppose the unsteady motion is associated with a small disturbance parameter, say ϵ , the small amplitude of oscillation. The Rankine-Hugoniot conditions (equations (3.3)) are then perturbed by ϵ to yield a set of perturbed shock conditions. They are useful in the formulation of a number of problems (e.g. see Hui's work, Ref. 68). In particular, the problems A and C are formulated according to these shock conditions.

Thus, substituting equations (2.13) and (3.4)b into equations (3.3) and collecting like terms of order $O(\epsilon)$ result in the following equations. For convenience, they are arranged in the matrix form as

$$\begin{pmatrix} c_1 & c_2 & c_3 & 0 & c_5 \\ c_1 & c_2 & c_3 & d_4 & d_5 \\ c_1 & c_2 & c_3 & e_4 & e_5 \\ t_1 & t_2 & 0 & 0 & 0 \\ s_1 & s_2 & s_3 & 0 & 0 \end{pmatrix} \begin{pmatrix} \frac{u}{u_*} \\ \frac{v}{u_*} \\ \frac{w}{u_*} \\ \frac{p}{p_*} \\ \frac{\rho}{\rho_*} \end{pmatrix} = \begin{pmatrix} c_t & c_x & c_z \\ 0 & d_x & d_z \\ e_t & e_x & e_z \\ 0 & t_x & 0 \\ 0 & s_x & s_z \end{pmatrix} \begin{pmatrix} Q_t \\ Q_x \\ Q_z \end{pmatrix}$$

(C.1)

where all the constants c_1, c_2, c_3, \dots etc. are given in equations (3.21)a and (3.21)b.

Writing

$$\left\{ \begin{array}{l} U = \frac{u}{u_*} \\ V = \frac{v}{u_*} \\ W = \frac{w}{u_*} \\ P = \frac{p}{p_*} \\ \text{and } R = \frac{\rho}{\rho_*} \end{array} \right. \quad (C.2)$$

and making use of the matrix (C.1) yields equation (3.19).

Note that when $\chi \rightarrow 0$, (C.1) reduces to four equations (as $w = 0$) previously given by Hui (Ref. 34), the shock condition for a oscillating wedge.

APPENDIX D

THE DERIVATIVES OF SOME FLOW PARAMETERS: DIFFERENTIATION METHOD

In the present derivation, consider M_∞ , γ and χ as fixed parameters.

D.1 The expression of $\frac{\partial}{\partial \alpha_0} \left(\frac{P_0}{P_\infty} \right)$

Knowing

$$\frac{P_0}{P_\infty} = \frac{2\gamma}{\gamma+1} (M_\infty^2 \sin^2 \beta_0 - 1) + 1$$

from the oblique shock relation, for given M_∞ , α_0 and χ

$$\frac{\partial}{\partial \alpha_0} \left(\frac{P_0}{P} \right) = \frac{2\gamma}{\gamma+1} M_\infty^2 \cdot \sin 2\beta_0 \left(\frac{\partial \beta_0}{\partial \alpha_0} \right) \quad (D.1)$$

where

$$\frac{\partial \beta_0}{\partial \alpha_0} = \sec^2 \alpha_0 \cdot \frac{1}{T'(\beta_0)} \quad (D.2) a$$

with $\beta_0 = \beta_0(\alpha_0)$ given from Appendix A (also see equation 2.3)

$$\text{and } T'(\beta_0) = \frac{\partial}{\partial \beta_0} \left[\frac{T_1(\beta_0)}{T_2(\beta_0)} \right] = \frac{T_2 \frac{\partial T_1}{\partial \beta_0} - T_1 \frac{\partial T_2}{\partial \beta_0}}{T_2^2}$$

$$T_1(\beta_0) = 2 \cot \beta_0 [M_\infty^2 \sin^2 \beta_0 - 1]$$

$$T_2(\beta_0) = M_\infty^2 (\gamma + \cos 2\beta_0) + 2$$

$$\frac{\partial T_1}{\partial \beta_0} = 2 [M_\infty^2 \cos 2\beta_0 + \csc^2 \beta_0]$$

$$\frac{\partial T_2}{\partial \beta_0} = -2 M_\infty^2 \sin 2\beta_0$$

Hence, with $\varphi_0 = \beta_0 - \alpha_0$

$$\frac{\partial \varphi_0}{\partial \alpha_0} = \frac{\partial \beta_0}{\partial \alpha_0} - 1 \quad (\text{D.2})_b$$

D.2 : The expression of $\frac{\partial P_s}{\partial \alpha_0}$

From equation (2.6)d, P_s reads

$$P_s = M_\infty^2 \cdot \left(\frac{\lambda}{M_0^2} \right) \frac{P_5}{P_6}$$

where

$$P_5 = \sin^2 \beta_1 \sin^2 \tau - \sin^2 \beta_0$$

$$P_6 = \gamma M_\infty^2 \sin^2 \beta_0 - \frac{1}{2} (\gamma - 1)$$

Thus,

$$\frac{\partial P_s}{\partial \alpha_0} = M_\infty^2 \cdot \left[\frac{\partial}{\partial \alpha_0} \left(\frac{\lambda}{M_0^2} \right) \cdot \left(\frac{P_5}{P_6} \right) + \frac{\lambda}{M_0^2} \cdot \frac{\partial}{\partial \alpha_0} \left(\frac{P_5}{P_6} \right) \right] \quad (\text{D.3})$$

i) The expression of $\frac{\partial}{\partial \alpha_0} \left(\frac{\lambda}{M_0^2} \right)$

The oblique shock relation gives

$$M_0 = \left(\frac{N_2}{N_1} \cdot \frac{1}{\sin^2 \varphi_0} \right)^{\frac{1}{2}}$$

where

$$N_1 = 2 \gamma M_\infty^2 \sin^2 \beta_0 - (\gamma - 1)$$

$$N_2 = 2 + (\gamma - 1) M_\infty^2 \sin^2 \beta_0$$

Hence

$$\frac{\partial M_0}{\partial \alpha_0} = \frac{1}{2M_0 \sin^2 \varphi_0} \cdot \left\{ \frac{\partial}{\partial \beta_0} \left(\frac{N_2}{N_1} \right) \cdot \left(\frac{\partial \beta_0}{\partial \alpha_0} \right) - 2 \cot \varphi_0 \left(\frac{N_2}{N_1} \right) \cdot \left(\frac{\partial \beta_0}{\partial \alpha_0} - 1 \right) \right\} \quad (D.4)$$

where

$$\frac{\partial}{\partial \beta_0} \left(\frac{N_2}{N_1} \right) = \frac{1}{N_1^2} \cdot \left[N_1 \frac{\partial N_2}{\partial \beta_0} - N_2 \frac{\partial N_1}{\partial \beta_0} \right]$$

where

$$\begin{cases} \frac{\partial N_1}{\partial \beta_0} = 2 \gamma M_\infty^2 \sin 2\beta_0 \\ \frac{\partial N_2}{\partial \beta_0} = (\gamma - 1) M_\infty^2 \sin 2\beta_0 \end{cases}$$

Now

$$\frac{\partial \lambda}{\partial \alpha_0} = \frac{M_0}{\lambda} \left(\frac{\partial M_0}{\partial \alpha_0} \right) \quad (D.5)$$

and

$$\frac{\partial}{\partial \alpha_0} \left(\frac{\lambda}{M_0^2} \right) = \frac{1}{M_0^3} \left[M_0 \frac{\partial \lambda}{\partial \alpha_0} - 2 \lambda \frac{\partial M_0}{\partial \alpha_0} \right] \quad (D.5a)$$

$$\frac{\partial}{\partial \alpha_0} \left(\frac{M_0^2}{\lambda} \right) = \frac{1}{\lambda^2} \left[2 \lambda M_0 \frac{\partial M_0}{\partial \alpha_0} - M_0^2 \frac{\partial \lambda}{\partial \alpha_0} \right] \quad (D.6b)$$

ii) The expression of $\frac{\partial}{\partial \alpha_0} \left(\frac{P_5}{P_6} \right)$

First, one needs to find the derivatives of the angles in the side plane and the oblique plane, namely $\frac{\partial \beta_1}{\partial \alpha_0}$ & $\frac{\partial \tau}{\partial \alpha_0}$. From equations (2.1) and (2.2) it is obtained

$$\frac{\partial \tau}{\partial \alpha_0} = \frac{\sin \chi \sin \alpha_0}{\sqrt{1 - \sin^2 \chi \cos^2 \alpha_0}} \quad (D.7)$$

and

$$\frac{\partial \beta_1}{\partial \alpha_0} = \frac{1}{\left(\frac{\partial T(\beta_1)}{\partial \beta_1}\right)} \left\{ \frac{1}{\cos \chi \cdot \cos^2 \alpha_1} - \left(\frac{\partial T}{\partial M_n}\right) \left(\frac{\partial M_n}{\partial \alpha_0}\right) \right\} \quad (D.8)$$

where

$$\left\{ \begin{array}{l} \frac{\partial T(\beta_1)}{\partial \beta_1} = \frac{T_2 \frac{\partial T_1}{\partial \beta_1} - T_1 \frac{\partial T_2}{\partial \beta_1}}{T_2^2} \\ T_1(\beta_1) = 2 \cot \beta_1 \cdot [M_n^2 \sin^2 \beta_1 - 1] \\ T_2(\beta_2) = M_n^2 (\gamma + \cos 2\beta_1) + 2 \\ \frac{\partial T_1(\beta_1)}{\partial \beta_1} = 2 [M_n^2 \cos 2\beta_1 + \csc^2 \beta_1] \\ \frac{\partial T_2(\beta_1)}{\partial \beta_1} = -2 M_n^2 \sin 2\beta_1 \end{array} \right. \left\{ \begin{array}{l} \frac{\partial T}{\partial M_n} = \frac{1}{T_2} T_2 \frac{\partial T_1}{\partial M_n} - T_1 \frac{\partial T_2}{\partial M_n} \\ \frac{\partial T_1}{\partial M_n} = 2 M_n \sin 2\beta_1 \\ \frac{T_2}{M_n} = 2 M_n (\gamma + \cos 2\beta_1) \end{array} \right.$$

and

$$\alpha_1 = \tan^{-1} \left[\frac{\tan \alpha_0}{\cos \chi} \right]$$

$$M_n = M_\infty \cdot \sqrt{1 - \sin^2 \chi \cos^2 \alpha_0}$$

$$\beta_1 = \beta_1(\alpha_1) \quad , \quad \text{given in Appendix B}$$

Thus

$$\frac{\partial}{\partial \alpha_0} \left(\frac{P_5}{P_6} \right) = \left(P_6 \frac{\partial P_5}{\partial \alpha_0} - P_5 \frac{\partial P_6}{\partial \alpha_0} \right) \cdot \frac{1}{P_6^2} \quad (D.9)$$

where

$$\begin{aligned} \frac{\partial P_5}{\partial \alpha_0} &= \sin^2 \tau \sin 2\beta_1 \left(\frac{\partial \beta_1}{\partial \alpha_0} \right) + \sin^2 \beta_1 \sin 2\tau \left(\frac{\partial \tau}{\partial \alpha_0} \right) \\ &\quad - \sin 2\beta_0 \left(\frac{\partial \beta_0}{\partial \alpha_0} \right) \end{aligned}$$

$$\frac{\partial P_6}{\partial \alpha_0} = \gamma m_\infty^2 \sin 2\beta_0 \left(\frac{\partial \beta_0}{\partial \alpha_0} \right)$$

with $\frac{\partial \beta_1}{\partial \alpha_0}$ & $\frac{\partial \tau}{\partial \alpha_0}$ given in equation (D.7) and (D.8) and $\frac{\partial \beta_0}{\partial \alpha_0}$

given in equation (D.2)

D.3 The expressions of $\frac{\partial H}{\partial \alpha_0}$ and $\frac{\partial \kappa}{\partial \alpha_0}$

As defined previously, $H = \lambda \tan \varphi_0$

Hence,

$$\frac{\partial H}{\partial \alpha_0} = \frac{\partial \lambda}{\partial \alpha_0} \cdot \tan \varphi_0 + \lambda \sec^2 \varphi_0 \left(\frac{\partial \beta_0}{\partial \alpha_0} - 1 \right) \quad (D.10)$$

As defined previously, $\kappa = \frac{M_0}{\lambda}$

Hence,

$$\frac{\partial \kappa}{\partial \alpha_0} = \frac{1}{\lambda^2} \left[\lambda \frac{\partial M_0}{\partial \alpha_0} - M_0 \frac{\partial \lambda}{\partial \alpha_0} \right] \quad (D.11)$$

with $\frac{\partial M_0}{\partial \alpha_0} \cdot \frac{\partial \lambda}{\partial \alpha_0}$ given in equations (D.4) and (D.5) and $\frac{\partial \beta_0}{\partial \alpha_0}$

given in equation (D.2).

D.4 The expression of $\frac{\partial \zeta_*}{\partial \alpha_0}$

From equation (4.6), ζ_* can be written as

$$\zeta_* = \lambda \cdot \left(\frac{z_u}{z_d} \right)$$

where

$$z_u = \lambda_* \sin \theta + \cos \theta$$

$$z_d = \lambda_* \cos \theta - \sin \theta$$

and

$$\lambda_* = \sqrt{m_*^2 - 1}$$

As given by equation (2.8a), M_* can be written as

$$M_*^2 = M_0^2 \cdot \left\{ \frac{\left(1 + \frac{M_0^2}{\lambda} \rho_s\right)}{\left(1 + \frac{\gamma M_0^2}{\lambda} \rho_s\right)} \cdot \left[(1 + u_s)^2 + w_s^2 \right] \right\}$$

and by equation (2.8b)

$$\theta = \tan^{-1} \left(\frac{w_s}{1 + u_s} \right)$$

i) The expression of $\frac{\partial w_s}{\partial \alpha_0}$ and $\frac{\partial u_s}{\partial \alpha_0}$

Rewrite w_s and u_s from equations (2.6a) and (2.6c) in the form

$$w_s = \left(\frac{U_\infty}{u_0} \right) \cdot \left[w_2 - \frac{w_3}{w_4} \cdot \sin \chi \right]$$

$$u_s = \left(\frac{U_\infty}{u_0} \right) \cdot \left[w_2 + \frac{w_3}{w_4} \cdot \cos \chi \right]$$

where

$$w_2 = \cos \tau \cos \chi$$

$$u_2 = \cos \tau \sin \chi$$

$$w_3 = \sin \tau \cos \beta_1$$

$$\frac{U_\infty}{u_0} = \frac{\cos \varphi_0}{\cos \beta_0}$$

$$w_4 = \cos \varphi_1$$

Thus

$$\frac{\partial w_2}{\partial \alpha_0} = -\sin \tau \cos \chi \cdot \left(\frac{\partial \tau}{\partial \alpha_0} \right)$$

$$\frac{\partial w_3}{\partial \alpha_0} = \cos \tau \cos \beta_1 \left(\frac{\partial \tau}{\partial \alpha_0} \right) - \sin \tau \sin \beta_1 \left(\frac{\partial \beta_1}{\partial \alpha_0} \right)$$

$$\frac{\partial w_4}{\partial \alpha_0} = -\sin (\beta_1 - \alpha_1) \cdot \left[\frac{\partial \beta_1}{\partial \alpha_0} - \frac{\partial \alpha_1}{\partial \alpha_0} \right]$$

where

$$\frac{\partial \alpha_1}{\partial \alpha_0} = \frac{1}{\cos \chi} \left(\frac{\sec \alpha_1}{\sec \alpha_0} \right)^2$$

$$\frac{\partial u_2}{\partial \alpha_0} = -\sin \tau \sin \chi \left(\frac{\partial \tau}{\partial \alpha_0} \right)$$

and

$$\frac{\partial}{\partial \alpha_0} \left(\frac{U_\infty}{u_0} \right) = \frac{\partial}{\partial \alpha_0} \left(\frac{\cos \varphi_0}{\cos \beta_0} \right) = \frac{1}{\cos^2 \beta_0} \sin \alpha_0 \cdot \left(\frac{\partial \beta_0}{\partial \alpha_0} \right) + \frac{\sin \varphi_0}{\cos \beta_0}$$

Hence

$$\frac{\partial w_s}{\partial \alpha_0} = \frac{\partial}{\partial \alpha_0} \left(\frac{U_\infty}{u_0} \right) \cdot \left[w_2 - \frac{w_3}{w_4} \sin \chi \right] + \left(\frac{U_\infty}{u_0} \right) \cdot \left[\frac{\partial w_2}{\partial \alpha_0} - \frac{\partial}{\partial \alpha_0} \left(\frac{w_3}{w_4} \right) \cdot \sin \chi \right] \quad (D.12)$$

$$\frac{\partial u_s}{\partial \alpha_0} = \frac{\partial}{\partial \alpha_0} \left(\frac{U_\infty}{u_0} \right) \cdot \left[u_2 - \frac{w_3}{w_4} \sin \chi \right] + \left(\frac{U_\infty}{u_0} \right) \cdot \left[\frac{\partial u_2}{\partial \alpha_0} + \frac{\partial}{\partial \alpha_0} \left(\frac{w_3}{w_4} \right) \cdot \cos \chi \right] \quad (D.13)$$

where

$$\frac{\partial}{\partial \alpha_0} \left(\frac{w_3}{w_4} \right) = \frac{1}{w_4^2} \left[w_4 \frac{\partial w_3}{\partial \alpha_0} - w_3 \frac{\partial w_4}{\partial \alpha_0} \right]$$

ii) The expression of $\frac{\partial \rho_s}{\partial \alpha_0}$

Rewrite ρ_s from equation (2.6)e in the form of

$$\rho_s = R_0 \cdot \left(\frac{\lambda}{m_0^2} \right) \cdot \left(\frac{P_5}{P_7} \right)$$

where

$$R_0 = \frac{2}{\sin^2 \beta_0}$$

$$P_7 = 2 + (\gamma - 1) M_\infty^2 \sin^2 \tau \sin^2 \beta_1$$

Thus,

$$\frac{\partial R_0}{\partial \alpha_0} = - \frac{4 \cos \beta_0}{\sin^3 \beta_0} \left(\frac{\partial \beta_0}{\partial \alpha_0} \right)$$

$$\frac{\partial P_7}{\partial \alpha_0} = (\gamma - 1) M_\infty^2 \sin 2\tau \sin^2 \beta_1 \left(\frac{\partial \tau}{\partial \alpha_0} \right) + \sin 2\beta_1 \sin^2 \tau \left(\frac{\partial \beta_1}{\partial \alpha_0} \right)$$

with $\frac{\partial \beta_0}{\partial \alpha_0}$ given in equation (D.2), $\frac{\partial \tau}{\partial \alpha_0}$ and $\frac{\partial \beta_1}{\partial \alpha_0}$ given in equations (D.7) and (D.8), and $\frac{\partial}{\partial \alpha_0} \left(\frac{\lambda}{M_0^2} \right)$ given in equation (D.6), the expression of $\frac{\partial P_s}{\partial \alpha_0}$ reads

$$\frac{\partial P_s}{\partial \alpha_0} = \left(\frac{P_5}{P_7} \right) \left[\frac{\partial R_0}{\partial \alpha_0} \cdot \left(\frac{\lambda}{M_0^2} \right) + \frac{\partial}{\partial \alpha_0} \left(\frac{\lambda}{M_0^2} \right) \cdot R_0 \right] + R_0 \left(\frac{\lambda}{M_0^2} \right) \cdot \frac{\partial}{\partial \alpha_0} \left(\frac{P_5}{P_7} \right)$$

(D.14)

where

$$\frac{\partial}{\partial \alpha_0} \left(\frac{P_5}{P_7} \right) = \frac{1}{P_7^2} \left(P_7 \frac{\partial P_s}{\partial \alpha_0} - P_5 \frac{\partial P_7}{\partial \alpha_0} \right)$$

iii) The expression of $\frac{\partial M_*}{\partial \alpha_0}$ and $\frac{\partial \theta}{\partial \alpha_0}$

Rewrite M_*^2 as

$$M_*^2 = M_0^2 \cdot \frac{m_u}{m_d}$$

where

$$m_u = \left(1 + \frac{M_0^2}{\lambda} \rho_s \right) \left[(1 + u_s)^2 + w_s^2 \right]$$

$$m_d = 1 + \gamma \frac{M_0^2}{\lambda} \rho_s$$

Thus,

$$\frac{\partial m_*}{\partial \alpha_0} = \frac{m_o}{m_*} \left(\frac{\partial m_o}{\partial \alpha_0} \right) \cdot \frac{m_u}{m_d} + \frac{m_o^2}{2m_*} \frac{\partial}{\partial \alpha_0} \left(\frac{m_u}{m_d} \right) \quad (D.15)$$

with

$$m_u = \left(\rho_s \frac{\partial}{\partial \alpha_0} \left(\frac{m_o^2}{\lambda} \right) + \frac{m_o^2}{\lambda} \frac{\partial \rho_s}{\partial \alpha_0} \right) \cdot \left[(1 + u_s)^2 + w_s^2 \right] \\ + \left(1 + \frac{m_o^2}{\lambda} \rho_s \right) \left[2(1 + u_s) \frac{\partial u_s}{\partial \alpha_0} + 2 \frac{\partial w_s}{\partial \alpha_0} w_s \right]$$

$$m_d = \gamma \cdot \left[\rho_s \cdot \frac{\partial}{\partial \alpha_0} \left(\frac{m_o^2}{\lambda} \right) + \frac{m_o^2}{\lambda} \cdot \frac{\partial \rho_s}{\partial \alpha_0} \right]$$

and

$$\frac{\partial}{\partial \alpha_0} \left(\frac{m_u}{m_d} \right) = \frac{1}{m_d^2} \left[m_d \frac{\partial m_u}{\partial \alpha_0} - m_u \frac{\partial m_d}{\partial \alpha_0} \right]$$

whereas

$$\frac{\partial \theta}{\partial \alpha_0} = \frac{1}{(1+u_s)^2 + w_s^2} \left[(1+u_s) \frac{\partial w_s}{\partial \alpha_0} - w_s \frac{\partial u_s}{\partial \alpha_0} \right] \quad (D.16)$$

Hence

$$\frac{\partial \zeta_*}{\partial \alpha_0} = \left(\frac{\partial \lambda}{\partial \alpha_0} \right) \left(\frac{z_u}{z_d} \right) + \lambda \cdot \frac{\partial}{\partial \alpha_0} \left(\frac{z_u}{z_d} \right) \quad (D.17)$$

where

$$\frac{\partial}{\partial \alpha_0} \left(\frac{z_u}{z_d} \right) = \frac{1}{z_d^2} \left[z_d \frac{\partial z_u}{\partial \alpha_0} - z_u \frac{\partial z_d}{\partial \alpha_0} \right]$$

$$\frac{\partial z_u}{\partial \alpha_0} = \frac{\partial \theta}{\partial \alpha_0} \cdot \left(\lambda_* \cos \theta - \sin \theta \right) + \frac{\partial \lambda_*}{\partial \alpha_0} \cdot \sin \theta$$

$$\frac{\partial z_d}{\partial \alpha_0} = -\frac{\partial \theta}{\partial \alpha_0} \cdot \left(\lambda_* \sin \theta + \cos \theta \right) + \frac{\partial \lambda_*}{\partial \alpha_0} \cdot \cos \theta$$

and

$$\begin{cases} \frac{\partial \lambda_*}{\partial \alpha_0} = \frac{M_*}{\lambda_*} \frac{\partial M_*}{\partial \alpha_0} \\ \frac{\partial \lambda}{\partial \alpha_0} = \frac{M_0}{\lambda} \frac{\partial M_0}{\partial \alpha_0} \end{cases} \quad (D.5)$$

D.5 The expressions of $\frac{\partial C}{\partial \alpha_0}$, $\frac{\partial A}{\partial \alpha_0}$, $\frac{\partial K}{\partial \alpha_0}$ and $\frac{\partial A_0}{\partial \alpha_0}$, $\frac{\partial B_0}{\partial \alpha_0}$ and $\frac{\partial D_0}{\partial \alpha_0}$

i) The coefficients C, A and K can be rearranged in the following forms

$$C = 2 \cdot \frac{C_1 \cdot C_2 \cdot C_3}{C_4} = 2 \cdot \frac{C_5}{C_4}$$

$$A = \frac{C_1 \cdot C_2 \cdot A_3}{A_4} = \frac{A_5}{A_4}$$

$$K = -K_1 \cdot K_2$$

where

$$\begin{cases} C_1 = \sin \varphi_0 \cos^3 \varphi_0 & * \\ C_2 = 1 - \frac{\rho_\infty}{\rho_0} \\ C_3 = 1 - \frac{\gamma-1}{2} \left(\frac{\rho_0}{\rho_\infty} - 1 \right) M_0^2 \sin^2 \varphi_0 \\ C_4 = 1 - M_0^2 \sin^2 \varphi_0 \end{cases}$$

* All the notations here are defined locally, to be distinguished from the main text.

$$\left\{ \begin{aligned} A_3 &= 1 + A_1 + A_2 \\ A_1 &= \left(\frac{\rho_0}{\rho_\infty} \right) H^2 \\ A_2 &= \gamma \left(1 - \frac{\rho_0}{\rho_\infty} \right) M_0^2 \sin^2 \varphi_0 \\ A_4 &= H \left(1 - M_0^2 \sin^2 \varphi_0 \right) \end{aligned} \right.$$

$$\left\{ \begin{aligned} K_1 &= \frac{\rho_0}{\rho_\infty} - 1 \\ K_2 &= \sin \varphi_0 \cos \varphi_0 \end{aligned} \right.$$

Also, denote the terms

$$\frac{\rho_0}{\rho_\infty} = \frac{R_2}{R_1}$$

and

$$M_0^2 \sin^2 \varphi_0 = \frac{N_2}{N_1}$$

where R_2 and R_1 reads

$$\left\{ \begin{aligned} R_2 &= (\gamma + 1) M_\infty^2 \sin^2 \beta_0 \\ R_1 &= (\gamma - 1) M_\infty^2 \sin^2 \beta_0 + 2 \end{aligned} \right.$$

N_2 and N_1 are given in equation (D.4),

Thus, the derivatives read

$$\left\{ \begin{aligned} \frac{\partial R_2}{\partial \alpha_0} &= (\gamma + 1) M_\infty^2 \sin 2\beta_0 \frac{\partial \beta_0}{\partial \alpha_0} \\ \frac{\partial R_1}{\partial \alpha_0} &= (\gamma - 1) M_\infty^2 \sin 2\beta_0 \frac{\partial \beta_0}{\partial \alpha_0} \\ \frac{\partial}{\partial \alpha_0} \left(\frac{\rho_0}{\rho_\infty} \right) &= \frac{1}{R_1^2} \left[R_1 \frac{\partial R_2}{\partial \alpha_0} - R_2 \frac{\partial R_1}{\partial \alpha_0} \right] \\ \frac{\partial}{\partial \alpha_0} \left(\frac{\rho_\infty}{\rho_0} \right) &= \frac{1}{R_2^2} \left[R_2 \frac{\partial R_1}{\partial \alpha_0} - R_1 \frac{\partial R_2}{\partial \alpha_0} \right] \end{aligned} \right.$$

Hence,

$$\left\{ \begin{aligned} \frac{\partial C_1}{\partial \alpha_0} &= (\cos^4 \varphi_0 - 3 \cos^2 \varphi_0 \sin^2 \varphi_0) \left(\frac{\partial \varphi_0}{\partial \alpha_0} \right) \\ \frac{\partial C_2}{\partial \alpha_0} &= -\frac{\partial}{\partial \alpha_0} \left(\frac{\rho_0}{\rho_\infty} \right) \\ \frac{\partial C_3}{\partial \alpha_0} &= -\left(\frac{\gamma-1}{2} \right) \left[\frac{\partial}{\partial \alpha_0} \left(\frac{\rho_0}{\rho_\infty} \right) M_0^2 \sin^2 \varphi_0 + \left(\frac{\rho_0}{\rho_\infty} - 1 \right) \frac{\partial}{\partial \alpha_0} \left(\frac{N_2}{N_1} \right) \right] \\ \frac{\partial C_4}{\partial \alpha_0} &= -\frac{\partial}{\partial \alpha_0} \left(\frac{N_2}{N_1} \right) \\ \frac{\partial C_5}{\partial \alpha_0} &= \frac{\partial C_1}{\partial \alpha_0} \cdot C_2 \cdot C_3 + \frac{\partial C_2}{\partial \alpha_0} \cdot C_1 \cdot C_3 + \frac{\partial C_3}{\partial \alpha_0} \cdot C_2 \cdot C_1 \\ \frac{\partial C}{\partial \alpha_0} &= \frac{2}{C_4^2} \cdot \left[C_4 \frac{\partial C_5}{\partial \alpha_0} - C_5 \frac{\partial C_4}{\partial \alpha_0} \right] \end{aligned} \right. \quad (D.18)$$

Also,

$$\left\{ \begin{aligned} \frac{\partial A_1}{\partial \alpha_0} &= H^2 \cdot \frac{\partial}{\partial \alpha_0} \left(\frac{\rho_0}{\rho_\infty} \right) + 2H \frac{\partial H}{\partial \alpha_0} \left(\frac{\rho_0}{\rho_\infty} \right) \\ \frac{\partial A_2}{\partial \alpha_0} &= \gamma \cdot \left[\left(1 - \frac{\rho_0}{\rho_\infty} \right) \frac{\partial}{\partial \alpha_0} \left(\frac{N_2}{N_1} \right) - M_0^2 \sin^2 \varphi_0 \frac{\partial}{\partial \alpha_0} \left(\frac{\rho_0}{\rho_\infty} \right) \right] \\ \frac{\partial A_3}{\partial \alpha_0} &= \frac{\partial A_1}{\partial \alpha_0} + \frac{\partial A_2}{\partial \alpha_0} \\ \frac{\partial A_4}{\partial \alpha_0} &= \frac{\partial H}{\partial \alpha_0} (1 - M_0^2 \sin^2 \varphi_0) - H \frac{\partial}{\partial \alpha_0} \left(\frac{N_2}{N_1} \right) \\ \frac{\partial A_5}{\partial \alpha_0} &= \frac{\partial C_1}{\partial \alpha_0} \cdot C_2 \cdot A_3 + \frac{\partial C_2}{\partial \alpha_0} \cdot C_1 \cdot A_3 + \frac{\partial A_3}{\partial \alpha_0} \cdot C_1 \cdot C_2 \end{aligned} \right.$$

Hence,

$$\frac{\partial A}{\partial \alpha_0} = \frac{1}{A_4^2} \left[A_4 \frac{\partial A_5}{\partial \alpha_0} - A_5 \frac{\partial A_4}{\partial \alpha_0} \right] \quad (D.19)$$

Now

$$\begin{cases} \frac{\partial K_1}{\partial \alpha_0} = \frac{\partial}{\partial \alpha_0} \left(\frac{\rho_0}{\rho_\infty} \right) \\ \frac{\partial K_2}{\partial \alpha_0} = \cos 2\varphi_0 \frac{\partial \varphi_0}{\partial \alpha_0} \end{cases}$$

Hence,

$$\frac{\partial K}{\partial \alpha_0} = - \left(K_1 \frac{\partial K_2}{\partial \alpha_0} + K_2 \frac{\partial K_1}{\partial \alpha_0} \right) \quad (D.20)$$

ii) The coefficients A_0 , B_0 and D_0 are

$$\begin{cases} A_0 = \frac{A}{C} \\ B_0 = -\frac{K}{C} \\ D_0 = \frac{D_1}{D_2} - A_0 \end{cases}$$

$$\text{where } \begin{cases} D_1 = 2H B_0 \\ D_2 = H'^2 \end{cases}$$

Their derivatives can be written as

$$\begin{cases} \frac{\partial A_0}{\partial \alpha_0} = \left[C \frac{\partial A}{\partial \alpha_0} - A \frac{\partial C}{\partial \alpha_0} \right] \frac{1}{C^2} & a \\ \frac{\partial B_0}{\partial \alpha_0} = \left(C \frac{\partial B}{\partial \alpha_0} - B \frac{\partial C}{\partial \alpha_0} \right) \frac{1}{C^2} & (D.21) \quad b \\ \frac{\partial D_0}{\partial \alpha_0} = \frac{1}{D_2^2} \cdot \left[D_2 \frac{\partial D_1}{\partial \alpha_0} - D_1 \frac{\partial D_2}{\partial \alpha_0} \right] - \frac{\partial A_0}{\partial \alpha_0} & c \end{cases}$$

$$\text{where } \begin{cases} \frac{\partial D_1}{\partial \alpha_0} = 2 \left[H \frac{\partial B_0}{\partial \alpha_0} + B_0 \frac{\partial H}{\partial \alpha_0} \right] \\ \frac{\partial D_2}{\partial \alpha_0} = -2H \left(\frac{\partial H}{\partial \alpha_0} \right) \end{cases}$$

D.6 The expression of $\frac{\partial w_s'}{\partial \alpha_0}$ and $\frac{\partial a_1'}{\partial \alpha_0}$

From equations (4.1) and (4.9) w_s' and a_1' are given by

$$w_s' = \chi \cdot \frac{\sin \varphi_0}{\cos \beta_0} \cdot \sin \alpha_0$$

$$a_1' = \frac{4}{\pi} \cdot \left(\frac{H w_s'}{A_0 + H} \right)$$

The derivative of w_s' is

$$\frac{\partial w_s'}{\partial \alpha_0} = \chi \cdot \frac{1}{\cos^2 \beta_0} \left[\cos \beta_0 \sin(\varphi_0 - \alpha_0) + \left(\frac{\partial \beta_0}{\partial \alpha_0} \right) \sin \alpha_0 \cos \alpha_0 \right] \quad (D.22)$$

$$\frac{\partial a_1'}{\partial \alpha_0} = \frac{4}{\pi} \cdot \frac{1}{(A_0 + H)^2} \left[(A_0 + H) \left(w_s' \frac{\partial H}{\partial \alpha_0} + H \frac{\partial w_s'}{\partial \alpha_0} \right) - H w_s' \left(\frac{\partial A_0}{\partial \alpha_0} + \frac{\partial H}{\partial \alpha_0} \right) \right] \quad (D.23)$$

D.7 The expression of $\frac{\partial P_c}{\partial \alpha_0}$

From equation (4.2a), the term a_n' can be written as

$$a_n' = a_1' \cdot \frac{b_n}{2n-1} \cdot \hat{d}_n$$

where

$$\left\{ \begin{aligned} b_1 &= \frac{1}{H'} \\ b_2 &= b_1 \cdot \frac{A_0 + \hat{c}_1 - 2D_0}{A_0 + \hat{c}_2} \\ b_k &= \frac{(\hat{c}_{k-2} - A_0) b_{k-2} - 2D_0 b_{k-1}}{A_0 + \hat{c}_k} \end{aligned} \right.$$

$k = 3, 4, 5, \dots$

$$\hat{c}_k = \tanh \sigma_k \quad ; \quad \sigma_k = (2k - 1) \sigma_0$$

$$\sigma_0 = \tanh^{-1} H$$

$$k = 1, 2, 3, \dots$$

and

$$\hat{d}_n = \operatorname{sech} \sigma_n \quad ; \quad \sigma_n = (2n - 1) \sigma_0$$

$$n = 1, 2, 3, \dots$$

First, the derivatives of \hat{c}_k and \hat{d}_n

$$\frac{\partial \hat{c}_k}{\partial \alpha_0} = \operatorname{sech}^2 \sigma_k \frac{\partial \sigma_k}{\partial \alpha_0}$$

$$k = 1, 2, 3, \dots$$

$$\frac{\partial \hat{d}_n}{\partial \alpha_0} = -\operatorname{sech} \sigma_n \tanh \sigma_n \frac{\partial \sigma_n}{\partial \alpha_0}$$

$$n = 1, 2, 3, \dots$$

where

$$\frac{\partial \sigma_k}{\partial \alpha_0} = (2k - 1) \frac{1}{H^2} \frac{\partial H}{\partial \alpha_0}$$

$$\frac{\partial \sigma_n}{\partial \alpha_0} = (2n - 1) \frac{1}{H^2} \frac{\partial H}{\partial \alpha_0}$$

Thus, the derivatives of b_1 , b_2 and b_k

$$\frac{\partial b_1}{\partial \alpha_0} = \frac{H}{H^3} \frac{\partial H}{\partial \alpha_0}$$

$$\frac{\partial b_2}{\partial \alpha_0} = \frac{\partial b_1}{\partial \alpha_0} \cdot \left[\frac{A_0 + \hat{c}_1 - 2D_0}{A_0 + \hat{c}_2} \right]$$

$$+ b_1 \cdot \frac{1}{(A_0 + \hat{c}_2)^2} \left\{ (A_0 + \hat{c}_2) \left[\frac{\partial A_0}{\partial \alpha_0} + \frac{\partial \hat{c}_1}{\partial \alpha_0} - 2 \frac{\partial D_0}{\partial \alpha_0} \right] - (A_0 + \hat{c}_1 - 2D_0) \cdot \left[\frac{\partial A_0}{\partial \alpha_0} + \frac{\partial \hat{c}_2}{\partial \alpha_0} \right] \right\}$$

$$\frac{\partial b_k}{\partial \alpha_0} = \frac{1}{(A_0 + \hat{c}_k)^2} \cdot \left\{ (A_0 + \hat{c}_k) \cdot \left[\frac{\partial b_{k-2}}{\partial \alpha_0} (\hat{c}_{k-2} - A_0) + b_{k-2} \left(\frac{\partial \hat{c}_{k-2}}{\partial \alpha_0} - \frac{\partial A_0}{\partial \alpha_0} \right) \right. \right. \\ \left. \left. - 2 \left(b_{k-1} \frac{\partial D_0}{\partial \alpha_0} + D_0 \frac{\partial b_{k-1}}{\partial \alpha_0} \right) \right] - [(\hat{c}_{k-2} - A_0) b_{k-2} - 2D_0 b_{k-1}] \right\} \\ \cdot \left(\frac{\partial A_0}{\partial \alpha_0} + \frac{\partial \hat{c}_k}{\partial \alpha_0} \right) \quad k = 3, 4, 5, \dots$$

Hence from equation (4.6)

$$P_c = \sum_{n=1}^{\infty} a_n'$$

the derivative is

$$\frac{\partial P_c}{\partial \alpha_0} = \sum_{n=1}^{\infty} \frac{\partial a_n'}{\partial \alpha_0}$$

where

$$\frac{\partial a_n'}{\partial \alpha_0} = \frac{1}{2n-1} \cdot \left\{ \frac{\partial a_1'}{\partial \alpha_0} \cdot b_n \cdot \hat{d}_n + \frac{\partial b_n}{\partial \alpha_0} \cdot a_1' \cdot \hat{d}_n + \frac{\partial \hat{d}_n}{\partial \alpha_0} \cdot a_1' \cdot b_n \right\}$$

This then completes the full derivation of the derivatives required in Sec. 4.3 .

APPENDIX E

ON OPERATORS REPRESENTING SPANWISE INTEGRATION

The full-range spanwise integral is defined as an operator

$$\mathcal{J}[P(\eta, \zeta)] = \int_{-\sqrt{1-\eta^2}}^{\sqrt{1-\eta^2}} P(\eta, \zeta) d\zeta = P(\eta) \quad (\text{E.1})$$

where $P(\eta, \zeta)$ is an even function in $(-\sqrt{1-\eta^2}, \sqrt{1-\eta^2})$.

For the integrands that are even

$$\mathcal{J}[P_\eta(\eta, \zeta)] = P'(\eta) + \frac{2\eta}{\sqrt{1-\eta^2}} P(\eta, \sqrt{1-\eta^2}) \quad (\text{E.2})$$

$$\mathcal{J}[\zeta P_\zeta(\eta, \zeta)] = 2\sqrt{1-\eta^2} P(\eta, \sqrt{1-\eta^2}) - P(\eta)$$

and for odd integrands, according to equation (5.17), they are all zero.

Also, define the following operator as

$$\mathcal{J}_H[P] = \lim_{\eta \rightarrow H} \mathcal{J}[P(\eta, \zeta)] = \int_{-H'}^{H'} P(H, \zeta) d\zeta = P(H) \quad (\text{E.3})$$

$$\mathcal{J}_0[P] = \lim_{\eta \rightarrow 0} \mathcal{J}[P(\eta, \zeta)] = \int_{-1}^1 P(0, \zeta) d\zeta = P(0)$$

at $\eta = H$

$$\mathcal{J}_H[P_H(\eta, \zeta)] = P'(H) + \frac{2H}{H'} \cdot P(H, H') \quad (\text{E.4})$$

$$\mathcal{J}_H[\zeta P_\zeta(H, \zeta)] = 2H' \cdot P(H, H') - P(H)$$

at $\eta = 0$

$$\begin{aligned} \mathcal{D}_0 [P_\eta(0, \zeta)] &= P'(0) \\ \mathcal{D}_0 [\zeta P_\zeta(0, \zeta)] &= 2 P(0, 1) - P(0) \end{aligned} \quad (\text{E.5})$$

Note that the above operation also holds for flow velocities $v(\eta, \zeta)$ and $u(\eta, \zeta)$.

Next, for the side velocity $w(\eta, \zeta)$ which is an odd function in $(-\sqrt{1-\eta^2}, \sqrt{1-\eta^2})$ the operator is defined as

$$\mathcal{D} [w(\eta, \zeta)] = \int_{-\sqrt{1-\eta^2}}^{\sqrt{1-\eta^2}} w(\eta, \zeta) \quad = W(\eta) \quad (\text{E.6})$$

Apparently,

$$\begin{aligned} \mathcal{D} [w(\eta, \zeta)] &= 0 \\ \mathcal{D} [w_\eta(\eta, \zeta)] &= 0 \\ \mathcal{D} [\zeta w_\zeta(\eta, \zeta)] &= 0 \end{aligned} \quad (\text{E.7})$$

but

$$\mathcal{D} [w_\zeta(\eta, \zeta)] = 2w(\eta, \sqrt{1-\eta^2})$$

Hence

at $\eta = H$

$$\mathcal{D}_H [w_\zeta] = 2w(H, H')$$

APPENDIX F

APPLICATION OF SPANWISE INTEGRAL IN THE
TSCHAPLYGIN PLANE

The Tschaplygin plane is defined (e.g. see Ref. 7) by the following Tschaplygin Transformation

$$\begin{cases} \sigma = \tanh^{-1} \eta \\ \mu = \sin^{-1} \frac{\zeta}{\sqrt{1-\eta^2}} \end{cases} \quad (F.1)$$

or

$$\begin{cases} \eta = \tanh \sigma \\ \zeta = \sin \mu \operatorname{sech} \sigma \end{cases} \quad (F.2)$$

Their derivative operators are related as

$$\begin{pmatrix} \frac{\partial}{\partial \sigma} \\ \frac{\partial}{\partial \mu} \end{pmatrix} = \begin{pmatrix} \operatorname{sech}^2 \sigma [-\sin \mu \operatorname{sech} \sigma \tanh \sigma] \\ 0 \quad \cos \mu \operatorname{sech} \sigma \end{pmatrix} \begin{pmatrix} \frac{\partial}{\partial \eta} \\ \frac{\partial}{\partial \zeta} \end{pmatrix} \quad (F.3)$$

$$\begin{pmatrix} \frac{\partial}{\partial \eta} \\ \frac{\partial}{\partial \zeta} \end{pmatrix} = \begin{pmatrix} \cosh^2 \sigma [\cosh^2 \sigma \tanh \sigma \tan \mu] \\ 0 \quad \cosh \sigma / \cos \mu \end{pmatrix} \begin{pmatrix} \frac{\partial}{\partial \sigma} \\ \frac{\partial}{\partial \mu} \end{pmatrix} \quad (F.4)$$

and hence

$$\begin{aligned} (\eta^2 - 1) \frac{\partial^2}{\partial \eta^2} + 2\eta\zeta \frac{\partial^2}{\partial \eta \partial \zeta} + (\zeta^2 - 1) \frac{\partial^2}{\partial \zeta^2} + 2\eta \frac{\partial}{\partial \eta} + 2\zeta \frac{\partial}{\partial \zeta} \\ = -\cosh^2 \sigma \left(\frac{\partial^2}{\partial \sigma^2} + \frac{\partial^2}{\partial \mu^2} \right) \end{aligned} \quad (F.5)$$

Making use of the transformations from equations (F.1) - (F.5) the LHS of equation (6.21) of problem D can now be transformed into the Tschaplygin plane as :-

$$\begin{aligned}
 & (\eta^2 - 1) \mathcal{O}_{\eta\eta} + 2\eta\zeta \mathcal{O}_{\eta\zeta} + (\zeta^2 - 1) \mathcal{O}_{\zeta\zeta} \\
 & = -\cosh^2 \sigma \left[(\mathcal{O}_{\sigma\sigma} + \mathcal{O}_{\mu\mu}) + 2(\mathcal{O}_{\sigma} \tanh \sigma + \mathcal{O}_{\mu} \tan \mu) \right] \quad (F.6)
 \end{aligned}$$

Next, define the full-range spanwise integral in the Tschaplygin coordinate (Refer to Fig. 1-J)

$$\mathcal{J}_{\sigma} [\mathcal{O}(\sigma, \mu)] = P(\sigma) = \int_{-\frac{\pi}{2}}^{\frac{\pi}{2}} \mathcal{O}(\sigma, \mu) \operatorname{sech} \sigma \cos \mu \cdot d\mu \quad (F.7) \quad a$$

thus

$$\frac{\partial}{\partial \sigma} [P(\sigma) \cosh \sigma] = \int_{-\frac{\pi}{2}}^{\frac{\pi}{2}} \mathcal{O}_{\sigma}(\sigma, \mu) \cos \mu \cdot d\mu \quad b$$

$$\frac{\partial^2}{\partial \sigma^2} [P(\sigma) \cosh \sigma] = \int_{-\frac{\pi}{2}}^{\frac{\pi}{2}} \mathcal{O}_{\sigma\sigma}(\sigma, \mu) \cos \mu \cdot d\mu \quad c$$

Also, given are the Mach cone condition (M.C.) for the upper and lower limits of the integrals of equations (F.7), i.e.

$$\begin{aligned}
 \mathcal{O}(\sigma, \frac{\pi}{2}) &= \mathcal{O}(\sigma, -\frac{\pi}{2}) = \mathcal{O}^*(\sigma) \\
 &= \mathcal{A}_1 + \mathcal{B}_1 \tanh \sigma + \mathcal{C}_1 \operatorname{sech} \sigma \quad (F.8)
 \end{aligned}$$

Applying the spanwise integral to equation (F.6) and writing in the notation introduced in equation (F.7) yields :-

$$\begin{aligned}
& \mathcal{D}_\sigma [(\eta^2 - 1) \mathcal{P}_{\eta\eta} + 2 \eta \zeta \mathcal{P}_{\eta\zeta} + (\zeta^2 - 1) \mathcal{P}_{\zeta\zeta}] \\
&= -\cosh^2 \sigma \cdot \mathcal{D}_\sigma [(\mathcal{P}_{\sigma\sigma} + \mathcal{P}_{\mu\mu}) + 2(\tanh \sigma \mathcal{P}_\sigma + \mathcal{P}_\mu \tan \mu)] \\
&= -\cosh^2 \sigma \cdot \left\{ \left(\frac{\partial^2}{\partial \sigma^2} - 1 \right) [P(\sigma) \cosh \sigma] \right. \\
&\quad \left. + 2 \tanh \sigma \frac{\partial}{\partial \sigma} [P(\sigma) \cosh \sigma] \right. \\
&\quad \left. - 2 P(\sigma) \cosh \sigma + 6 \mathcal{P}^*(\sigma) \right\} \tag{F.9}
\end{aligned}$$

On the other hand, applying the spanwise integral to the RHS of equation (6.21) results in

$$\begin{aligned}
& -\mathcal{D}_\sigma [2\kappa^2(\eta p^{(0)} + \zeta p^{(0)})] \\
&= -2\kappa^2 \cdot \left\{ \tanh \sigma \frac{\partial}{\partial \sigma} [P^{(0)}(\sigma) \cosh \sigma] - P^{(0)}(\sigma) \cosh \sigma \right\} \\
&\quad - 2\kappa^2 p^{(0)*}(\sigma) \tag{F.10}
\end{aligned}$$

Finally, equations (F.9) and (F.10) are transformed back to the (η, ζ) plane. Hence the full-range spanwise integral expression of equation (6.21) reads

$$\begin{aligned}
(1 - \eta^2) P''(\eta) + 2\eta P'(\eta) - 2P(\eta) &= -2\kappa^2 [\eta P^{(0)'}(\eta) - P^{(0)}(\eta)] \\
&\quad - \frac{I^*}{\sqrt{1 - \eta^2}}
\end{aligned}$$

where

$$I^* = 4\kappa^2 p^{(0)*}(\sigma) + 6 \mathcal{P}^*(\sigma) \tag{F.11}$$

Equation (F.11) is precisely equation (6.30).

APPENDIX G

THE PRESSURE FORMULATION FOR THE WEDGE FLOW :
A SPECIAL CASE

It can be shown that (Chapter 3) when letting the sweptback angle χ approach zero, problems A and C reduce to the in-phase flow and out-of-phase for a wedge. Hence, Hui's wedge solution (Ref. 34) is recovered from the outer flow formulation. The task here is to attempt to recover the wedge solution from the inner flow formulation, i.e. problem B and D by reinstating the X dependence of the flow and removing the M.C. Thus, in this way the formulation is expressed solely in pressure as the dependent variable of the problem.

Introducing the coordinate transformation

$$\begin{cases} \xi = X \\ \eta = \frac{Y}{X} \\ \zeta = \frac{Z}{X} \end{cases}$$

the D.E., the T.C. and the S.C. of equation (3.28) can be written generally as

$$\begin{aligned} \text{D.E.} \quad & \xi^2 p_{\xi\xi}^{(0)} - 2\xi(\eta p_{\eta\xi}^{(0)} + \zeta p_{\zeta\xi}^{(0)}) + (\eta^2 - 1) p_{\eta\eta}^{(0)} \\ & + 2\eta\zeta p_{\eta\zeta}^{(0)} + (\zeta^2 - 1) p_{\zeta\zeta}^{(0)} + 2(\eta p_{\eta\gamma}^{(0)} + \zeta p_{\zeta\gamma}^{(0)}) = 0 \quad a \\ \left\{ \begin{aligned} & \xi p_{\xi}^{(0)} - (\eta p_{\eta}^{(0)} + \zeta p_{\zeta}^{(0)}) + v_{\eta}^{(0)} + w_{\zeta}^{(0)} = 0 \\ & \xi v_{\xi}^{(0)} - (\eta v_{\eta}^{(0)} + \zeta v_{\zeta}^{(0)}) + p_{\eta} = 0 \\ & \xi w_{\xi}^{(0)} - (\eta w_{\eta}^{(0)} + \zeta w_{\zeta}^{(0)}) + p_{\zeta} = 0 \end{aligned} \right. \quad (G.1) \end{aligned}$$

continued ...

$$\text{T.C.} \quad p_{\eta}^{(0)} = 0 \quad \text{at } \eta = 0 \quad \text{b}$$

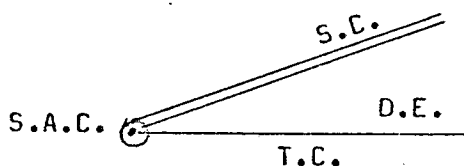
$$\text{S.C.} \quad \left\{ \begin{array}{l} p^{(0)} = C [\xi G_{\xi}^{(0)} + G^{(0)} - \zeta G_{\zeta}^{(0)}] \\ v^{(0)} = A [\xi G_{\xi}^{(0)} + G^{(0)} - \zeta G_{\zeta}^{(0)}] \\ u^{(0)} = E [\xi G_{\xi}^{(0)} + G^{(0)} - \zeta G_{\zeta}^{(0)}] \\ w^{(0)} = K G_{\zeta}^{(0)} \end{array} \right. \quad \text{at } \eta = H \quad \text{c}$$

$$(G.1)$$

$$\text{where } G^{(0)}(\xi, \zeta) = \frac{Q^{(0)}(X, Z)}{X}$$

Clearly, for the case of delta wing, $p^{(0)} = p^{(0)}(\eta, \zeta)$ and $G^{(0)} = G^{(0)}(\zeta)$ equations (G.1) become equations (6.13). For the case of wedge flow, $\zeta = 0$, hence $p^{(0)} = p^{(0)}(\xi, \eta)$, $G^{(0)} = G^{(0)}(\xi)$ and $w^{(0)} = 0$, the above formulation for $p^{(0)}(\xi, \eta)$ reads

THE IN-PHASE FLOW :



$$\text{D.E.} \quad \xi^2 p_{\xi\xi}^{(0)} - 2\xi\eta p_{\eta\xi}^{(0)} + (\eta^2 - 1) p_{\eta\eta}^{(0)} + 2\eta p_{\eta}^{(0)} = 0 \quad \text{a}$$

$$\text{T.C.} \quad \begin{array}{l} p_{\eta}^{(0)} = 0 \\ v^{(0)} = 1 \end{array} \quad \text{at } \eta = 0 \quad \text{b}$$

$$\text{S.C.} \quad (A_0 + H) \xi p_{\xi}^{(0)} + H^2 p_{\eta}^{(0)} = 0 \quad \text{at } \eta = H \quad \text{c}$$

$$(G.2)$$

$$\left\{ \begin{array}{l} p^{(0)} = C [\xi G^{(0)'}(\xi) + G^{(0)}(\xi)] \\ v^{(0)} = A [\xi G^{(0)'}(\xi) + G^{(0)}(\xi)] \\ u^{(0)} = E [\xi G^{(0)'}(\xi) + G^{(0)}(\xi)] \end{array} \right. \quad \text{c}$$

$$\text{S.A.C.} \quad \left[\xi G(\xi) \right]_{\xi \rightarrow 0} = -\lambda x_0 \quad \text{d}$$

From the T.C. and the S.C., the solutions representing again a uniform flow are obtained as

$$p^{(0)}(\xi, \eta) = \frac{C}{A} \quad \text{a}$$

$$v^{(0)}(\xi, \eta) = 1 \quad \text{(G.3) b}$$

$$u^{(0)}(\xi, \eta) = \frac{E}{A} \quad \text{c}$$

The solution of the perturbed in-phase shock shape results from solving the following problem

$$\xi G^{(0)'}(\xi) + G^{(0)}(\xi) = \frac{1}{A}$$

with S.A.C. $\left[\xi G(\xi) \right]_{\xi \rightarrow 0} = -\lambda x_0$ as its initial condition.

The solution thus reads

$$G^{(0)}(\xi) = \frac{1}{A} - \frac{\lambda x_0}{\xi} \quad \text{(G.3) d}$$

or in terms of $Q^{(0)}$

$$Q^{(0)}(x) = \frac{x}{A} - \lambda x_0 \quad \text{e}$$

The solutions obtained in equation 3 are identically the solutions obtained by Hui (Ref. 38, equation 19), i.e.

$$Q^0(x) = \frac{x}{\tilde{A}_w} - x_0$$

Similarly the problem D can be put down in general as (see equations 6.18)

$$\begin{aligned} \text{D.E. } \xi^2 p_{\xi\xi}^{(1)} - 2\xi(\eta p_{\eta\xi}^{(1)} + \zeta p_{\zeta\xi}^{(1)}) + (\eta^2 - 1) p_{\eta\eta}^{(1)} \\ + 2\eta\zeta p_{\eta\zeta}^{(1)} + (\zeta^2 - 1) p_{\zeta\zeta}^{(1)} + 2(\eta p_{\eta\gamma}^{(1)} + \zeta p_{\zeta\gamma}^{(1)}) = \\ - 2\kappa^2 \xi(\eta p_{\eta\gamma}^{(0)} + \zeta p_{\zeta\gamma}^{(0)}) \end{aligned} \quad \text{(G.4) a}$$

$$\begin{cases} \xi p_{\xi}^{(1)} - (\eta p_{\eta}^{(1)} + \zeta p_{\zeta}^{(1)}) + v_{\eta}^{(1)} + w_{\zeta}^{(1)} = \xi b^{(0)} \\ \xi v_{\xi}^{(1)} - (\eta v_{\eta}^{(1)} + \zeta v_{\zeta}^{(1)}) + p_{\eta}^{(1)} = -\xi v^{(0)} \\ \xi w_{\xi}^{(1)} - (\eta w_{\eta}^{(1)} + \zeta w_{\zeta}^{(1)}) + p_{\zeta}^{(1)} = -\xi w^{(0)} \end{cases} \quad (G.4)$$

where $b^{(0)} = \frac{1}{\lambda} U^{(0)} - \kappa^2 p^{(0)}$

T.C. $\begin{cases} p_{\eta}^{(1)} = -2\xi \\ v^{(1)} = \xi - x_0 \end{cases}$ at $\eta = 0$ b

S.C. $\begin{cases} p^{(1)} = C [G^{(1)} + \xi G_{\xi}^{(1)} - \zeta G_{\zeta}^{(1)}] + D [\xi G^{(0)}(\xi, \zeta)] \\ v^{(1)} = A [G^{(1)} + \xi G_{\xi}^{(1)} - \zeta G_{\zeta}^{(1)}] + B [\xi G^{(0)}(\xi, \zeta)] \\ w^{(1)} = K G_{\zeta}^{(1)} \end{cases}$ c

where $G^{(1)}(\xi, \zeta) = \frac{Q^{(1)}(X, Z)}{X}$

Clearly, for the case of wedge flow, $\zeta = 0$, hence $p^{(1)} = p^{(1)}(\xi, \eta)$, $G^{(1)} = G^{(1)}(\xi)$ and $w^{(1)} = 0$, the above formulation for $p^{(1)}$ thus reads

D.E. $\xi^2 p_{\xi\xi}^{(1)} - 2\xi\eta p_{\eta\xi}^{(1)} + (\eta^2 - 1) p_{\eta\eta}^{(1)} + 2\eta p_{\eta}^{(1)} = 0$ a

T.C. $p_{\eta}^{(1)} = -2\xi$ at $\eta = 0$ b

S.C. $(A_0 + H) \xi p_{\xi}^{(1)} + (1 - H^2) p_{\eta}^{(1)} + \xi \cdot \left(\frac{E^{(0)}}{A} - H b^{(0)} + 1 \right) = 0$ c

S.A.C. $p^{(1)} = -I x_0$ at $\eta = 0$
 $\xi = 0$ d

where $\begin{cases} E^{(0)} = B - A_0 D \\ b^{(0)} = \frac{1}{A} \left(\frac{E}{\lambda} - \kappa^2 C \right) \\ I = \frac{C}{A} [1 - \lambda E^{(0)}] \end{cases}$ (G.5)

Note that the equations (G.5) still remain a hyperbolic-type problem.

Following the similar procedure as for problem D, a solution of the form

$$p^{(1)}(\xi, \eta) = \xi \mathcal{P}(\eta) - I x_0 \quad (G.6)$$

is sought.

Thus, equations (G.5) can be reduced to an ordinary differential equation formulation, i.e.

$$\text{D.E.} \quad \mathcal{P}''(\eta) = 0 \quad a$$

$$\text{T.C.} \quad \mathcal{P}'(0) = -2 \quad (G.7) \quad b$$

$$\text{S.C.} \quad (A_0 + H) \mathcal{P}(H) + (1 - H^2) \mathcal{P}'(H) = (Hb^{(0)} - 1 - \frac{E^{(0)}}{A}) \quad c$$

where $0 \leq \eta \leq H < 1$

The solution reads

$$\mathcal{P}(\eta) = b_1 \eta + a_1 \quad (G.8)$$

$$\text{where} \quad \begin{cases} a_1 = \frac{2(A_0 H + 1) + Hb^{(0)} - 1 - \frac{E^{(0)}}{A}}{A_0 + H} & a \\ b_1 = -2 & b \end{cases}$$

Hence the total out-of-phase pressure is obtained

$$p^{(1)}(\xi, \eta) = \xi (a_1 + b_1 \eta) - I x_0 \quad (G.9)$$

Making use of the following conversion (given in Appendix I) to the wedge-flow notation

$$\begin{aligned} \tilde{A}_w &= \lambda A & \tilde{C}_w &= M_0 C \\ \tilde{B}_w &= \lambda B & \tilde{D}_w &= M_0 D \end{aligned}$$

together with the pressure notation

$$p_w^1 = \frac{M_0}{\lambda} p^1$$

equation (G.9) becomes

$$p_w^1(x, y) = A_1' x + B_1' y - I x_0 \quad (G.10)$$

where $A_1' = \kappa a_1$

$$= \kappa \left\{ \frac{\frac{E_w H}{\kappa} b_0 + 2 \kappa H + E_w \left(1 - \frac{\tilde{B}_w}{\tilde{A}_w} \right) + \frac{\tilde{D}_w}{\tilde{A}_w}}{1 + \frac{E_w H}{\kappa}} \right\}$$

and $B_1' = -2 M_0$

Referred to Ref. 34 (Hui), equation (G.10) above is proved identical to Hui's solution (equation 19, Ref. 34).

Finally, the out-of-phase shock shape, $G^{(1)}(\xi)$ can be determined by solving any one of the equations (G.4)c thus

$$\xi G^{(1)'}(\xi) + G^{(1)}(\xi) = \left[\frac{a_1 + b_1 H - \frac{D}{A}}{c} \right] \cdot \xi + \left[\frac{D \lambda - I}{c} \right] x_0$$

with S.A.C.

$$\xi G^{(1)}(\xi) \Big|_{\xi \rightarrow 0} = 0 \quad (G.11)$$

Hence the solution reads

$$G^{(1)}(\xi) = \left[\frac{a_1 + b_1 H - \frac{D}{A}}{2c} \right] \cdot \xi + \left[\frac{D \lambda - I}{c} \right] \cdot x_0 \quad (G.12)$$

Again, in terms of Hui's wedge solution expression, equation (G.12)

becomes : -

$$Q^1(x) = \left[\frac{A_1' - 2\kappa H - \frac{\tilde{D}_w}{\tilde{A}_w}}{2\tilde{C}_w} \right] x^2 + \left[\frac{\tilde{D}_w - I_w}{\tilde{C}_w} \right] x_0 \cdot x \quad (G.13)^*$$

where $I_w = \kappa I$

This is indeed Hui's out-of-phase shock shape solution. Hence, the proof of a reduction to the wedge case is complete.

Some remarks concerning the present pressure formulation are in order as follows :

i) Although the present method of solution does seem less direct than that given by Hui, (Ref. 37), the method is a formal one. Following the same general formulation for the 3D flow, the present method of solution is also consistent with the 3D method of solution.

ii) To formulate the problem in terms of P alone has merit in studying other related problems with attached shock waves, i.e.

(a) small perturbation in geometry: either the thickness or the incidence can be the perturbed parameter for studying the airfoil curvature - shock reflected wave effects (see Lighthill, Ref. 31).

(b) small perturbation in flow condition :

For studying the locally subsonic flow behind the curved shock wave of the finite wedge the perturbed parameter λ_0 can be used ($\lambda_0 = \sqrt{1 - M_0^2}$). Here the local Mach number immediately behind the shock at the apex is defined as

M_0 , $M_0 \lesssim 1$. (see Tamada, Ref. 69, and Oguchi, Ref. 70).

* Apparently, Hui's shock shape (equation (19), Ref. 37) is in error. In the second term of his expression 1 should be replaced by \tilde{D}_w and a factor of x_0 is multiplied to be term.

In the studies of Lighthill and Oguchi, the formulations were expressed in terms of a 'pressure potential' alone in the differential equation but no single equation was obtained for the shock-wave boundary condition.

Hence, it would be interesting to apply the present formulation (equation (G.5)) to these problems.

APPENDIX H

AN IMPROVED PERTURBATION SCHEME TO THE INNER PROBLEMS

At the end of Chapter 1 and Chapter 8, the approximate nature of Problems B and D was pointed out and possible improvement was indicated. In the present appendix, an improved perturbation scheme is proposed as follows :

H.1 The Scheme :

Let δ and ϵ be the small perturbation parameters representing 2-D departure and the small amplitude of oscillation respectively*, the new scheme thus reads

$$\bar{u} = u_0 \left[(1 + \delta u) + \epsilon (U_0 + \delta U_1) \right] \quad a$$

$$\bar{v} = u_0 \left[\delta v + \epsilon (V_0 + \delta V_1) \right] \quad b$$

$$\bar{w} = u_0 \left[\delta w + \epsilon (W_0 + \delta W_1) \right] \quad (H.1) \quad c$$

$$\bar{p} = p_0 \left[1 + \frac{\gamma M_0^2}{\lambda} \left[\delta p + \epsilon (P_0 + \delta P_1) \right] \right] \quad d$$

$$\bar{\rho} = \rho_0 \left[1 + \frac{M_0^2}{\lambda} \left[\delta \rho + \epsilon (R_0 + \delta R_1) \right] \right] \quad e$$

Corresponding to equations (2.12), $\delta u = u_\delta$, $\delta v = v_\delta$, $\delta w = w_\delta$, $\delta p = p_\delta$ and $\delta \rho = \rho_\delta$; and $U_0 + \delta U_1 = \hat{U}$, $V_0 + \delta V_1 = \hat{V}$... and so on.

The subscript $()_0$ represents the oscillatory solution of the wedge flow obtained by Hui (Ref. 37). The subscript $()_1$ represents

* Since the purpose here is to demonstrate the new perturbation scheme, for convenience some notations are re-defined.

the oscillatory solution of the 2-D departure flow now to be sought.

For example, U_0 and U_1 are expressed as

$$U_0(X, Y, T) = \left[U_0^{(0)} + ik_0 U_0^{(1)}(X, Y) \right] e^{ik_0 T} \quad (H.2)$$

$$U_1(X, Y, Z, T) = \left[U_1^{(0)}(X, Y, Z) + ik_0 U_1^{(1)}(X, Y, Z) \right] e^{ik_0 T}$$

where $()^{(0)}$ and $()^{(1)}$ indicate the in-phase flow and out-of-phase flow as usual.

Hence, V_0 , V_1 , P_0 , P_1 ... and so on, can be expressed in the like manner. Note that $W_0 \equiv 0$, by definition of the wedge flow.

In checking the limits of the perturbation procedure :

letting $\epsilon \rightarrow 0$, $\bar{u} \rightarrow u_\Delta$, reduces \bar{u} to the steady mean flow delta wing solution ;

letting $\delta \rightarrow 0$, $\bar{u} \rightarrow u_0 (1 + \epsilon U_0)$ reduces \bar{u} to the oscillatory wedge solution ;

letting $k_0 \rightarrow 0$, $\bar{u} \rightarrow u_\Delta + \epsilon (U_0^{(0)} + \delta U_1^{(0)})$ reduces \bar{u} to the in-phase mean flow delta wing solution.

Indeed, they all approach to the correct limits.

H.2 The x-momentum equation : an example

For demonstration of the new perturbation scheme, the x-momentum equation (equation (3.1)b) is selected as an example, i.e.

$$\frac{\partial \bar{u}}{\partial t} + \bar{u} \frac{\partial \bar{u}}{\partial t} + \bar{v} \frac{\partial \bar{u}}{\partial y} + \bar{w} \frac{\partial \bar{u}}{\partial z} = -\frac{1}{\bar{\rho}} \frac{\partial \bar{p}}{\partial x} \quad (H.3)$$

Following the inner-region coordinate system, equation (2.9), and substituting equation (H.1) into equation (H.3), yield two perturbed equations in $O(\epsilon)$ and in $O(\epsilon k_0)$

$O(\epsilon)$:

$$\frac{\partial U_0}{\partial T} + \frac{\partial U_0}{\partial X} + \frac{1}{\lambda} \frac{\partial P_0}{\partial X} = 0 \quad (\text{H.4}) \text{ a}$$

$O(\epsilon k_0)$:

$$\begin{aligned} \frac{\partial U_1}{\partial T} + \frac{\partial U_1}{\partial X} + \frac{1}{\lambda} \frac{\partial P_1}{\partial X} = & - \left[U_0 \frac{\partial U}{\partial X} + \lambda V_0 \frac{\partial U}{\partial Y} - \kappa^2 R_0 \frac{\partial P}{\partial X} \right] \\ & - \left[U \frac{\partial U_0}{\partial X} + \lambda V \frac{\partial U_0}{\partial Y} - \kappa^2 \rho \frac{\partial P_0}{\partial X} \right] \end{aligned} \quad (\text{H.4}) \text{ b}$$

Clearly, equation (H.4)a is the unsteady wedge equation and equation (H.4)b is the 'new' unsteady delta wing equation. The RHS of equation (H.4)b are all known terms to be treated as inhomogeneous terms in the formulation.

Next, substituting equation (H.2) into equation (H.4)b yield two perturbed equations in $O(\epsilon \delta)$ and in $O(\epsilon \delta k_0)$

$O(\epsilon \delta)$:

$$\begin{aligned} \frac{\partial U_1^{(0)}}{\partial X} + \frac{1}{\lambda} \frac{\partial P_1^{(0)}}{\partial X} = & - \left[U_0^{(0)} \frac{\partial U}{\partial X} + \lambda V_0^{(0)} \frac{\partial U}{\partial Y} - \kappa^2 R_0^{(0)} \frac{\partial P}{\partial X} \right] \\ = & h_{\Delta}^{(0)}(X, Y, Z) \end{aligned} \quad (\text{H.5}) \text{ a}$$

$O(\epsilon \delta k_0)$:

$$\begin{aligned} \frac{\partial U_1^{(1)}}{\partial X} + \frac{1}{\lambda} \frac{\partial P_1^{(1)}}{\partial X} = & - U_1^{(0)} - \left\{ \left[U_0^{(1)} \frac{\partial U}{\partial X} + \lambda V_0^{(1)} \frac{\partial U}{\partial Y} - \kappa^2 R_0^{(1)} \frac{\partial P}{\partial X} \right] \right. \\ & \left. + \left[U \frac{\partial U_0^{(1)}}{\partial X} + \lambda V \frac{\partial U_0^{(1)}}{\partial Y} - \kappa^2 \rho \frac{\partial P_0^{(1)}}{\partial X} \right] \right\} \\ = & - U_1^{(0)} + h_{\Delta}^{(1)}(X, Y, Z) \end{aligned} \quad (\text{H.5}) \text{ b}$$

Equations (H.5)a and (H.5)b are the 'new' in-phase and out-of-phase equations. The inhomogeneous terms on the RHS of (H.5)a, $h_{\Delta}^{(0)}$, represent the interaction between the in-phase wedge flow (equation (H.4)a) and the mean flow of a delta wing (equation (3.7)). The inhomogeneous term on the RHS of (H.5)b, $h_{\Delta}^{(1)}$, represents the interaction between the out-of-phase wedge flow and the mean flow of a delta wing. Clearly, in the present formulation, $h_{\Delta}^{(0)}$ and $h_{\Delta}^{(1)}$ were dropped in order to simplify the problem.

H.3 Proposed Method of solution

When equation (H.5)a is expressed in the conical coordinates, it becomes

$$\eta u_1^{(0)} \eta + \zeta u_1^{(0)} \zeta + \frac{1}{\lambda} \left[\eta p_1^{(0)} \eta + \zeta p_1^{(0)} \zeta \right] = - \left\{ u_o^{(0)} (\eta u_{\eta} + \zeta u_{\zeta}) + \lambda v_o^{(0)} u_{\eta} + \kappa^2 R_o^{(0)} (\eta p_{\eta} + \zeta p_{\zeta}) \right\}$$

Together with the other form equations derived for the in-phase flow then, $u_1^{(0)}$, $v_1^{(0)}$, $w_1^{(0)}$, and $R_1^{(0)}$ can be eliminated in the same way as Problem B. Consequently, a $p_1^{(0)}$ formulation is possible and the equation reads

$$(\eta^2 - 1)p_1^{(0)} \eta \eta + 2\eta \zeta p_1^{(0)} \eta \zeta + (\zeta^2 - 1)p_1^{(0)} \zeta \zeta + 2\eta p_1^{(0)} \eta + 2\zeta p_1^{(0)} \zeta = N_{\Delta}^{(0)}(\eta, \zeta) \quad (H.7)$$

It is in the same form as equation (6.13) except that $N_{\Delta}^{(0)}(\eta, \zeta)$ involves many known terms of interaction. The boundary conditions can be perturbed and result in a similar form as equation (6.13). This allows the 'new' method of solution to follow the same method used in Chapter 6, except one needs to cope with all the inhomogeneous terms.

If one applies the method of spanwise integration, the formulation then becomes an O.D.E. with inhomogeneous terms. This presents little problem, as the solution technique is standard (see equations (6.31) and (6.32)).

Similarly, the out-of-phase solution of (H.5)b can be obtained following the same method of solution.

APPENDIX I

CONVERSION TABLES FOR VARIABLES AND COEFFICIENTS
FOR VARIOUS PROBLEMS IN THE PRESENT FORMULISM.

DEPENDENT VARIABLES

Inner Region (HDP)	Outer Region	Wedge Flow (HWP)
$\frac{m_o^2 p_o}{\lambda P_*} \cdot \hat{p}$	P	$\gamma M_o P_w$
$\frac{u}{u_*} \cdot \hat{v}$	V	V_w
$\frac{u}{u_*} \cdot \hat{u}$	U	U_w
$\frac{u}{u_*} \cdot \hat{w}$	W	0
$\frac{\rho_o m_o^2}{\rho_* \lambda} \cdot \hat{R}$	R	$M_o R_w$
$\frac{1}{\lambda} \hat{Q}$	Q	Q_w

INDEPENDENT VARIABLES

Inner
Region : $\begin{pmatrix} X \\ Y \\ Z \\ T \end{pmatrix}$
(HDP)

Outer
Region : $\begin{pmatrix} x \\ y \\ z \\ t \end{pmatrix}$

Wedge
Flow
(HWP) $\begin{pmatrix} x \\ y \\ \theta \\ T \end{pmatrix}$

$(x, \frac{y}{\lambda}, \frac{z}{\lambda})$

(x, y, z)

(x, y)

$T \cdot \frac{u}{u_*}$

t

$T \cdot \frac{u}{u_*}$

S.C. COEFFICIENTS

Inner Region <2D>	Outer Region	Wedge Flow
λA	\tilde{A}_1	\tilde{A}_w
0	\tilde{A}_2	0
λB	\tilde{B}	\tilde{B}_w
$\gamma M_o^2 C$	\tilde{C}_1	$\gamma M_o \tilde{C}_w$
0	\tilde{C}_2	0
$\gamma M_o^2 D$	\tilde{D}	$\gamma M_o \tilde{D}_w$
λE	\tilde{E}_1	\tilde{E}_w
0	\tilde{E}_2	0
λF	\tilde{F}	\tilde{F}_w
$M_o^2 G$	\tilde{G}_1	$M_o \tilde{G}_w$
0	\tilde{G}_2	0
$M_o^2 J$	\tilde{J}	$M_o \tilde{J}_w$
K	\tilde{K}	0

REFERENCES

1. TOWNEND, L.H. Some design aspects of space shuttle orbitors.
RAE TR 70139, 1970
2. NONWEILER, T.R.F. Aerodynamic problems of manned space vehicles.
Journal of the Royal Aeronautical Society, Vol. 63,
No. 585, September 1959, 521-528
3. FOWELL, L.R. Exact and approximate solutions for the supersonic
delta wing.
J.Aeronaut.Sci. 8, 1956, 709-720
4. BABAEV, D.A. Numerical solution of the problem of supersonic flow
past the lower surface of a delta wing.
AIAA J., Vol. 1, No. 9, 2224-2231
5. VOSKRESENSKI, G.P. Numerical solution of the problem of a supersonic gas
flow past an arbitrary surface of a delta wing in the
compression region.
Izv. Akad. Nauk SSSR, Mekh. Zhidk., Gaza, No. 4,
1968, 134-142
6. SOUTH, J.C. &
KLUNKER, E.B. Methods for calculating non-linear conical flows.
NASA SP 228, Oct. 1969, 131-156
7. HUI, W.H. Supersonic and hypersonic flow with attached shock
waves over delta wings.
Proc. Roy. Soc., London, A325, 1971, 251-268
8. HUI, W.H. Methods for calculating non-linear flows with
attached shock waves over conical wings.
AIAA J., Vol. 11, No. 10, October 1973, 1443-1445
9. GARRICK, I.E. and
RUBINOW, S.I. Theoretical study of air forces on an oscillating or
steady thin wing in a supersonic main stream.
NACP Rep. 872, 1947
10. STEWARD, H.J. and
LI, T.Y. Source-superposition method of solution of a
periodically oscillating wing at supersonic speeds.
Quar. of Appl. Math. 9, 1951, 31-45
11. STEWARTSON, K. On the linearized potential theory of unsteady
supersonic motion I.
Quar. F. Mech. Appl. Math. 3, 1950, 182-199
12. STEWARTSON, K. On the linearized potential theory of unsteady
supersonic motion II.
Quar. J. Mech. Appl. Math. 5, 1952, 137-154
13. MILES, J.W. On damping in pitch for delta wings.
Jour. Aero. Sci. 16, 1949, 574-575
14. MILES, J.W. Potential Theory of Unsteady Supersonic Flow.
Cambridge monographs on Mech. & Appl. Math., 1959

15. ADAMS, M.C. and SEARS, W.R. Slender body theory - Review and extension. Jour. Aero. Sci. 20, 1953, 85-98
16. GUNN, J.C. Linearized supersonic aerofoil theory, Parts. I & II. Phil. Trans. A, 240, 1947, 327-373
17. MALVESTUTO, F. and MARGOLIS, K. Theoretical stability derivatives of thin sweptback wings tapered to a point with sweptback or swept-forward training edges for a limited range of supersonic speeds. NACA TN1761, 1949
18. MARTIN, J., MARGOLIS, K. and JEFFREYS, I. Calculation of lift and pitching moments due to angle of attack and steady pitching velocity at supersonic speeds for thin sweptback tapered wings with stream-wise tips and supersonic leading and trailing edges. NACA TN 2699, 1952
19. NELSON, H.C. Lift and moment on oscillating triangular and related wings with supersonic edges. NACA TN 2494, 1951
20. FROELICH, J.E. Nonstationary motion of purely supersonic wings. Jour. Aero. Sci. 18, 1951, 298-310
21. LANDAHL, M.T. Unsteady Transonic Flow. Pergamon Press, New York, 1961, p. 39
22. LANDAHL, M.T. Unsteady flow around thin wings at high Mach numbers. Jour. Aero. Sci. 24, 33-38
23. Van DYKE, M.D. Supersonic flow past oscillating airfoils including non-linear thickness effects. NACA PT 1183, 1945
24. HAYES, W.D. and PROBSTEIN, R.F. Hypersonic Flow Theory. Academic Press, 1966
25. LIGHTHILL, M.J. Oscillating airfoils at high Mach number. Jour. Aero. Sci., Vol. 20, June 1953
26. MORGAN, H., RUNYAN, H. and HUCKEL, V. Theoretical consideration of flutter at high Mach numbers. Jour. Aero. Sci. 25, 1958, 371-381
27. ZARTARIAN, G., HSU, P.T. and ASHLEY, H. Dynamic airloads and aeroelastic problems at entry Mach numbers. Jour. Aero. Sci. Vol. 28, No. 3, 1961
28. ASHLEY, H. and ZARTARIAN, G. Piston Theory - A new aerodynamic tool for the Aeroelastician. Jour. Aero. Sci. Vol. 23, No. 12, December 1956, 1109-1118

29. MILES, J.W. Newtonian flow over a stationary body in unsteady flow.
AIAA J., Vol. 4, No. 1, 1966, 38-40
30. ARDESTY, J., CHARWAT, A.F., CHEN, S.Y. and COLE, J.D. A snowplow model of hypersonic unsteady flows. The Rand Corporation Report, February 1967, (AD 647267)
31. LIGHTHILL, M.J. The flow behind a stationary shock. Phil. Mag. Vol. 40, 1949, 214-220
32. CHU, B.T. On weak interaction of strong shock and Mach wave generated downstream of the shock. Jour. Aero. Sci. Vol. 19, 1952, 433-446
33. CHERNYI, G.G. Introduction of Hypersonic Flow. Academic Press, N.Y. and London, 1961
34. HUI, W.H. A perturbation theory of unsteady hypersonic and supersonic flows. Ph.D. Thesis, University of Southampton, April 1968.
35. APPLETON, J.P. Aerodynamic pitching derivatives of a wedge in hypersonic flow. AIAA J., Vol. 2, 1964, 2034-3036
36. McINTOSH, S.C. Jr. Hypersonic flow over an oscillating wedge. AIAA J., Vol. 3, No. 3, March 1965, 433-440
37. HUI, W.H. Stability of oscillating wedges and caret wings in hypersonic and supersonic flows. AIAA J., Vol. 7, No. 8, August 1969, 1524-1530
38. Van DYKE, M. 'The circle at low Reynolds number at a test of the method of series truncation' Appl. Mech. proceedings of the 11th International Congress of Applied Mechanics, 1964. Published by Springer-Verlag, 1165-1169
39. SWIGART, R.J. A theory of asymmetric hypersonic blunt body flow. AIAA J., Vol. 1, No. 5, May 1963, 1034-1042
40. CHANG, S. S-H A theory of supersonic flow past steady and oscillating blunt bodies of revolution. AIAA J., Vol. 9, No. 8, September 1971, 1754-1762
41. TELENIN, G.F. and LIPNITSKII, Iu M. Nonstationary supersonic flow around blunt bodies with a detached shock. Izvestiya Akademii Nauk SSSR, Mekhanika Zhidkosti i Gaza, No. 4, 1966, 19-29
42. MESSITER, A.F. Lift of slender delta wings according to Newtonian Theory. AIAA J. Vol. 1, 1963, 794-802

43. HIDA, K. Thickness effects on the force of slender wings in hypersonic flow.
AIAA J., Vol. 3, 1965, 427
44. SQUIRE, L.C. Calculated pressure distribution and shock shapes on thick conical wings at high supersonic speeds.
Aero.Quar. Vol. XVIII, May 1967, 185
45. MALMUTH, N. A new area rule for hypersonic wing-bodies.
AIAA J., Vol. 9, No. 12, 2460-2462
46. HUI, W.H. Unified area rule for hypersonic and supersonic wing-bodies.
AIAA J. Vol. 10, No. 7, July 1972, 961-962
47. NACA AMES STAFF Equation, Tables and Charts for compressible flow.
NACA RT 1135, 1953
48. ORLIK-RUCKEMANN, K.J. and LABERGE, J.G. Static and dynamic longitudinal stability characteristics of a series of delta and sweepback wings at supersonic speeds.
National Research Council of Canada, Aero. Report LR 396, January 1966
49. HALL, G.Q., and OSBORNE, L.A. Transonic and supersonic derivative measurement on the planforms of the Ministry of Aviation flutter and vibration committee's first Research Programme.
Hawker Siddeley Dynamic Ltd., Report ARL 64/9 A:R.C. 26016, FV 139, 1964
50. KIND, R.J. and ORLIK-RUCKEMANN, K.J. Stability derivatives of sharp cones in viscous hypersonic flow.
AIAA Jour., August 1966, 1469-1471
51. TOBAK, M. and WEHREND, W.R. Stability derivatives of cones at supersonic speeds.
NACA TN 3788, 1956
52. Van DYKE, M.D. On supersonic flow past an oscillating wedge.
Quar. Appl. Math., Vol. 11, No. 3, 1953
53. HUI, H.W. On axisymmetric and two-dimensional flow with attached shock waves.
Astronautica Acta, Vol. 18, 1973, 35-44
54. HUI, W.H. The caret wing at certain off-design conditions.
Aero. Quar. Vol. XXIII, November 1972, 263-275
55. LIU, D.D. On the design conditions of a caret wing.
University of Southampton AASU RT327, April 1973
56. Van DYKE, M.D. Perturbation methods in fluid mechanics.
Academic Press, New York
57. FRANKLE, F.I. and KARPOVICH, E.A. Gas Dynamics of Thin Bodies.
Interscience, New York, 1953

58. MALMUTH, N. Hypersonic flow over a delta wing of moderate aspect ratio.
AIAA Jour., Vol. 4, No. 3, March 1966, 555-556
59. MALMUTH, N. Pressure fields over hypersonic wing-bodies at moderate incidence.
J. Fluid Mech. Vol. 59, Part 4, 1973, 673-691
60. ROE, P.L. A result concerning the supersonic flow below a plane delta wing.
RAE TR 72077, May 1972
61. CLARKE, J.H. and WALLACE, J. Uniform second-order solution for supersonic flow over delta wing using reverse-flow integral method.
J. Fluid Mech. 18, 225-238
62. CROCCO, L. Coordinate perturbation and multiple scale in gas dynamics.
Phil. Trans. of Roy. Soc., Vol. 272, A1222
63. LIGHTHILL, M.J. A technique for rendering approximate solutions to physical problems uniformly valid.
Phil. Mag. 40, 1179-1201
64. PRITULO, M.F. On the determination of uniformly accurate solutions of differential equations by the method of perturbation of coordinates.
J. Appl. Math. Mech. 26, 661-667
65. HILL, W.G. A convenient, explicit formula for oblique-shock calculations.
AIAA Jour. Vol. 5, No. 5, September 1968, p. 509
66. THOMPSON, M.J. A note on the calculation of oblique shock-wave characteristics.
J.A.S. Vol. 17, No. 11, November 1950, p. 741
67. ABROMOWITZ and STEGUN Handbook of Mathematical Functions.
SI272, Dover 1965, p. 17
68. HUI, W.H. Effects of upstream unsteadiness on hypersonic flow past a wedge.
Physics of Fluids, Vol. 15, No. 10, October 1972, 1747-1750
69. TAMADA, K. On the detachment of shock wave from the leading edge of a finite wedge.
J. of the Phy. Soc. of Japan, Vol. 8, No. 2, March-April 1953, 212-247
70. OGUCHI, H. On the sonic flow behind the bow wave of a finite wedge.
J. of the Phy. Soc. of Japan, Vol. 9, No. 2, March-April 1954, 249-225
71. LIGHTHILL, M.J. The diffraction of blast.
Proc. Roy. Soc. (London) A200, 1950, 554-565

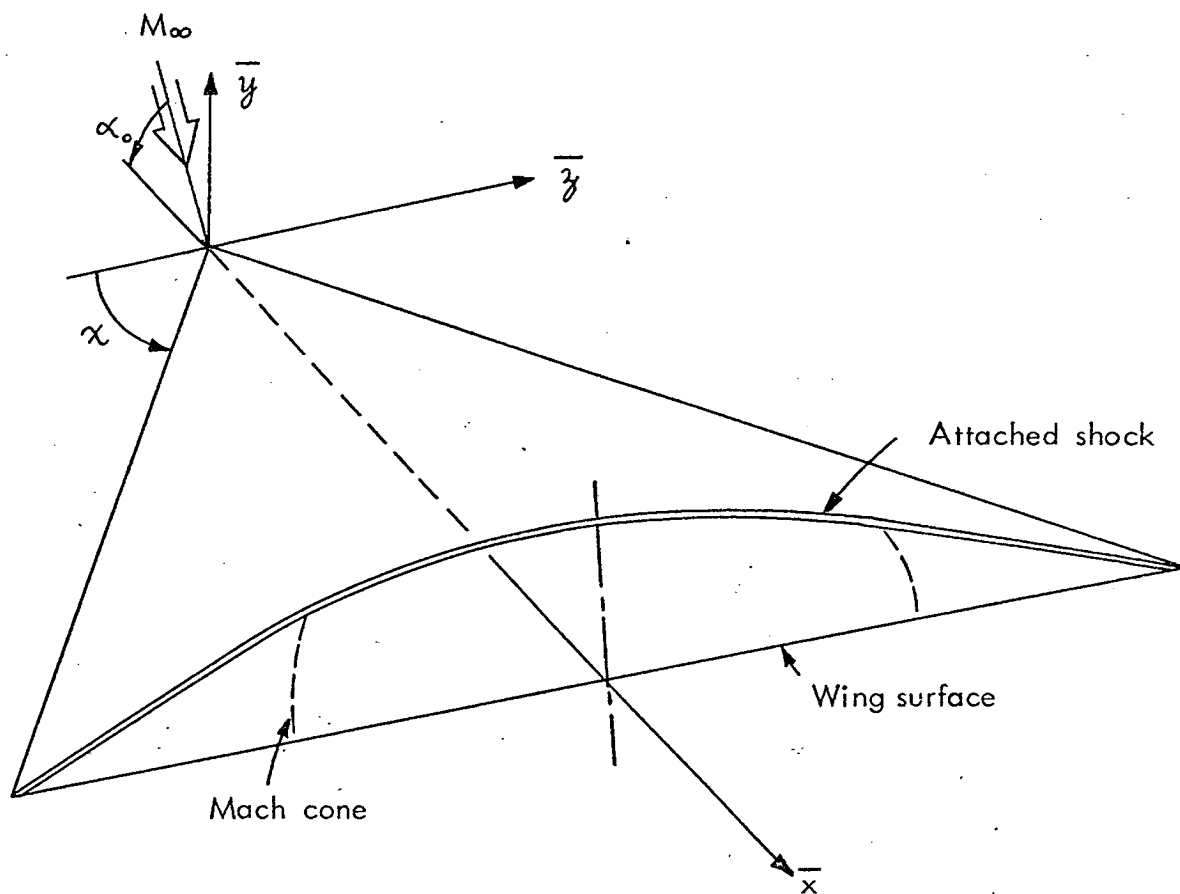


FIG. 1A. FLAT-BOTTOM DELTA WING PLACED IN THE CARTESIAN CO-ORDINATE.

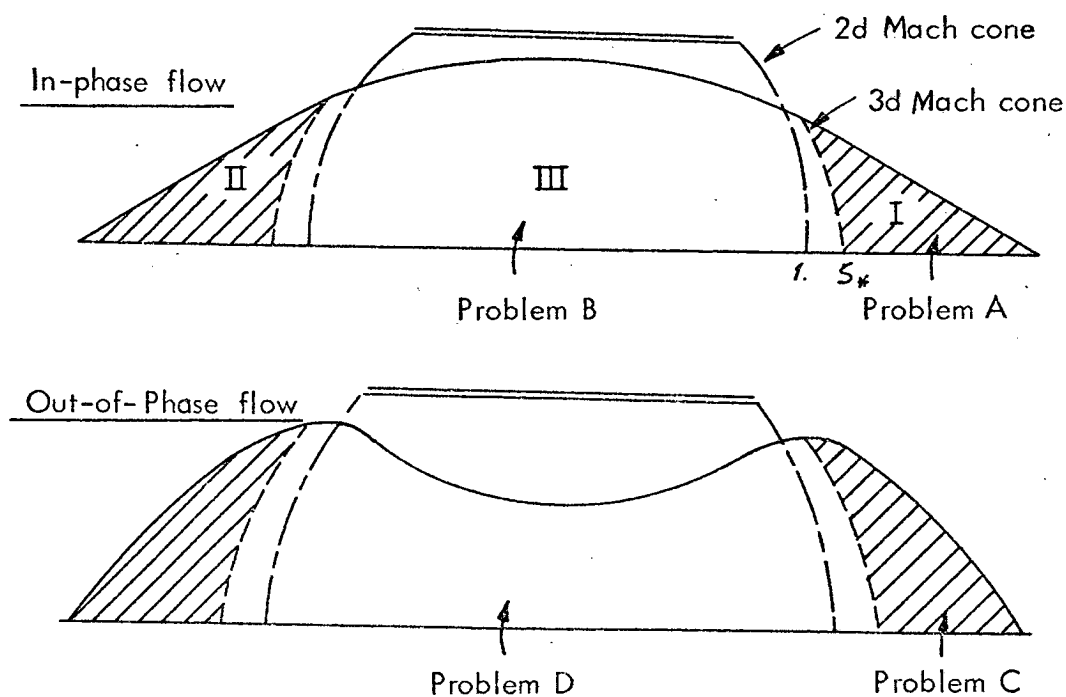


FIG. 1-B PROBLEMS A, B, C & D AND THE DEFINED REGIONS.

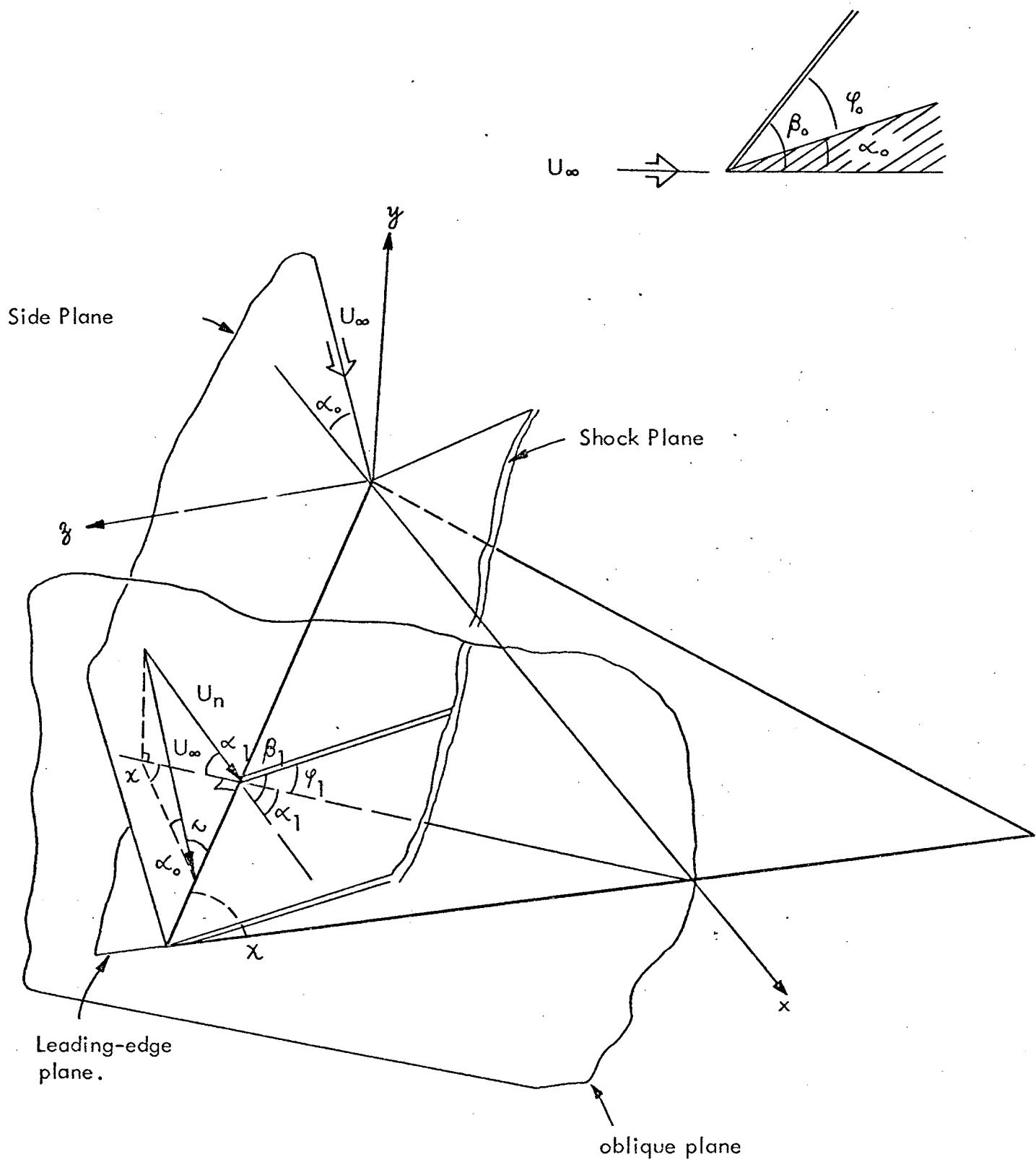


FIG.1-C DELTA WING SHOWING NOTATIONS.

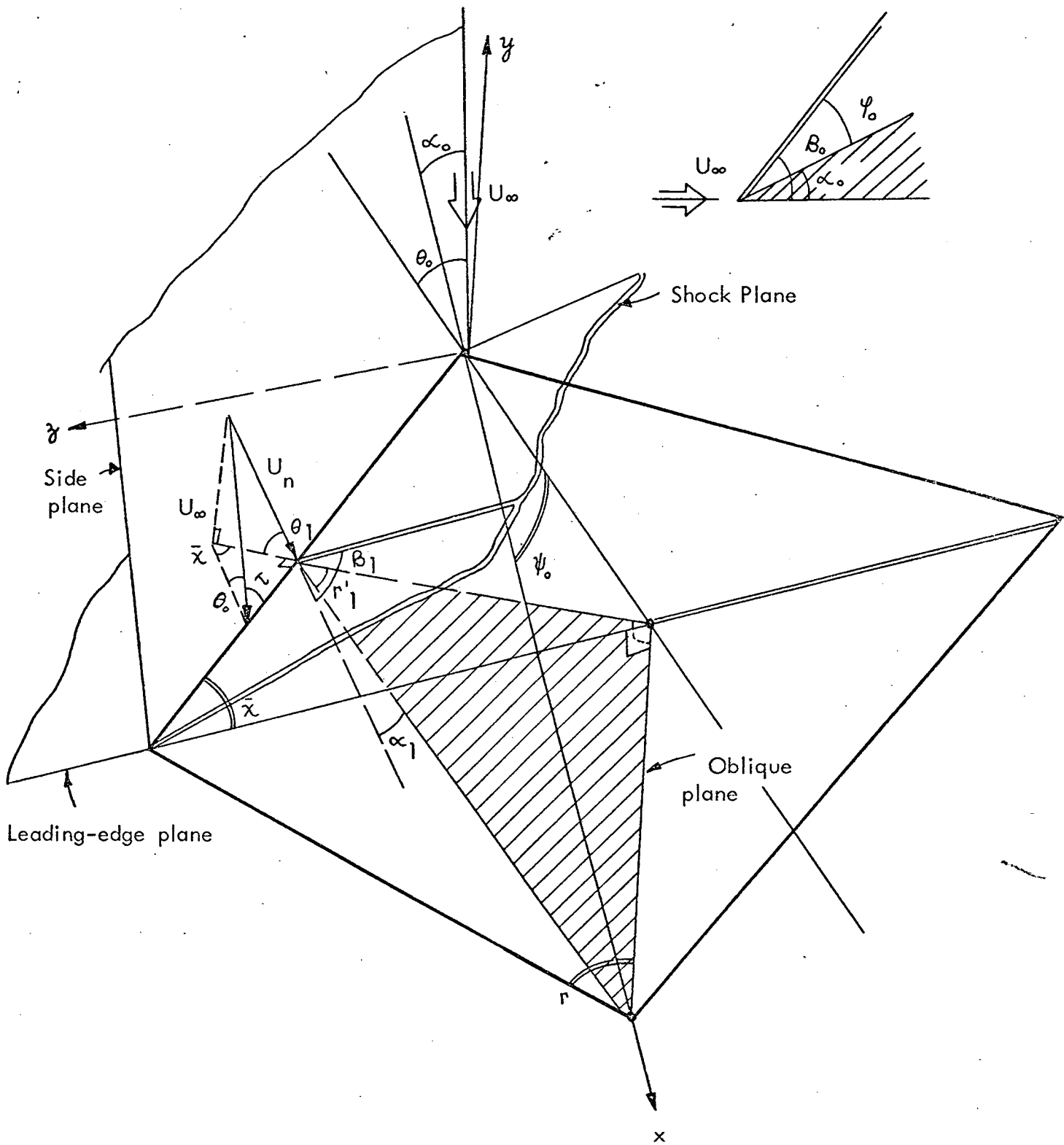


FIG. 1-D CARET WING SHOWING NOTATIONS.

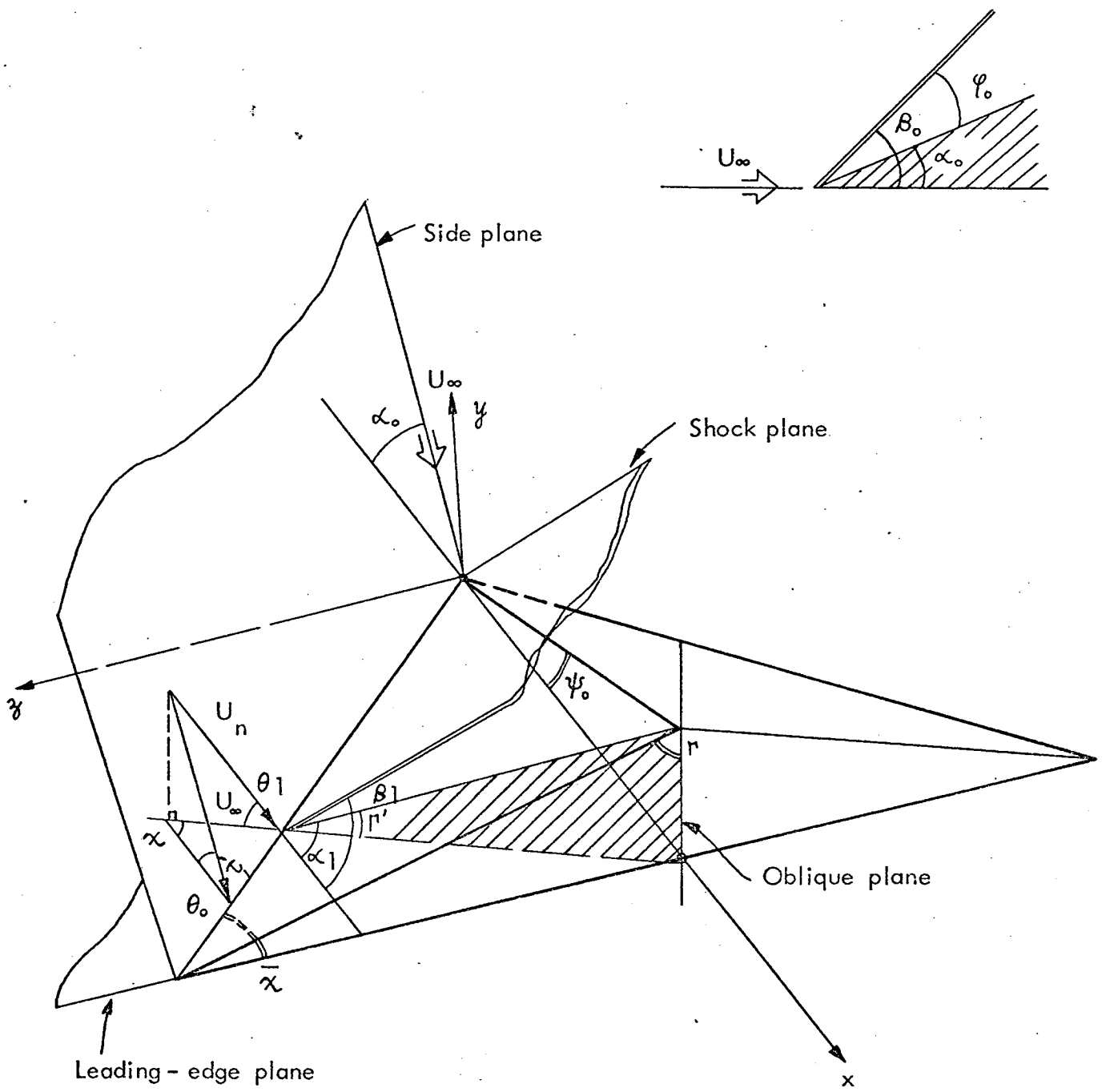
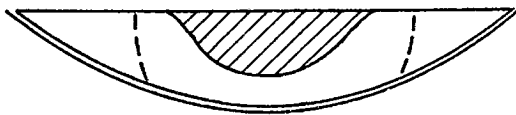


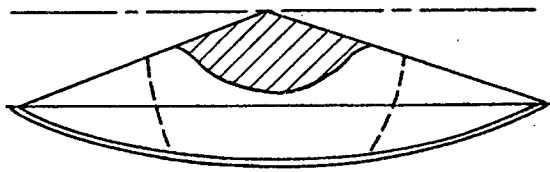
FIG.1-E DIAMOND WING SHOWING NOTATIONS.

(I) Large α_o cases ($\alpha_o > 0$)

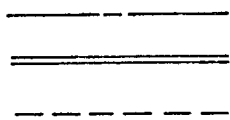
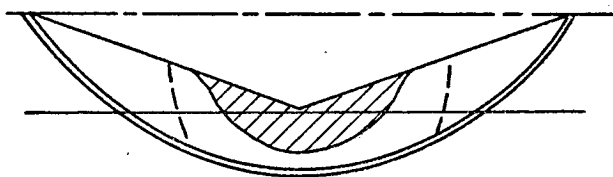
Generalized flat bottom



Generalized caret bottom



Generalized V bottom



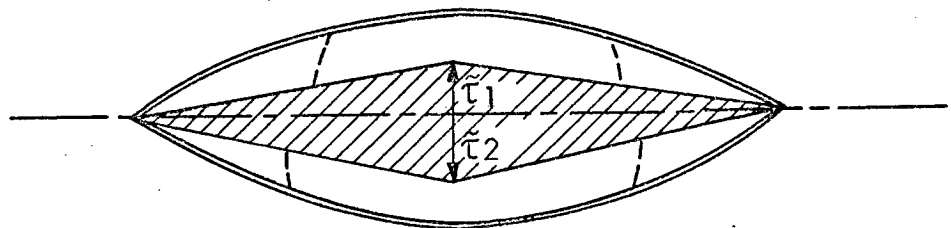
Wedge flow reference line.

Attached shock.

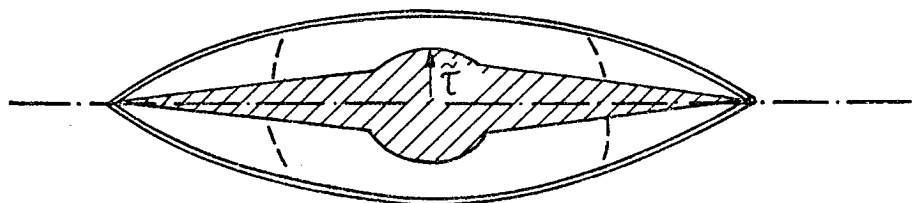
Mach Cone.

(II) Small α_o cases ($\tilde{\tau} > \alpha_o, \alpha_o \geq 0$)

Full diamond



Diamond wing-body



Full caret

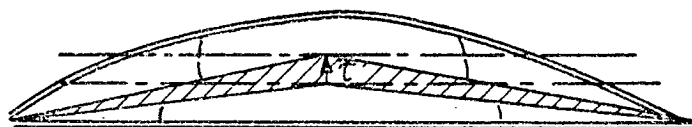


FIG. 1-F APPLICABLE CONFIGURATIONS.

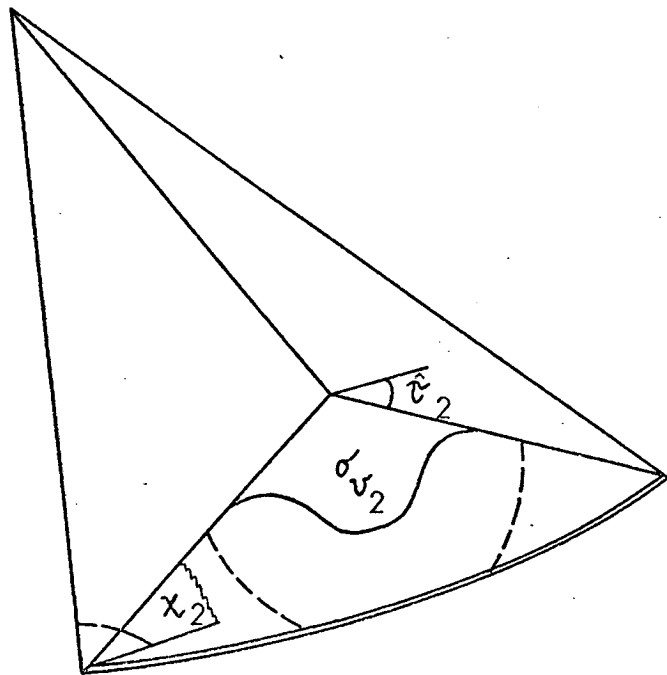
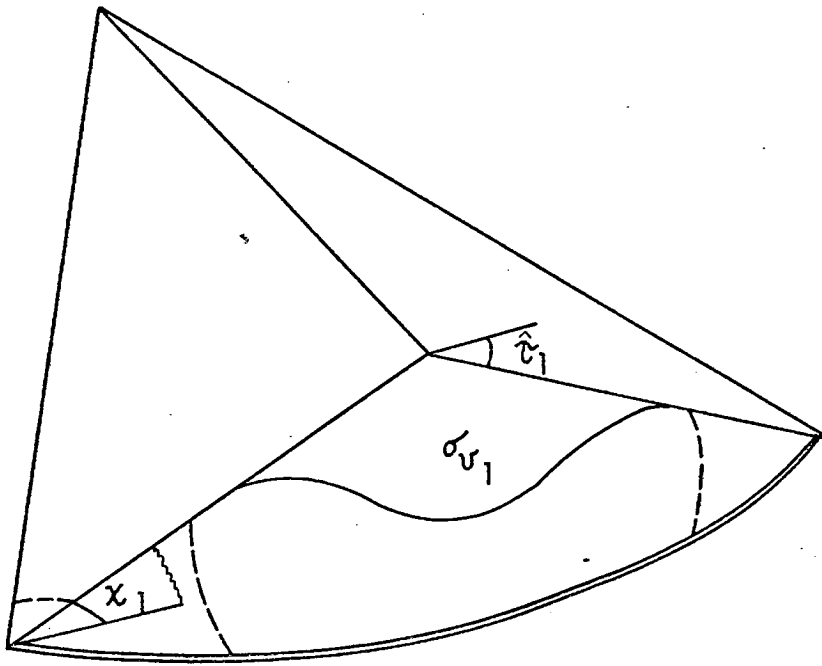


FIG.1G CARET WINGS WITH ADDED VOLUMES.
OF NON-AFFINE SHAPES

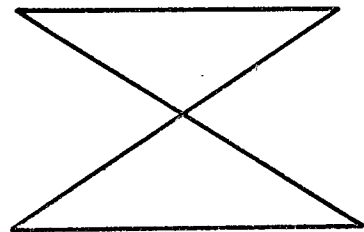
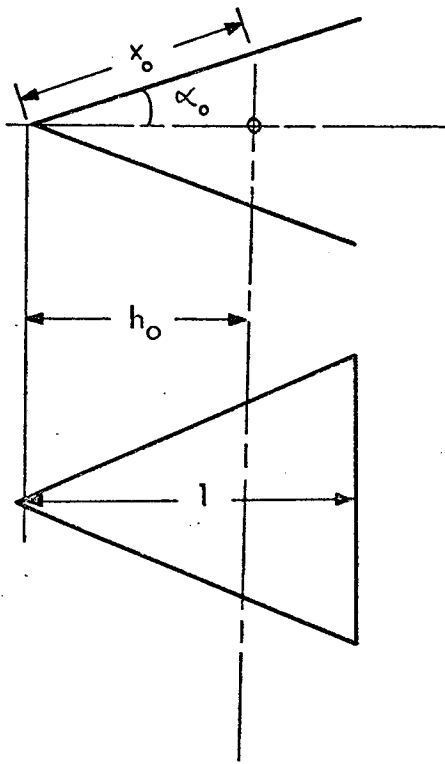
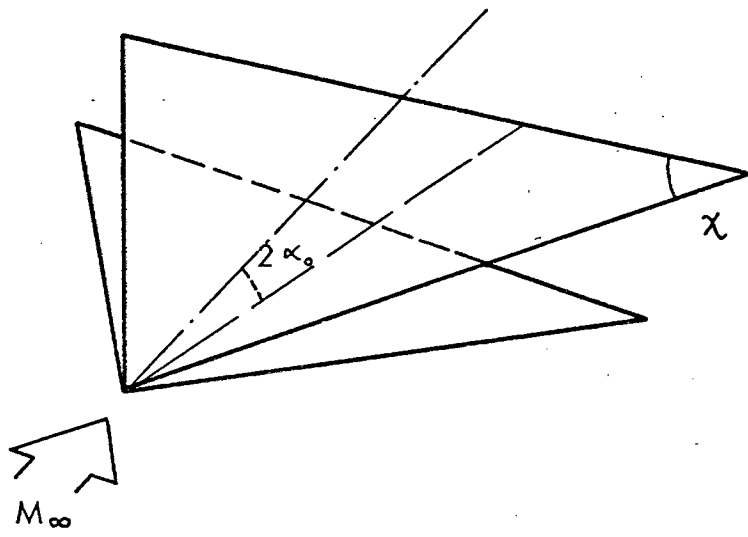
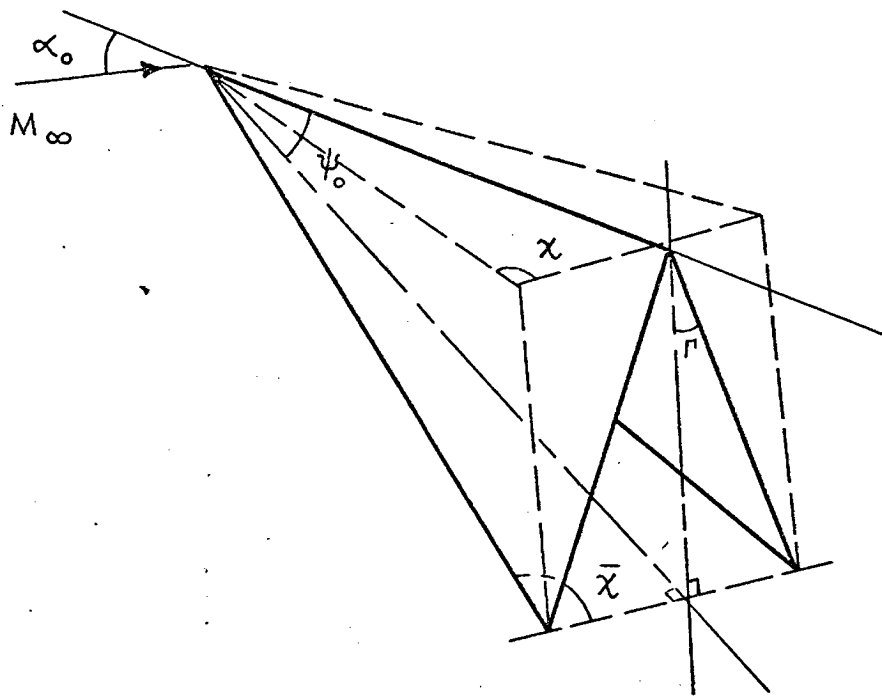


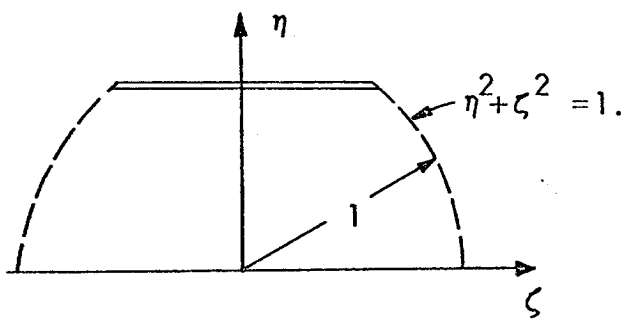
FIG. 1-H TWO-SIDE WING GEOMETRY.



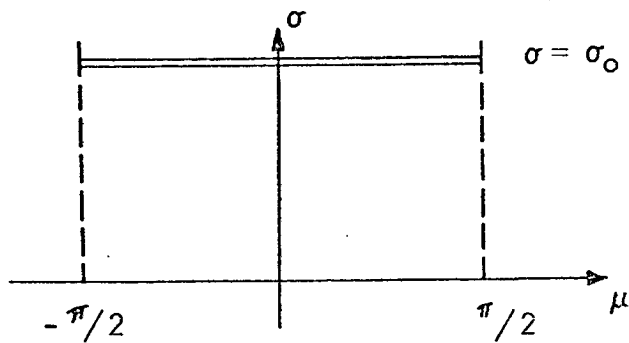
$$\tan \chi \tan r \tan \psi_0 = 1.$$

$$\tan \bar{\chi} \tan r \tan \psi_0 = 1.$$

FIG. 1-I PROJECTION PLANE OF A CARET WING.



(Conical Plane)



(Tschaplygin Plane)

FIG. 1-J THE TSCHAPLYGIN TRANSFORM PLANE.

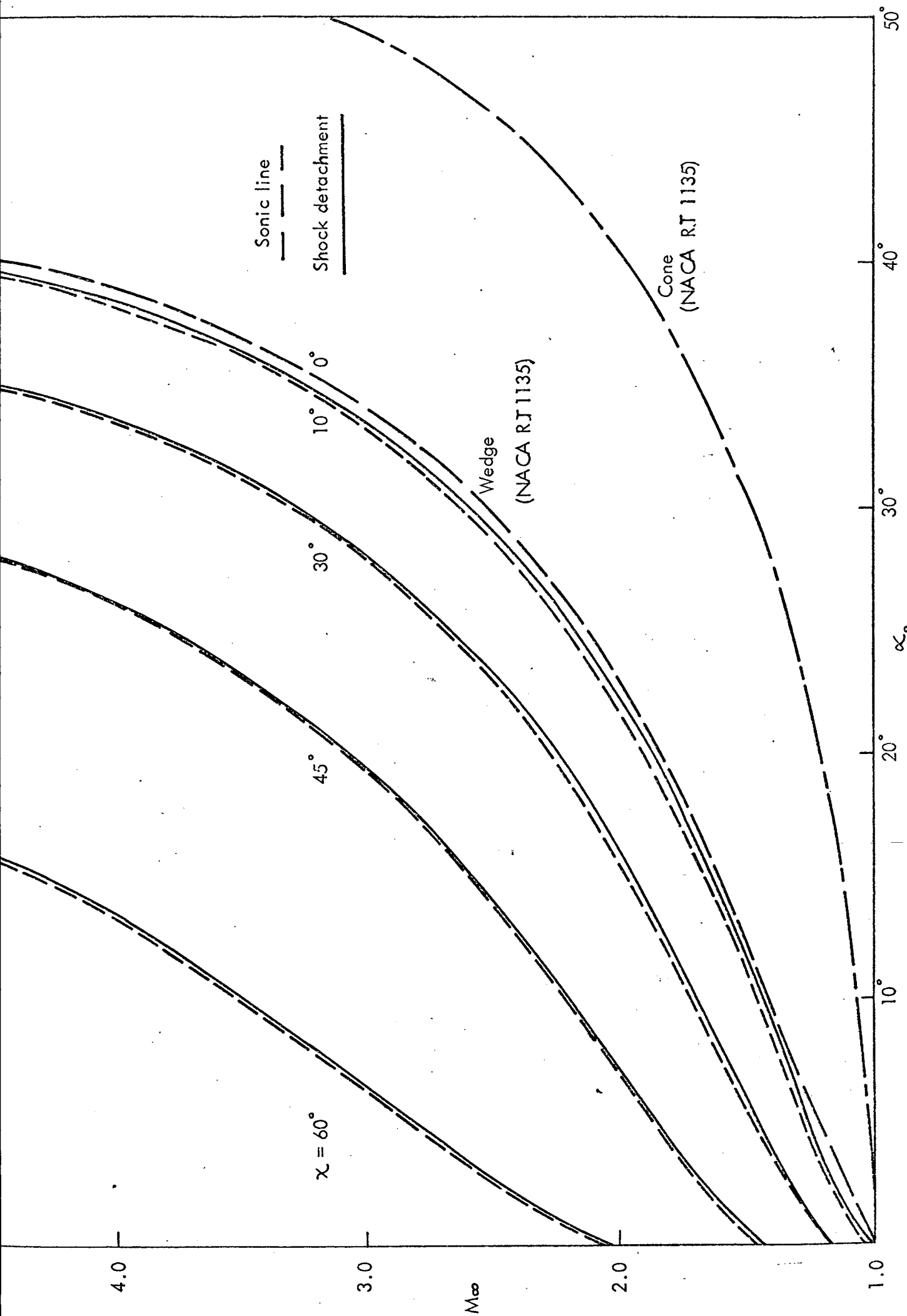


FIG. 2 SHOCK-ATTACHMENT CRITERION FOR CONE, WEDGE AND FLAT DELTA WINGS ($M_\infty - \alpha_0$ DIAGRAM.)

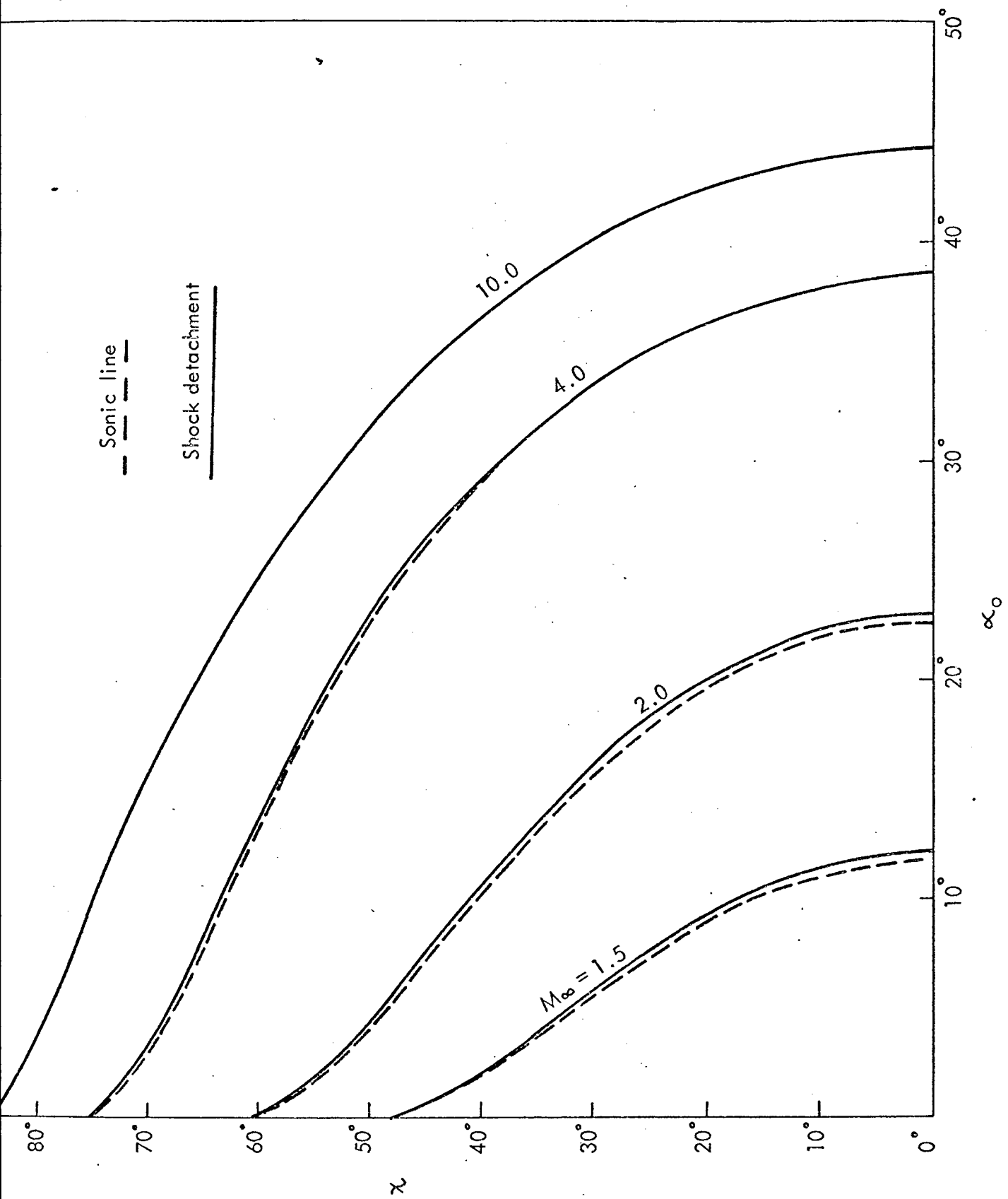


FIG. 3 SHOCK-ATTACHMENT CRITERION FOR FLAT DELTA WINGS (α - α_0 DIAGRAM) $r = 90^\circ$.

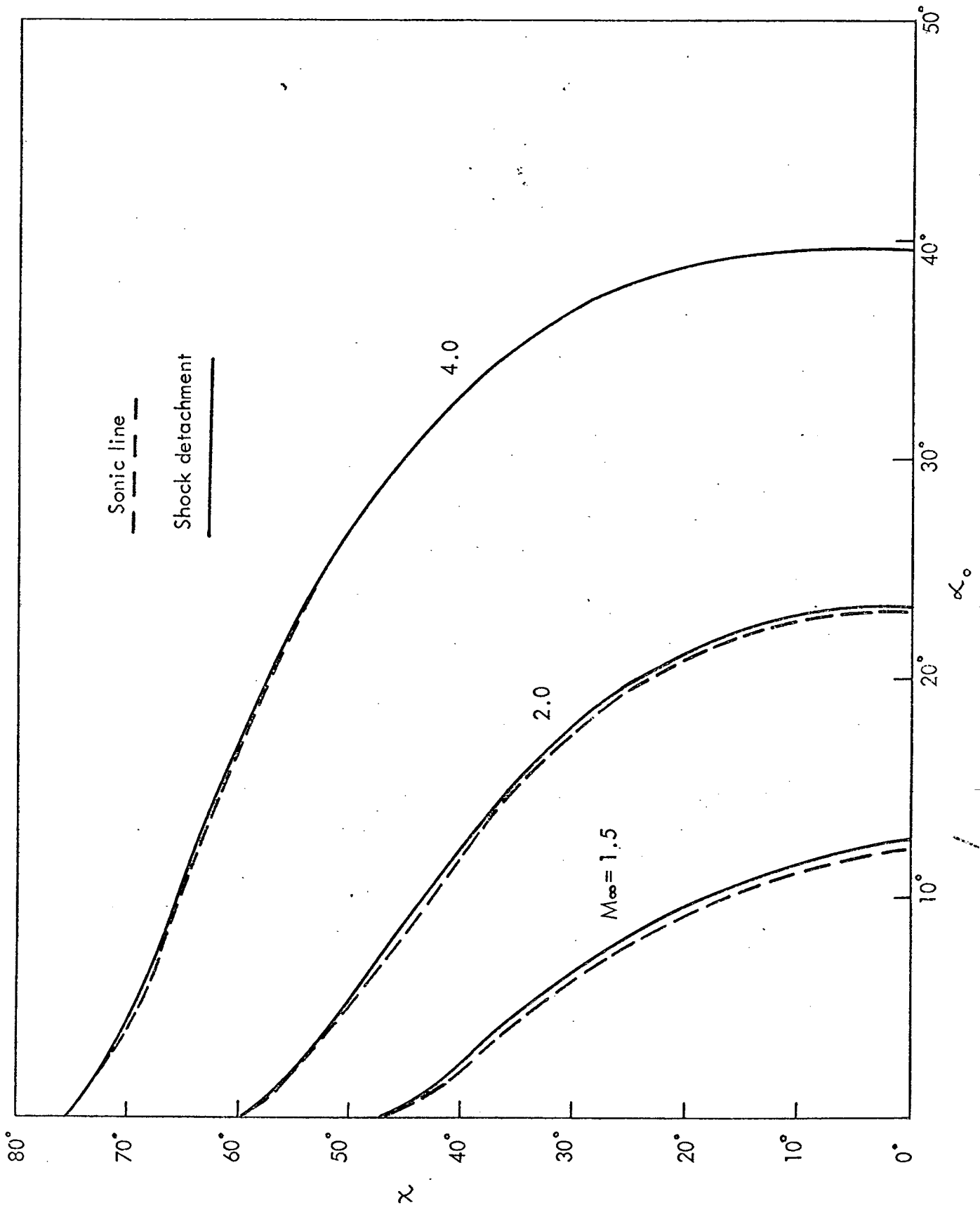


FIG. 4 SHOCK-ATTACHMENT CRITERION FOR CARET WINGS ($\chi - \alpha_0$ DIAGRAM) $\Gamma = 80^\circ$.

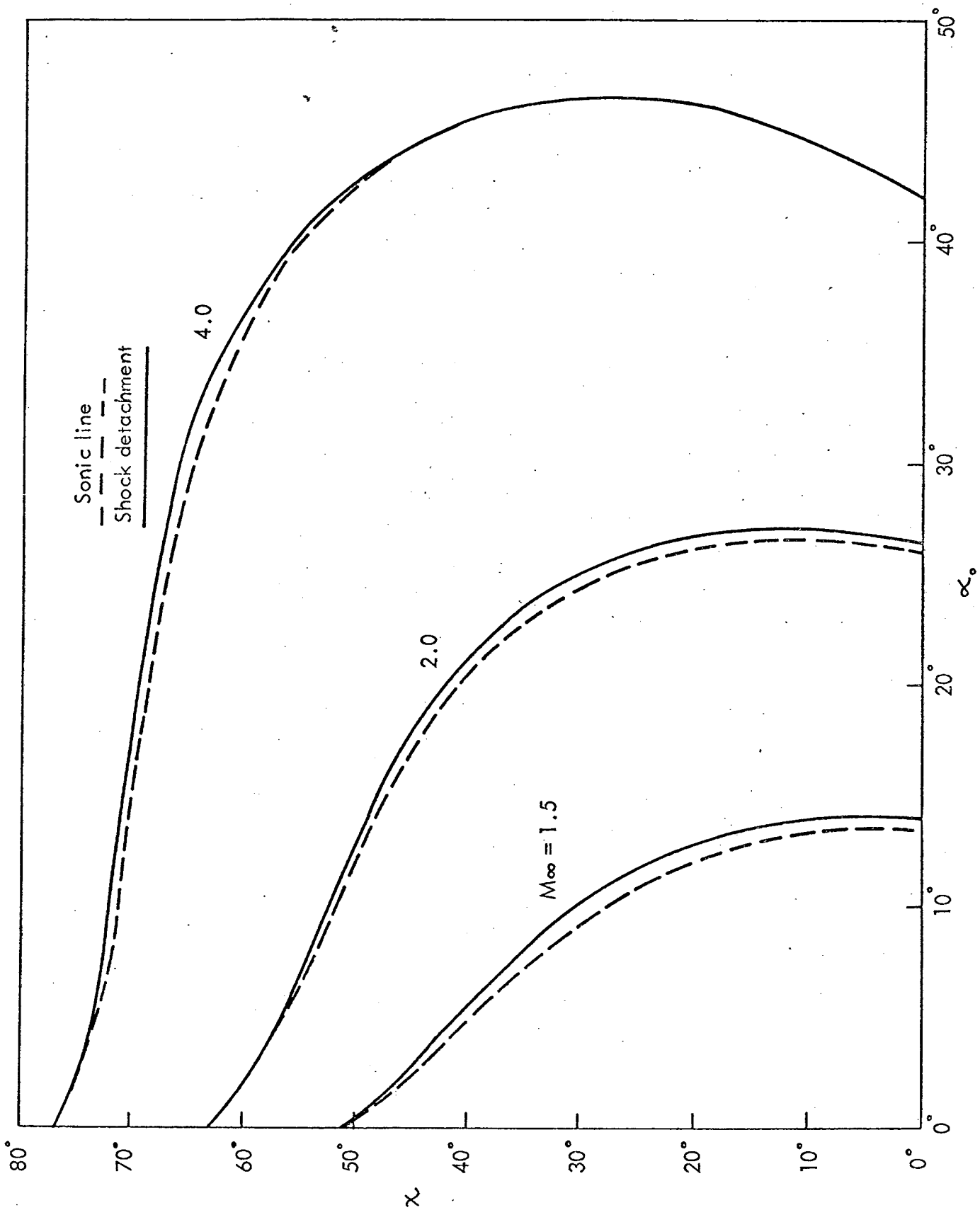


FIG. 5 SHOCK-ATTACHMENT CRITERION FOR CARET WINGS ($\gamma = 60^\circ$)

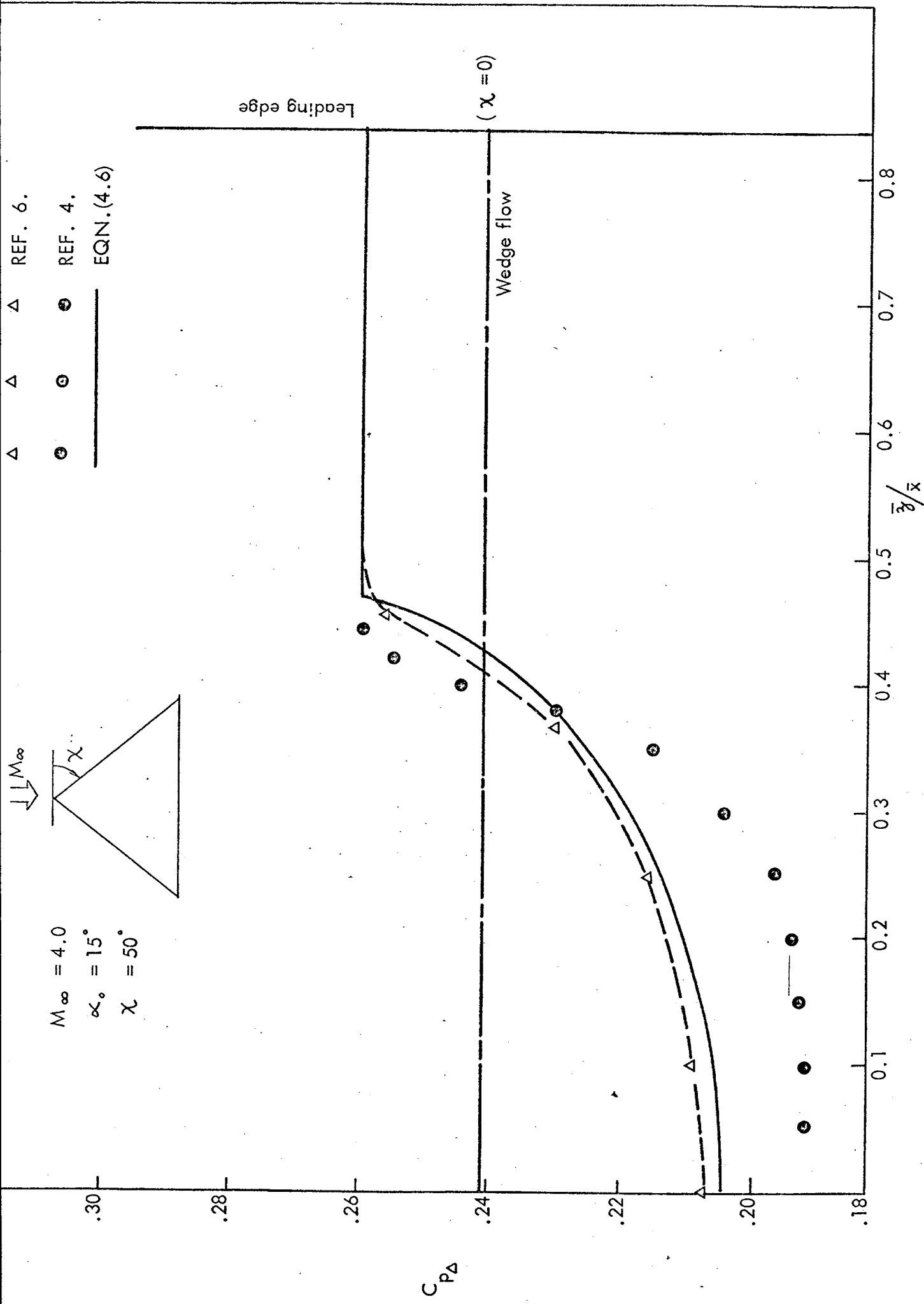


FIG. 6. TYPICAL PRESSURE DISTRIBUTION ACCORDING TO HUI'S THEORY (Ref 7)

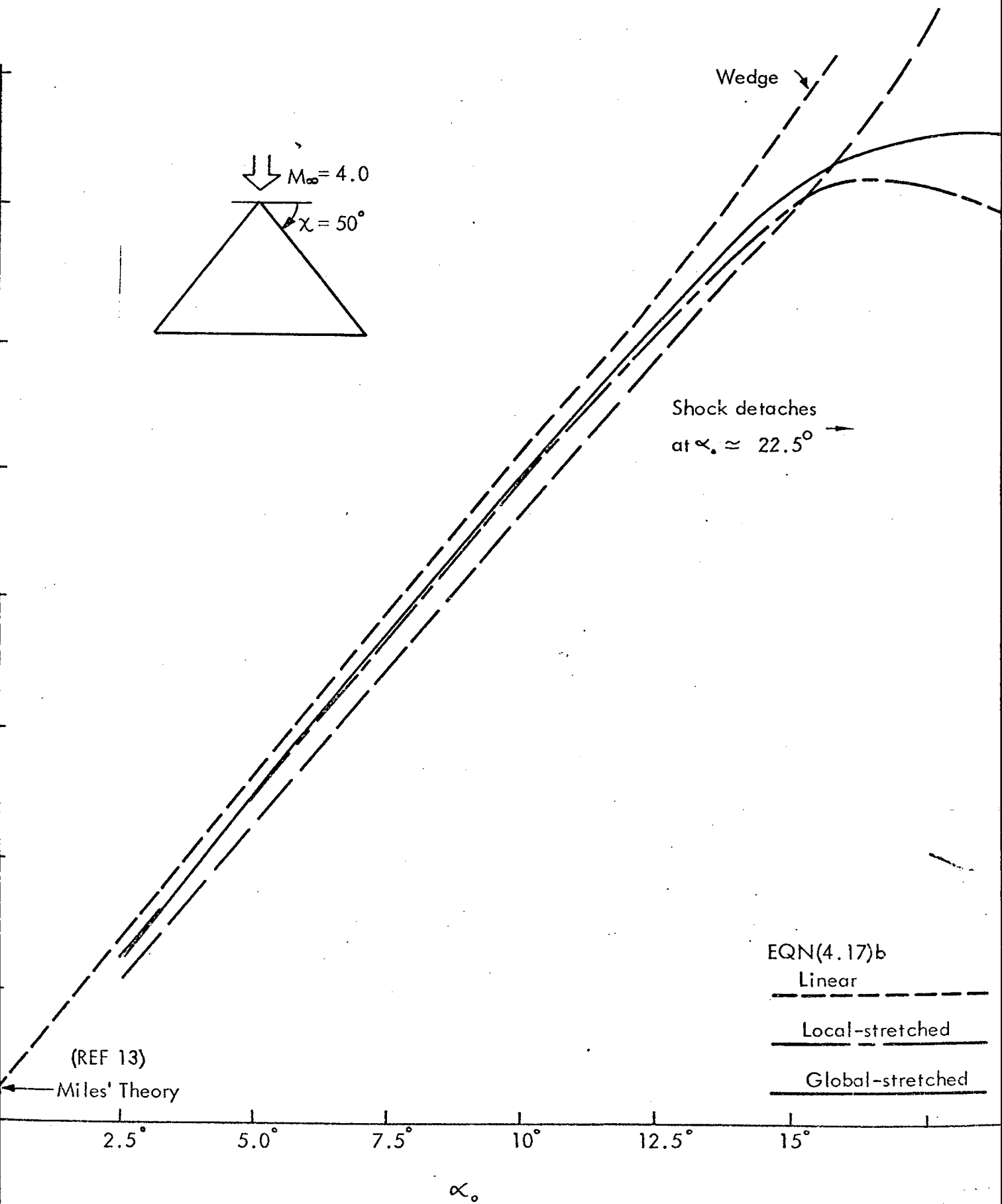


FIG.7 $C_{L\alpha}$ vs α_0 ACCORDING TO DIFFERENT METHODS.

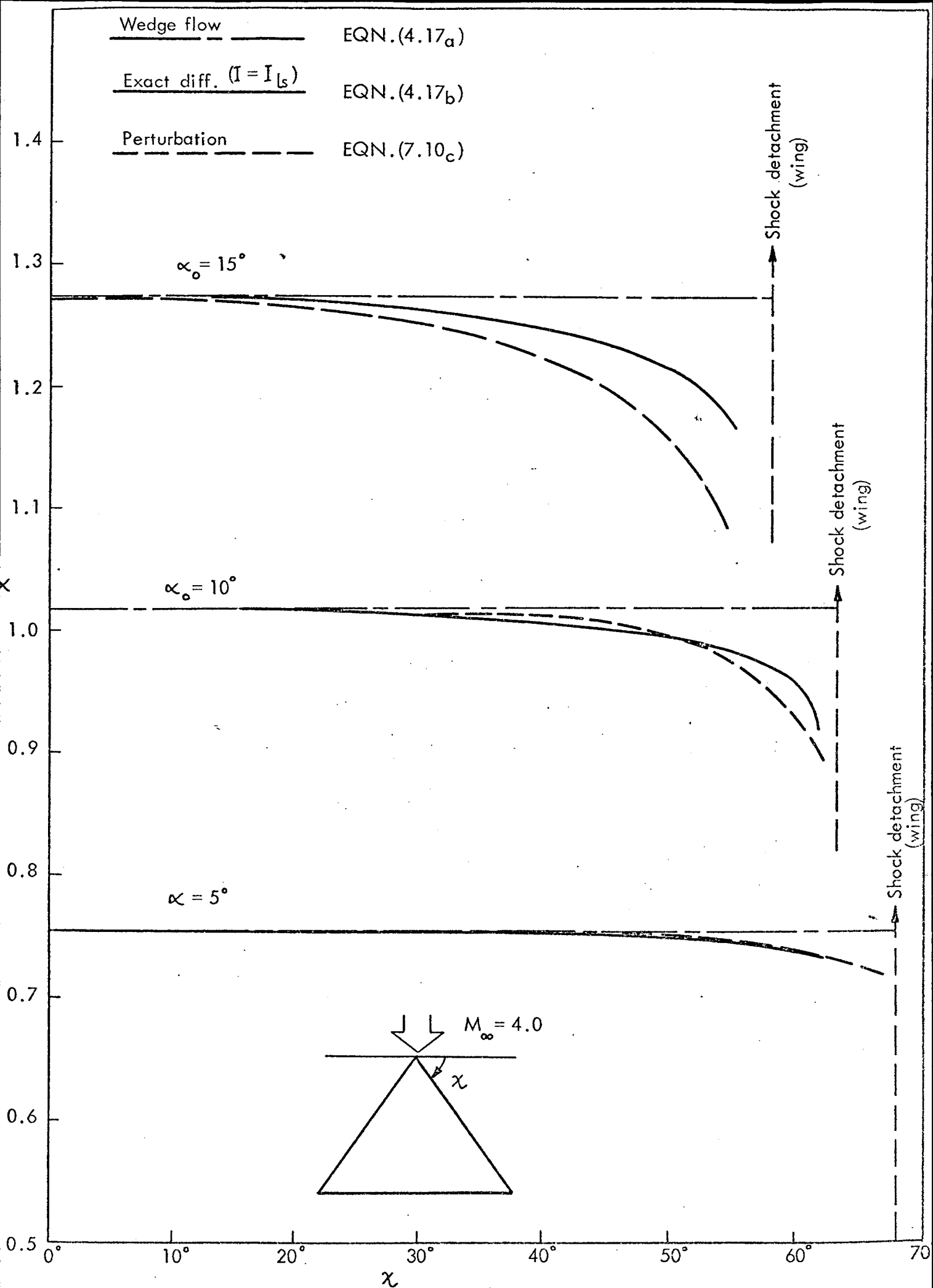


FIG 8. $C_{L\alpha}$ vs χ ACCORDING TO DIFFERENT METHODS.

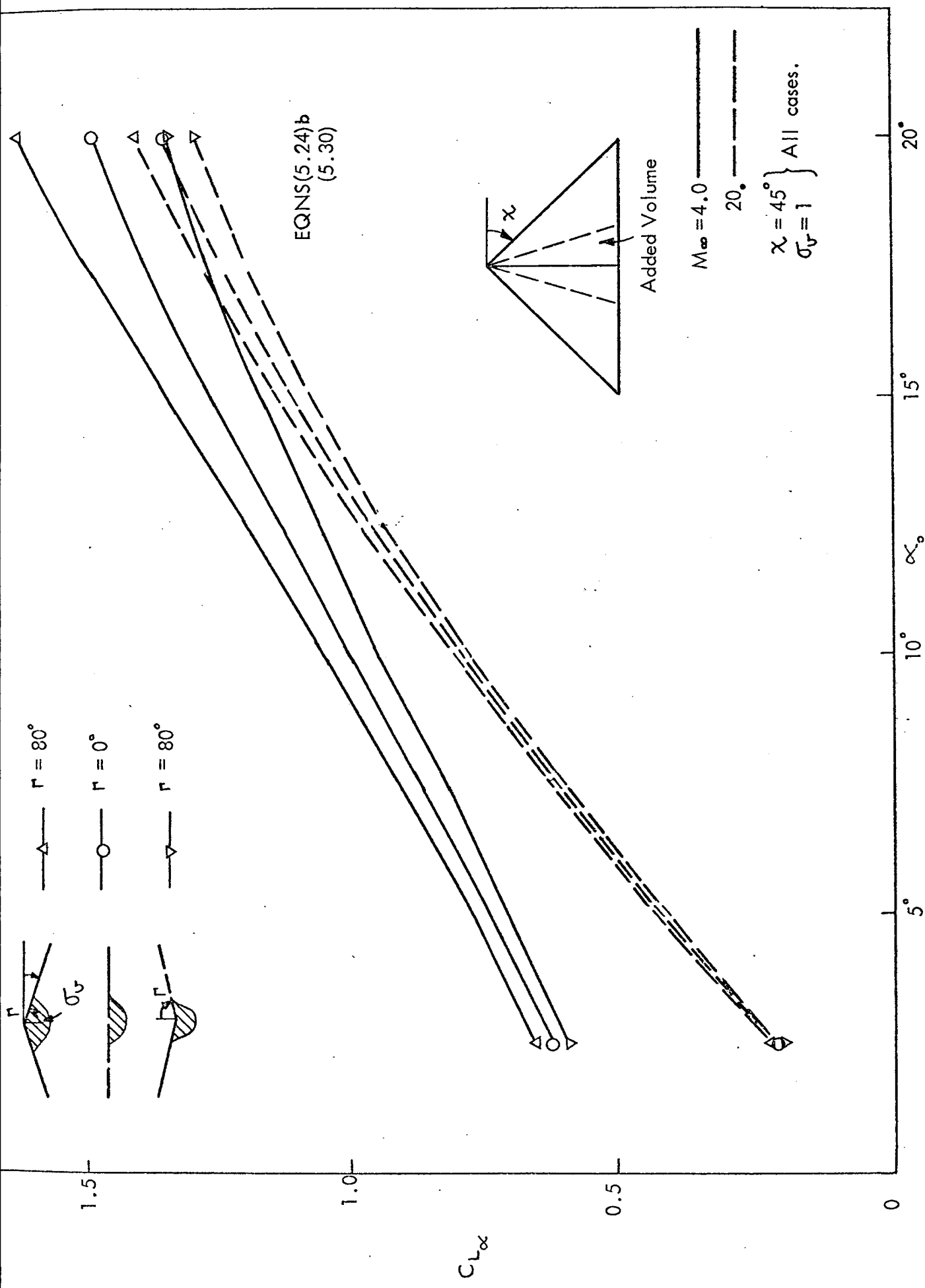


FIG. 9 $C_{L\alpha}$ vs α_0 FOR VARIOUS WING-BODY COMBINATIONS.

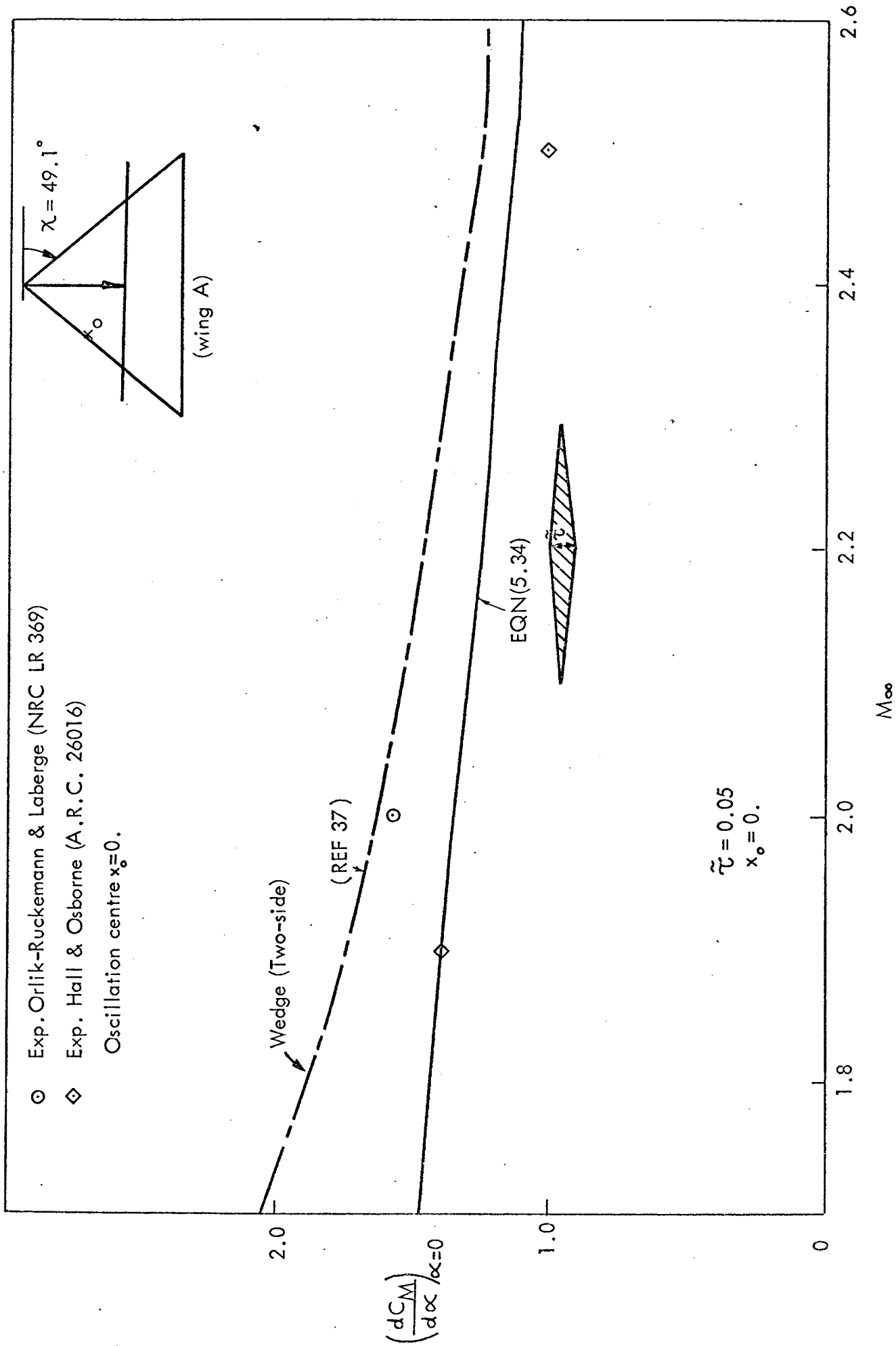


FIG. 10 $C_{M\alpha}$ vs M_∞ : COMPARISON WITH EXPERIMENTAL DATA.

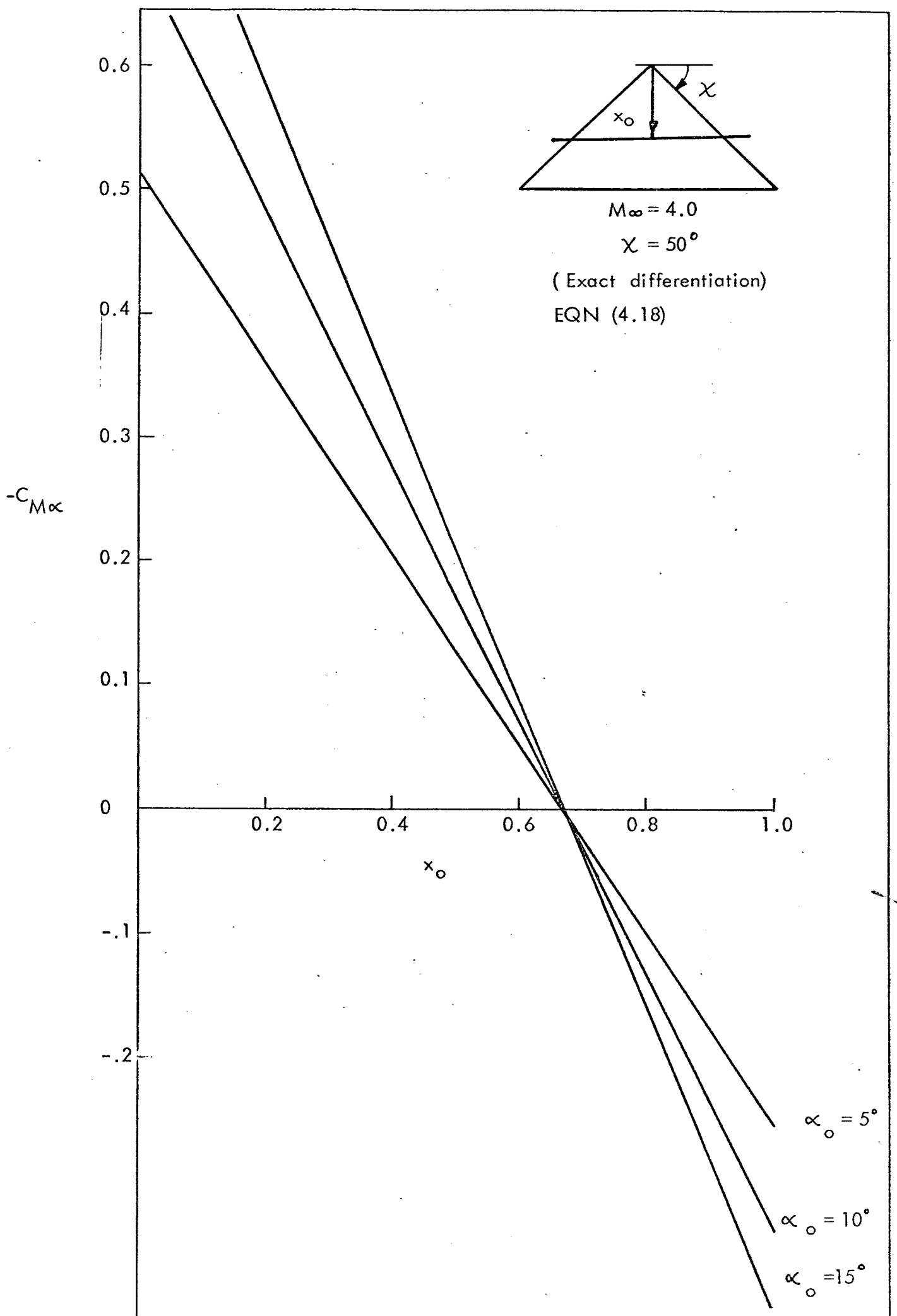


FIG.11 $-C_{M\alpha}$ vs x_0 AT DIFFERENT INCIDENCES.

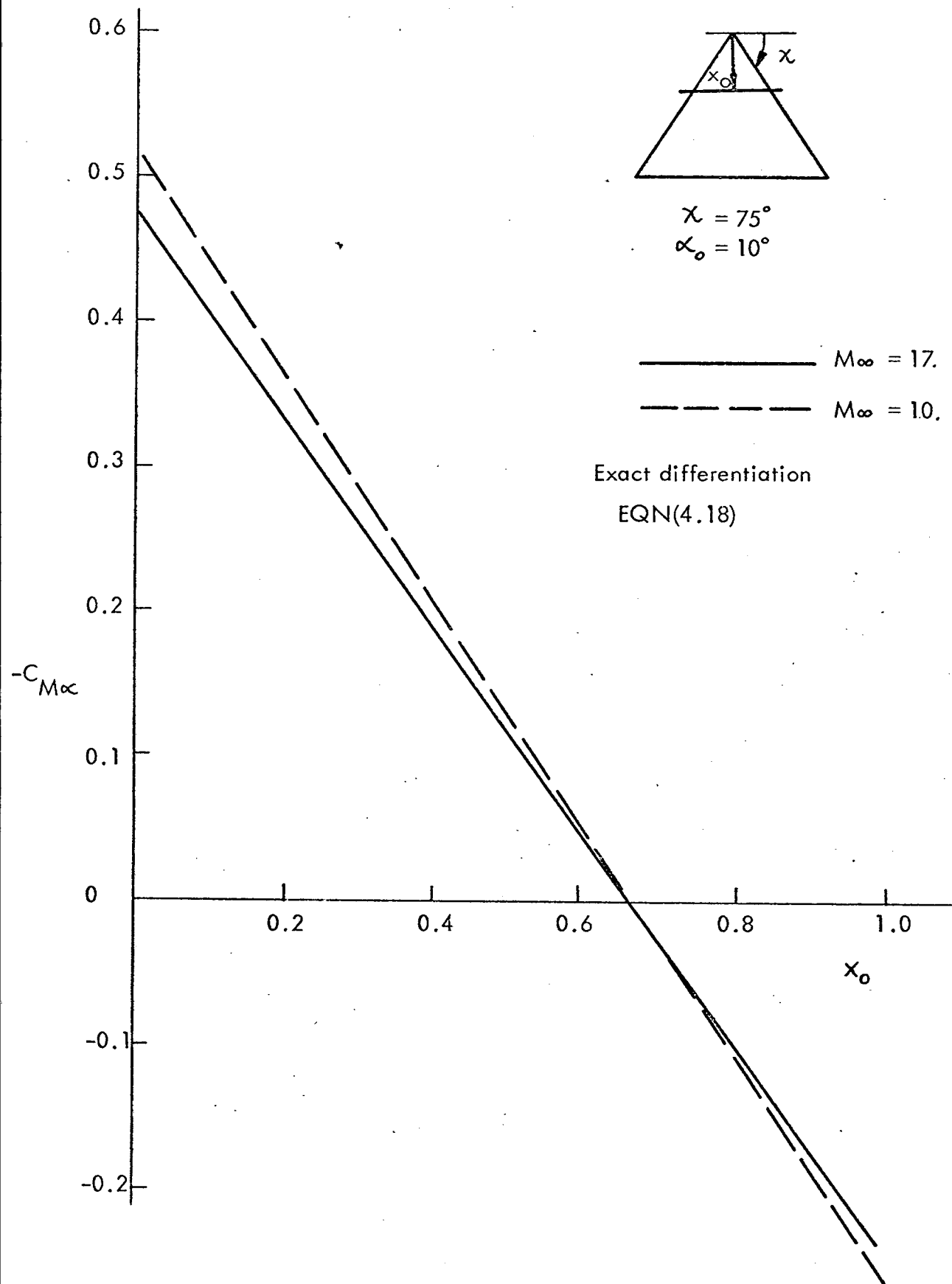


FIG. 12 $-C_{M\alpha}$ vs x_0 AT HIGH MACH NUMBERS.

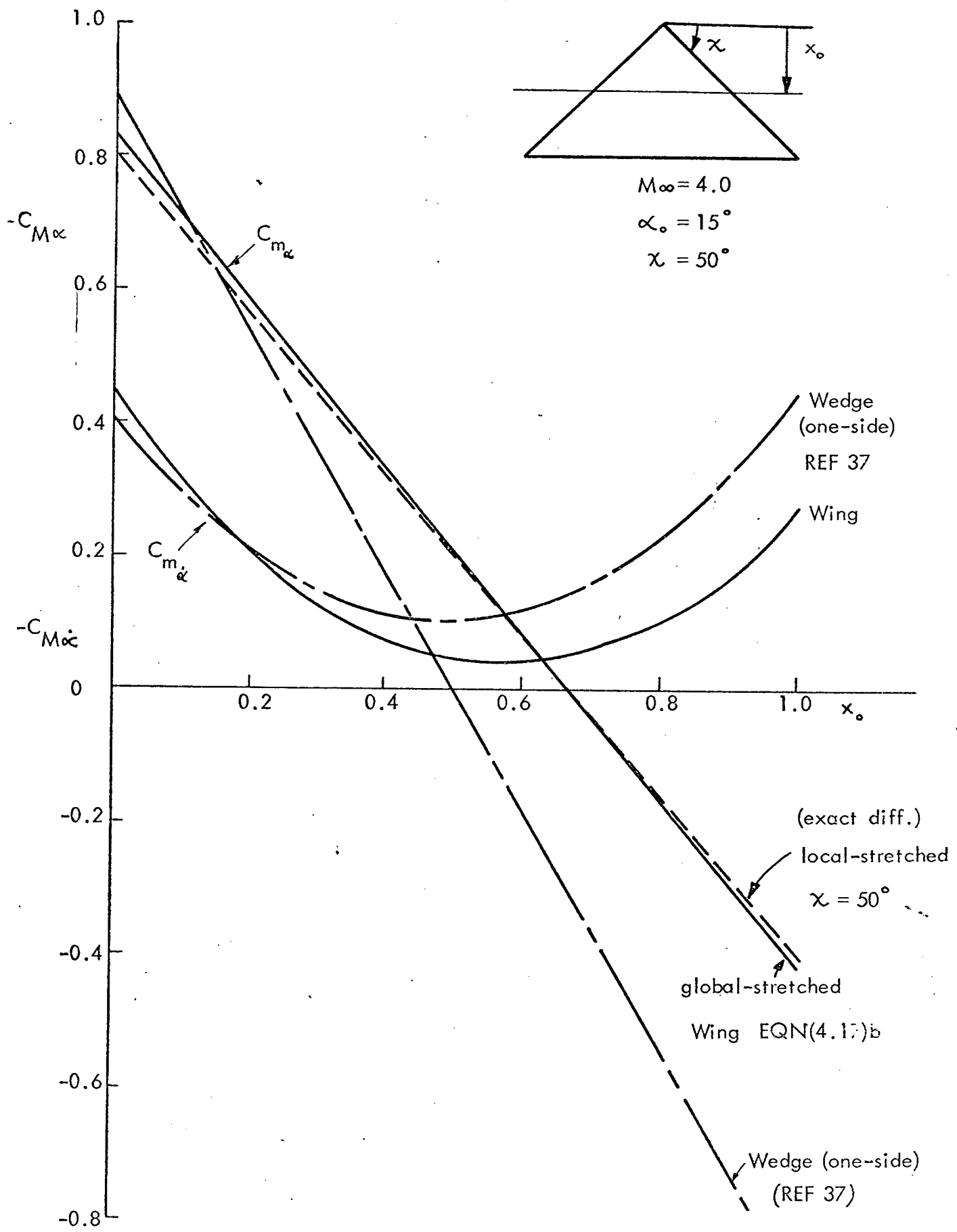


FIG.13 COMPARISON OF STIFFNESS DERIVATIVE AND DAMPING DERIVATIVES FOR DELTA WING OF $\chi = 50^\circ$

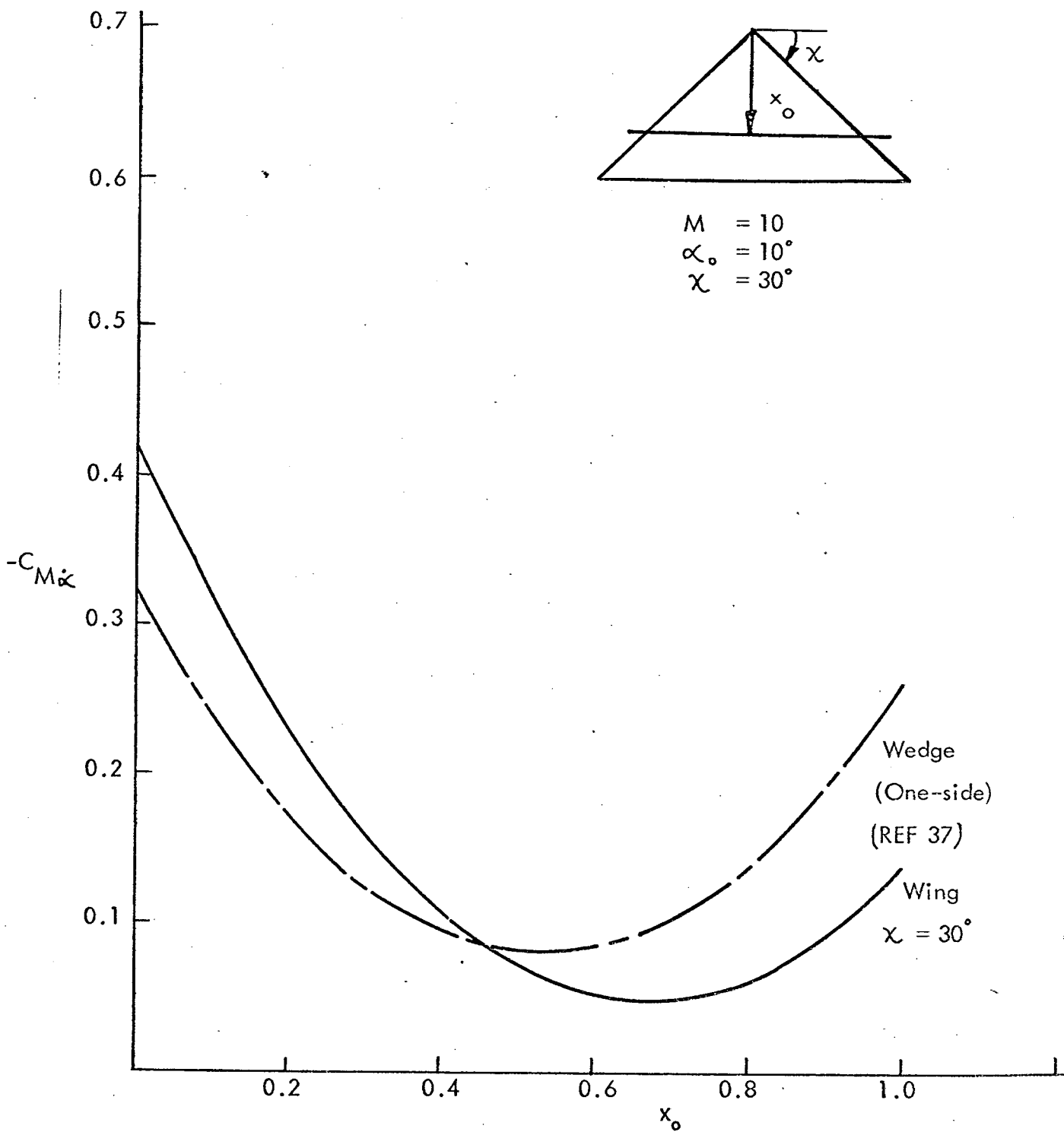


FIG. 14 $-C_{M\dot{\alpha}}$ vs x_0 FOR DELTA WING & WEDGE.

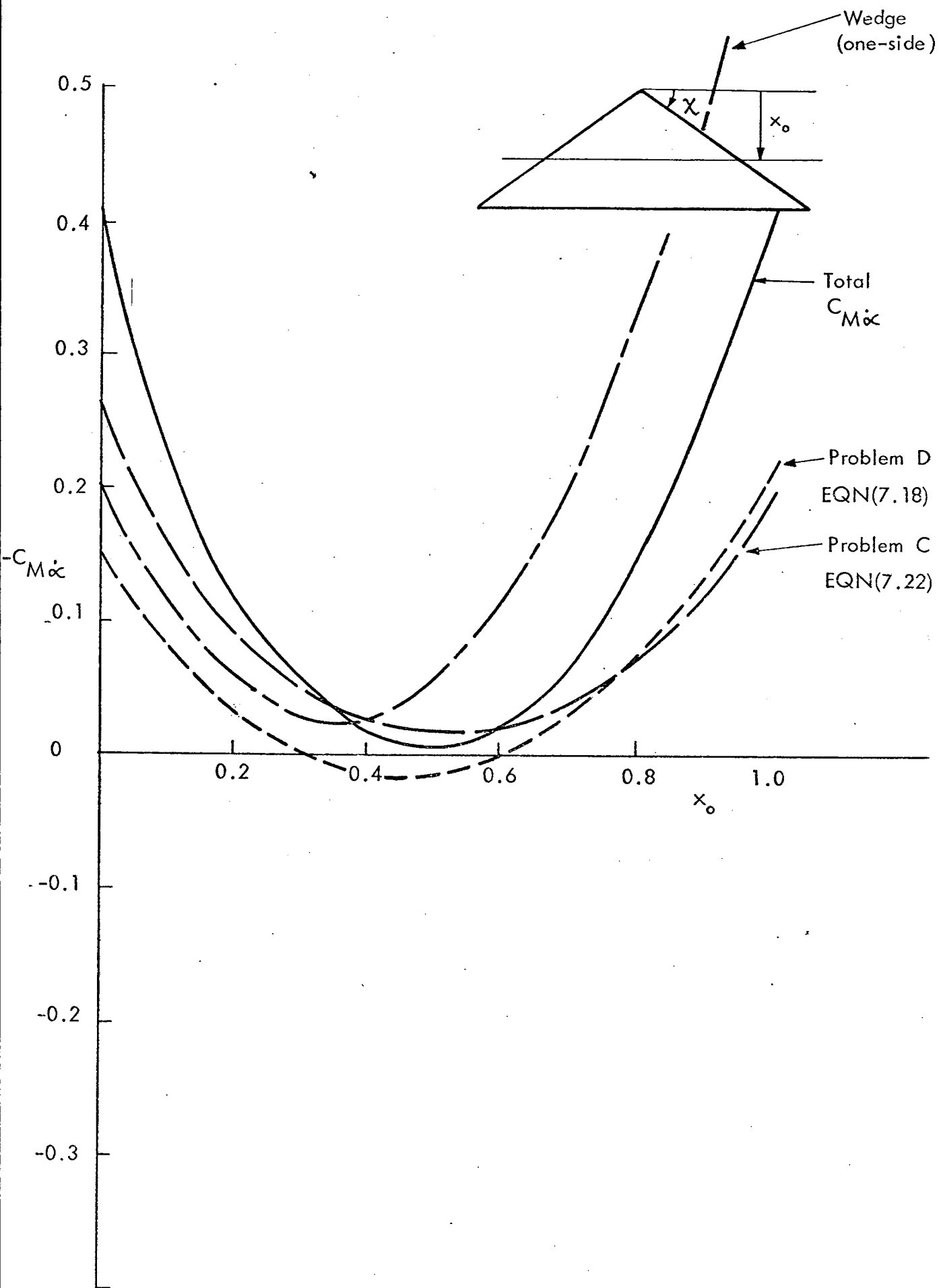


FIG.15 $-C_{M\dot{\alpha}}$ vs x_0 : CONTRIBUTION DUE TO INNER AND OUTER REGIONS.

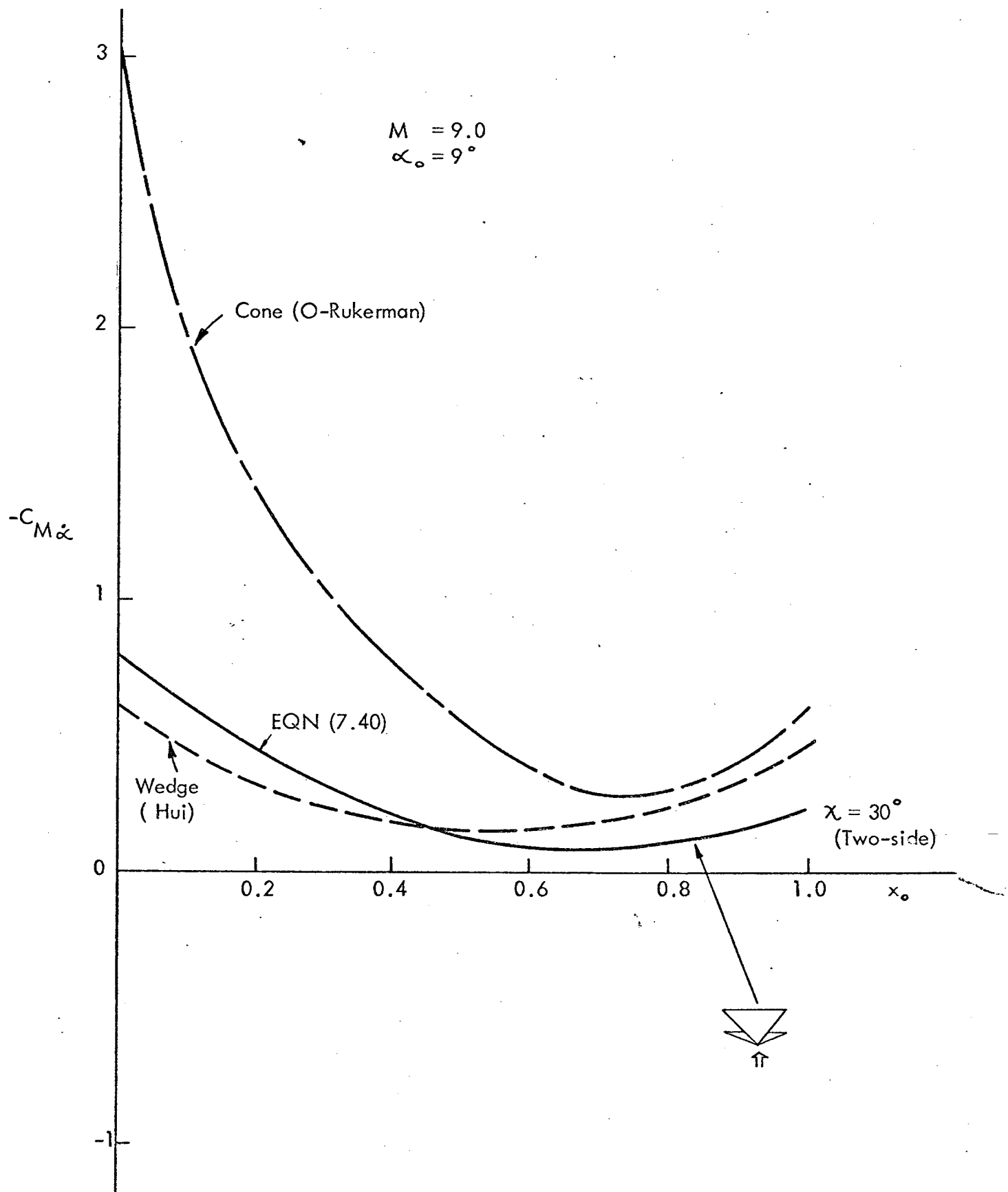


FIG. 16 $-C_{M\dot{\alpha}}$ vs x_0 COMPARISON OF DAMPING DERIVATIVES FOR A CONE, A WEDGE AND A DELTA WING OF $\chi = 30^\circ$ ALL WITH SEMI-APEX ANGLE $\alpha_0 = 9^\circ$

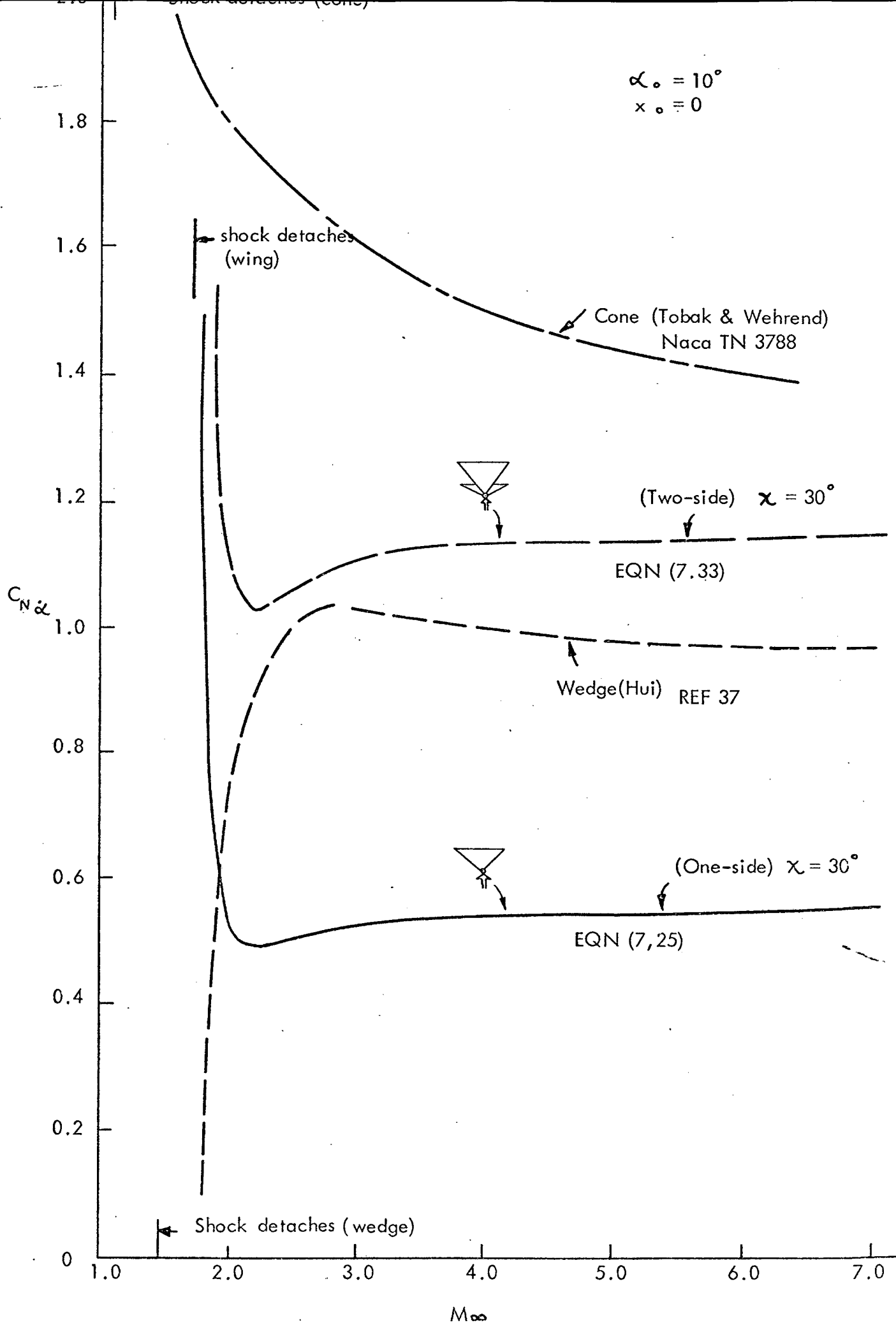


FIG. 17 $C_{N\alpha}$ vs M_∞ : COMPARISON OF OUT-OF-PHASE LIFTS FOR A CONE, WEDGES AND DELTA WING OF $\chi = 30^\circ$, ALL WITH SEMI-APEX ANGLE $\alpha_o = 10^\circ$.

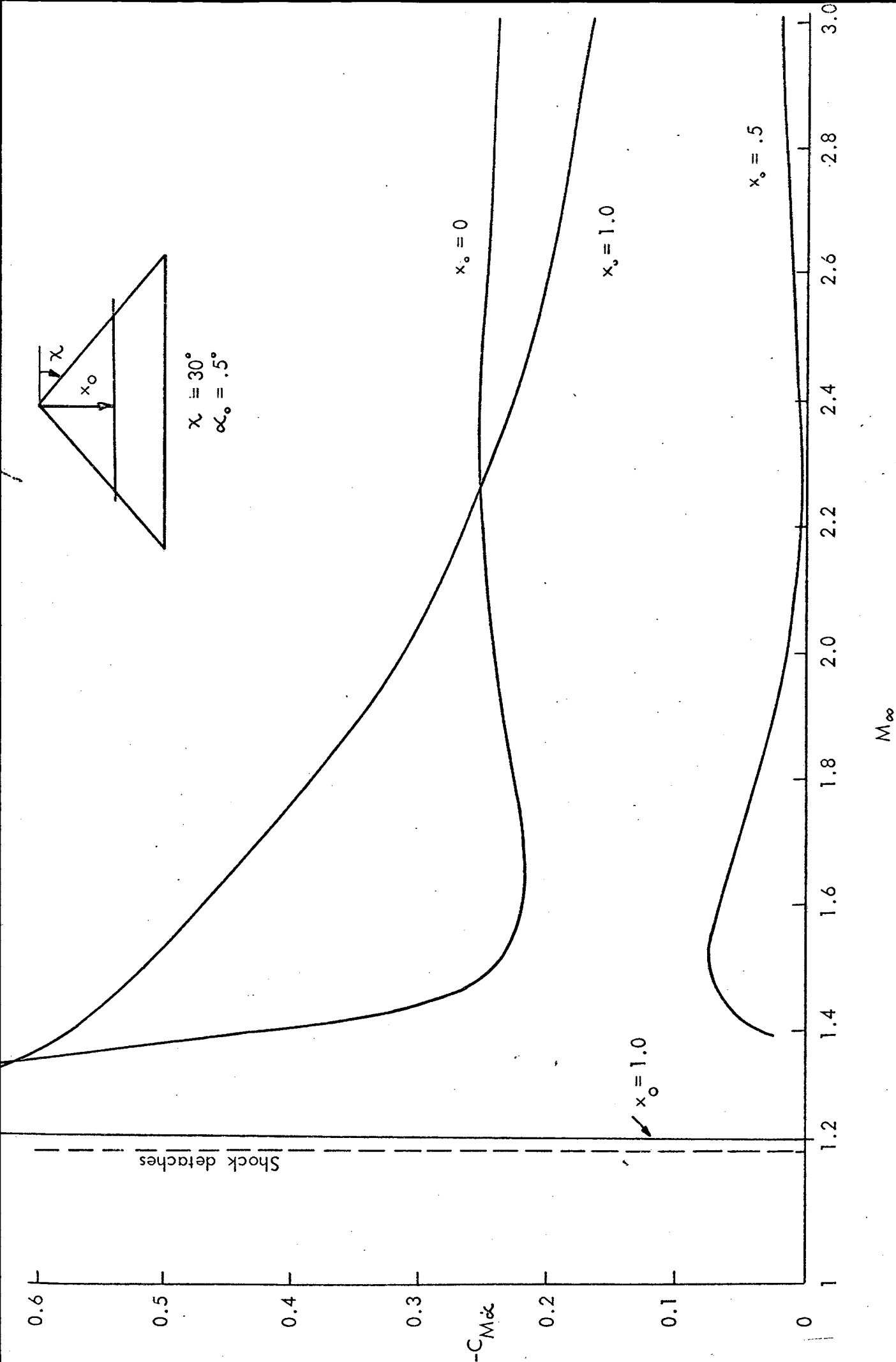


FIG.18 $-C_{M\alpha}$ IN LOWER MACH NUMBER RANGE.

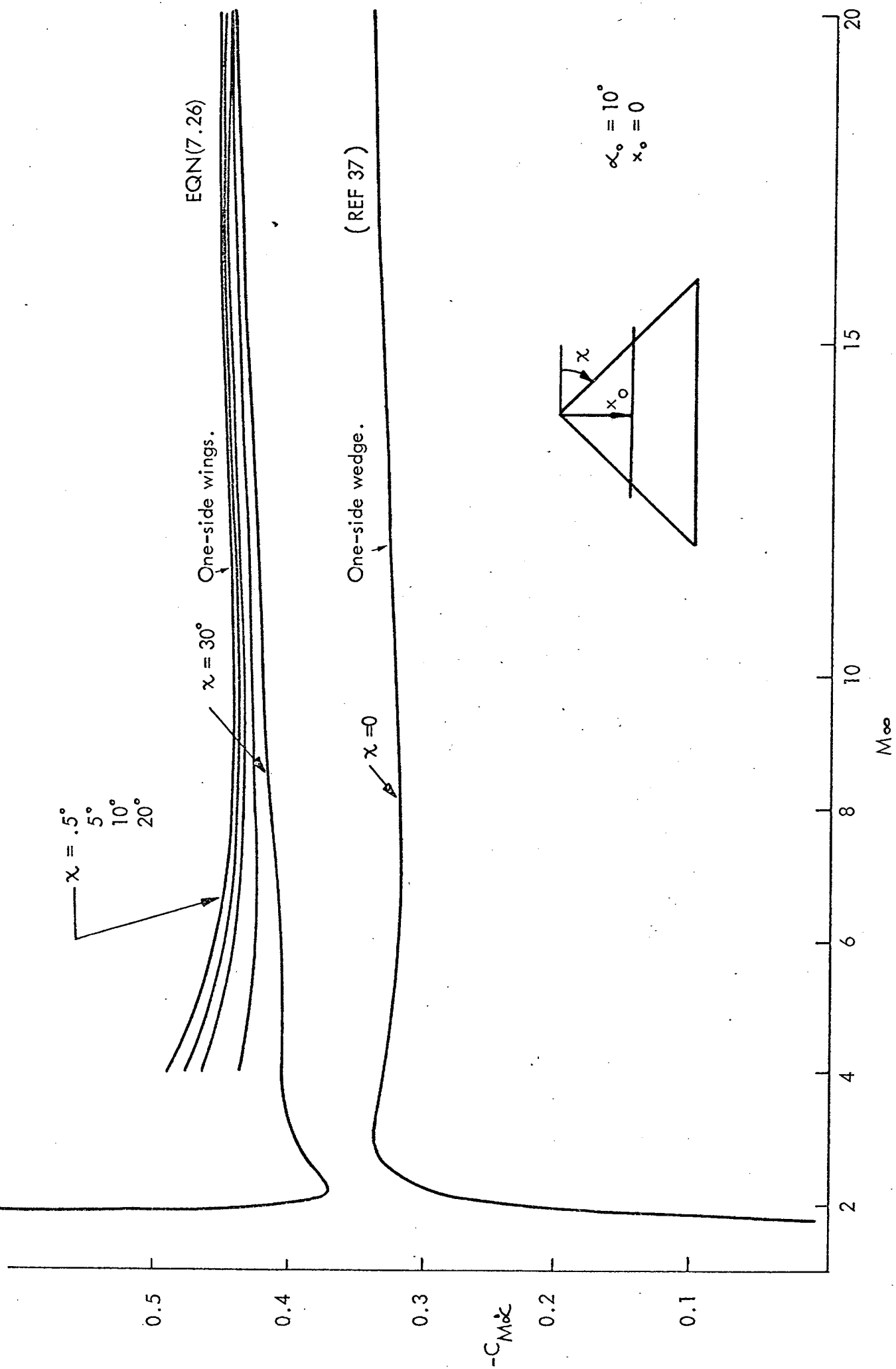
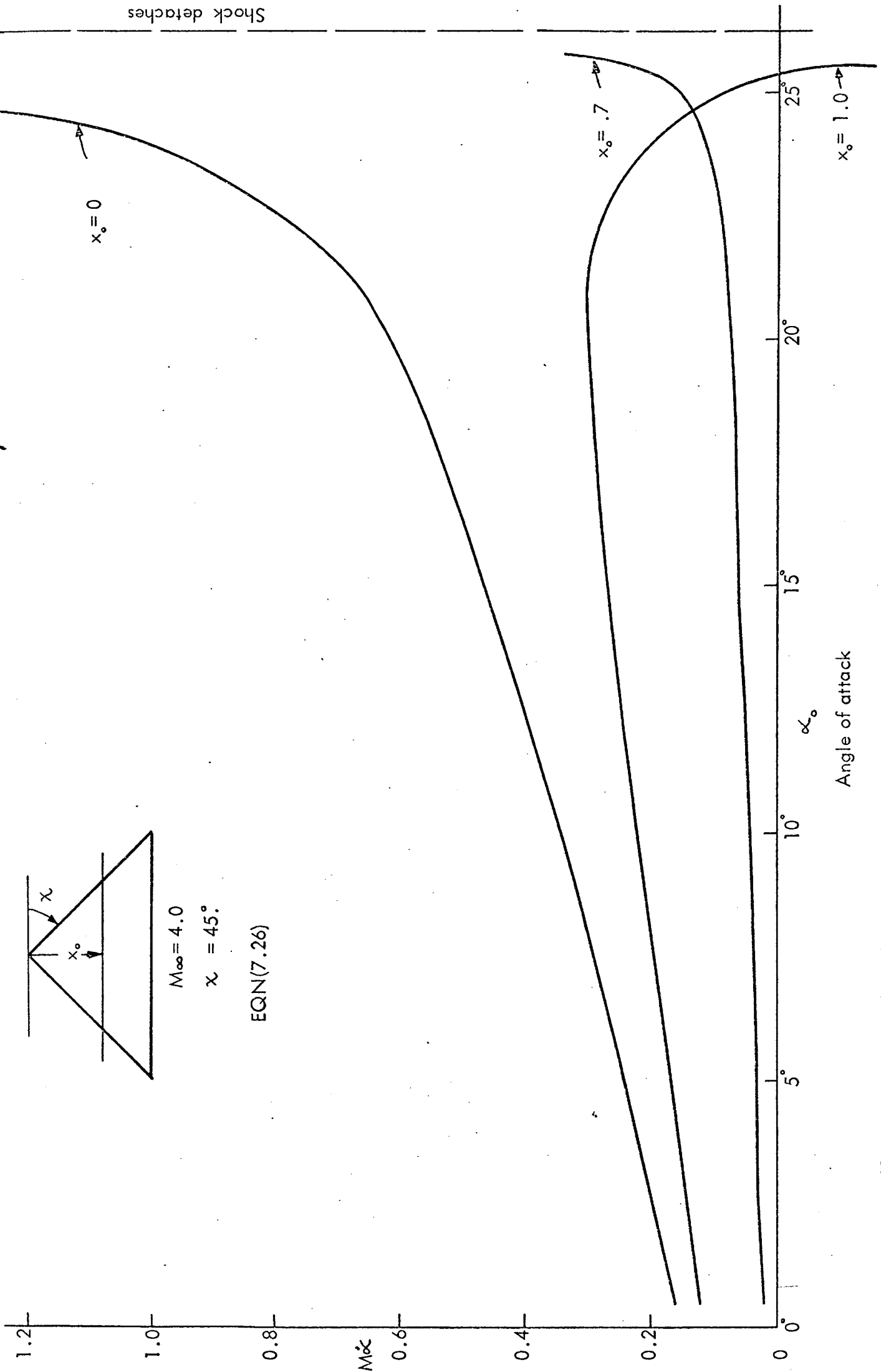


FIG. 19 $-C_{M\alpha}$ VARIATION FROM LOW TO HIGH MACH NUMBERS.



$M_\infty = 4.0$

$\chi = 45^\circ$

EQN(7.26)

FIG. 20 $-C_{M\alpha}$ vs α_0 AT VARIOUS x_0 's.

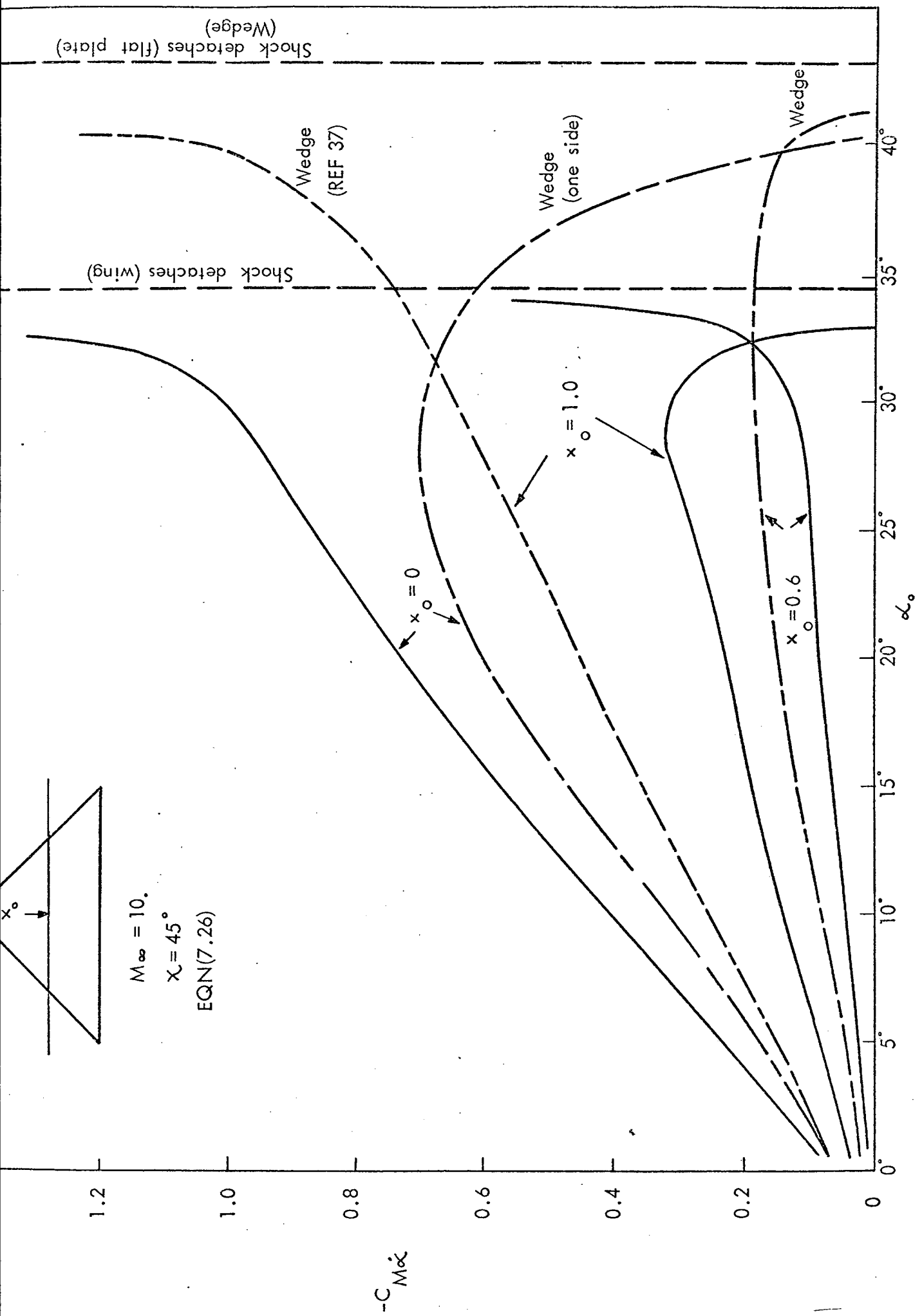


FIG.21 $-C_{M\alpha}$ vs α_0 : COMPARISON OF A WEDGE AND A DELTA WING OF $\chi = 45^\circ$ AT VARIOUS x_0 's.

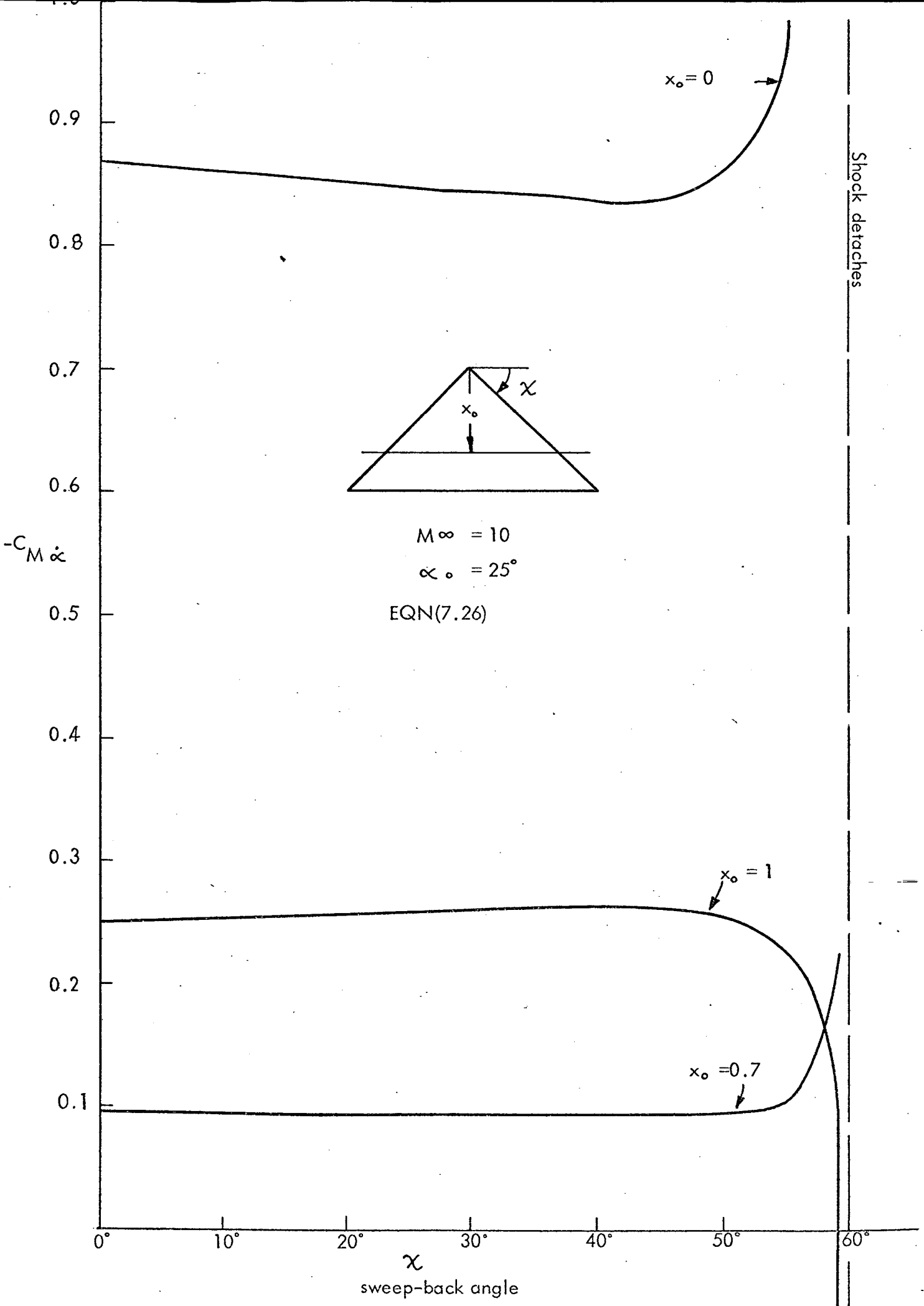


FIG. 22 $-C_{M\dot{\alpha}}$ vs χ AT VARIOUS x_0 's. ($M_\infty = 10$.)

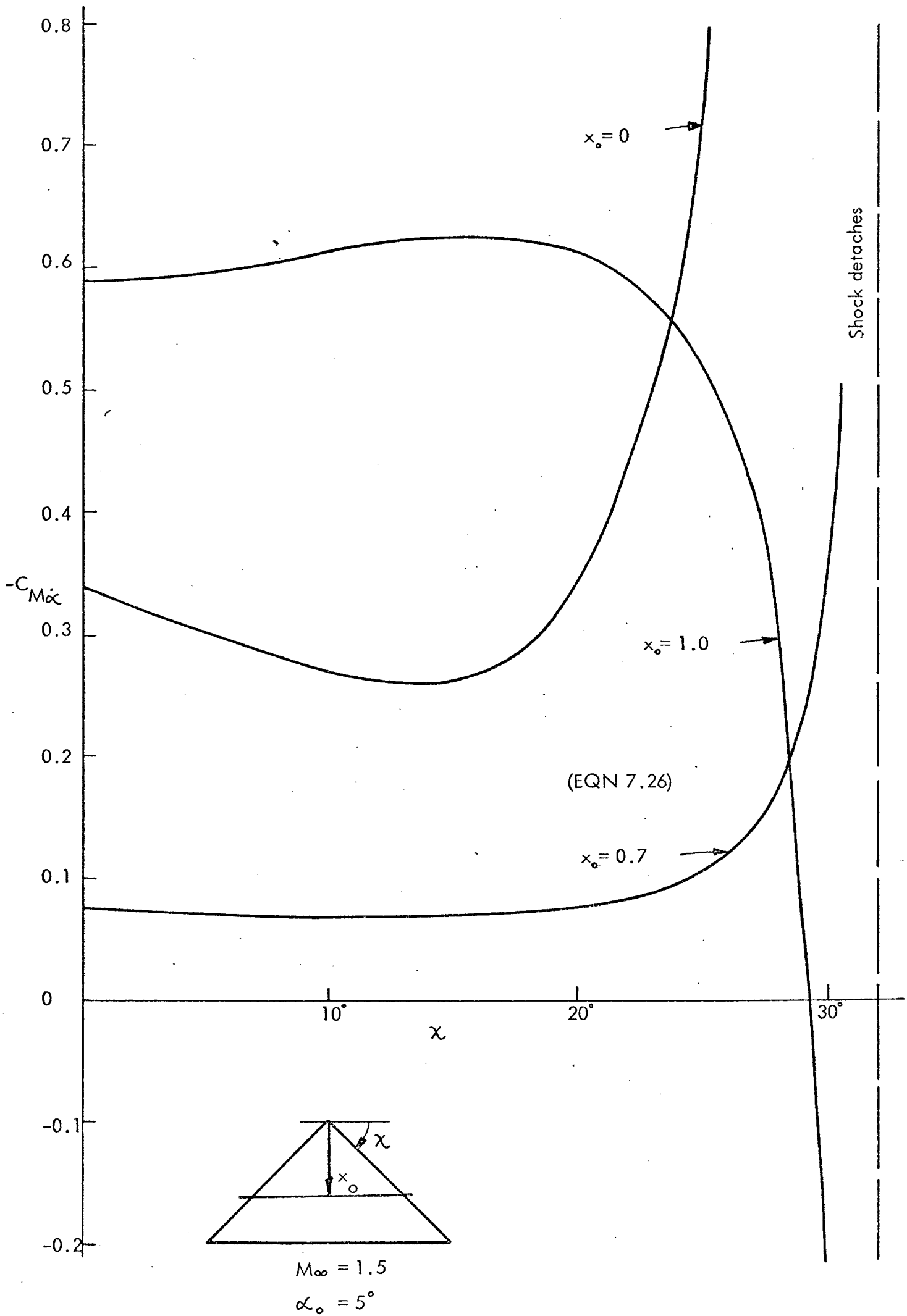


FIG. 23 $-C_{M\dot{\alpha}}$ vs χ AT VARIOUS x_0 'S . ($M_\infty = 1.5$).

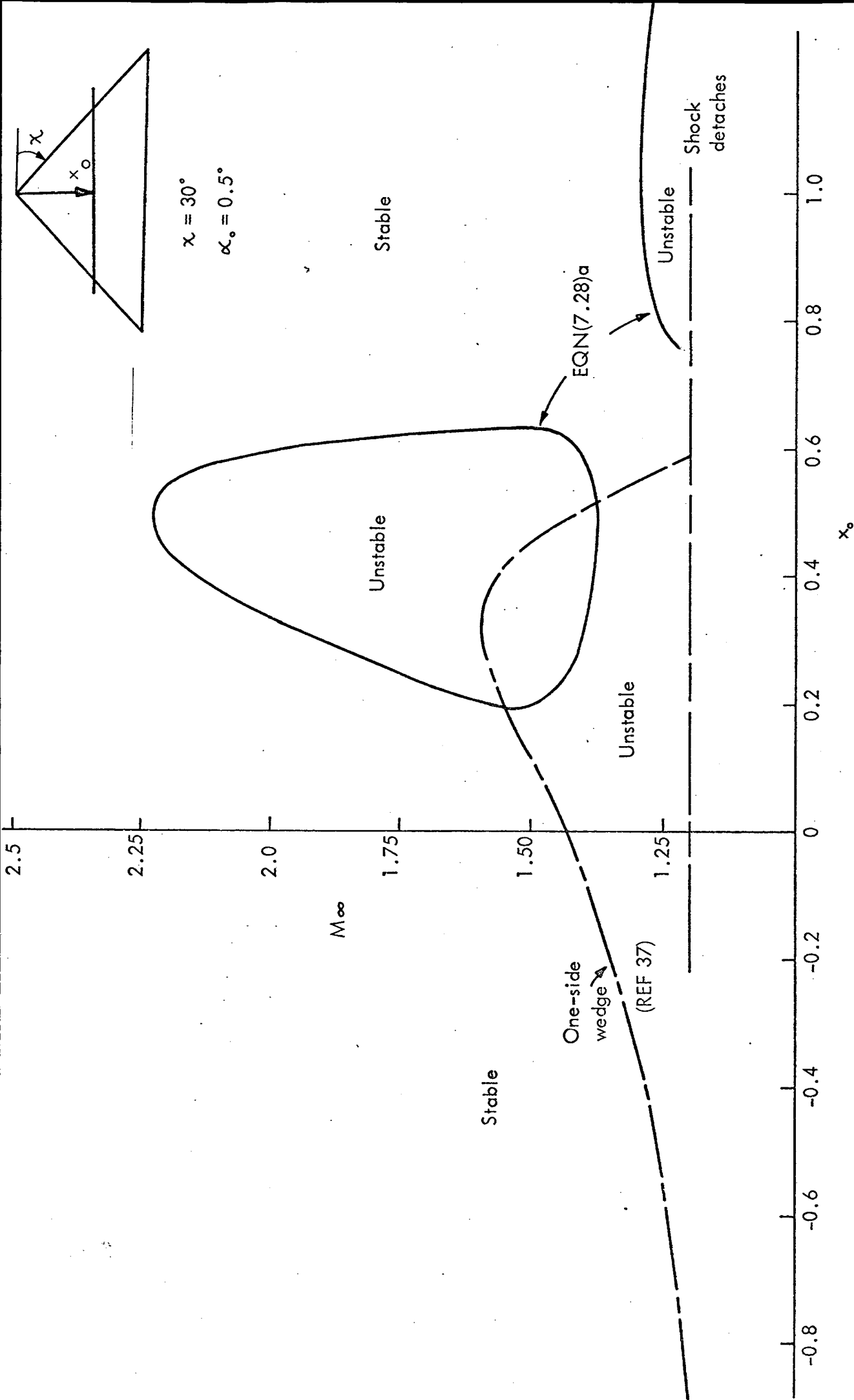


FIG.24 STABILITY BOUNDARIES OF A WEDGE AND A DELTA WING.

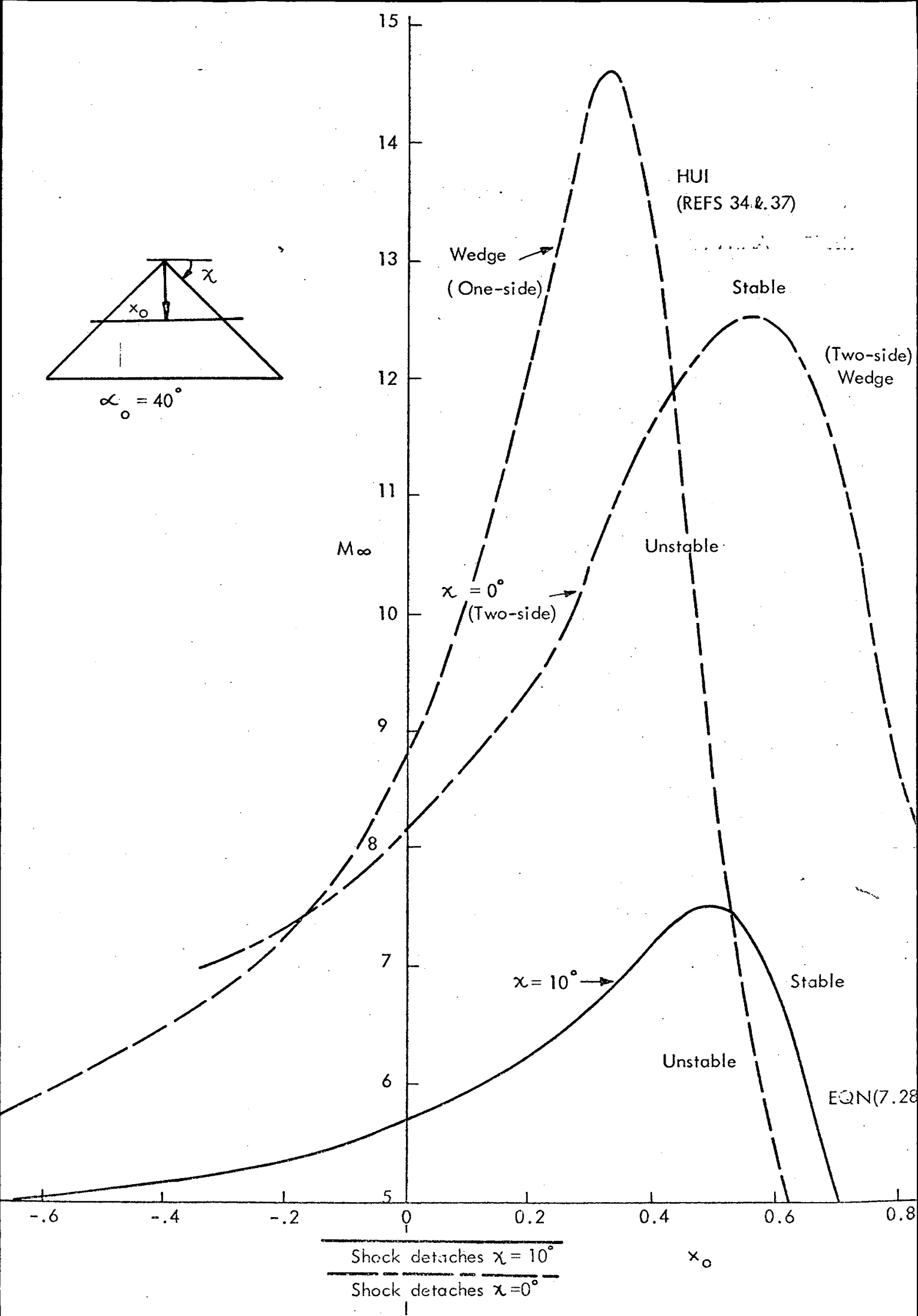
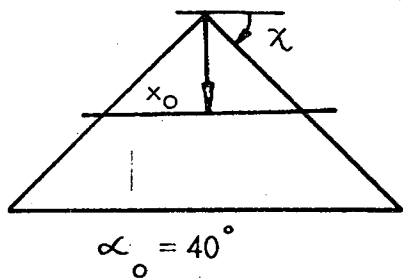


FIG.25 STABILITY BOUNDARIES OF DAMPING FOR WEDGES AND A DELTA WING.

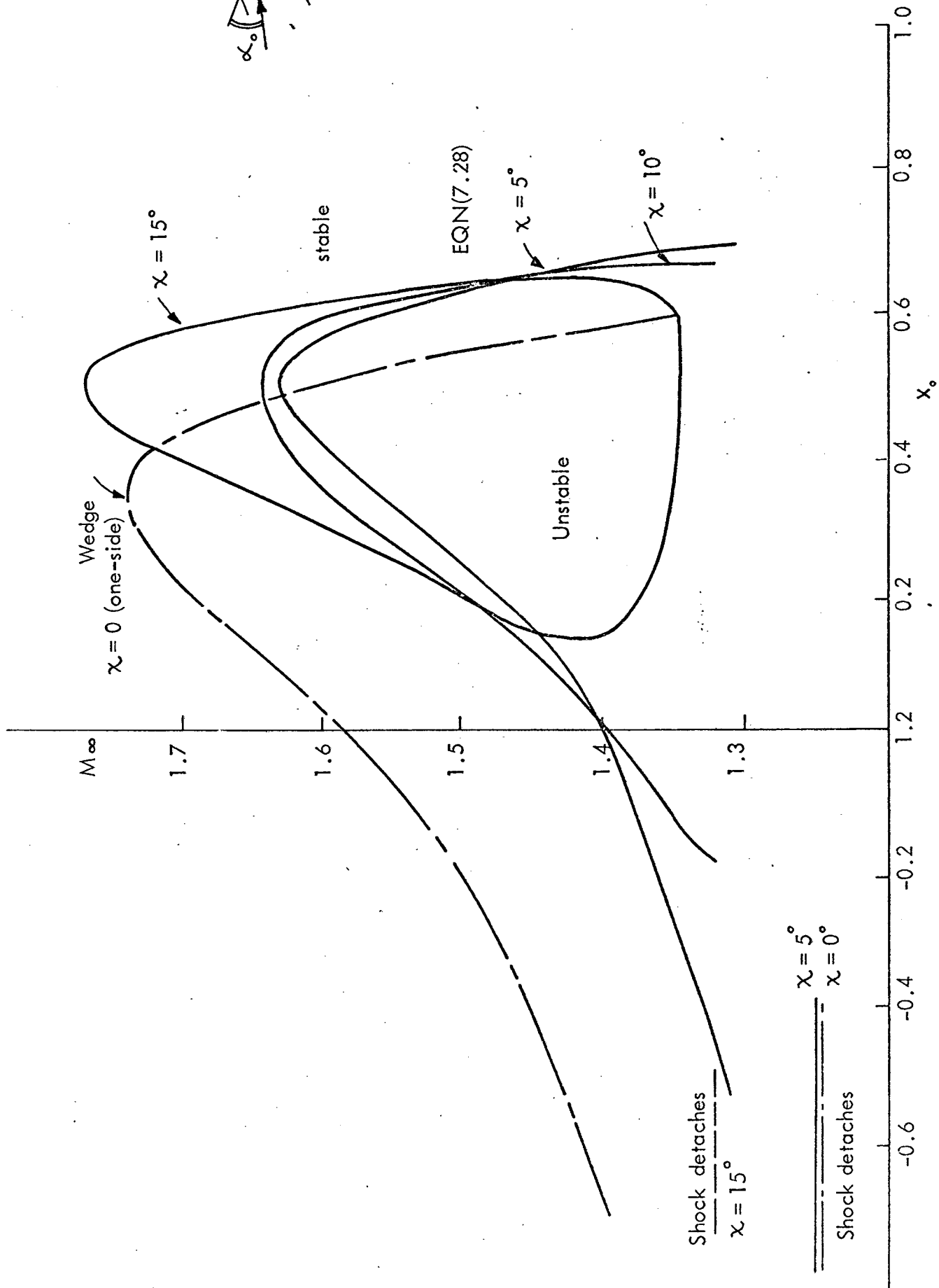


FIG. 26. STABILITY BOUNDARIES FOR DELTA WINGS OF VARIOUS χ .

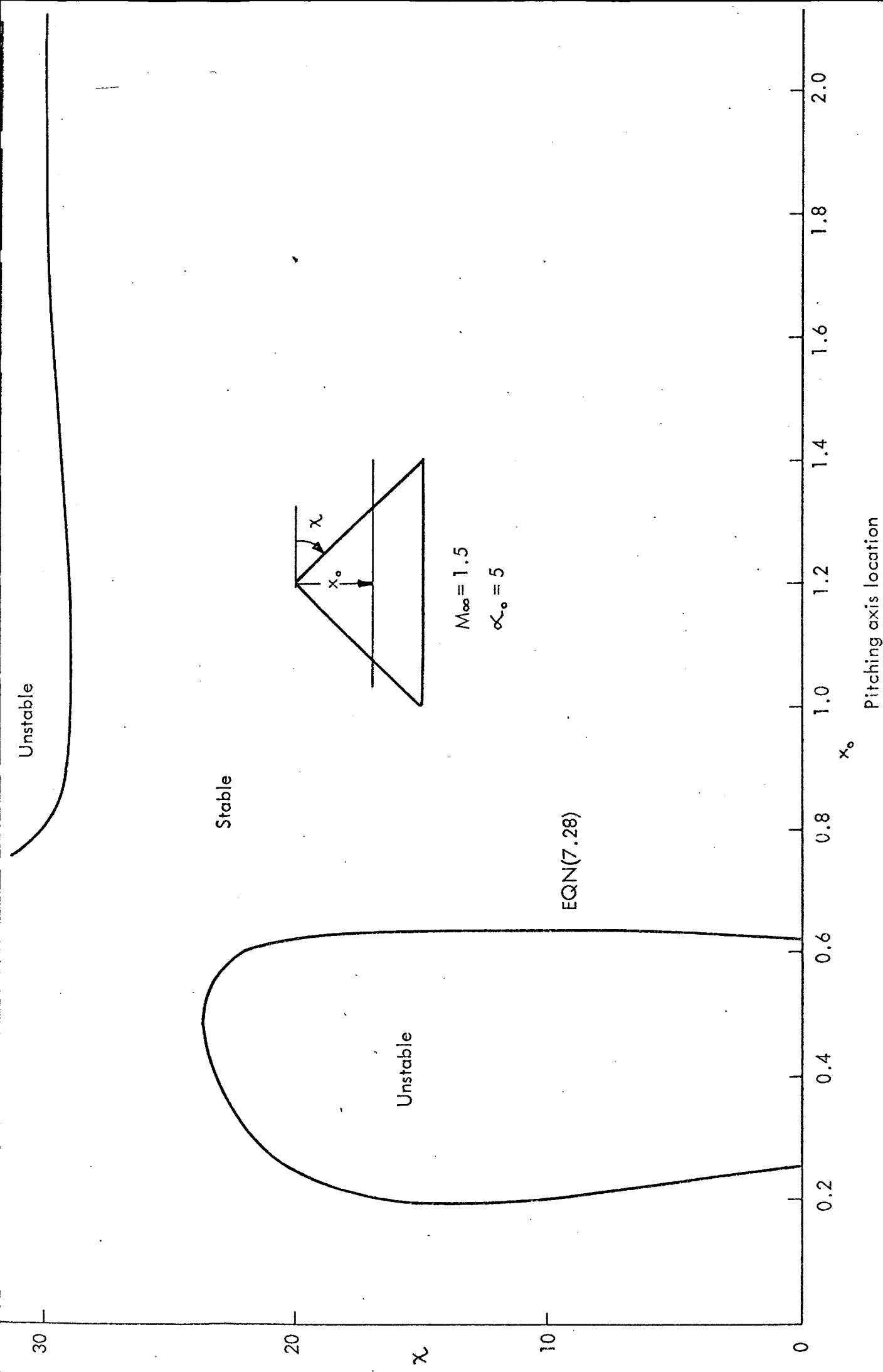


FIG. 27. STABILITY BOUNDARIES SHOWING IN $\chi - x_0$ DIAGRAM.

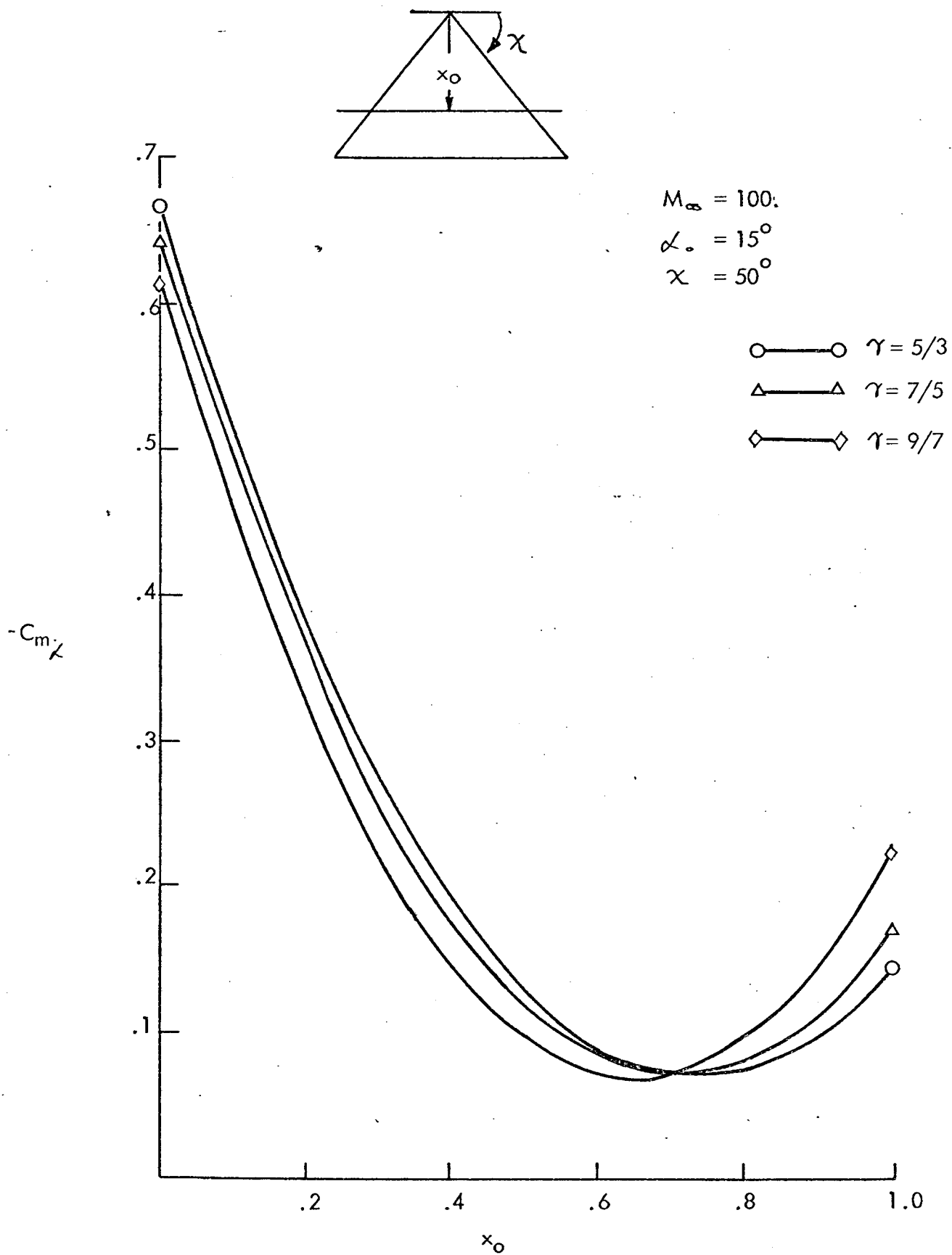


FIG. 28. $C_{m\chi}$ vs x_0 FOR DIFFERENT RATIOS OF SPECIFIC HEATS.

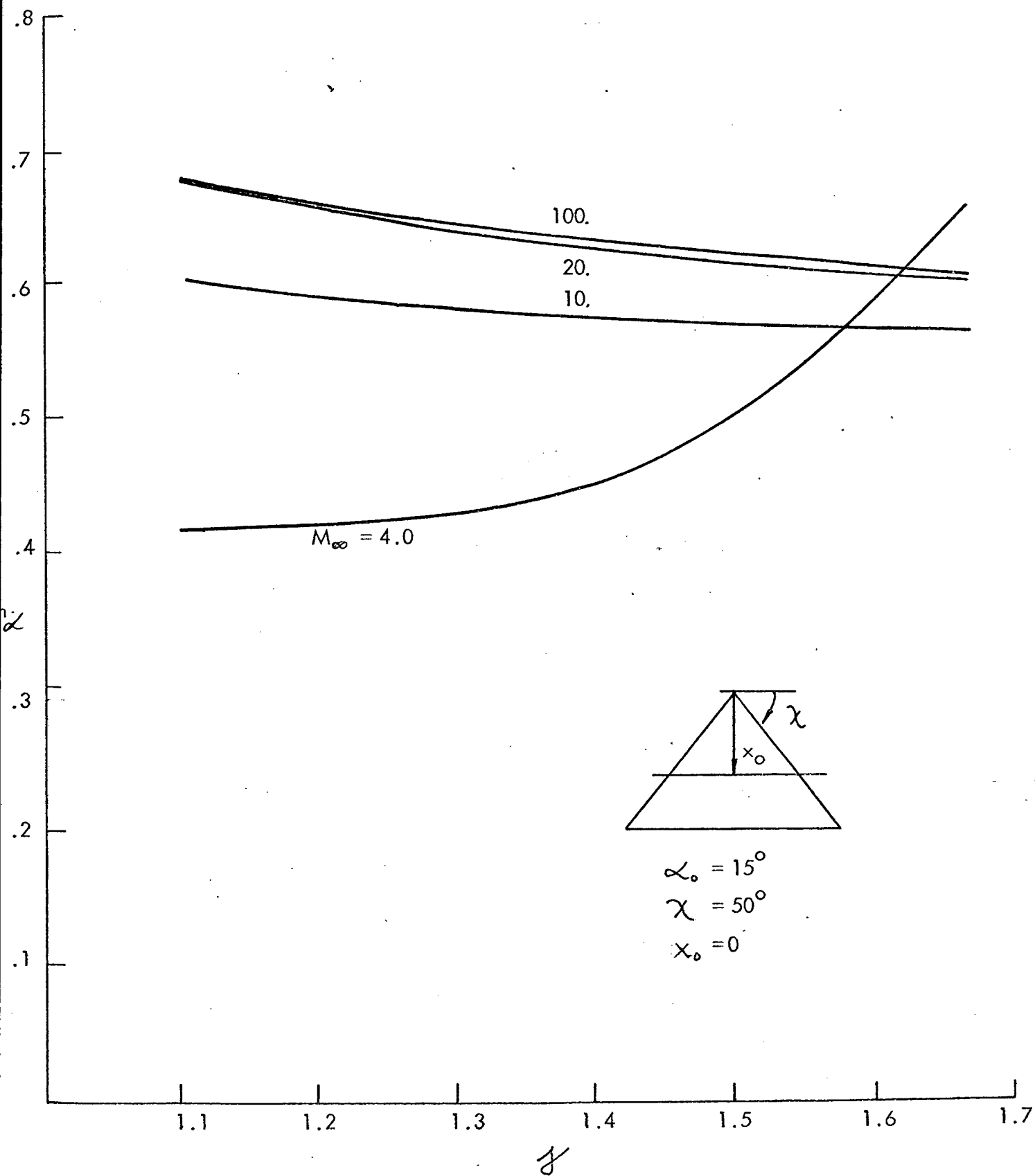


FIG.29. EFFECTS OF THE RATIOS OF SPECIFIC HEATS ON DAMPING-IN-PITCH $C_{m\dot{\alpha}}$